SGW-50776
Revision 1

Model Package Report: Vadose Zone Model for the River Corridor

Version 1.0

Prepared for the U.S. Department of Energy
Assistant Secretary for Environmental Management

Contractor for the U.S. Department of Energy
under Contract DE-AC06-08RL14788

CH2MHILL
Plateau Remediation Company
P.O. Box 1600
Richland, Washington 99352

Model Package Report: Vadose Zone Model for the River Corridor

Version 1.0

Document Type: ENV Program/Project: EP&SP

S. Mehta
CH2M HILL Plateau Remediation Company

J. L. Smoot
CH2M HILL Plateau Remediation Company

T. J. Budge
CH2M HILL Plateau Remediation Company

C. Cheng
INTERA

J. L. Ludwig
INTERA

N. Hasan
INTERA

A. H. Aly
CH2M HILL Plateau Remediation Company

M. I. Wood
CH2M HILL Plateau Remediation Company

W. E. Nichols
CH2M HILL Plateau Remediation Company

H. Rashid
INTERA

J. M. Sigda
INTERA

Date Published
May 2013

Prepared for the U.S. Department of Energy
Assistant Secretary for Environmental Management

Contractor for the U.S. Department of Energy
under Contract DE-AC06-08RL14788

CH2MHILL
Plateau Remediation Company
P.O. Box 1600
Richland, Washington 99352

APPROVED
By Shauna Adams at 12:49 pm, May 14, 2013

Release Approval Date

**Approved for Public Release;
Further Dissemination Unlimited**

TRADEMARK DISCLAIMER

Reference herein to any specific commercial product, process, or service by tradename, trademark, manufacturer, or otherwise, does not necessarily constitute or imply its endorsement, recommendation, or favoring by the United States Government or any agency thereof or its contractors or subcontractors.

Printed in the United States of America

Model Package Report

Vadose Zone Model for the River Corridor

Version 1.0

May 2013

Prepared for:

River Corridor RI/FS Projects

Prepared by:

S. Mehta
A.H. Aly
T.J. Budge
W.E. Nichols
J.L. Smoot
M.I. Wood
(CH2M HILL Plateau Remediation Company)

C. Cheng
N. Hasan
H. Rashid
J.L. Ludwig
J.M. Sigda
(INTERA, Inc.)

Executive Summary

This model package report documents the development of vadose zone (VZ) flow and transport models for the River Corridor portion of the U.S. Department of Energy's Hanford Site, Washington, in support of remedial activities that are currently underway. The results of the flow and transport models are intended for use in evaluating the potential long-term impact of residual VZ contamination on groundwater and surface water quality from waste sites located in various geographic areas in the River Corridor. The modeling results are used in calculating the soil screening levels and preliminary remediation goals (PRGs) for various contaminants to support the clean-up decisions in an effort to protect the groundwater and surface water resources. The goal is to determine and apply these threshold concentrations to a geographic area within the River Corridor without focusing on any given waste site. Because this methodology is designed to be applicable to all waste sites within a given geographic area, the calculations are performed with a conservative set of assumptions. These conservatively determined bounding concentrations provide an efficient way in identifying waste sites, with a high degree of confidence where residual contamination poses acceptable risk, and differentiating them from those waste sites where more careful evaluation of long-term impacts may be needed.

The report discusses the current understanding of nature and extent of various contaminants of interest in the various geographic areas in the River Corridor, with focus on hexavalent chromium. Results from sampling in recent boreholes drilled near high-risk waste sites and potentially contaminated areas are also presented. The development of representative stratigraphic columns and corresponding one-dimensional numerical models for various geographic areas in the River Corridor is described along with the technical basis for specific model parameters, contamination zone, and boundary conditions. A description of modeling assumptions and modeling conservatisms is also provided. The methodology used in predicting the peak concentrations in the groundwater from residual contamination in the VZ and derivation of soil screening levels and PRGs for protection of groundwater and surface water is described in detail. The overall objective of the modeling effort is to provide a basis for making informed remedial action decisions.

Uncertainty and sensitivity analyses have been conducted to determine the model parameters that impact the prediction of peak concentration. The results indicate that depending upon the vertical extent of contamination, either the vadose zone hydrologic parameters or the hydraulic gradient in the aquifer is important in determining the peak concentrations, if the sorption parameters are held constant.

Contents

Figures

Tables

Abbreviations and Acronyms

ACM	alternative conceptual model
AMU	atomic mass unit
bgs	below ground surface
CCC	Criterion Continuous Concentration
CERCLA	Comprehensive Environmental Response, Compensation, and Liability Act
CHPRC	CH2M-HILL Plateau Remediation Company
Ci	curie(s)
cm	centimeter(s)
cm/s	centimeters per second
cm^3/g	cubic centimeters per gram
COPC	contaminant of potential concern
Cr	chromium
Cr(III)	trivalent chromium
Cr(VI)	hexavalent chromium
DOE	U.S. Department of Energy
DWS	Drinking Water Standards
EPA	U.S. Environmental Protection Agency
EPC	exposure point concentration
ET	evapotranspiration
FEPs	Features, Events, and Processes
FS	Feasibility Study
ft	feet
FY	fiscal year
g	gram(s)
GA	Graded Approach
h	hour(s)
HEIS	Hanford Environmental Information System
HISI	Hanford Information System Inventory
HMS	Hanford Meteorology Station
in	inch
ISRM	In Situ Redox Manipulation
kg	kilogram(s)
km	kilometer(s)
km^2	square kilometer(s)
µg/L	micrograms per liter
m	meter(s)
m/s	meters per second
mg/kg	milligrams per kilogram
mi	mile(s)

mi^2	square mile(s)
mm/yr	millimeters per year
mph	miles per hour
ms/cm	microsiemens per centimeter
NPL	National Priority List
OU	operable unit
pCi/g	picocuries per gram
PNNL	Pacific Northwest National Laboratory
PRG	Preliminary Remediation Goal
QA/QC	quality assurance/quality control
RI	Remedial Investigation
RPO	Remedial Process Optimization
ROD	Record of Decision
RUM	Ringold Upper Mud
STOMP	Subsurface Transport Over Multiple Phases
SZ	saturated zone
TIN	Triangulated Irregular Network
VZ	vadose zone
WCH	Washington Closure Hanford
WQS	water quality standard
yr	year

1. Introduction

Remediation of contaminated waste sites located in the River Corridor of the U.S. Department of Energy's (DOE's) Hanford Site is currently underway. For the purpose of remediation, the River Corridor was divided into different geographic areas (Figure 1-1): 100-BC, 100-K, 100-D, 100-H (managed as 100-D/H), 100-N, 100-F, 100-IU-2, 100-IU-6 (managed as 100-F/IU-2/IU-6), and the 300 Area.

Modeling activities have been undertaken in the River Corridor to support the clean-up process through evaluation of the long-term impact of waste site residual vadose zone (VZ) contamination on groundwater and surface water quality. For purposes of modeling, the waste sites in the River Corridor were sorted into geographic areas and models representative of the generalized geology and surface soil type of each area were developed. In addition to geographic proximity, the nature of waste disposed during waste site operations (e.g., resulting from a nuclear reactor operations) was considered in assigning geographic areas for modeling purposes so that similar remedial action can be considered. The geographic areas are generally large areas and may include groundwater Operable Unit (OU), source OUs, and facilities that encompass the National Priority List (NPL) sites. For example, the 100-BC geographic area consists of the 100-BC-1 and 100-BC-2 Source OUs as well as the 100-BC-5 Groundwater OU. The discussion in this report follows the geographic area nomenclature.

1.1 Modeling Need

Modeling is needed to determine the residual contaminant concentration in the vadose zone that would be protective of groundwater and surface water as defined by the water quality standards (drinking water standards and aquatic water quality standards) in support of risk assessment studies in the River Corridor.

The soil screening levels and preliminary remediation goals (PRGs) provide estimate of the residual contaminant concentration under different set of modeling conditions, which when left behind will not pose unacceptable risk. The goal is to define these threshold concentrations that are applicable to geographic areas within the River Corridor without attempting to forecast future conditions under any given waste site. This approach provides an efficient way of identifying waste sites, with a high degree of confidence, where residual contamination poses potential risk, and thereby differentiating them from those waste sites where more careful evaluation of long-term impacts are needed. The soil screening level and PRG calculation is important because separately assessing each of the hundreds of waste sites within River Corridor with detailed characterization and modeling is neither pragmatic nor necessary if the residual contamination in the VZ underneath most of the sites is so small that it will not pose risk to groundwater or surface water quality.

Since this methodology is designed to be applicable to all waste sites within a given geographic area, the calculations are performed with a conservative set of assumptions, such as, extended vertical zone of contamination under the waste site, higher recharge rates, ignoring dilution and gradient reversals due to Columbia river stage fluctuations, choosing minimum vadose zone thickness in the soil columns, choosing sorption parameter values from lower end of the empirical distribution functions, ignoring attenuation between groundwater under the waste site and the point of discharge in the Columbia River or mixing within the surface water body, etc. Furthermore, the calculations are performed in one-dimension to maximize the vertical transport to the water table thereby ignoring any lateral spreading of contaminants. Due to conservative choice of modeling inputs and boundary conditions, the screening levels and PRG concentrations are deemed to be bounding estimates (i.e., lead to the lowest threshold concentrations). The goal is not to accurately predict the contaminant concentrations over time, for which

a site specific model will be required, but to estimate a bounding impact from residual contamination that may be left behind under a waste site on groundwater and surface water.

An attempt has also been made to summarize the nature and extent of contamination in various geographic areas in the River Corridor (except for the 100-N and 300 Areas) with particular attention given to chromium (Cr) contamination. Insights gained from Cr leachability tests are presented to support the conceptual model development. The vertical extent of contamination observed in the recently completed remedial investigation (RI) boreholes is also summarized to support the modeling assumptions.

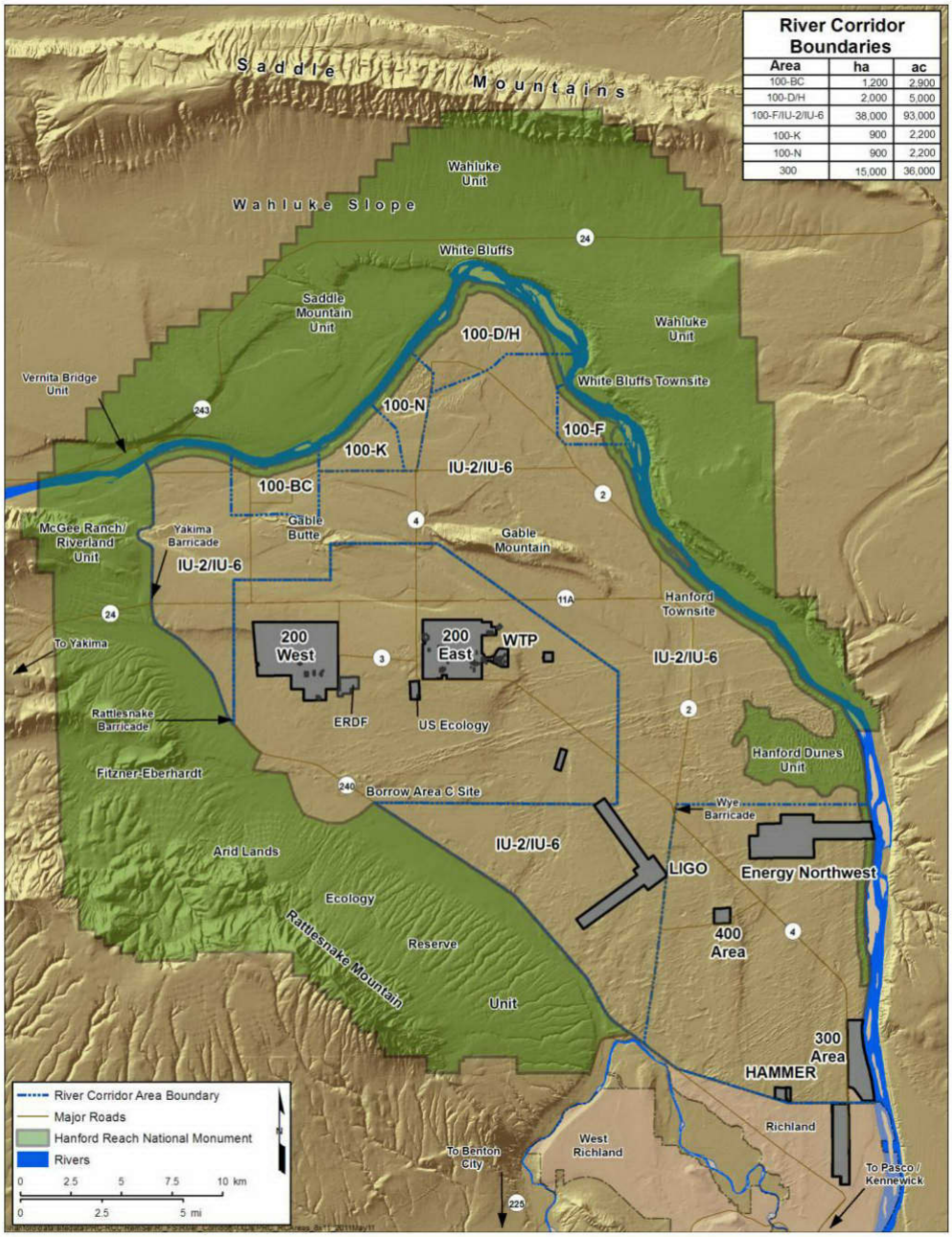

Figure 1-1. River Corridor Area at the Hanford Site

1.2 Background

To manage cleanup activities at the Hanford Site, waste sites are grouped within OUs so that the Comprehensive Environmental Response, Compensation, and Liability Act (CERCLA) cleanup process can be efficiently implemented. The OUs includes source OUs (i.e., surface and vadose zone areas where waste was disposed) and groundwater OUs (areas in the saturated zone where contamination exists) to perform separate characterization in recognition of the differences between localized contaminants in the soil column at the sources and the more widespread co-mingled contamination in groundwater. Most of the OUs are source OUs. There are five groundwater OUs in the 100 Area, namely, 100-BC-5, 100-KR-4, 100-NR-2, 100-HR-3, and 100-FR-3.

Assessment of potential impacts from soil contamination currently present in the vadose zone (VZ) focuses on the magnitude and timing of solute fluxes to the underlying aquifer and potential migration towards the Columbia River. Migration of VZ contamination towards groundwater and surface water resources is the principal exposure pathway for contaminants deeper than 4.6 meters (m) (15 feet [ft]), the depth to which the contaminated soil from the waste sites is typically removed. The contaminant migration from waste sites through the VZ to the underlying aquifer is controlled by driving forces for water movement in porous media (such as gravity, recharge, and matric potential), interactions between water and sediments, and interactions between the contaminants and the sediment. Because of past waste disposal practices, the type of the contaminant and extent of contamination (spatially and vertically) varies across different geographic areas, and thus calculations specific to each geographic area need to be performed in support of risk assessment studies. The types of sediments and their thicknesses and properties can also vary from one geographic area to another and can affect the rate and direction of solute and water movement to the aquifer. The non-linear physics governing flow and solute transport in the VZ under arid climate conditions can lead to very long travel times (hundreds to thousands of years or more) for some contaminants before the contaminant concentration in groundwater approaches or exceeds water quality standards (WQSs). The concentration of contaminant in the groundwater is dependent on a variety of features and processes, such as solute flux from the VZ, aquifer thickness and dilution from mixing with the groundwater, retardation and dispersion in the aquifer, and river water and groundwater interaction.

To evaluate the impact of residual contamination in VZ on groundwater and surface water quality at the waste site boundary, the modeling is conducted using the Graded Approach (GA). The GA allows for evaluating the impact of residual contamination underneath the waste sites in a gradational or stepwise fashion through rapid differentiation of relatively low-risk sites from higher-risk sites so that resources (data-collection related and modeling related) can be focused on the potentially high-risk sites. By evaluating waste sites in a gradational fashion, the GA assesses sites using the entire range of conservative simplifications to rigorous site specifics. Using soil concentrations obtained by employing very conservative but relatively simple contaminant transport model, the GA first identifies waste sites that are unlikely to constitute a risk to groundwater protection. The remaining waste sites, which pose a greater risk to groundwater and surface water protection, are again evaluated in a stepwise manner that matches the complexity and data needs of the assessment to the risk posed. The GA thus provides efficient, conservative, and rigorous evaluation of sites by allocating evaluation and characterization resources to those sites for which groundwater protection is a significant problem.

Figure 1-2 shows the logic flow chart for the GA (DOE/RL-2011-50 Rev. 0, *Regulatory Basis and Implementation of a Graded Approach to Evaluation of Groundwater Protection*). The decisions are shown as diamonds and actions as rectangles. Boxes with rounded corners provide descriptive

information for the various decisions and actions. The first action in the GA is to compare the exposure point concentration (EPC) of an analyte at the site with a screening level to determine if it should be designated as a contaminant of potential concern (COPC). If the EPC for a given analyte is less than or equal to the screening level, then that analyte does not pose a significant risk to groundwater and passes the screen. However, if the EPC exceeds its screening level, it fails the screen and is designated a COPC. The soil screening level calculation is important because separately assessing each of the hundreds of waste sites within River Corridor with individual models is neither pragmatic nor necessary if the residual contamination in the VZ underneath most of the sites is so small that it will not pose risk to groundwater or surface water quality. The screening level for each contaminant is defined as the larger of a background level, a practical quantification limit, or a calculated screening level that was computed using the Subsurface Transport Over Multiple Phases (STOMP) code (PNNL-12030, *STOMP Subsurface Transport Over Multiple Phases Version 2.0 Theory Guide;* PNNL-11216, *STOMP Subsurface Transport Over Multiple Phases: Application Guide*; PNNL-15782, *STOMP Subsurface Transport Over Multiple Phases Version 4.0 User's Guide*), and a highly conservative set of assumptions for the site or its vicinity (see Section 2.1 for more details).

Although the assumptions that underlie the screening level calculation are deliberately highly conservative and typically are not representative of site conditions, the site of each contaminant that fails the screening assumptions is further evaluated in Decision 2 based on additional information:

- If the screening assumptions represent site conditions, or if available site data and information are not sufficient to modify the assumptions used to develop the screening values, then the site is directly carried into the Feasibility Study (FS) (Action 4).
- If sufficient information is available to use a more site specific representative calculation, then the COPC is evaluated using PRGs, which are the initial or proposed cleanup goals developed in the CERCLA process to provide risk reduction targets or candidate cleanup levels (see Section 2.2) (Decisions 3 and 4).

It is more likely that all of the COPCs that fail screening will be carried into the site assessment using the PRG evaluation step rather than be directly carried into the FS because the highly conservative assumptions underpinning the screening levels are not expected to be representative of conditions at many waste sites. Furthermore, if a site shows concentration levels that are higher than the screening levels, additional information is typically gathered at the site to assist in the risk evaluation. This information is what enables the evaluation against the screening assumptions.

For the Hanford site, PRGs will be calculated with the assumption that once the remedial actions are completed, native xerophytic vegetation will be re-established as the land cover. PRGs for other remedial alternatives, such as an evapotranspiration barrier, can be calculated as well.

Transitioning a site from one step of the GA to another can occur with the addition of new information, such as additional data, analyses, and modeling. A more thorough discussion of the GA is given in DOE/RL-2011-50 Rev. 0.

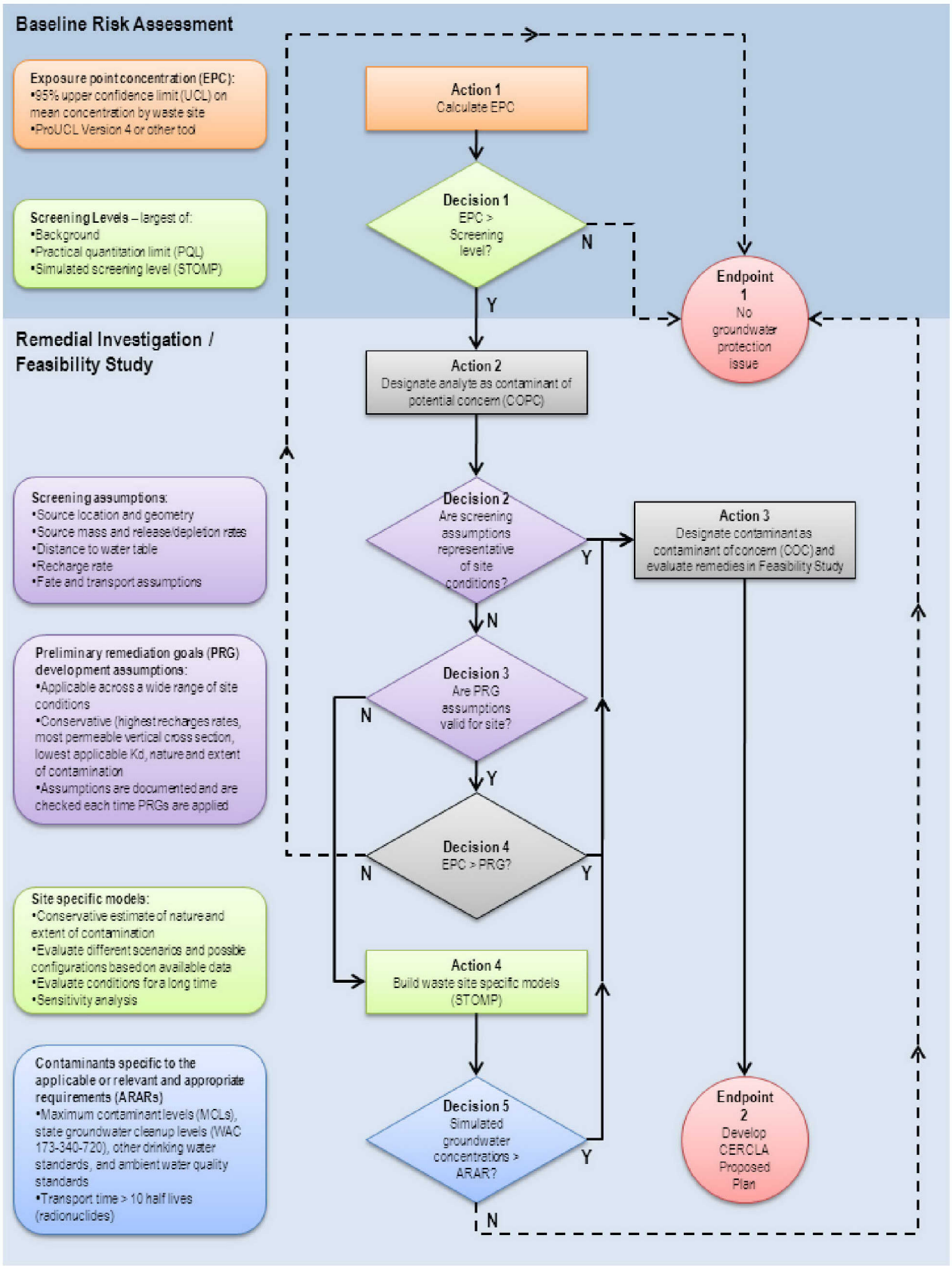

Figure 1-2. Logic Flow Chart for the Graded Approach

1.3 Document Organization

The document is organized into three basic parts: (1) basis for development of the model; (2) model implementation and modeling results; and (3) uncertainty and sensitivity analyses. The organization of this model package report follows the guidance set forth in the "Quality Assurance Project Plan for Modeling" found in Appendix G of CHPRC-00189 Rev. 9, *CH2M HILL Plateau Remediation Company Environmental Quality Assurance Program Plan*. Section 2 sets forth the modeling objectives. Section 3 presents the geology of the River Corridor and the modeling relevant Features, Events, and Processes (FEPs) that impact the flow and transport in the 100 Area, along with the modeling assumptions and the nature and extent of contamination. Because contamination of hexavalent chromium [Cr(VI)] is prevalent but varies among the geographic areas in the 100 Area, a more detailed discussion of Cr(VI) contamination is presented with discussion of desorption test results based on leachability experiments. Section 4 describes the modeling implementation details, initial conditions, boundary conditions, and parameter values. Modeling results are presented in Section 5 both for the screening levels and PRG calculations for each geographic area while Section 6 discusses the sensitivity and uncertainty analyses. Section 7 provides the details related to configuration management of the model inputs and outputs including the software used.

2. Model Objectives

The purpose of modeling is to develop bounding residual contaminant concentration levels in the VZ rock matrix, underneath the waste sites located in the River Corridor, such that that the effluent concentrations resulting from the residual contamination would not exceed the surface water and groundwater quality standards. Two separate calculations are performed to determine the residual contaminant concentration level in the VZ: The first is a geographic area-specific screening level calculation where modeling is performed using a conservative set of parameter values and modeling assumptions of fully contaminated VZ and maximum possible recharge rate (irrigation scenario) to determine the minimum residual contaminant concentration values in the rock matrix that would be protective of surface water and groundwater quality standards. If the VZ contaminant concentrations underneath the waste sites are found to be below the screening level then no remedial action is needed. The second calculation is geographic area specific PRG calculation where modeling is performed using assumption of fully contaminated VZ but with base (expected) recharge rates that are consistent with the soil type. Both calculations are performed for 192 non-radionuclides and 28 radionuclides in groundwater and 192 non-radionuclides in surface water (specifically, the Columbia River).

The calculations are performed with a conservative set of assumptions, such as, extended vertical zone of contamination under the waste site, higher recharge rates, ignoring dilution and gradient reversals due to Columbia river stage fluctuations, choosing minimum vadose zone thickness in the soil columns, choosing sorption parameter values from lower end of the empirical distribution functions, ignoring attenuation between groundwater under the waste site and the point of discharge in the Columbia River or mixing within the surface water body, etc. Furthermore, the calculations are performed in one-dimension to maximize the vertical transport to the water table thereby ignoring any lateral spreading of contaminants. Due to conservative choice of modeling inputs and boundary conditions, the screening levels and PRG concentrations are deemed to be bounding estimates (i.e., lead to the lowest threshold concentrations).

In the calculation methodology, the saturated zone is assumed to be initially uncontaminated, which may not always be true since plumes can migrate from upgradient locations over time. However, due to several in-built modeling conservatisms mentioned above, the screening level and PRG calculations are deemed to remain bounding when compared to the results derived from a more sophisticated site-specific predictive model that incorporates all the features and processes relevant at the scale of the model, including any contaminant migration from upgradient locations. Stated differently, groundwater is not expected to remain contaminated above cleanup levels (or discharge to the Columbia River above ambient water quality standards) any longer because former waste sites are closed with the screening values or PRGs calculated using this methodology.

2.1 Screening Levels

Soil screening levels are neither cleanup standards nor are they definitions of "unacceptable" levels of soil contaminants (EPA/540/R-95/128, *Soil Screening Guidance: Technical Background Document*). Rather, screening levels are used to separate contaminants from COPCs and determine which COPCs warrant further evaluation or investigation (EPA/540/R-96/018, *Soil Screening Guidance: Users Guide*; EPA/540/R-95/128; DOE-STD-1153-2002, *A Graded Approach for Evaluating Radiation Does to Aquatic and Terrestrial Biota*).

The screening level is defined as the largest of the following:

- Some statistically defined upper bound on the range of background values (e.g., 90th percentile).
- A practical limit for measuring the contaminant's concentration or activity (if radionuclide).
- A simulated minimum amount of material (concentration or activity) that will not cause groundwater cleanup standards to be exceeded, even under conservative assumptions within an extended time frame (e.g., 1,000 years).

The calculated screening level for any contaminant is simply the ratio of the applicable WQS to the simulated peak groundwater concentration (or radioisotope activity) for a unit initial contaminant source concentration (or radioisotope activity). It is calculated by the following equation:

$$SL = aC_I \frac{WQS}{CPK} \qquad \text{Eqn. 2-1}$$

where:

SL	=	calculated screening level (contaminant mass or activity/kilogram [kg] of soil)
a	=	a constant selected to balance units
C_I	=	the initial contaminant concentration associated with the rock matrix in the VZ (typically contaminant mass or activity/mass of soil)
WQS	=	water quality standard (contaminant mass or activity/liter [L] of water)
CPK	=	peak groundwater concentration caused by C_I (typically contaminant mass or activity/L of water)

The surface WQSs were utilized to compute screening levels protective of surface water, whereas the groundwater WQSs were used to compute screening levels protective of groundwater.

The simulations were run using the STOMP code (PNNL-12030) to yield a peak groundwater concentration for each contaminant within the uppermost 5 m of the aquifer, representing the screened interval of a water table monitoring well. Simulations for calculating the screening levels for the waste sites in the 100 Area for protection of surface water and groundwater were carried out separately for each geographic area with highly conservative assumptions to maximize the peak concentration in the aquifer. A very conservative sets of hydraulic and transport properties related to saturated hydraulic conductivity, saturated volumetric water content, residual volumetric water content, dispersivity, van Genuchten α and n parameters, and bulk density was assumed for screening calculations. Distribution of contaminants in the soil column (i.e., fully or partially contaminated), an important driving force for Screening Level calculations, was assumed based on the distribution coefficients of the contaminants. The details on this assumption are described in Section 5 of this document. Other conservative assumptions used to calculate screening levels focused on the driving forces, specifically, relatively large recharge through the VZ under irrigation scenario and lower aquifer flux rate to minimize dilution. However, it is crucial that assumptions are selected to balance conservatism with site appropriate conditions. For example, selecting a lowest-observed hydraulic gradient value that applies to only one of many sites is not warranted if this low value is well outside the range of values observed for similar aquifer formations.

2.2 Preliminary Remediation Goals

PRGs are residual contaminant concentration in the soil that will be protective of groundwater and surface water under specific site conditions. The PRGs represent the maximum quantity of contaminant concentration or radioisotope activity in the rock matrix that can remain in the VZ without causing an exceedance of applicable water quality standards (the federal and/or state drinking water standards and aquatic water quality standards). The PRGs can be defined for protection of groundwater or for protection of surface water simply by the choice of the applicable standard used in the calculation. They are developed to guide risk assessment decisions and evaluate selected remedies.

The value of a 100 Area PRG for a particular contaminant depends on a small number of key factors. Waste site characteristics, specifically, source mass distribution and distance to the water table, are key factors. Another key factor is land cover condition and the associated recharge rate. The interactions between the VZ geology and water movement and between VZ geology and contaminant chemistry are the two remaining key factors. PRGs were calculated assuming that the entire VZ thickness is fully or partially contaminated based on the distribution coefficients of the contaminants (See Section 5 for details) and that ambient recharge rate is a function of natural land cover and varies over time (as opposed to irrigation based recharge for the screening level calculations). PRGs were calculated with the assumption that once the remedial actions are completed, native land cover vegetation will be reestablished after 30 years. The recharge rate associated with this land cover varies over time as the land cover transitions from bare soil (highest recharge rate), to grasses and immature shrub steppe (reduced recharge rate), to mature shrub steppe (lowest recharge rate).

Variability in hydraulic properties was incorporated into PRG development by selection of conservative values. Hydraulic properties include saturated hydraulic conductivity, porosity, and unsaturated flow parameters such as the Mualem-van Genuchten α, n, and residual water content parameters (Mualem [1976], "A New Model for Predicting the Hydraulic Conductivity of Unsaturated Porous Media"; van Genuchten [1980], "A Closed-Form Solution for Predicting the Conductivity of Unsaturated Soils"). PRG values can be relatively sensitive to the saturated hydraulic conductivity values for the aquifer, so values from the lower end of the range were chosen, yielding a more conservative PRG value. PRG development captures the effects of geologic variability by simulating flow and transport through a set of representative stratigraphic columns for each geographic area. Peak groundwater concentrations are simulated for each representative column and PRGs are calculated for each column. The minimum value is adopted as the final PRG for each geographic area for each contaminant.

The PRG calculation for each contaminant is performed using the same equation (Equation 2-1) as that for the screening level except that the inputs are different as mentioned above.

3. Model Conceptualization

The VZ models for the River Corridor consider porous media flow and transport through the unsaturated portion of the various geographic areas. The stratigraphy and thickness of the vadose and saturated zone plays an important role in determining the peak concentration of contaminants in the groundwater. This section provides an overview of the conceptual model development based on the geology in the 100 Area and the thickness of vadose and saturated zone. Modeling relevant Features, Events, and Processes (FEPs) are also presented to help in developing the flow and transport models. The nature and extent of contamination in the geographic areas is also presented to aid model development for screening value and PRG calculations.

3.1 Geology of River Corridor

There are two distinct hydrostratigraphic units present in the VZ and upper unconfined aquifer of the 100 Area: the younger is known as the Hanford formation and the older as the E unit of the Ringold Formation. Overlying the Hanford formation is a thin cover of more recent Holocene alluvium and eolian deposits.

Composed of silt, sand, and gravel, the recent Holocene surficial sediments were deposited by a combination of aeolian and alluvial processes. These deposits are observed as a thin layer (2 m or less) across the 100 Area where the surface has not been disturbed or altered by construction, and are treated as part of the Hanford formation for this study.

The Hanford formation is characterized by mostly unconsolidated coarse and fine-grained sediments including large to very large cobble-boulder fragments, sand, silt, and gravel. Three facies of the Hanford formation have been identified in the 100 Area: (1) gravel-dominated facies, (2) sand-dominated facies, and (3) an interbedded sand to silt-dominated facies (DOE/RL-2002-39, *Standardized Stratigraphic Nomenclature for Post-Ringold-Formation Sediments within the Central Pasco Basin).* Within the 100 Area, the coarse-grained unconsolidated sand and gravel-dominated facies are most common, the result of high-energy fluvial deposition processes caused by the cataclysmic Missoula Floods (SGW-44022 Rev. 0, *Geologic Data Package in Support of 100-BC-5 Modeling*). For this reason the Hanford formation in the 100 Area tends to be coarser and contain a larger gravel component than other areas of the Hanford Site.

Below the Hanford formation, the Ringold Formation contains two units: one is a fluvial gravel referred to as the Ringold Unit E, and the other is a lower-energy sand, silt, and a clay interval referred to as the Ringold Upper Mud (RUM). The saturated hydraulic conductivity of the Ringold E is several orders of magnitude lower than that of the Hanford formation, whereas the RUM, an aquitard that is the base of the unconfined aquifer, has the lowest hydraulic conductivity of all hydrostratigraphic units in the 100 Area. The RUM directly underlies the Hanford formation where Ringold E was removed by the Missoula Floods (SGW-40781 Rev. 1, *100-HR-3 Remedial Process Optimization Modeling Data Package*).

The Hanford-Ringold contact was formed by cataclysmic paleo-floods that first reworked the Ringold Formation surface by eroding into the older sediments and creating paleochannels constrained by uplifted basalt (the bedrock in the region). Hanford formation sediments were subsequently deposited over this reworked Ringold surface (SGW-41213 Rev. 0, *100-KR-4 Remedial Process Optimization Modeling Data Package*). Given the large differences in saturated hydraulic conductivity values for the two formations, the location of the Hanford-Ringold contact relative to the water table is important to predicting contaminant migration in the unconfined aquifer. Where the Hanford-Ringold contact occurs

below the water table, water and solute fluxes toward the Columbia River can be orders of magnitude larger than those when the contact is located above the water table (PNNL-14702 Rev. 1, *Vadose Zone Hydrogeology Data Package for Hanford Assessments*). Figure 3.1 depicts the generalized geology of the 100 Area. Figure 3.2 presents the top of the Ringold E surface (the Hanford-Ringold E contact) in plan view.

3.1.1 Representative Stratigraphy

Although the stratigraphy of the VZ and the unconfined aquifer within the 100 Area are limited to the Hanford formation and the Ringold E unit, their presence and thicknesses vary within and between each of the geographic areas. These variations can in turn cause important variations in solute fluxes and peak concentrations for contaminants, thereby leading to a range of potential PRG values among various geographic areas. Because of natural variability in the thickness of various hydrostratigraphic units it is not practical to calculate PRG for all possible variations in thicknesses observed in the various boreholes. Instead, representative stratigraphic columns were identified for each geographic area: D/H, K, BC, F, IU-2, and IU-6. Figures 3.3 through 3.5 illustrate the borehole locations used for each geographic area to produce representative soil columns for modeling purposes.

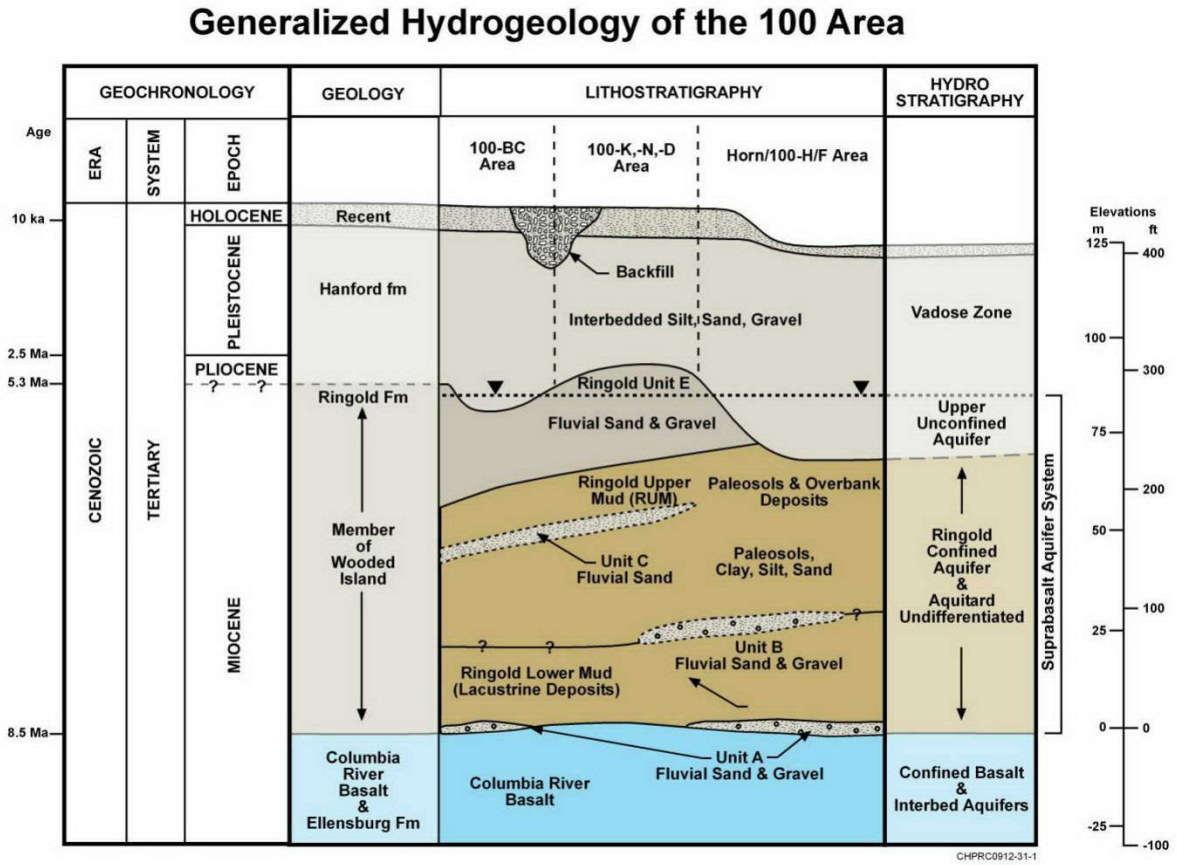

Source: SGW-44022 Rev. 0

Figure 3-1. Generalized Geology of the 100 Area

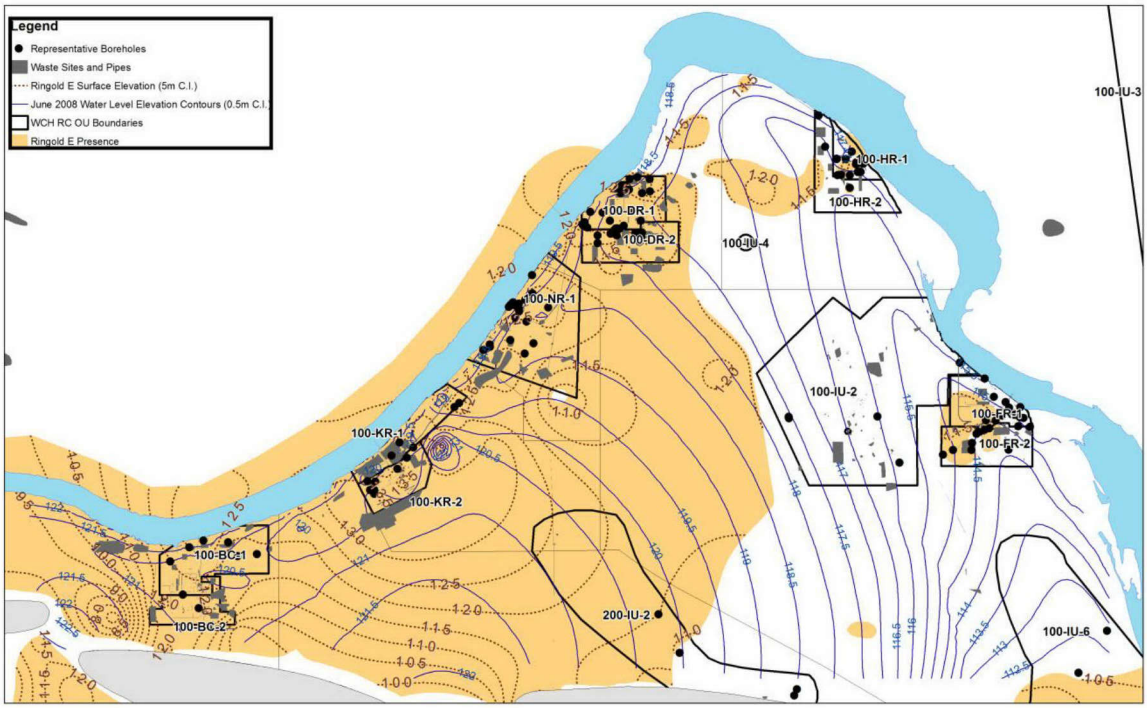

Figure 3-2. Elevation Contours for Top of Ringold E and Water Table

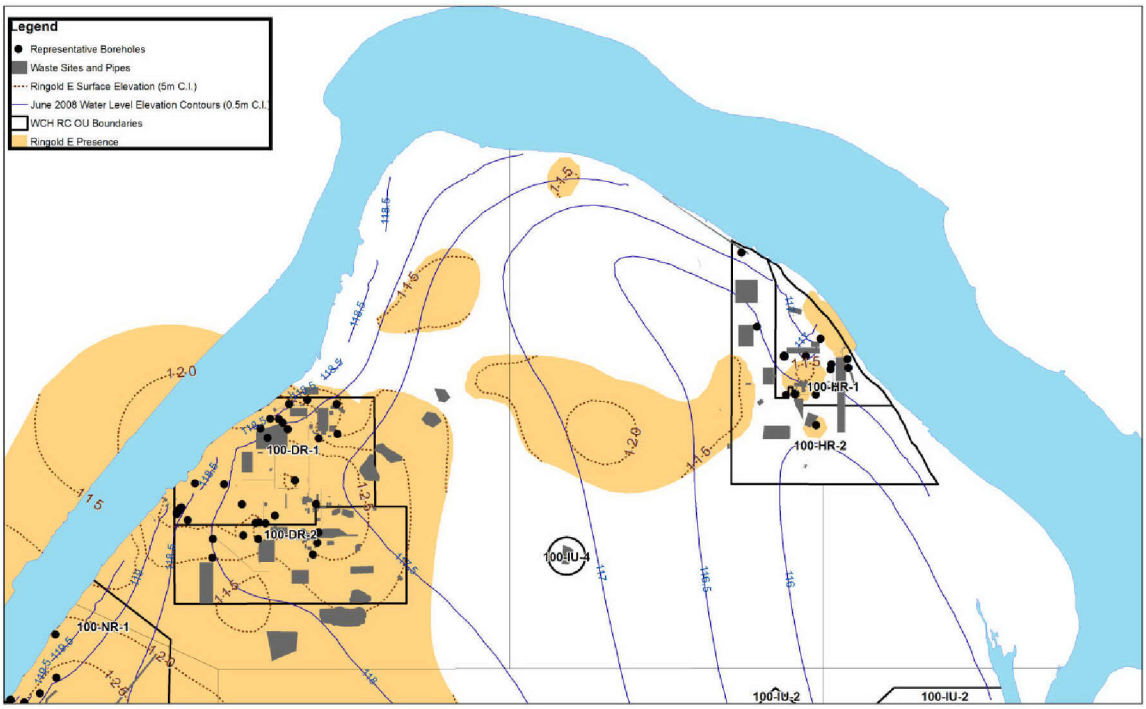

Figure 3-3. Borehole Locations for 100-D and 100-H Areas

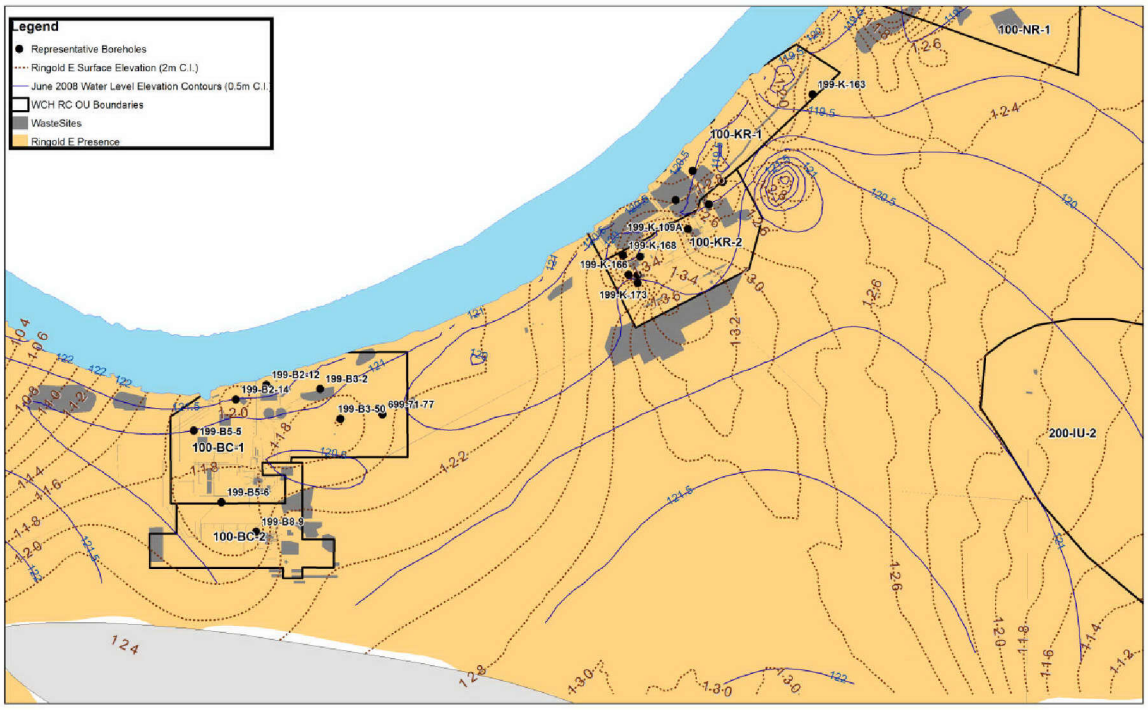

Figure 3-4. Borehole Locations for 100-B and 100-K Areas

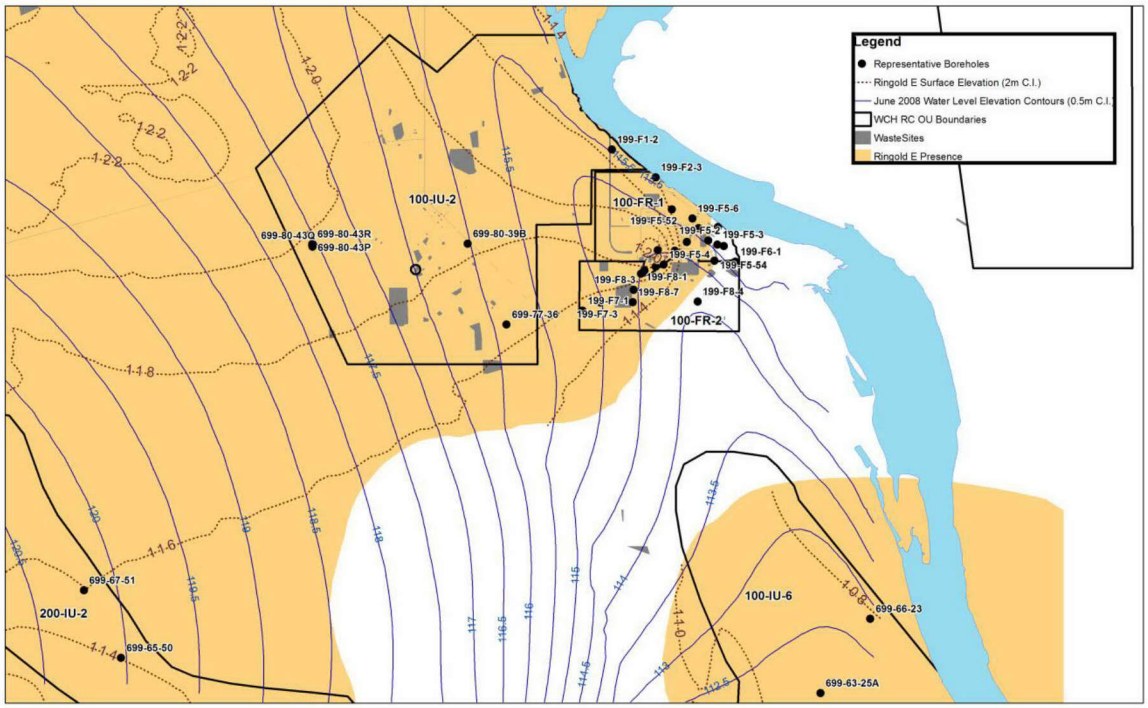

Figure 3-5. Borehole Locations for 100-F and 100-IU Areas

Representative columns were identified by collecting and reviewing geologic data from 86 boreholes nearest to the waste sites in each geographic area. All borehole data were taken from the Hanford Environmental Information System (HEIS) borehole database. The columns include the VZ and the unconfined aquifer. Using the June 2008 water table elevations to represent the annually occurring highest water table, a conservative (smaller) thickness of the VZ was computed for each borehole. The borehole data also provided estimates of the thicknesses of each lithologic unit within the VZ and within the aquifer. The boreholes in each geographic area were divided into groups based on the proportion of each lithologic unit and total VZ thickness. A representative stratigraphic column was selected for each borehole group within each geographic area, yielding two to seven stratigraphic columns for each (see Section 4.3.1 below).

The total column thickness, VZ thickness, and aquifer thickness of the representative columns vary with the borehole geology for each geographic area. Only the thickness of the clean backfill was held constant at 4.6 m (15 ft) for all representative columns based on the Interim Action Record of Decision (ROD) for the 100 Area sites (EPA/ROD/R10-99/039, *EPA Superfund Record of Decision: Hanford 200-Area (USDOE) and Hanford 100-Area (USDOE)*). Thickness of the VZ, the thickness of the SZ, and the percentages of the different lithologic units in each zone were determined using the selected borehole logs. Table 3-1 presents the number of boreholes evaluated in each geographic area along with the range in vadose zone and saturated zone thickness. For a given borehole, a conservative (thinner) estimate of VZ thickness was calculated by taking the difference between ground surface elevation and the June 2008 water table elevation, which is representative of the seasonal high water table elevation. Boreholes belonging to the 100-IU-2 and 100-IU-6 geographic areas were combined to produce shared representative columns. This was done due to lack of borehole data across both geographic areas.

Table 3-1. Vadose and Saturated-Zone Thicknesses in the 100 Area Geographic Areas

Geographic area	Number of Boreholes	Vadose Zone Thickness (m)			Saturated Zone Thickness (m)		
		Minimum	Average	Maximum	Minimum	Average	Maximum
100-D	18	16.7	23.6	26.6	1.2	5.7	8.1
100-H	17	8.4	11.8	13.4	2.3	5.2	8.2
100-K	8	15.8	21.8	25.1	14.9	25.3	28.7
100-BC	8	12.2	19.2	30	30.9	34.5	48.2
100-F	17	7.5	10.9	13.4	1.2	6.4	11.8
100-N	10	19.2	21.0	25.4	8.8	11.6	16.2
100-IU-2 & 100-IU-6	8	7.4	14.5	40.0	4.6	8.9	24.0

Representative stratigraphic columns for each geographic area were derived from groupings of the borehole data by VZ thickness and lithologic composition (Tables 3-2 to 3-7). However, it should be

noted that some of the representative columns may change based on new information regarding the extent of stratigraphic units.

The objective was to create a limited number of representative stratigraphic columns for each geographic area so that the number of STOMP simulations would be feasible given resource constraints, while capturing the range of variability within each area. This was accomplished by dividing the boreholes for each geographic area into groups based on a range of VZ-thickness intervals and then identifying one or more representative lithologic compositions (see Appendix A for more details). For example, the set of 100-D boreholes was divided into three groups according to VZ thickness: 25, 20, and 15 m, whereas the 100-H boreholes were divided into two groups with 12 and 8 m thicknesses, respectively (Tables 3-2 and 3-3). Examination of all wells within the 100-D 25-m-thickness group revealed a range of compositions for the VZ, but the 12 boreholes in this group were divided into three sub-groups based on relative fraction of lithologies:

- 100% Hanford formation
- 80% Hanford formation – 20% Ringold E unit
- 60% Hanford formation – 40% Ringold E unit (Table 3-2)

If the thickness of the SZ was greater than 5 m, then the representative thickness of the SZ was used in STOMP simulations. If the thickness of the SZ was less than 5 m, then the thickness of the SZ was assumed to be 5 m so that a 5-m-long monitoring well screen could be simulated. Tables 3-2 through 3-7 compare the actual versus representative compositions for each geographic area. The procedure for determining representative boreholes and thickness of VZ and SZ is presented in Appendix A.

Table 3-2. Determination of Vadose Zone Thickness and Geology for Geographic Area 100-D

Representative Column Index	Representative VZ Thickness (m)	Representative VZ Composition	Thickness of Hanford in VZ (m)	Thickness of Ringold E in VZ (m)	Corresponding Wells	Actual VZ Composition	Actual VZ Thickness (m)	Actual Aquifer Thickness (m)	Average Aquifer Thickness (m)	SZ Composition
1	25	100% Hanford	25	0	199-D4-83	100% Hanford	24.32	5.25	6.48	100% Hanford
					199-D5-17		25.4	6.15		
					199-D5-97		25.81	7.41		
					199-D5-99		26.09	7.29		
					199-D8-4		25.21	6.31		
2	20	100% Hanford	20	0	199-D2-5	100% Hanford	22.64	4.80	5.13	100% Hanford
					199-D8-97		23.14	5.06		
					199-D8-98		20.37	5.53		
3	25	75% Hanford 25% Ringold E	20	5	199-D4-101	76% Hanford 24% Ringold E	25.35	6.66	7.35	100% Ringold E
					199-D5-103	83% Hanford 17% Ringold E	25.69	8.05		
4	20	80% Hanford 20% Ringold E	16	4	199-D8-89	80% Hanford 20% Ringold E	19.76	4.01	4.01	100% Ringold E
5	25	60% Hanford 40% Ringold E	15	10	199-D4-25	63% Hanford 37% Ringold E	24.79	6.15	4.91	100% Ringold E
					199-D5-12	59% Hanford 41% Ringold E	25.96	1.17		
					199-D5-120	63% Hanford 37% Ringold E	25.76	7.16		
					199-D5-19	63% Hanford 37% Ringold E	24.14	4.66		
					199-D5-34	62% Hanford 38% Ringold E	26.6	5.40		
6	15	60% Hanford 40% Ringold E	9	6	199-D8-54B	63% Hanford 37% Ringold E	16.82	6.35	5.34	100% Ringold E
					199-D8-55	55% Hanford 45% Ringold E	16.7	4.33		

Note; VZ: vadose zone; SZ: saturated zone

Table 3-3. Determination of Vadose Zone Thickness and Geology for Geographic Area 100-H (VZ: vadose zone; SZ: saturated zone)

Representative Column Index	Representative VZ Thickness (m)	Representative VZ Composition	Thickness of Hanford in VZ (m)	Thickness of Ringold E in VZ (m)	Corresponding Wells	Actual VZ Composition	Actual VZ Thickness (m)	Actual Aquifer Thickness (m)	Average Aquifer Thickness (m)	SZ Composition
1	12	100% Hanford	12	0	199-H3-1	100% Hanford	12.90	4.17	5.25	100% Hanford
					199-H3-25		11.31	5.75		
					199-H3-2A		11.39	5.37		
					199-H3-2B		11.26	6.11		
					199-H3-2C		11.36	5.40		
					199-H4-1		11.62	6.14		
					199-H4-11		10.82	7.16		
					199-H4-14		11.42	6.56		
					199-H4-2		11.66	8.15		
					199-H4-46		13.07	5.53		
					199-H4-49		13.36	3.40		
					199-H4-69		12.53	5.75		
					199-H4-70		12.97	4.10		
					199-H4-72		11.90	5.17		
					199-H4-9		11.34	2.83		
					199-H6-2		12.92	2.32		
2	8	100% Hanford	8	0	699-99-41	100% Hanford	8.35	3.84	3.84	100% Hanford

Note; VZ: vadose zone; SZ: saturated zone

Table 3-4. Determination of Vadose Zone Thickness and Geology for Geographic Area 100-K (VZ: vadose zone; SZ: saturated zone)

Representative Column Index	Representative VZ Thickness (m)	Representative VZ Composition	Thickness of Hanford in VZ (m)	Thickness of Ringold E in VZ (m)	Corresponding Wells	Actual VZ Composition	Actual VZ Thickness (m)	Actual Aquifer Thickness (m)	Average Aquifer Thickness (m)	SZ Composition
1	25	100% Hanford	25	0	199-K-173	100% Hanford	25.12	28.07	28.07	8% Hanford 92% Ringold E (100% Ringold E selected in the model)
2	15	70% Hanford 30% Ringold E	10.5	4.5	199-K-32B	70% Hanford 30% Ringold E	15.77	25.68	20.305	100% Ringold E
					199-K-163	66% Hanford 34% Ringold E	18.6	14.93		
3	20	50% Hanford 50% Ringold E	10	10	199-K-109A	52% Hanford 48% Ringold E	22.71	24.54	24.51	100% Ringold E
4	20	40% Hanford 60% Ringold E	8	12	199-K-111A	38% Hanford 62% Ringold E	21.01	26.33	26.33	100% Ringold E
5	20	30% Hanford 70% Ringold E	6	14	199-K-165	35% Hanford 65% Ringold E	24.96	28.69	27.67	100% Ringold E
					199-K-166	34% Hanford 66% Ringold E	24.02	27.26		
					199-K-106A	28% Hanford 72% Ringold E	22.48	27.05		

Note; VZ: vadose zone; SZ: saturated zone

Table 3-5. Determination of Vadose Zone Thickness and Geology for Geographic area 100-F

Representative Column Index	Representative VZ Thickness (m)	Representative VZ Composition	Thickness of Hanford in VZ (m)	Thickness of Ringold E in VZ (m)	Corresponding Wells	Actual VZ Composition	Actual VZ Thickness (m)	Actual Aquifer Thickness (m)	Average Aquifer Thickness (m)	SZ Composition
1	12	100% Hanford	12	0	199-F5-46	100% Hanford	12.40	4.82	6.14	100% Hanford
					199-F5-45		11.81	3.89		
					199-F5-52		12.22	7.90		
					199-F5-2		11.38	11.79		
					199-F5-54		11.53	9.74		
					199-F5-47		13.42	5.63		
					199-F5-4		12.10	3.14		
					199-F8-4		11.31	2.86		
					199-F8-2		11.00	5.46		
2	10	100% Hanford	10	0	199-F5-5	100% Hanford	10.77	11.18	10.39	100% Hanford
					199-F5-6		10.95	10.08		
					199-F5-3		9.90	9.91		
3	8	100% Hanford	8	0	199-F5-1	100% Hanford	9.00	9.90	4.94	100% Hanford
					199-F8-3		7.45	1.70		
					199-F6-1		8.28	6.96		
					199-F8-7		8.53	1.22		
4	12	40% Hanford 60% Ringold E	4.8	7.2	199-F5-48	43% Hanford 57% Ringold E	12.76	3.09	3.09	100% Ringold E

Note; VZ: vadose zone; SZ: saturated zone; *Some representative columns may be subject to change

Table 3-6. Determination of Vadose Zone Thickness and Geology for Geographic area 100-BC

Representative Column Index	Representative VZ Thickness (m)	Representative VZ Composition	Thickness of Hanford in VZ (m)	Thickness of Ringold E in VZ (m)	Corresponding Wells	Actual VZ Composition	Actual VZ Thickness (m)	Actual Aquifer Thickness (m)	Average Aquifer Thickness (m)	SZ Composition
1	14	100% Hanford	14	0	199-B3-2	100% Hanford	14.24	32.4	32.4	100% Hanford
2	23		23	0	699-71-77		23.61	31.26	31.26	2% Hanford 98% Ringold E (100% Ringold E selected in the model)
3	14		14	0	199-B5-5		14.34	48.15	48.15	4% Hanford 96% Ringold E (100% Ringold E selected in the model)
4	30		30	0	199-B8-9		29.98	34.49	34.49	15% Hanford 85% Ringold E
5	22		22	0	199-B3-50		22.18	31.77	32.9	17% Hanford 83% Ringold E (15% Hanford 85% Ringold E selected in the model)
					199-B5-6		24.18	34.03		12% Hanford 88% Ringold E (15% Hanford 85% Ringold E selected in the model)
6	12	30% Hanford 70% Ringold E	3.6	8.4	199-B2-12	32% Hanford 68% Ringold E	12.16	33.41	33.41	100% Ringold E
7	13	80% Hanford 20% Ringold E	10.4	2.6	199-B2-14	78% Hanford 22% Ringold E	12.65	30.85	30.85	100% Ringold E

Note; VZ: vadose zone; SZ: saturated zone

Table 3-7. Determination of Vadose Zone Thickness and Geology for Geographic areas 100-IU-2 and 100-IU-6

Representative Column Index	Representative VZ Thickness (m)	Representative VZ Composition	Thickness of Hanford in VZ (m)	Thickness of Ringold E in VZ (m)	Wells	Actual VZ Composition	Actual VZ Thickness (m)	Actual Aquifer Thickness (m)	Average Aquifer Thickness (m)	SZ Composition
1	40	100% Hanford	40	0	699-67-51	100% Hanford	40.02	23.99	23.99	17% Hanford; 83% Ringold E
2	22	100% Hanford	22	0	699-65-50	100% Hanford	22.54	12.51	12.51	100% Hanford
3	10	100% Hanford	10	0	699-76-36	100% Hanford	10.19	5.05	6.49	100% Hanford
					699-80-43P		9.11	4.61		
					699-63-25A		9.10	9.80		
4	8	100% Hanford	8	0	699-80-39B	100% Hanford	7.42	5.69	5.11	100% Hanford
					699-80-43Q		8.84	4.88		
					699-80-43R		8.94	4.78		

Note; VZ: vadose zone; SZ: saturated zone

3.2 Modeling Features, Events, Processes, and Assumptions

This section provides a summary of key FEPs that are considered in the development of the VZ flow and transport models for the River Corridor. These FEPs are important in developing the conceptual models as they affect the transport of contaminants through the VZ. Section 3.2.5 lists key modeling assumptions.

3.2.1 Climate and Vegetation

The DOE's Hanford Site lies within the semiarid shrub-steppe Pasco Basin of the Columbia Plateau in south-central Washington State. The region's climate is greatly influenced by the Pacific Ocean and the Cascade Mountain Range to the west, and other mountain ranges to the north and east. The Pacific Ocean moderates temperatures throughout the Pacific Northwest, and the Cascade Range generates a rain shadow effect that limits rain and snowfall in the eastern half of Washington State. The Cascade Range also serves as a source of cold air drainage, which has a considerable effect on the wind regime on the Hanford Site. Mountain ranges to the north and east of the region shield the area from the severe winter storms and frigid air masses that move southward across Canada. The following climate information summary is extracted from information reported in PNNL-6415 Rev. 18, *Hanford Site National Environmental Policy Act (NEPA) Characterization*.

Climatological data for the Hanford Site are compiled at the Hanford Meteorology Station (HMS), which is located on the Hanford Site's Central Plateau, just outside the northeast corner of the 200 West Area and about 4 kilometers (km) (3 miles [mi]) west of the 200 East Area. Meteorological measurements have been made at the HMS since late 1944. Before the HMS was established, local meteorological observations were made at the old Hanford town site (1912 through late 1943) and in Richland (1943 to 1944). A climatological summary for Hanford is provided in a report by PNNL-15160, *Hanford Site Climatological Summary 2004 with Historical Data*. Data from the HMS capture the general climatic conditions for the region and describe the specific climate of the Hanford Site's Central Plateau. The size of the Hanford Site and its topography give rise to substantial spatial variations in wind, precipitation, temperature, and other meteorological characteristics. To characterize meteorological differences accurately across the Hanford Site, the HMS operates a network of monitoring stations. These stations, which currently number 30, are situated throughout the Hanford Site and in neighboring areas.

The prevailing surface winds on Hanford's Central Plateau are from the northwest and occur most frequently during the winter and summer. During the spring and fall, there is an increase in the frequency of winds from the southwest and a corresponding decrease in winds from the northwest. Monthly and annual joint-frequency distributions of wind direction versus wind speed for the HMS are reported in PNNL-15160. Monthly average wind speeds 15.2 m (50 ft) above the ground are lower during the winter months, averaging 2.7 to 3.1 m/s (6 to 7 miles per hour [mph]) and faster during the spring and summer, averaging 3.6 to 4.0 m/s (8 to 9 mph). The fastest wind speeds at the Hanford Site are usually associated with flow from the southwest. However, the summertime drainage winds from the northwest frequently exceed speeds of 13 m/s (30 mph). The maximum speed of the drainage winds (and their frequency of occurrence) tends to decrease at locations toward the southeast. The HMS averages 156 days per year with peak wind gusts greater than or equal to 11 m/s (25 mph) (ranging from a low of about 7 days in December to a high of nearly 20 days in June and July) and 57 days with peak gusts greater than or equal to 16 m/s (35 mph) (from a low of about 3 days in September and October to a high of about 6 days during the months of April through July).

Monthly averages and extremes of temperature, dew point, and humidity are presented in PNNL-15160. Based on data collected from 1946 through 2004, the average monthly temperatures at the HMS range from a low of -0.7°C (31°F) in January to a high of 24.7°C (76°F) in July. The highest winter monthly average temperature was 6.9°C (44°F) in February 1958 and February 1991, and the lowest average monthly temperature was -11.1°C (12°F) in January 1950. The highest monthly average temperature was 27.9°C (82°F) in July 1985, and the lowest summer monthly average temperature was 17.2°C (63°F) in June 1953. Daily maximum temperatures at the HMS vary from an average of 2°C (35°F) in late December and early January to 36°C (96°F) in late July. There are, on average, 52 days during the summer months with maximum temperatures greater than or equal to 32°C (90°F) and 12 days with maxima greater than or equal to 38°C (100°F). From mid-November through early March, the average daily minimum temperature is below freezing; the daily minimum in late December and early January is -6°C (21°F). On average, the daily minimum temperature of less than or equal to -18°C (approximately 0°F) occurs only 3 days per year; however, only about one winter in two experiences such low temperatures. The annual average relative humidity at the HMS is 55%. It is highest during the winter months, averaging about 76%, and lowest during the summer, averaging about 36%. The annual average dew point temperature at the HMS is 1°C (34°F). In the winter, the dew point temperature averages about -3°C (27°F), and in the summer it averages about 6°C (43°F).

Average annual precipitation at the HMS is 17 centimeters (cm) (6.8 inches [in.]). During 1995, the wettest year on record, 31.3 cm (12.3 in.) of precipitation was measured; during 1976, the driest year, only 7.6 cm (3 in.) was measured. The wettest season on record was the winter of 1996-1997, with 14.1 cm (5.4 in.) of precipitation; the driest season was the summer of 1973, when only 0.1 cm (0.03 in.) of precipitation was measured. Most precipitation occurs during the late autumn and winter, with more than half of the annual amount occurring from November through February. Days with greater than 1.3 cm (0.50 in.) precipitation occur on average less than one time each year. Average snowfall ranges from 0.25 cm (0.1 in.) during October to a maximum of 13.2 cm (5.2 in.) during December, and decreases to 1.3 cm (0.5 in.) during March. The record monthly snowfall of 59.4 cm (23.4 in.) occurred during January 1950. The seasonal record snowfall of 142.5 cm (56.1 in.) occurred during the winter of 1992-1993. Snowfall accounts for about 38% of all precipitation from December through February.

Vegetation communities in this region are subject to change depending on soil type, climate conditions, physical disturbance, and plant succession. Figure 3-6 illustrates the distribution of vegetation types and areas on the Hanford Site before the major fire that occurred in 2000 (Legend for Figure 3-6 is provided in Figure 3-7). The extent of the year 2000 fire is shown in Figure 3-8.

Shrublands occupy the largest area in terms of acreage and comprise seven of the nine major plant communities on the Hanford Site (PNNL-13688, *Vascular Plants of the Hanford Site*). Of the shrubland types, sagebrush-dominated communities are predominant, with other shrub communities varying with changes in soil and elevation. About 287 square kilometers (km^2) (111 square miles [mi^2]) of shrub habitat dominated by big sagebrush was destroyed in the 2000 fire and is in various stages of recovery. Of the vegetation types found on the Hanford Site, those with a shrub component (i.e., big sagebrush, threetip sagebrush [*Artemisia tripartita*], bitterbrush [*Purshia tridentata*], gray rabbitbrush [*Ericameria nauseous,* previously *Chrysothamnus nauseosus*], green rabbitbrush [*Chrysothamnus viscidiflorus*], black greasewood [*Sarcobatus vermiculatus*], winterfat [*Krascheninnikovia (Ceratoides) lanata*], snow buckwheat [*Eriogonum niveum*], and spiny hopsage [*Grayia (Atriplex) spinosa*]) are considered shrub-steppe. These stands typically have an understory dominated by bunchgrasses such as bluebunch wheatgrass (*Pseudoroegnaria spicata,* previously *Agropyron spicatum*), Sandberg's bluegrass (*Poa sandbergii [secunda]*), needle-and-thread grass (*Hesperostipa comate,* previously *Stipa comata*), Indian

ricegrass (*Achnatherum hymenoides,* previously *Oryzopsis hymenoides*), bottlebrush squirreltail (*Elymus elymoides,* previously *Sitanion hysterix*), and prairie junegrass (*Koeleria cristata*), as well as a number of broad-leaf forbs. Heavily grazed or disturbed areas often have an understory dominated by cheatgrass. Heterogeneity of species composition varies with soil, slope, and elevation. Vegetation types with a significant cheatgrass component are generally of lower habitat quality than those with bunchgrass understories.

Most grasses occur as understory in shrub-dominated plant communities. Because shrubs have been removed by fire in many areas, there are large areas of grass-dominated communities on the Hanford Site. Cheatgrass has replaced many native perennial grass species and is well established in many low-elevation (less than 244 m [800 ft]) and/or disturbed areas. Of the native grasses that occur on the Hanford Site, bluebunch wheatgrass occurs at higher elevations. Sandberg's bluegrass is widely distributed throughout the Columbia Basin and the intermountain west. Needle-and-thread grass, Indian ricegrass, and thickspike wheatgrass (*Elymus macrourus,* previously *Agropyron dasytachyum*) occur in sandy soils and dune habitats.

Within the past few hundred years, the Hanford Site upland landscape had few trees and the Columbia River shoreline supported a few scattered cottonwood (*Populus spp.*) or willows (*Salix spp.*). Homesteaders and Manhattan Project construction workers planted trees in association with agricultural areas and housing camps. Shade and ornamental trees were planted in the 1950s around former military installations and industrial areas on the Hanford Site. Currently, approximately 23 species of trees occur on the Site. The most commonly occurring species are black locust (*Robinia pseudo-acacia*), Russian olive (*Eleagnus angustifolia*), cottonwood (*Populus trichocarpa*), mulberry (*Morus alba*), sycamore (*Platanus occidentalis*), and poplar (*Populus spp.*). These trees are not commonly found in waste disposal locations.

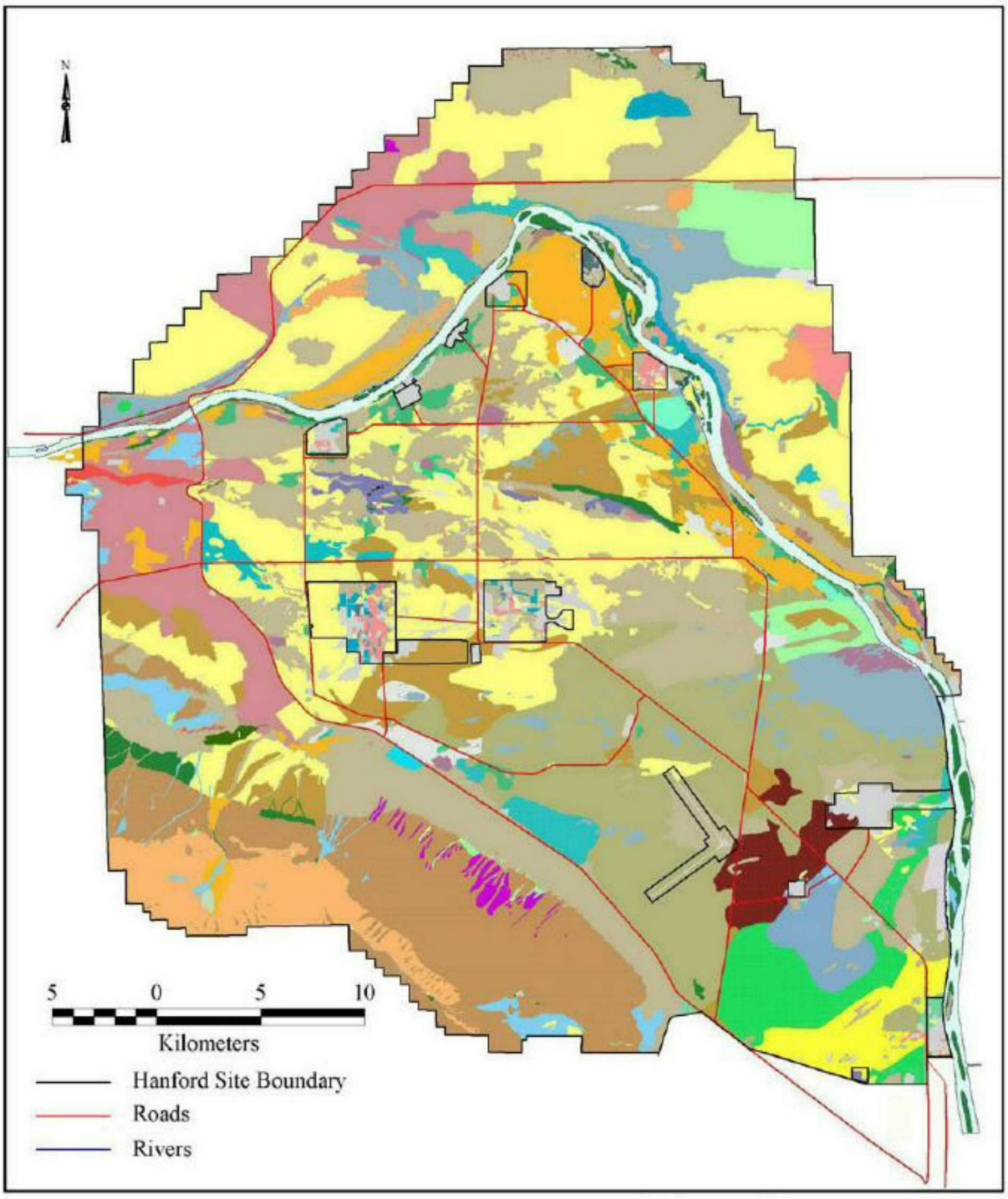

Source: PNNL-6415 Rev. 18

Figure 3-6. Distribution of Vegetation Types and Areas on the Hanford Site, Washington, before the Year 2000 Fire

Source: PNNL-6415 Rev. 18

Figure 3-7. Legend for Figure 3-6

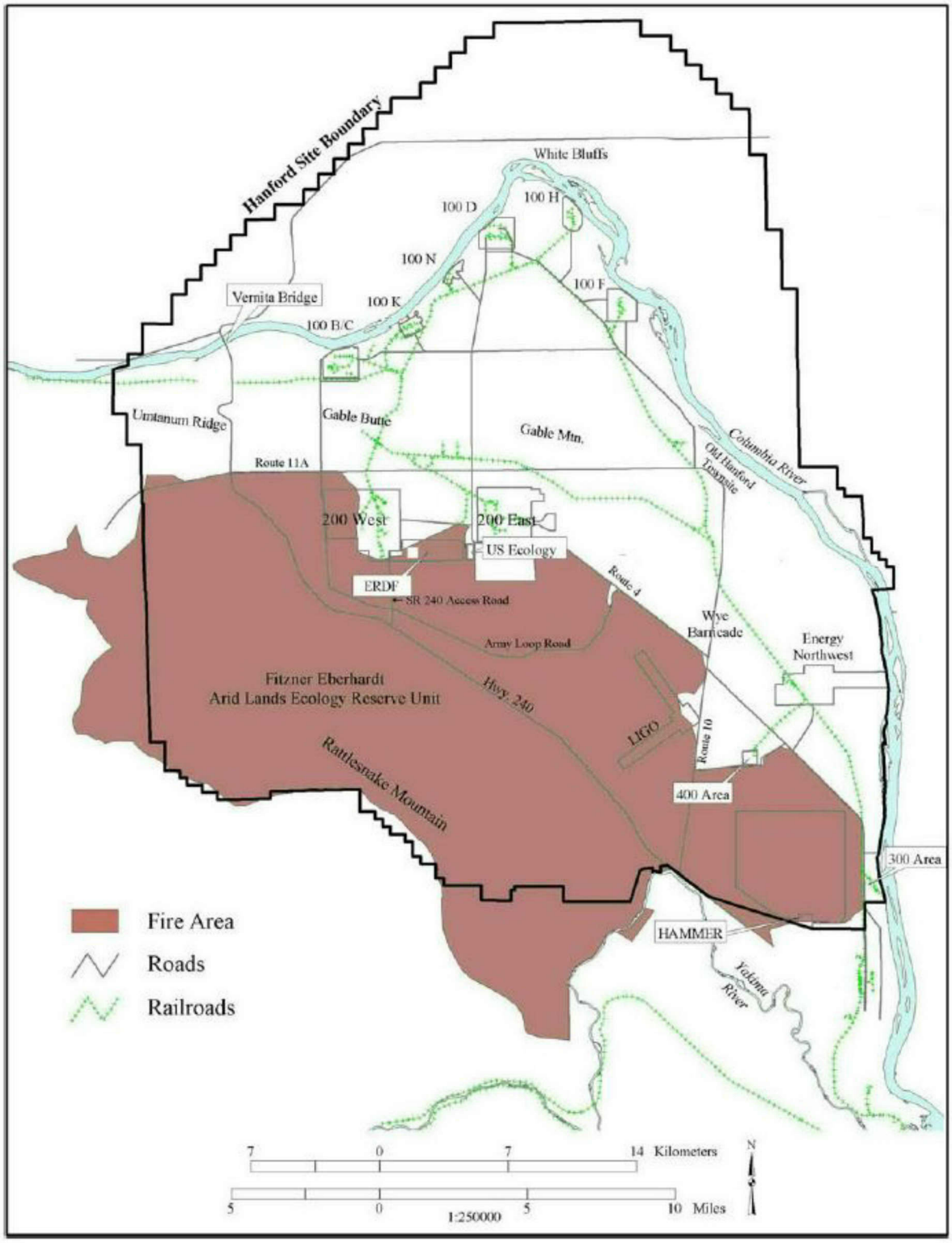

Source: PNNL-6415 Rev. 18

Figure 3-8. Extent of Hanford Site, Washington, Burned as a Result of the June 27 to July 2, 2000 Wildfire

3.2.2 Recharge and Evapotranspiration

Recharge is the flux of water transmitted across the water table from the VZ to the SZ. Direct measurement of recharge at the water table is typically impractical due to the inaccessibility, especially at Hanford where the water table is commonly located at depths below ground surface (bgs) of 80 m or more. Natural recharge is that recharge that originates as meteoric water. Other aquifer-influencing operations, such as artificial discharges (from anthropogenic discharges such as those associated with past waste management operations at the Hanford Site) or perturbations to the aquifer system from remedial action pump and treat systems, where present, would complicate efforts at making a direct measurement of natural recharge for a deep water table. Instead, measurements and analyses in the unsaturated zone at shallow depths are used to characterize deep drainage, defined here as the water flux leaving the depth below which the processes of evapotranspiration can return water from the unsaturated soil to the atmosphere (PNNL-17841, *Compendium of Data for the Hanford Site (Fiscal Years 2004 to 2008) Applicable to Estimation of Recharge Rates*). This deep drainage, with sufficient time, will be manifest as the natural recharge flux. The time required for this to happen will depend on the thickness and hydraulic properties of the VZ and the deep drainage rate itself. Changes in the deep drainage rate, such as would result from changes in surface vegetative conditions that increase or decrease the evapotranspiration rate, can take many years to be reflected in the recharge rate for a thick VZ in arid conditions such as at the Hanford Site and can be an important consideration in characterizing recharge as well (PNNL-17841).

Important physical properties and processes that influence recharge include climate, soil hydraulic properties and stratigraphy, vegetative cover, land use, and topography (PNNL-17841). Climate determines the driving forces for recharge, namely the quantity of precipitation available for the land surface water balance, and the energy fluxes that are determinant in the partitioning of precipitation into evaporation, transpiration, and recharge. Soil hydraulic properties and stratigraphy determine the rate at which water is transmitted through the VZ, and hence the effective time for processes of evaporation and transpiration to influence the net downward flux. Vegetative cover determines the strength of the transpiration portion of the land surface water balance. Land use will change the influencing factors including the vegetative cover and surface soils, and hence the hydraulic properties and soil stratigraphy of a site, and hence transpiration rates. Topography is the primary determinant for the portion of precipitation that is subject to overland flow, either "run-on" or "run-off," for a given site. Knowledge of all of the influences is important to the estimation of recharge at a given location.

There has been considerable study devoted to estimation of recharge rates at the Hanford Site to support flow and transport modeling needs. PNL-10285, *Estimated Recharge Rates at the Hanford Site*, produced a defensible map of estimated recharge rates across the Hanford Site for current climate and 1991 vegetation/and use patterns. Various recharge data packages have been prepared to support performance assessments (e.g., PNNL-13033, *Recharge Data Package for the Immobilized Low-Activity Waste 2001 Performance Assessment*, PNNL-14744, *Recharge Data Package for the 2005 Integrated Disposal Facility Performance Assessment*; PNNL-16688, *Recharge Data Package for Hanford Single-Shell Tank Waste Management Areas*) and site-wide assessments (e.g., PNNL-14702 Rev. 1). These studies, in turn, have been supported by a significant field research program (e.g., PNL-6403, *Recharge at the Hanford Site: Status Report*; PNL-6810, *The Field Lysimeter Test Facility (FLTF) at the Hanford Site: Installation and Initial Tests*; PNL-7209, *Field Lysimeter Test Facility: Second Year (FY 1989) Test Results*; Gee et al. [2005], "Measurement and Prediction of Deep Drainage from Bare Sediments at a Semiarid Site"; Gee et al. [2007], "Hanford Site Vadose Zone Studies: An Overview"; PNNL-17841).

For numerical simulation, two general approaches are available with regard to addressing recharge. In the first, the surface energy and fluid balance can be explicitly simulated as part of the larger VZ model numerical implementation. In this approach, meteorological data (precipitation, wind speed, humidity, solar radiation, air temperature), surface soil parameters, and vegetation parameters (root density and depth with time, leaf area index with time, growth cycle dates, etc.) would be used to directly simulate the surface water balance and thereby estimate net deep recharge. Under this approach, the processes simulated for the upper boundary would dominate time step control of the simulation, particularly as this approach would require high-temporal-resolution meteorological data (e.g., hourly) to support a reasonably accurate simulation of the processes in question. A second approach is to segregate the simulation of the surface balance processes to arrive at a net recharge rate used for deeper VZ simulations. In this approach the full process-based simulation described for the surface soil is still performed, but only for the near surface. This has been done, and the effective net recharge rates are available in references such as PNNL-14702 Rev. 1 for application to deeper VZ simulations. The second approach is clearly more efficient and is preferred. It is noted that the recharge rates from the second approach are strongly a function of vegetation cover and surface soil type, and that due to land surface condition changes in time, these rates will change over time. A typical progression might be from a pre-operational natural vegetation cover (low recharge due to vegetation efficiently returning a high proportion of meteoric water to the atmosphere through transpiration) to an operational cover (such as gravel maintained vegetation-free with high recharge) to a transitional period following remediation with declining recharge rates, and finally a return to a mature native plant community with low recharge once again. Thus, the historic and projected land cover condition is the determining factor for selecting recharge rates to apply with time.

3.2.3 Columbia River – Aquifer Interactions

The groundwater flow in the aquifer and exchange with the Columbia River impacts contaminant transport within the geographic areas in the River Corridor. Flow paths in the groundwater/river zone of interaction vary with daily and seasonal fluctuations in river stage. River water infiltrates the banks during high river stages, moves inland, then reverses flow as the river stage subsides, and moves back through the hyporheic zone and discharges to the riverbed. Monitoring and modeling studies suggest that this back-and-forth motion of groundwater and river is very cyclical in response to the diurnal river stage cycle, which typically includes two high stages and two low stages in response to power peaking demands on the Priest Rapids hydroelectric dam located upstream of the Hanford Site. Review of past modeling studies in addition to new studies conducted for the Remedial Process Optimization (RPO) and 100-Area RI/FS suggests that there is a significant back-and-forth or sloshing action due to flow reversals within the aquifer resulting from river stage changes. For example, an individual Cr(VI) atom may experiences a discontinuous path on its way to the river. It will experience numerous reversals in flow direction before it eventually reaches the water column in the river.

The flow reversal is very significant process with respect to the fate and transport of Cr(VI) (the most prevalent contaminant in the 100 Area) because it allows for the partial replenishment or resetting of the geochemical factors that promote reduction, adsorption, and precipitation of Cr(VI) that are close to being maxed out (nutrient limited, adsorption site limited) towards the distal end of the groundwater flow path. Modeling studies (e.g., PNNL-13674, *Zone of Interaction Between Hanford Site Groundwater and Adjacent Columbia River*) indicate that the movement of groundwater in response to river stage is predominantly piston-type flow. This action likely replenishes the geochemical environment and allows for continued reduction, adsorption, and precipitation in the hyporheic zone and adjacent groundwater.

Work by the Pacific Northwest National Laboratory (PNNL) at the Integrated Field Research Challenge site at the Hanford 300 Area illustrates the water action in terms of river stage versus contaminant concentration in the hyporheic zone. In this case, the contaminant of concern is uranium. The figure below (Figure 3-9) shows uranium concentration in hyporheic zone in black versus the river stage (gray line). There is a pronounced inverse relationship in which, as the river elevation rises, there is a corresponding drop in the uranium concentration which may be due to reversal of flow direction and/or dilution. Similar observations have been made for years in the 100-Area of Cr(VI) concentrations in response to the spring runoff.

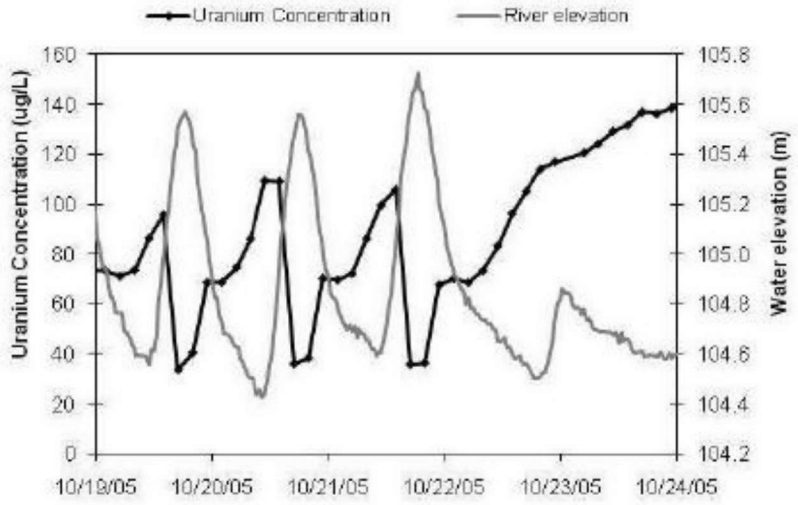

Figure 3-9. Relationship of Uranium Concentration to River Stage in the 300 Area Hyporheic Zone

Studies of Cr(VI) reduction in river water (Świetlik, 2002, "Kinetic Study of Redox Processes of Chromium in Natural River Water") indicate Cr(VI) reduction rates with a half life ($t_{½}$) on the order of 2–19 hours, indicating that Cr(VI) will be fully reduced in a river within a day to a week's time. As a result of the river-stage changes, river water of differing chemistry is brought into contact with the near-field groundwater system adjacent to the river. This "rinsing" action allows the geochemical properties of the aquifer matrix to be refreshed, and allows for continued geochemical reduction, adsorption, and precipitation of contaminated groundwater upon contact with the sediment when the river stage drops and groundwater flows towards the river.

An important addition to our understanding of the fate and transport of Cr(VI) is that in addition to chemical reduction of Cr(VI) to Cr(III) the reduction also may occur biologically, mediated by bacteria. Chandler et al. (1997), "Phylogenetic Diversity of Archaea and Bacteria in a Deep Subsurface Paleosol," described the wide variety of microbes present in the Hanford subsurface. Their studies focused on the VZ. A number of studies have been conducted on deeper Hanford bacteria in the groundwater. Recent studies of 100-H Area groundwater microbial ecology (Han et al., 2010, *Physiological and Transcriptional Studies of Cr(VI) Reduction Under Aerobic and Denitrifying Conditions by an Aquifer-Derived Pseudomonad*) suggest that bacteria can use multiple electron donors to reduce Cr(VI), depending on whether conditions are aerobic or anaerobic. PNNL-18784, *Hanford 100-D Area Biostimulation Treatability Test Results*, described results from biostimulation treatability tests at 100-D.

They observed that following the injection of a carbon substrate, "…microbial activity and ability to reduce the targeted species were observed throughout the monitored zone." These general mechanisms are described in the *Chromium(VI) Handbook* (CRC Press, 2005).

A field study conducted by Washington Closure Hanford (WCH-380 Rev. 0, *Field Summary Report for Remedial Investigation of Hanford Site Releases to the Columbia River, Hanford Site, Washington*) in 2010 involved the collection of pore water samples under extremely low-stage river-stage conditions. The study included preliminary mapping and measurement of site contaminants in sediment, pore water, and surface water in areas where groundwater upwelling occurred. Trident probe and associated river-stage-specific sampling was used to collect samples of pore water at 20 to 31 cm (8 to 12 in.) below the riverbed surface. Sediment coring and grab sampling techniques were then used concurrently with the Trident probe to assess the likelihood of potential ecological risk where contaminated groundwater was found entering the river. In total, 972 sample locations were measured. Groundwater upwelling locations were mapped using conductivity and temperature at 685 sample locations. Study results showed groundwater upwelling was not uniformly distributed, and varied by water depth, season, and proximity to the shoreline. Evaluation of laboratory quality assurance/quality control (QA/QC) results indicates that a number of initially high values were unsubstantiated due to laboratory analysis issues coupled with poor comparison to low total Cr values. Pore-water samples collected from the hyporheic zone in the river-bed sediments indicate that total Cr is occasionally present in the river substrate at selected locations and is detected above aqueous WQS both near shore and offshore. However, the Trident probe measurement methodology collects a sample within tens of minutes and does not meet the 4-day criteria to estimate the Criterion Continuous Concentration (CCC). [The CCC is an estimate of the highest concentration of a material in surface water to which an aquatic community can be exposed indefinitely without resulting in an unacceptable effect.]

Review of the geochemistry of the aquifer matrix and groundwater at the 100-HR-3 and 100-KR-4 OUs indicates the presence of conditions that favor moderate amounts of reduction, adsorption, and precipitation of Cr(VI). PNNL-14202, *Mineralogical and Bulk-Rock Geochemical Signatures of Ringold and Hanford Formation Sediments*, conducted mineralogical studies of the Ringold formation and the Hanford formation. The results of these studies suggest that both formations contain sufficient iron, mica, and other critical components to be able to foster Cr(VI) reduction as well as adsorption of the anionic Cr(VI) species to positively charged surfaces such as along the edges of mica sheets and related clay weathering products. While these mechanisms act continuously in the aquifer, they are not likely to have a statistically significant measurable impact on highly contaminated Cr(VI) plumes; however, as active remediation such as pump-and-treat systems operate and Cr(VI) concentrations in the aquifer decline, these mechanisms become significant at lower concentrations.

Very high concentrations of Cr(VI) at the main hotspot in the 100-D South plume and relatively high concentrations in the adjacent 100-D North plume continue to be problematic. The DR-5 pump-and-treat system has removed relatively large amounts of Cr(VI) from just four extraction wells in this area; however, impact on the overall footprint of the plumes from DR-5 operation is minimal. The In Situ Redox Manipulation (ISRM) Barrier, which enhances the natural reductive capacity of the aquifer through the addition of sodium dithionite, was installed downgradient of the south plume in Year 2000. However, the barrier has exhibited uneven performance, although it appears to work well at the upstream end where the aquifer is thicker and the concentrations in the aquifer are lower along the east margin of the plume. Immediately downgradient of the hotspot, there is breakthrough of the plume. Most likely, the barrier is reducing Cr(VI) at a fairly steady rate across the length of the barrier, or at least per unit

thickness of aquifer. At the location where the aquifer is thinner and the concentrations are higher, the reduction capacity is likely being exceeded, resulting in the observed break through.

An important outcome of the Expert Panel study (SGW-39305, 2008) was the recommendation to assess the 1:1 factor within the context of the U.S. Environmental Protection Agency (EPA) guidance on attenuation[1]. As the EPA guidance notes, the primary mechanism for attenuation of Cr(VI) is the natural reduction in the environment in the presence of iron and enhanced by bacteria. Additional attenuation can occur via chemical precipitation and adsorption to mineral grains. Biostimulation of bacterial growth via addition of carbon substrates is a common method of accelerating this reduction. However, the ambient bacterial population will still generate Cr(VI) reduction at some rate.

The Expert Panel on groundwater-surface water interaction correctly noted that much of the flow within the aquifer adjacent to the hyporheic zone is likely to be laminar flow. While some mixing can and will occur under these conditions, it is likely to be relatively minimal owing to local variations in hydraulic conductivity. The main mechanism will be the transgression and regression of river water through the hyporheic zone and into the adjacent aquifer. This movement must obey the usual rules of flow within a potential field such as that found in groundwater; consequently, the resulting movement will be much like piston flow with river water invading and receding from the formation. The significance of this action is that the geochemical reduction capacity of the aquifer matrix is refreshed with each successive wave of fresh water that pulses through the aquifer. Some adsorption likely occurs, although it is probably limited given the $Cr_2O_4^{-2}$ forms the majority of the Cr. Adsorption sites in the more concentrated portions of the plumes are likely saturated until remediation has advanced to a point where enough Cr(VI) has been removed from the system to free up binding sites. This may allow Cr precipitates such as $Cr(OH)_3$ to be removed as particles.

The EPA guidance recommends evaluating concentrations along a flow path and estimating the attenuation that is occurring. A good example is looking at the margins of the diffuse plume in the Horn area between 100-D and 100-H. Figure 3-10 shows the evolution of Cr(VI) and specific conductance along an approximate streamline through wells 699-97-45 and 699-99-44 and aquifer tube C6288. In the wells in the aquifer, specific conductance is constant at about 420 microsiemens per centimeter (µS/cm) while Cr(VI) drops from 55 to 45 micrograms per liter (µg/L). Further downgradient at the aquifer tube, specific conductance has dropped to about 220 µS/cm and Cr(VI) to 12 µg/L. Typical specific conductance in the river is 100–125 µS/cm; a river effect is apparent. The specific conductivity has dropped in half. If the same mechanism was operating on the Cr(VI), the expected value might be closer to 22 than 12 µg/L, suggesting that other mechanisms are impacting Cr(VI) concentrations.

The main factors of Cr(VI) attenuation are chemical and biological factors of reduction, precipitation, and adsorption. Reduction occurs within the aquifer and appears to be enhanced where river water refreshes the geochemical sites on the aquifer matrix in and adjacent to the hyporheic zone. Pore-water samples collected from the hyporheic zone in river-bed sediments indicate that Cr(VI) is occasionally present in the river substrate at selected locations at concentrations that exceed the ambient water quality criterion.

[1] The interim groundwater cleanup target for Cr(VI) in the pump and treat system (22 µg/L) have been set with the expectation that the groundwater discharging to the river will be subject to at least a 1:1 dilution, which will result in concentrations below the ambient freshwater aquatic life chronic toxicity target value of 11 µg/L.

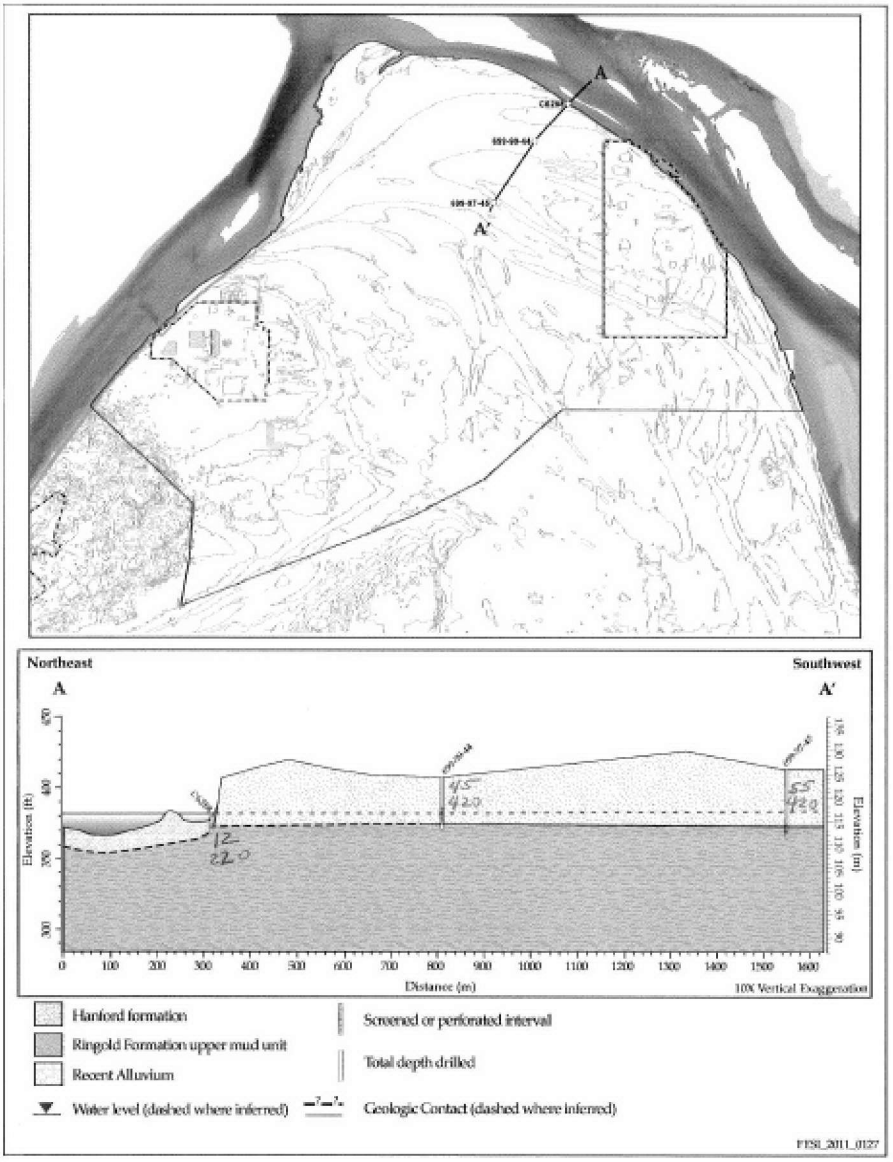

Figure 3-10. Cross Section Along a Streamline in the Horn Area Showing Cr(VI) Concentration (upper number) and Specific Conductance (lower number) as Groundwater Discharges to the Columbia River

3.2.4 Historical Discharges and Unintended Releases

Irradiated uranium fuel production at the 100 Area sites containing the original eight reactors generated large volumes of effluent waste water over a span of 22 years. Reactor processes were similar at all eight reactors leading to similar waste products at all sites. The primary generating process for these wastes was the production, use and disposal of reactor cooling water. Maximum quantities of cooling water were used because cooling water passed through each system once and was then discharged, hence the description of these reactors as single pass reactors.

To generate cooling water, several processes were needed. First, river water was collected and treated to remove impurities. Then other chemicals were added to enhance cooling water performance. After passage through the reactor, cooling water was discharged directly into the Columbia River or diverted to a series of retention basins and trenches to allow for short-term radioactive decay and cooling before discharge into the Columbia River. Fluid losses from the various facilities used to generate and transfer coolant after use were common occurrences. The fraction of total coolant and other waste volumes that discharged directly into the Columbia River versus into the subsurface through leaking facilities is not well known. However, leaking fluid volumes from retention basins, storage tanks, trenches, cribs and pipelines were sufficient to create and sustain groundwater mounds underneath them throughout operations. The fluids contained additive chemicals and radionuclides from ruptured fuel elements. These constituents have been and continue to be the primary sources of groundwater contamination. The most widespread subsurface contaminant is Cr, which was added to minimize corrosion of aluminum cooling pipes in the reactor cores. Cumulative estimates of coolant volumes and Cr inventory at each of the reactors are shown in Table 3-8.

In addition to reactor coolant, decontamination fluids and gas purification condensates were discharged. The decontamination fluids were generated by cleanup of reactor parts and typically contaminated with nitric and chromic acid and radionuclides. Finally, raw water basins leaked extensively into the subsurface and influenced the local groundwater flow patterns significantly.

In the following sections, the large discharge storage and disposal facilities are described. Where available for historical record, waste fluid types, fluid volumes, and estimates of Cr and total radionuclide inventories are summarized.

Table 3-8. Cumulative Reactor Coolant Volumes and Cr Quantities Used in Single Pass Reactor Operations

Reactor	Operations Period	Coolant Volume (L)	Cr(VI) Inventory (kg)
B and C	1944-1969	5.3E+12	2.8E+6
KE and KW	1955-1971	1.2E+13	6.3E+6
D and DR	1944-1967	4.5E+12	2.6E+6
H	1949-1965	2.1E+12	1.4E+6
F	1945-1965	2.3E+12	1.6E+6

100-BC Area Liquid Discharges

The information summarized here is taken from DOE/RL-2008-46-ADD3 Rev 0, Integrated 100 Area Remedial Investigation/Feasibility Study Work Plan Addendum 3: 100-BC-1, 100-BC-2, and 100-BC-5 Operable Units. The major structures used to create, use, and dispose of reactor coolant at the 100 B/C Area are shown in Figure 3-11. River water was pumped and stored in the 182-B reservoir prior to transfer to 183-B and 183-C. At 183-B and 183-C, Columbia River water was purified and transferred to 190-B and 190-C, respectively, where sodium dichromate was added. Concentrated sodium dichromate starting materials, first as solids (until the mid 1950s at 105-C and around 1960 at 105-B) and then solutions, were stored at 190-B and 190-C and added to the purified Columbia River water to make reactor coolant. Some loss of the highly concentrated sodium dichromate solution occurred around the storage tank at 183-C.

The reactor coolant was then routed through the reactors (105-B and 105-C) and piped to either the 116-B-11 or 116-C-5 retention basins. From these facilities, most of the coolant was then discharged to the river through three outfalls. Because of intermittent overflow of the retention basins or decisions to sequester specific coolant volumes contaminated by exposure to ruptured fuel elements, reactor coolant was also routed to the 116-B-1 and 116-C-1 trenches. An additional discharge event occurred during early operations (1946) in which highly contaminated fuel storage basin water was discharged to the 116-B-2 trench. Leaks were ubiquitous in pipelines and the retention basin. However, the fraction of discharged volume that entered the Columbia River versus leakage into the VZ through infrastructure leaks is not known.

Decontamination solutions were typically discharged into cribs such as 116-B-4 (shown in Figure 3-11) 116-B-3, 116-B-6A and 116-B-6B. Reported cumulative discharge volumes at these sites are less than a million L except for 116-B-4 (10 million L). A unique set of waste streams were sent to the 116-B-5 trench, including waste water from tritium production in the early 1950s and then laboratory waste associated with ruptured fuels examination.

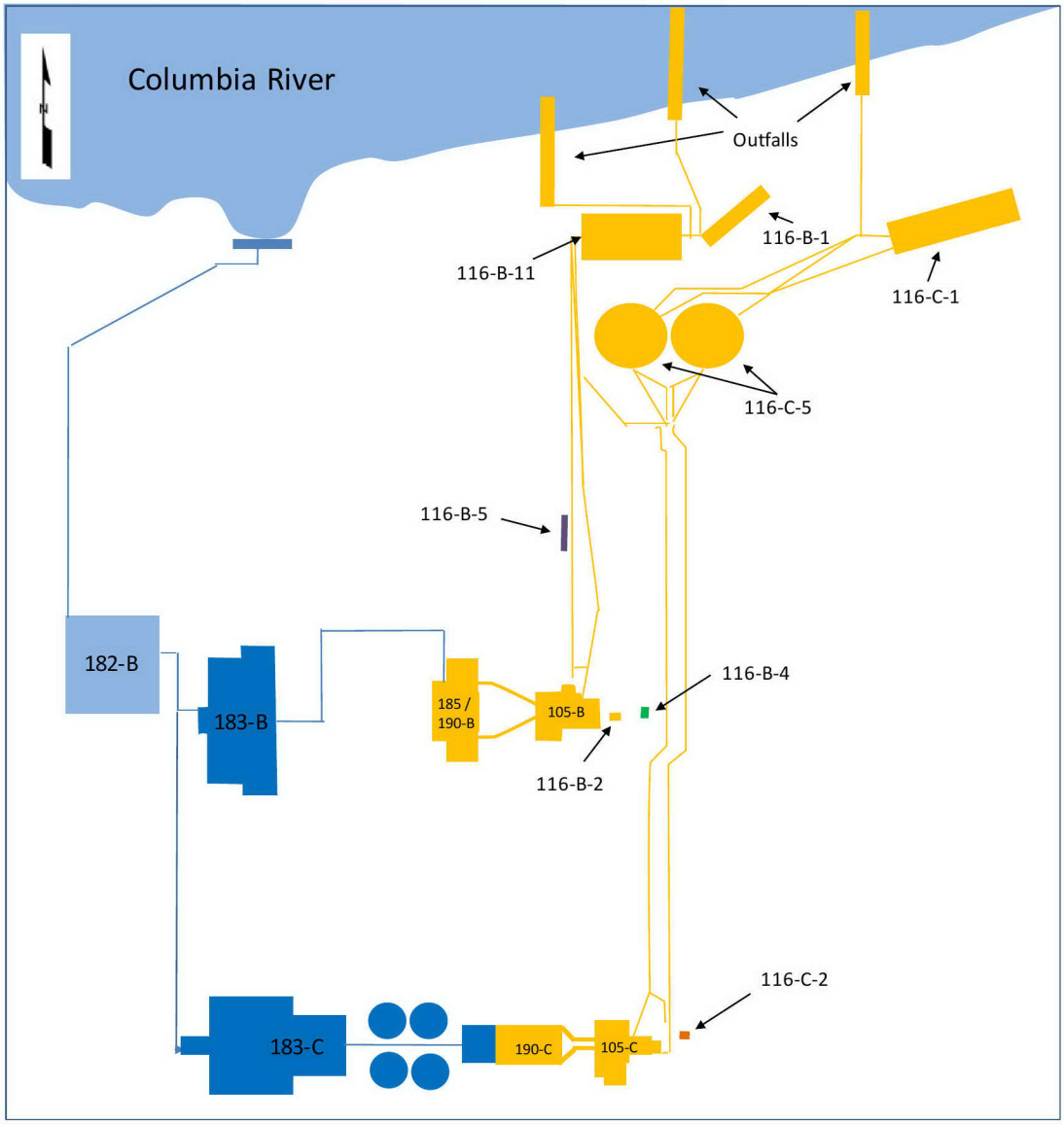

Figure 3-11. Map of Major 100 B/C Area Liquid Storage and Discharge Locations

Characteristics of the discharged liquids are summarized in Table 3-9**.** Small volume Cr discharges have also been reported, including an accidental discharge of concentrated sodium dichromate solution (53,980 L) into the sewer at 183-C in 1966 (4,000 kg in 4,000 L), and small quantities of chromic acid to the 116-B-6A/6B crib (a total of 38 kg of Cr [PNL-6456, *Hazard Ranking System Evaluation of CERCLA Inactive Waste Sites at Hanford*]). A mixture of radionuclides has been measured frequently in characterized soils including cesium-137, strontium-90, cobalt-60, europium isotopes, and uranium isotopes.

Table 3-9. Liquid Discharge Characteristics at the Major 100 B/C Area Sites

Facility	Waste Characteristics	Contaminant Inventory
116-B-1 Trench	Operation Period: 1946-1955 Waste Type: Reactor Coolant Discharge Volume: 6E+7 L	Chromium: 23 kg Radionuclides: 3.1 Ci
116-B-2 Trench (Fuel Storage Basin Trench)	Operation Period: 1946 Waste Type: Fuel Storage Basin Coolant Discharge Volume: 4E+6 L	Chromium: No estimate Radionuclides: 15 Ci
116-B-4 Trench	Operation Period: 1957-1968 Waste Type: Decontamination Fluids Discharge Volume: 3E+5 L	Chromium: 380 kg Radionuclides: 2 Ci
116-B-5 Crib	Operation Period: 1950-1968 Waste Type: Tritium Production Waste, Laboratory Waste Discharge Volume: 1E+7 L	Chromium: None Radionuclides: 190 Ci of tritium as of 1988
116-B-11 Retention Basin	Operation Period: 1944-1968 Waste Type: Reactor Coolant Discharge Volume: No estimate	Chromium: No estimate Radionuclides: No estimate
116-C-1 Trench	Operation Period: 1952-1968 Waste Type: Reactor Coolant Discharge Volume: 1E+8 to 7E+8 L plus 1968 Infiltration Test Water Volume of 1E+10 L	Chromium: 38 kg Radionuclides: 150 Ci
116-C-2 Crib	Operation Period: 1952-1968 Waste Type: Reactor Coolant, Decontamination Fluids Discharge Volume: 7.5E+6 L	Chromium: 376 kg Radionuclides: < 1 Ci
116-C-5 Retention Basins	Operation Period: 1952-1969 Waste Type: Reactor Coolant Discharge Volume: No estimate	Chromium: No estimate Radionuclides: No estimate

100-K Area Liquid Discharges

The information summarized here is taken from DOE/RL-2008-46-ADD2 Rev 0, Integrated 100 Area Remedial Investigation/Feasibility Study Work Plan Addendum 2: 100-KR-1, 100-KR-2, and 100-KR-4 Operable Units. The major structures used to create, use, and dispose of reactor coolant at the 100 K Area are shown in Figure 3-12. Two reactors (105-KW and 105-KE) were constructed and operated with separated systems for creating reactor coolant. Columbia River water was pumped at two pump houses, one for each reactor, and transferred to 183-KW and 183-KE. At 183-KW and 183-KE, This water was purified and transferred to 190-KW and 190-KW, respectively, where sodium dichromate was added.

Concentrated sodium dichromate liquid starting materials were stored in tanks (120-KW-5 and 120-KE-6) next to the 183-KW and 183-KE sedimentation basins. Some losses of the highly concentrated sodium dichromate solution occurred around the storage tanks (120-KW-5 and 120-KE-6) during transfer from railroad cars and are presumed to be the primary sources of the maximum groundwater concentration zones underlying the reactors. The high concentration solutions were then piped underneath these basins to a mixing tank at 190-KW and 190-KE. Two dilution steps were completed to make up reactor coolant concentrations.

The reactor coolant was then routed through the reactors (105-KW and 105-KE) and piped to the 116-KW-3 or 116-KE-4 retention basins, respectively. From these facilities, coolant was then discharged to either the 116-K-1/116-K-2 system or the river through the 1908 outfall. Leaks were ubiquitous in pipelines and retention basins. Estimates at 116-KE-4 were on the order of 57,000 to 114,000 L/min. The 116-K-2 trench also overflowed frequently. Other much smaller liquid waste discharges to cribs were condensate from reactor gas purification systems (116-KE-1 and 116-KW-1) and cleanup column waste from the 1706-KER facility that was used to test the performance of various reactor components.

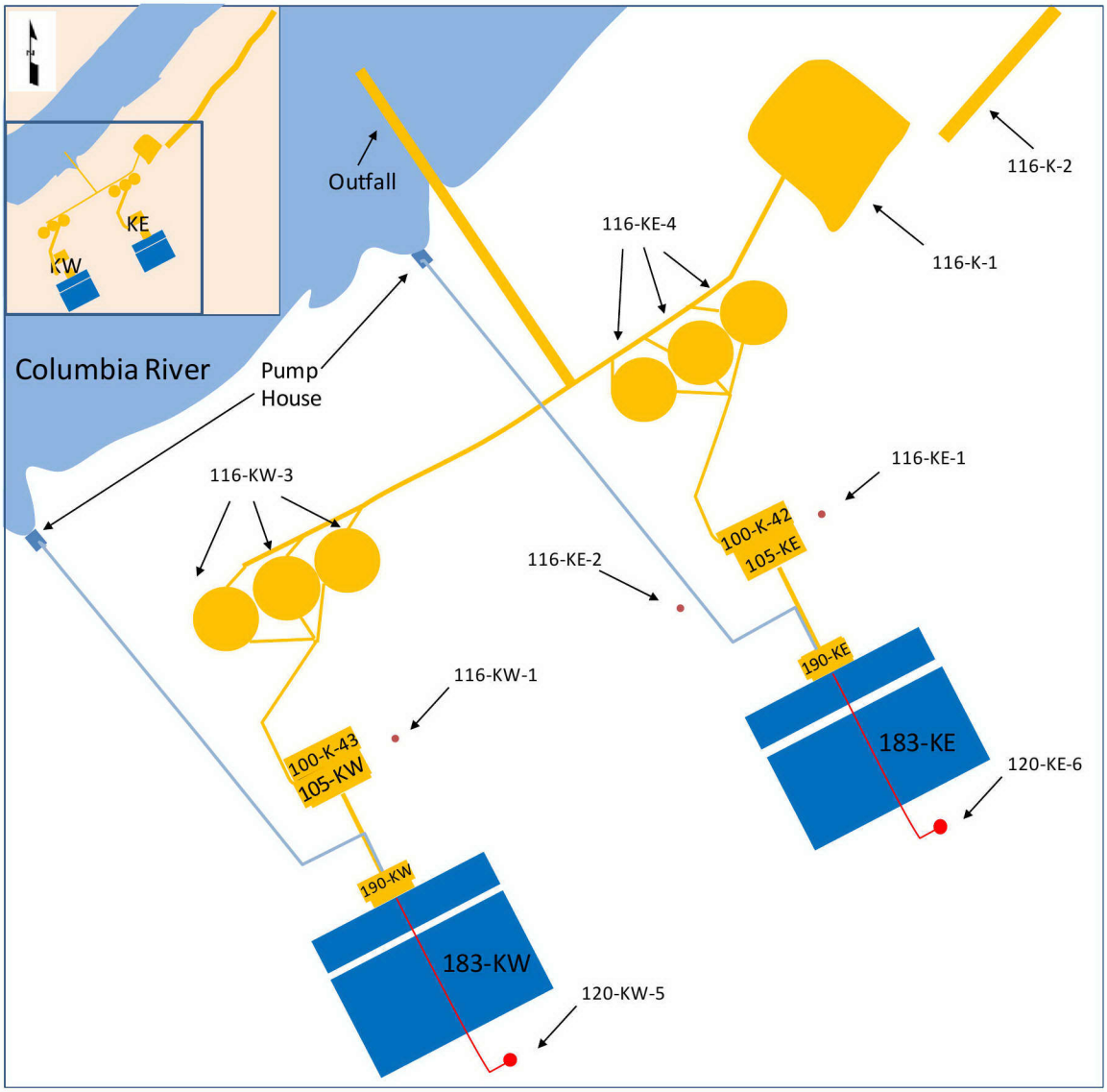

Figure 3-12. Map of Major 100 K Area Liquid Storage and Discharge Locations

Characteristics of the discharged liquids are summarized in Table 3-10. The great majority of fluids discharged to the Columbia River or the retention basin/trench system were reactor coolants. Because of extensive leakage of these systems and variable Cr content over time, the fraction of Cr that discharged directly into the Columbia River versus the subsurface is uncertain. The estimate for the 116-K-2 facility (300,000 kg) is an approximation for the VZ discharge, and constitutes about 5% of the total amount used during operations of 105-KW and 105-KE. The estimated radionuclide releases from reactor coolant, fuel storage basin coolant, and decontamination fluids are also dominated by the 116-K-2 trench estimate of about 2,100 Ci. Primary radionuclides in this estimate include europium isotopes, nickel-63, and cesium-137. The gas purification system condensate contained mostly carbon-14 and tritium, and the cleanup column waste contained a mixture of fission products including cobalt-60, strontium-90, and europium isotopes.

Table 3-10. Liquid Discharge Characteristics at the Major 100 K Area Sites

Facility	Waste Characteristics	Contaminant Inventory
116-K-1 Crib	Operation Period: 1955-1971 Waste Type: Reactor Coolant Discharge Volume: 4E+7 L	Chromium: 15 kg Radionuclides: 46 Ci
116-K-2 Trench	Operation Period: 1955-1971 Waste Type: Reactor Coolant, Fuel Storage Basin Coolant Discharge Volume: 3E+11 L	Chromium: 114,000 kg Radionuclides: 2,100 Ci
116-KE-1 Crib	Operation Period: 1955-1971 Waste Type: Gas Purification System Condensate Discharge Volume: 8E+5 L	Chromium: 0 kg Radionuclides: < 240 Ci (C-14, H-3)
116-KW-1 Crib	Operation Period: 1955-1971 Waste Type: Gas Purification System Condensate Discharge Volume: 8E+5 L	Chromium: 0 kg Radionuclides: < 240 Ci (C-14, H-3)
116-KE-2 Crib	Operation Period: 1955-1971 Waste Type: Cleanup Column Waste from Reactor Component Tests Discharge Volume: 3E+6 L	Chromium: 0 kg Radionuclides: 38 Ci
116-KW-3 and 116-KE-4 Retention Basins	Operation Period: 1955-1971 Waste Type: Reactor Coolant Discharge Volume: No estimate (extensive leakage)	Chromium: No estimate Radionuclides: No estimate
120-KE-6 and 120-KW-5 Sodium Dichromate Storage Tanks	Operation Period: 1955-1971 Waste Type: Reactor Coolant, Decontamination Fluids Discharge Volume: No estimate	Chromium: No estimate Radionuclides: 0 Ci

100-D Area Liquid Discharges

The information summarized here is taken from DOE/RL-2008-46-ADD1 Rev. 0, Integrated 100 Area Remedial Investigation/Feasibility Study Work Plan Addendum 1: 100-DR-1, 100-DR-2, 100-HR-1, 100-HR-2, and 100-HR-3 Operable Units. The major structures used to create, use, and dispose of reactor coolant at the 100 D Area are shown in Figure 3-13. Coolant production went through a number of modifications over time. In all cases, the process began with pumping Columbia River water and storing it in the 182-D reservoir prior to transfer to 108-D until about 1950, and thereafter to 183-D and 183-DR. At these facilities, the river water was treated to reduce total dissolved solids in preparation for the addition of Cr and other chemicals to make reactor coolant.

The initial sodium dichromate preparation process was done at 108-D between 1944 and 1950. Crystalline sodium dichromate was dissolved in water to make up the so-called 10% to 15% solution containing about 43 to 64 g/L of Cr, and then piped either to 105-D directly or to 185-D and 190-D where mixing with the treated Columbia River water caused additional dilution of Cr to about 700 µg/L. This diluted solution was then pumped through reactor 105-D.

After 1950, 108-D was eliminated from the coolant production process, and at some point, starting materials were switched from solids to liquids with Cr concentrations of about 466 g/L, referred to as the 70% solution. Around 1959–1960, the 100-D-12 transfer station was built, which is where the 70% solution was supplied by rail car and tankers. This solution was then pumped to storage tanks at 185-D and diluted to the 10% to 15% solution. For coolant supply to 105-D, the 10% to 15% solution was again diluted to the 700 µg/L level as it passed through 190-D and into the 105-D reactor. For coolant supply to 105-DR, the 10% to 15% solution was piped to 183-DR and then 190-DR for mixing with Columbia River water to achieve the 700 µg/L reactor coolant levels.

Following passage through the reactors, coolant was pumped to a retention basin system and associated smaller cribs. The facilities receiving the bulk of the reactor coolant volume are listed in Table 3-11 with Cr estimates where available. Most fluids went to the retention basins and then directly to the outfalls. Piping and basin structures leaked extensively, and some fraction of the total volume went directly into the subsurface in quantities sufficient to create and sustain groundwater mounds under these facilities. A notable exception to this practice was a deliberate coolant discharge event in 1967 when three months worth of coolant production (1.3E+10 L) was deliberately discharged into 116-DR 1 & 2 in an attempt to provide a longer transport path to the Columbia River. This event propagated a large plume eastward across the Horn. Discharges at the 100-D-12 transfer station are also listed in Table 3-11 because the 70% solution was regularly discharged into a French drain at the end of a transfer process when rail cars were sluiced after the bulk of the fluids had been transferred into the transfer station. The volume of clean out fluids discharged in this manner is not quantifiable, but hundreds to thousands of kilograms of Cr could have gone down the French drain because of maximum concentrations in the 70% solution. Several hundred thousand kilograms of Cr were transferred through 100-D-12.

Other large volumes of uncontaminated water were released at the 120-D-1 Pond and from a leaking 182-D Reservoir which is still operating. Discharge and leakage has been sufficient to create and sustain groundwater mounds underneath these facilities.

Characteristics of the discharged liquids are summarized in Table 3-11. The major contaminant in these facilities is Cr with variable amounts of radionuclides. A mixture of radionuclides has been measured frequently in characterized soils including cesium-137, strontium-90, cobalt-60, europium isotopes, and uranium isotopes.

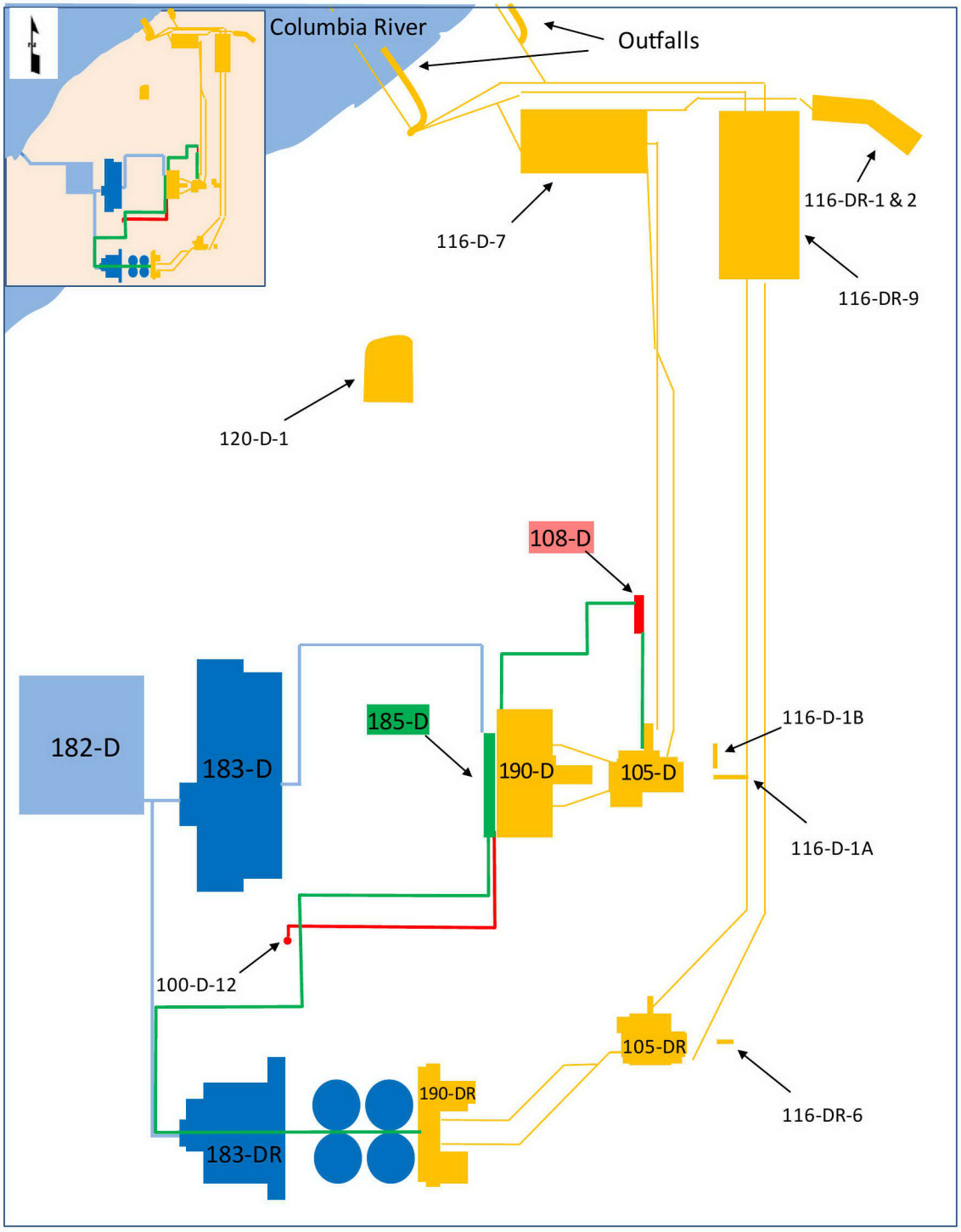

Figure 3-13. Map of Major 100 D Area Liquid Storage and Discharge Locations

Table 3-11. Characteristics of Significant Liquid Discharges at the 100 D Area Sites

Facility	Waste Characteristics	Contaminant Inventory
116-D-1A Trench	Operation Period: 1947-1952 Waste Type: Fuel Storage Basin Coolant Discharge Volume: 2E+5 L	Chromium: 380 kg Radionuclides: 4.7 Ci
116-D-1B Trench	Operation Period: 1953-1967 Waste Type: Fuel Storage Basin Coolant, Reactor Coolant Discharge Volume: 8E+6 L	Chromium: 266 kg Radionuclides: 2.6 Ci
116-D-7 Retention Basin	Operation Period: 1944-1967 Waste Type: Reactor Coolant Discharge Volume: No estimate	Chromium: No estimate Radionuclides: 5-400 Ci
116-DR-9 Retention Basin	Operation Period: 1950-1967 Waste Type: Reactor Coolant Discharge Volume: No estimate	Chromium: No estimate Radionuclides: 5-400 Ci
116-DR-1 & 2 Trench	Operation Period: 1950-1967 Waste Type: Reactor Coolant Discharge Volume: 4E+7 L (does not include the volume [1.3E+10 L] discharged intentionally in 1967)	Chromium: 30 kg Radionuclides: 3.1 Ci
116-DR-6-Trench	Operation Period: 1953-1965 Waste Type: Reactor Coolant and Decontamination Fluid Discharge Volume: 7E+6 L	Chromium: 0.8 kg Radionuclides: No estimate
120-D-1 Pond	Operation Period: 1977-1994 Waste Type: Filtered Water from 183-D Sand Filter and 185/189 Discharge Volume: 2E+9 L	Chromium: None Radionuclides: None
100-D-12 Transfer Station	Operation Period: 1959-1965 Waste Type: Concentrated Sodium Dichromate Discharge Volume: No estimate	Chromium: No estimate Radionuclides: None

100-H Area Liquid Discharges

The information summarized here is taken from DOE/RL-2008-46-ADD1 Rev. 0. The major structures used to create, use, and dispose of reactor coolant at the 100-H Area are shown in Figure 3-14. River water was pumped and stored in the 182-H reservoir prior to transfer to 183-H. At 183-H, Columbia River water was purified and transferred to 190-H, where sodium dichromate was added. Concentrated sodium dichromate starting materials, first as solids (until 1959) and then solutions, were stored at 190-H and added to the purified Columbia River water to make reactor coolant. Unlike processes at the 100-D and 100-K Areas, there is no indication of concentrated sodium dichromate leaks or discharges into the subsurface.

The reactor coolant was then routed through the reactor (105-H) and piped to the 116-H-7 retention basin. From this facility, most of the coolant was then discharged to the river, primarily through the 1904-H

(116-H-5) outfall. Because of intermittent overflow of the 116-H-7 retention basin, reactor coolant was also routed to the 116-H-1 trench. An additional discharge route was also used early in the operations period in which reactor coolant used to cool fuel in the fuel storage basin at the reactor was routed to the 116-H-4 crib (1950–1952). Leaks were ubiquitous in pipelines and the retention basin. However, the fraction of discharged volume that entered the Columbia River is not known. Decontamination solutions were typically discharged into the 116-H-3 French drain and sometimes mixed with reactor coolant pumped through the 116-H-7 retention basin.

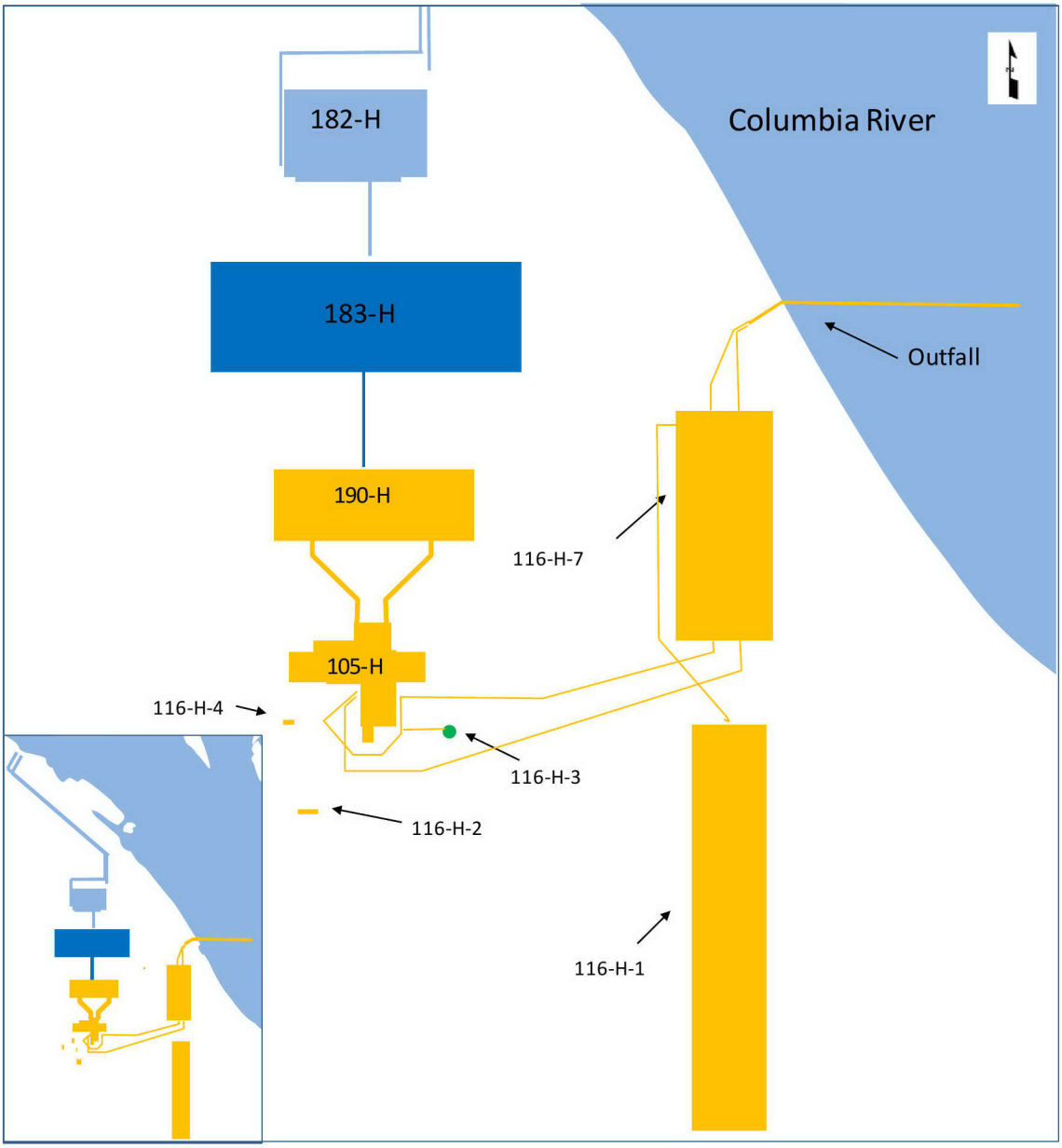

Figure 3-14. Map of Major 100 H Area Liquid Storage and Discharge Locations

Characteristics of the discharged liquids are summarized in Table 3-12**.** The major contaminant in these facilities is Cr with variable amounts of radionuclides. The high inventory for the 116-H 3 French drain

may indicate a chromic acid component in the decontamination fluids. Mixtures of radionuclides have been measured frequently in characterized soils, including cesium-137, strontium-90, cobalt-60, europium isotopes, and uranium isotopes.

Table 3-12. Characteristics of Significant Liquid Discharges at the 100 H Area Sites

Facility	Waste Characteristics	Contaminant Inventory
116-H-1 Trench	Operation Period: 1952-1965 Waste Type: Reactor Coolant Discharge Volume: 9E+7 L	Chromium: 60 kg Radionuclides: 33 Ci
116-H-2 Trench	Operation Period: 1953-1965 Waste Type: Reactor Coolant Discharge Volume: 6E+8 L	Chromium: 400 kg Radionuclides: 1.4 Ci
116-H-3 French Drain	Operation Period: 1950-1965 Waste Type: Decontamination Fluids Discharge Volume: 4E+5 L	Chromium: 1330 kg Radionuclides: 0.07 Ci
116-H-4 Crib	Operation Period: 1950-1952 Waste Type: Reactor Coolant Discharge Volume: No estimate	Chromium: 466 kg Radionuclides: 270 Ci in 1953
116-H-7 Trench	Operation Period: 1949-1965 Waste Type: Reactor Coolant Discharge Volume: 4E+7 L	Chromium: No estimate Radionuclides: No estimate

100-F Area Liquid Discharges

The information summarized here is taken from DOE/RL-2008-46-ADD4 Rev. 0 REISSUE, Integrated 100 Area Remedial Investigation/Feasibility Study Work Plan Addendum 4: 100-FR-1, 100-FR-2, 100-FR-3, 100-IU-2, and 100-IU-6 Operable Units. The major structures used to create, use, and dispose of reactor coolant at the 100-F Area are shown in Figure 3-15. River water was pumped and stored in the 182-F reservoir prior to transfer to 183-F. At 183-F, Columbia River water was purified and transferred to 190-F, where sodium dichromate was added. Concentrated sodium dichromate starting materials, first as solids (until 1959) and then solutions, were stored at 190-F and added to the purified Columbia River water to make reactor coolant. Unlike processes at the 100-D and 100-K Areas, there is no indication of concentrated sodium dichromate leaks or discharges into the subsurface.

The reactor coolant was then routed through the reactor (105-F) into the 100-F-19 pipeline system to either the 116-F-4 retention basin, and to a much smaller extent, to the Lewis Canal (116-F-1). From these facilities, most of the coolant was then discharged to the river, primarily through the 1904-F (116-F-8) outfall. Because of intermittent overflow of the 116-F-4 retention basin, reactor coolant was also routed to the 116-F-2 trench. An additional discharge route was also used early in the operations period in which reactor coolant used to cool fuel in the fuel storage basin at the reactor was routed to the 116-F-3 crib (1947-1951). Leaks were ubiquitous in pipelines and the retention basin. However, the fraction of discharged volume that entered the Columbia River is not known. Decontamination solutions were typically discharged into the Lewis Canal and the 116-F-10 and 116-F-11 French drains.

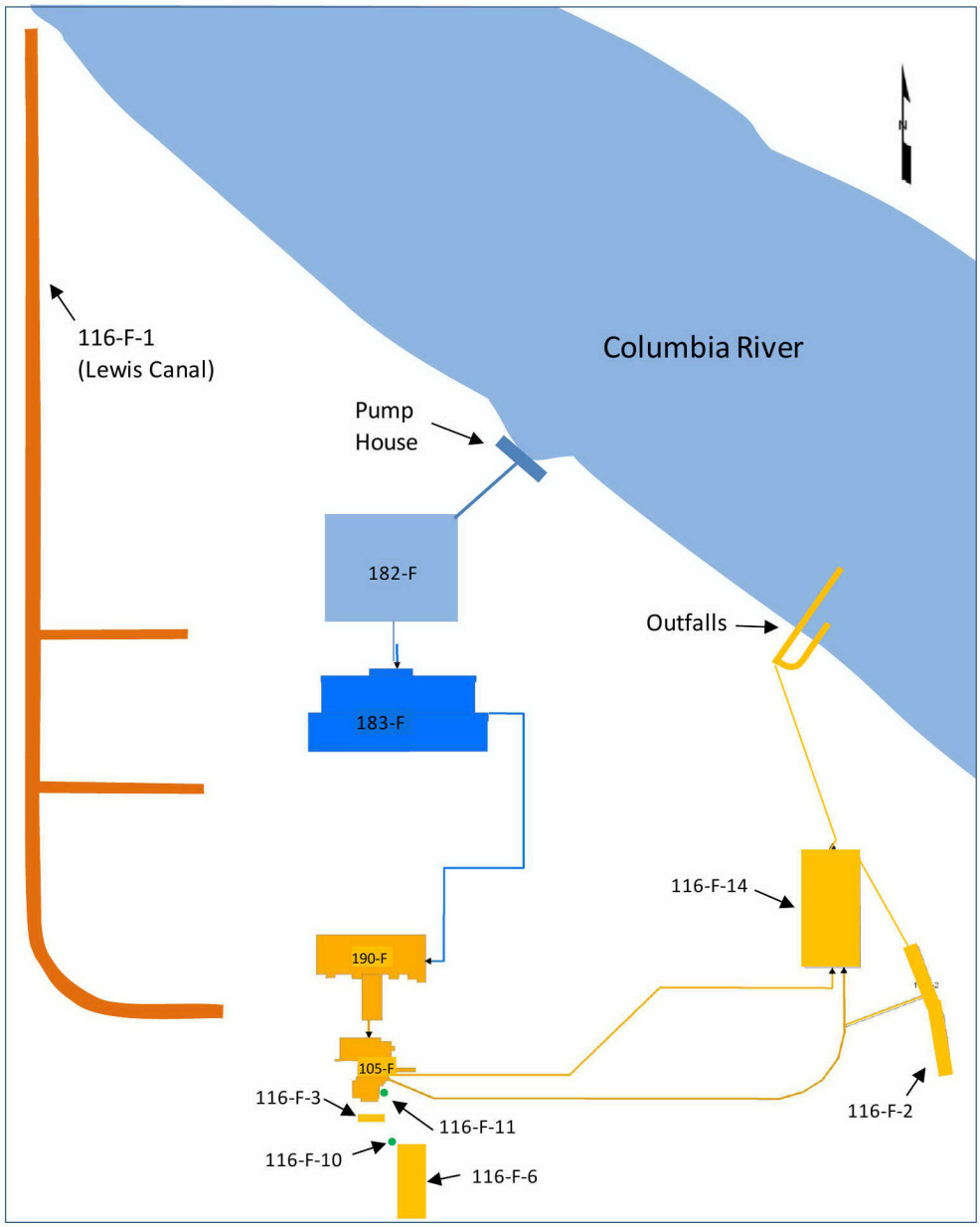

Figure 3-15. Map of Major F Area Liquid Storage and Discharge Locations

Characteristics of the discharged liquids are summarized in Table 3-13. Cr estimates for 116-F-2 appears to be conservatively high. Cr concentrations in reactor coolant were highest early in the operations period and were typically about 0.7 mg/L. Assuming this value and the reported discharge volumes, the Cr mass estimate from 116-F-2 would be 42 kg. The high inventory for the 116-3 trench may indicate a chromic acid component in the decontamination fluids. A mixture of radionuclides has been measured frequently in characterized soils, including cesium-137, strontium-90, cobalt-60, europium isotopes, and uranium isotopes.

Table 3-13. Liquid Discharge Characteristics at the Major 100 F Area Sites

Facility	Waste Characteristics	Contaminant Inventory
116-F-1 Trench (Lewis Canal)	Operation Period: 1953-1965 Waste Type: Reactor Coolant, Decontamination Fluid Discharge Volume: 1E+8 L	Chromium: 40 kg Radionuclides: 3.4 Ci
116-F-2 Trench	Operation Period: 1950-1965 Waste Type: Reactor Coolant Discharge Volume: 6E+7 L	Chromium: 228 kg Radionuclides: 15 Ci
116-F-3 Trench	Operation Period: 1947-1951 Waste Type: Reactor Coolant Discharge Volume: 7E+6 L	Chromium: 1.5 kg Radionuclides: 0.0021 Ci
116-F-6 Trench	Operation Period: 1952-1965 Waste Type: Reactor Coolant Discharge Volume: 1E+5 L	Chromium: No estimate Radionuclides: 6.5 Ci
116-F-10 French Drain	Operation Period: 1948-1965 Waste Type: Decontamination and Radioactive Liquid Water Rinses Discharge Volume: 4E+5 L	Chromium: 760 kg Radionuclides: 6.5 Ci
116-F-11 French Drain	Operation Period: 1953-1965 Waste Type: Decontamination Fluids Discharge Volume: 2E+5 L	Chromium: No estimate Radionuclides: No estimate
116-F-14 Retention Basin	Operation Period: 1945-1965 Waste Type: Reactor Coolant, Fuel Storage Basin Coolant Discharge Volume: 8.2E+10 to 1.6E+11 L	Chromium: No estimate Radionuclides: No estimate

3.2.5 Modeling Assumptions

Various modeling assumptions are made to perform the PRG and screening level calculations. Some of the key assumptions are:

- The vadose zone is considered to be homogeneous in nature, within the stratigraphic cross sections developed for the simulations, without consideration to the presence of thin finer-grained material, which can retard the downward migration of contaminants.
- Groundwater is assumed to have negligible mixing with the Columbia River. In calculating the values for surface water protection, the point of compliance is assumed at the groundwater below the waste site. No attenuation or decay of contaminants is assumed between the source area and the groundwater or the river.
- The vadose zone is assumed to be fully or partially contaminated depending on the distribution coefficient of the contaminant. For fully contaminated vadose zone scenario, two nodes above the water table were kept clean to avoid numerical issues due to boundary effects. This scenario is referred as effective fully contaminated in this document. The screening level calculations use an irrigation recharge scenario but the PRG calculations use base case recharge scenario based on reestablishment of natural infiltration.

- The calculations apply a derived K_d for Cr(VI) of 0.8 ml/g, which is taken from the lower end of the empirical cumulative distribution function based on the results of the batch leach testing at the 100 Area (ECF-Hanford-11-0165 Rev. 0, *Evaluation of Hexavalent Chromium Leach Test Data Conducted on Vadose Zone Sediment Samples from the 100 Area*) and summarized below in Section 3.3.4.
- The initial conditions for matric potential at the start of the flow and transport simulations represent a wetter vadose zone than is expected for such gravel-dominated sediments in an arid climate, thus allowing significantly higher water and solute flux values.
- The median hydraulic gradient value for each source area may be too small for waste sites near the Columbia River and may be several times too large for waste sites that are far inland from the river.
- In the modeling, revegetation of the area (from bare soil condition) is assumed to start after five years, with bare soil present for the first five years. This assumption results in more water infiltrating to the vadose zone than may actually occur.
- A minimum saturated aquifer thickness of 5 m is assumed.
- The longitudinal dispersivity in the transport calculations is set to zero to maximize the peak concentration in the groundwater.

Due to several of the above mentioned conservative choices, the screening levels and PRG concentrations are deemed to be bounding estimates (i.e., lead to the lowest reasonable threshold concentrations).

3.3 Nature and Extent of Contamination

This section presents an overview of the nature and extent of contamination by geographic area to be simulated with the model. This discussion is not comprehensive in the manner that will be presented in the RI reports to be prepared for these OUs, but does present sufficient information that is necessary to guide the development of this model.

3.3.1 Geographic area-Specific Distribution of Contaminants in VZ

The 100 Area RI/FS process has identified and characterized residual contamination within the VZ. As a potential source of contamination to groundwater and the environment, understanding the distribution of contaminants in the subsurface is critical to developing numerical models to support risk assessment. The discussion is broken up into two parts. First, the general distribution of contaminants at each geographic area in the 100 Area is summarized. The summaries are based on information used to develop the work plans for each geographic area. Second, data collected as part of the RI/FS process are used to illustrate observed contaminant levels in the soil column in contrast to soil background levels, and where available the calculated screening levels and final PRG values. The screening levels and PRG values are calculated using Equation 2-1 and discussed in Section 5.2.

100-BC

Characterization of the 100-BC geographic area included field investigations of over 29 high-priority waste sites. Strontium-90, Cr(VI), and tritium were identified as contaminants of interest for groundwater within the 100-BC geographic area (DOE/RL-93-37 Rev. 0, *Field Investigation Report for the 100-BC-5 Operable Unit*, DOE/RL-2008-46-ADD3 Rev. 0). Characterization showed that waste sites that received

enough liquid effluent to impact groundwater have contamination at varying levels throughout most of the VZ, especially for the more mobile contaminants. Contaminants with low contaminant distribution coefficients (near zero), such as Cr(VI), have migrated through the VZ and into the groundwater when the waste sites were operational. Where remediation has been completed, residual amounts of Cr(VI) exist in the VZ. However, limited data are available to quantify the quantities and distribution of mobile contaminants, including nitrate, tritium, and Cr(VI) in the VZ. Concentrations of less mobile contaminants generally decrease with depth below the disposal facility. Some waste sites only received small amounts of dilute liquids and are generally found to have soil contamination extending limited distances into the VZ beneath waste sites (i.e., burial grounds, reactor structures, and some unplanned releases).

In general, the following can be stated concerning the extent of contamination in the 100-BC geographic area based on contaminant soil-water partitioning coefficient (DOE/RL-2008-46-ADD4 Rev. 0 REISSUE):

- **High soil partitioning contaminants:** The highest soil contaminant concentrations are expected within and near the point of release. Sufficiently high volumes of liquids discharged into a waste site can increase the vertical extent of contamination in the vadose zone. Where little or no liquid effluents were discharged to a waste site, soil contamination is expected to remain within and only slightly below the point of release.
- **Low soil partitioning contaminants:** The highest soil contaminant concentrations are expected to be away from the point of release but elevated levels may continue through the vadose zone to groundwater, depending on the discharge volume and infiltration rate. Soil contaminant levels generally decrease with depth, but contamination can be found at higher levels in lenses of fine materials. Limited data are available to evaluate vertical contaminant distribution behavior for several contaminants including nitrate, tritium, and Cr(VI).

100-K

The distribution of contaminants below high-volume remediated liquid waste disposal sites in the 100-K geographic area are highest at the bottom of the disposal facility and generally decrease with depth. Some of the contaminants are arsenic, total Cr, Cr(VI), mercury, lead, Cs-1 37, Co-60, Eu-152, Ni-63, Pu-239/240, U-238, and U-233/234. Soil samples collected and analyzed during interim remedial actions indicate residual contamination is located well above the water table and periodically re-wetted zone (the part of VZ that gets saturated periodically due to river stage fluctuations). Wastes sites that received small amounts of liquid are generally found to have soil contamination extending limited distances into the VZ beneath the waste sites (i.e., burial ground, some unplanned releases, and liquid sites). Adverse impacts to groundwater are not expected from these sites (DOE/RL-2008-46-ADD2, Rev. 0).

100-D, H

Cr(VI) is the principal environmental threat in 100-D/H geographic area. Other contaminants that are potential risks to human health and ecological receptors such as, arsenic, nitrate, tritium, U-233/234, U-235, and U-238, Tc-99, and Sr-90 are also present (DOE/RL-2008-46-ADD1 Rev. 0). Field data indicate that contaminant distributions at high volume liquid waste sites like 116-DR-1&2 are highest near the bottom of the engineered structure and generally decrease with depth with occasional increases in contamination throughout the VZ. Soil samples collected at this site indicate that most of the contamination is high above the water table and does not exceed remedial action goals. However, soil

data have not been collected throughout the VZ to make a complete assessment of contaminant distribution. Waste sites that received small amounts of dilute liquids are generally expected to have soil contamination extending limited distances into the VZ beneath waste sites (i.e., burial grounds, reactor structures, and some unplanned releases). There is little reason to believe that groundwater was impacted at waste sites that received minimal discharges. Field data from 116-DR-1&2 and 116-H-1 indicate that contaminant concentrations at high-volume liquid waste sites for contaminants (e.g., arsenic, total Cr, mercury, Cr(VI), lead, Cs-137, Co-60, Eu-152, Ni-63, Pu-239/240, U-238, and U-233/234) are highest at the bottom of the waste site and generally decrease with depth with observed sporadic increases throughout the VZ. Soil samples collected and analyzed during interim remedial actions (Borehole B8786 at 116-DR-1&2) indicate that residual contamination is located above the water table and the periodically re-wetted zone (DOE/RL-2008-46-ADD1 Rev. 0).

100-F

Contaminants of interest for the 100-F geographic area include arsenic, Cr(VI), manganese, nitrate/nitrite, strontium-90, and tritium (DOE/RL-93-83, *Limited Field Investigation Report for the 100-FR-3 Operable Unit*). Contaminant profiles for sediments below the 116-F-4 crib and 116-F-14 retention basin indicate that contaminant concentrations generally decrease with depth, with the exception of total Cr. Higher concentrations are generally present between 1.5 to 3 m (10 ft) bgs and are associated with the bottom of the engineered structure (DOE/RL-2008-46-ADD4 Rev. 0).

100-N

The primary environmental threat in the 100-N geographic area is strontium-90 but six contaminants are identified in the sampling and analysis plan (DOE/RL-2009-42, *Sampling and Analysis Plan for the 100-NR-1 and 100-NR-2 Operable Units Remedial Investigation/Feasibility Study*). The highest concentrations of strontium-90 were found in surface sediments of the 116-N-1 and 116-N-3 cribs and the 116-N-1 trench. An estimated 2,454 Ci of strontium-90 was released to the 100-N cribs and trenches during reactor operations (DOE/RL-2008-46-ADD5 Rev. 0, *Integrated 100 Area Remedial Investigation Feasibility Study Work Plan Addendum 5 100-NR-1 and 100-NR-2 Operable Units*). The acidic nature of the discharge (pH less than 2) at 100-N may have increased the mobility of the strontium-90 (HW-34499, *Adsorption and Retention of Strontium by Soils of the Hanford Project*; HW-56582, *Influence of Limestone Neutralization on the Soil Uptake of Sr-90 from a Radioactive Waste*). The effects can be observed in historic groundwater measurements with some wells recording pH levels around 2 (e.g., 199-N-14 in 1993) and several others exhibiting pH around 5. Operational conditions are considered to be potential drivers for the areal extent of the strontium-90 plume estimated at 100-N. Concentrations of other less-mobile contaminants generally decrease with depth below the disposal structure. The available data indicate that residual concentrations of strontium-90 and tritium remain in the VZ (DOE/RL-2008-46-ADD5 Rev. 0).

3.3.2 RI/FS Borehole Data

Several contaminants have been identified in the 100 Area Groundwater OUs. Table 3-14 lists the contaminants of interest for the Groundwater OUs in the 100 Area. As part of developing the RI/FS, VZ samples were collected from a variety of locations within the 100 Area. The selection of the locations was biased towards high-risk waste sites in order to increase the likelihood that existing contamination could be located. At the time of publishing this report, a total of 33 soil borings with samples in the VZ were available. Borings in this dataset were taken from the 100-D, 100-H, 100-K, 100-F, and 100-BC

geographic areas. Figures 3-16 through 3-20 consist of scatter plots of observed contaminant concentrations versus fraction of depth below ground surface to the observed water table. The figures also include indicators of the background concentrations (DOE/RL-92-24 Rev. 4, *Hanford Site Background*; PNNL-18577, *A Review of Metal Concentrations Measured in Surface Soil Samples Collected on and Around the Hanford Site*; ECF-Hanford-11-0038 Rev. 0, *Soil Background Data for Interim Use at the Hanford Site*) and regulatory levels (ECF-Hanford-11-0063 Rev. 5, *STOMP 1-D Vadose Zone Modeling for Determination of Preliminary Remediation Goals for 100 Area D, H, and K Source Operable Units*) for comparison purposes. Only analytical results for which detectable levels of contaminants were found were included in the figures. In most cases where background values were available, more than half of the measurements for all geographic areas were measured below this level, however, concentration of some contaminants exceed the background levels. In the case of strontium-90, the majority of detectable measurements were above background, however, the concentration levels of strontium-90 are orders of magnitude below screening levels and PRGs (when calculated) in all geographic areas. The details of screening level and PRG calculations are presented in Section 5.2. The zone of contamination for most contaminants, including Cr(VI), extends through lower half of the VZ thickness.

Table 3-14. Contaminants of Interest In the 100 Area Groundwater OUs

Contaminant	100-KR-4	100-HR-3			100-BC-5	100-FR-3
		100-D Source Exposure Area	100-H Source Exposure Area	Horn Exposure Area		
Carbon tetrachloride				X		
Carbon-14	X					
Chromium	X	X				
Hexavalent chromium	X	X	X	X	X	X
Nitrate	X	X				X
Nitrate						
Strontium-90	X		X		X	X
Sulfate		X				
Trichloroethene						X
Tritium	X				X	

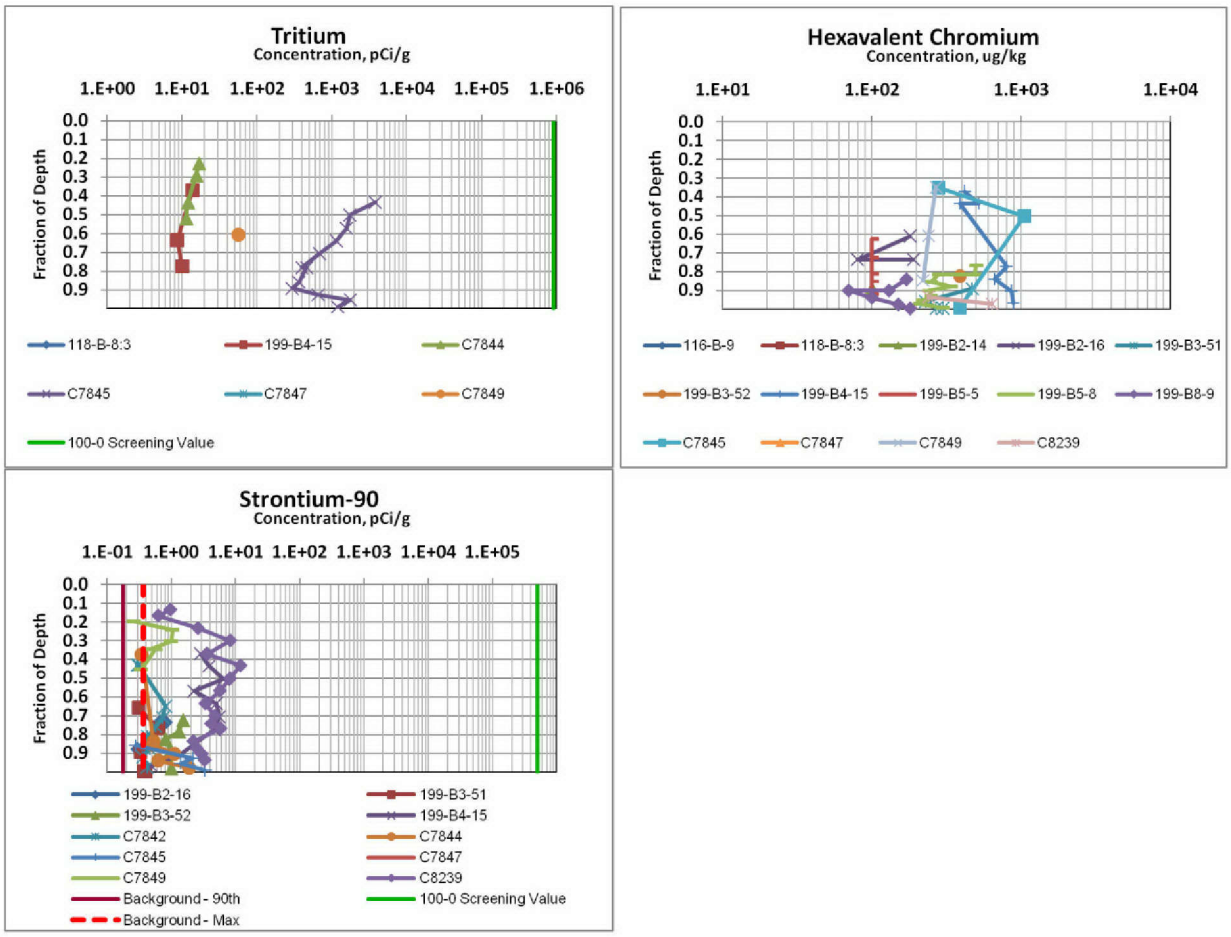

Note: Screening level and PRG values, wherever shown, are based on smaller of the surface water and groundwater PRG values. These values may have changed in the latest revision of the environmental calculations.

Figure 3-16. Contaminant Concentrations Plotted against the Fraction of the Depth within the VZ for all Wells in the 100-BC Geographic Area where a Detectable Concentration was Registered.

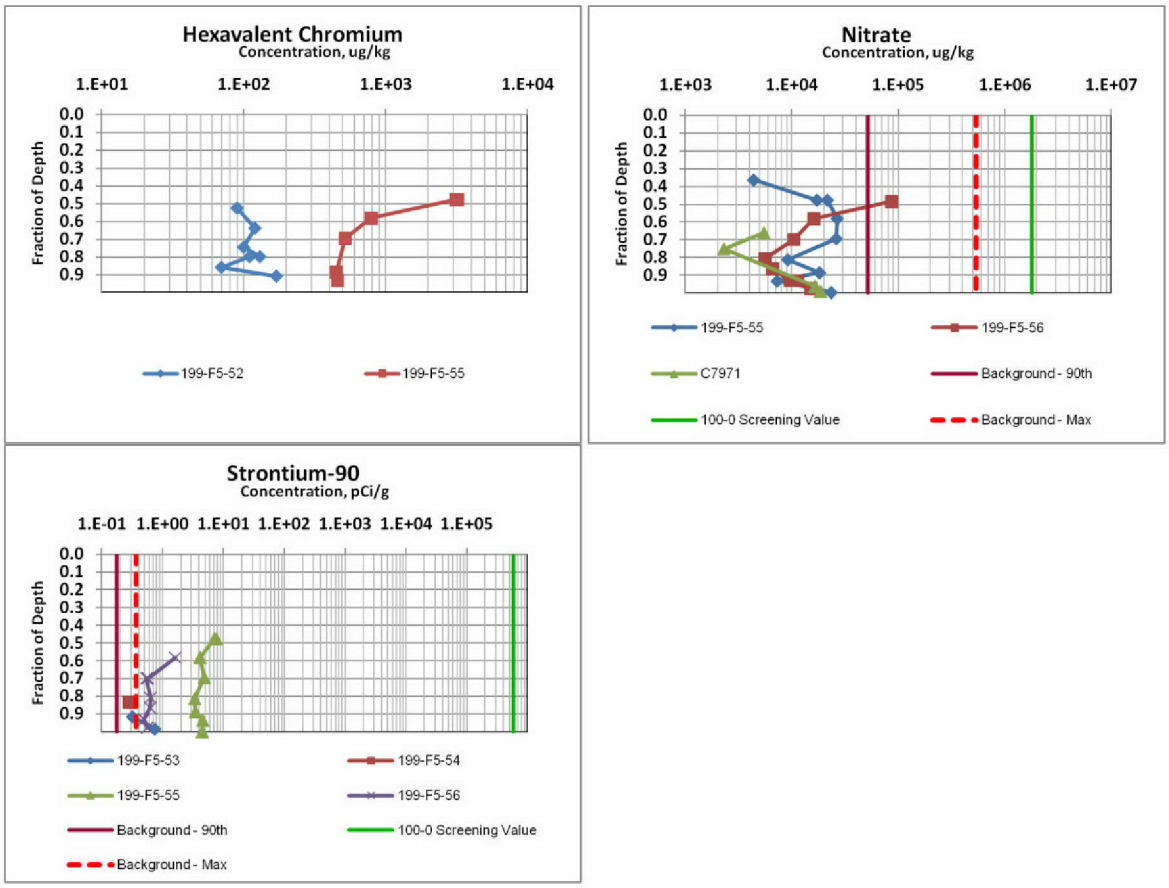

Note: Screening level and PRG values, wherever shown, are based on smaller of the surface water and groundwater PRG values. These values may have changed in the latest revision of the environmental calculations.

Figure 3-17. Contaminant Concentrations Plotted against the Fraction of the Depth within the VZ for all Wells in the 100-F Geographic Area where a Detectable Concentration was Registered.

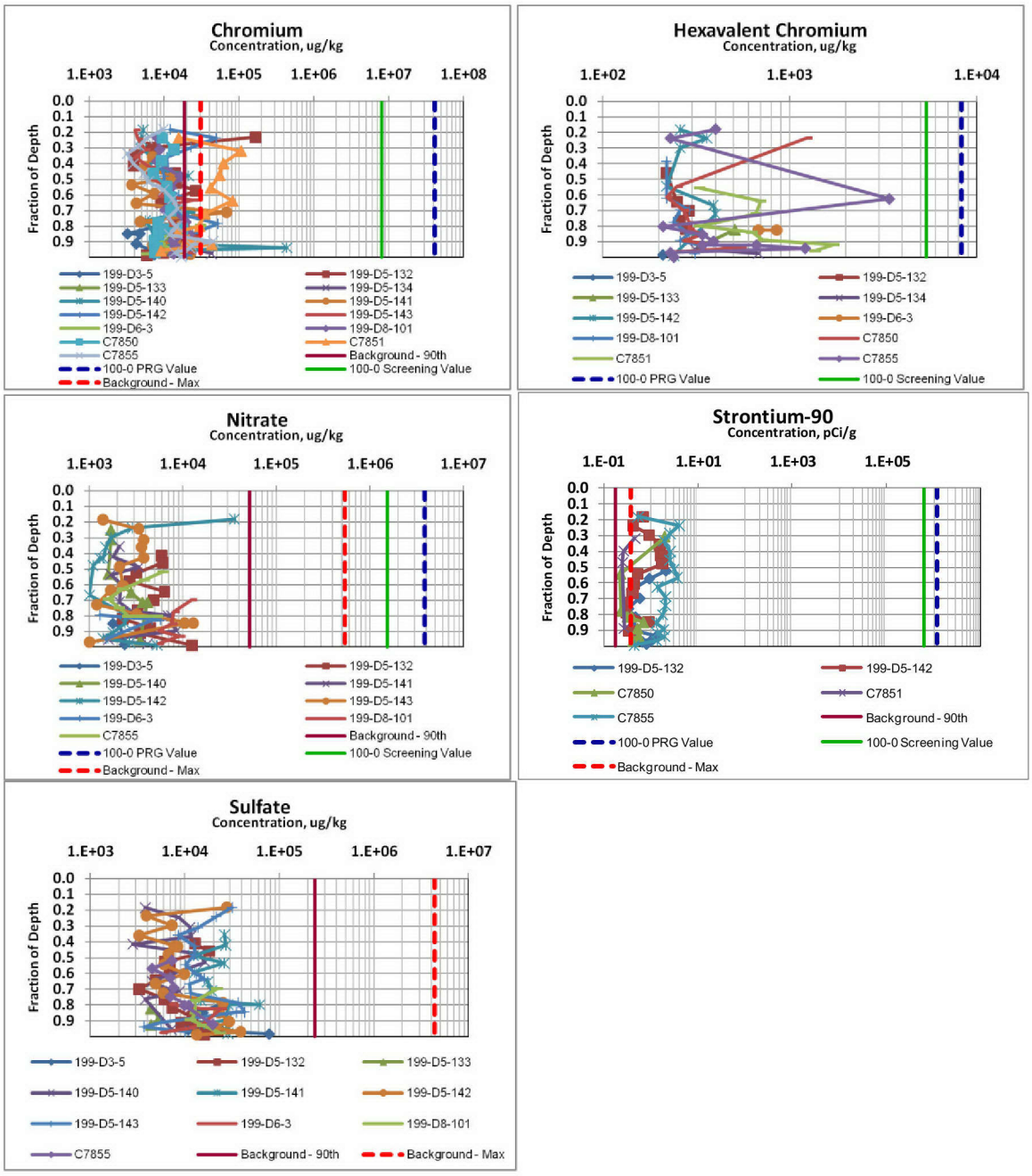

Note: Screening level and PRG values, wherever shown, are based on smaller of the surface water and groundwater PRG values. These values may have changed in the latest revision of the environmental calculations.

Figure 3-18. Contaminant Concentrations Plotted against the Fraction of the Depth within the VZ for all Wells in the 100-D Geographic Area where a Detectable Concentration was Registered.

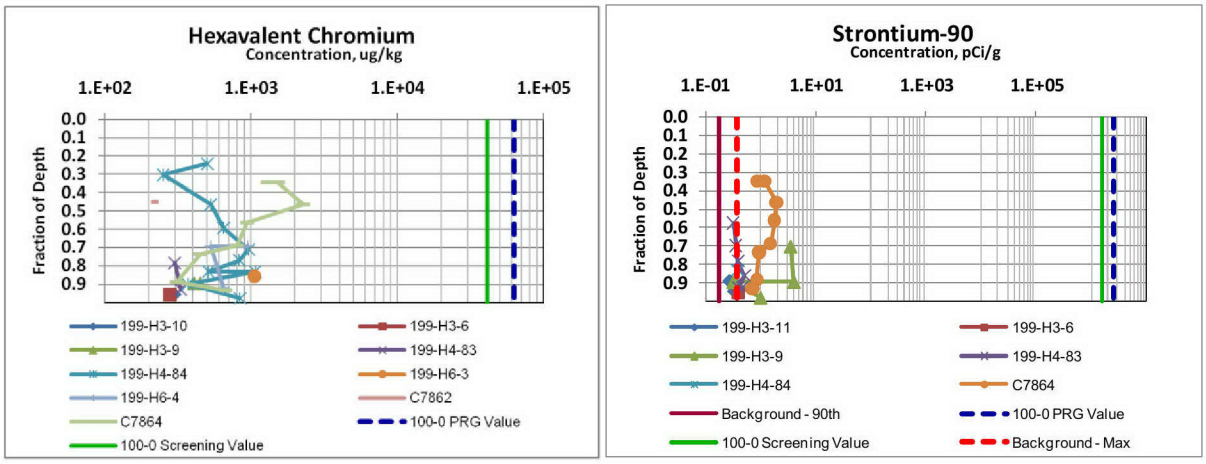

Note: Screening level and PRG values, wherever shown, are based on smaller of the surface water and groundwater PRG values. These values may have changed in the latest revision of the environmental calculations.

Figure 3-19. Contaminant Concentrations Plotted against the Fraction of the Depth within the VZ for all Wells in the 100-H Geographic Area where a Detectable Concentration was Registered.

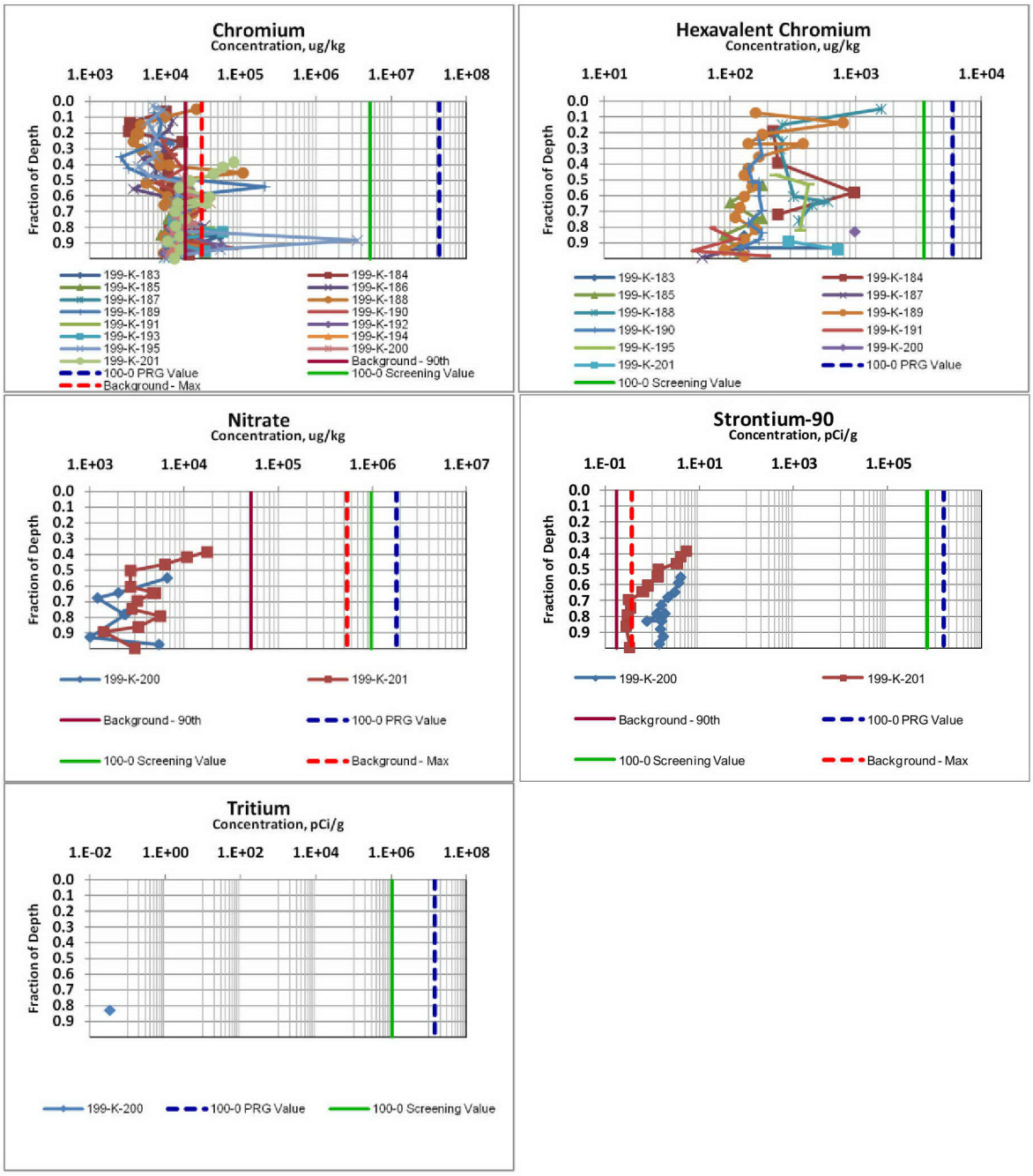

Note: Screening level and PRG values, wherever shown, are based on smaller of the surface water and groundwater PRG values. These values may have changed in the latest revision of the environmental calculations.

Figure 3-20. Contaminant Concentrations Plotted against the Fraction of the Depth within the VZ for all Wells in the 100-K Geographic Area where a Detectable Concentration was Registered.

3.3.3 Cr(VI) Distribution in VZ and Aquifer

Cr(VI) is a common contaminant in the subsurface at reactor operations locations in the 100 Areas along the Columbia River. It is present because the compound sodium dichromate was routinely added to reactor cooling water to inhibit metal corrosion of the piping system. The significance of this contaminant is linked to concern for salmon and other aquatic life in the Columbia River. Fall Chinook salmon spawning areas have been observed near 100-BC (Figure 3-21). Shoreline areas provide rearing habitat for young salmon and steelhead, as well as for many of the other species of fish in the river (DOE/RL-2005-40 Draft B, *100-BC Pilot Project Risk Assessment Report*). Historical records show that Cr(VI)-bearing materials (mostly liquids) were released into the subsurface during the addition of sodium dichromate to cooling water for use in the reactors and after cooling water use in the reactors. Cr(VI) concentrations in cooling water were set at maximum levels (about 700 µg/L) during early operations because the concentration needed for adequate corrosion inhibition was not well understood. Over time, reactor operations determined that lower concentrations (about 350 µg/L) were adequate. After a single pass through these reactors, the cooling waters were discharged to the surrounding environment by various routes.

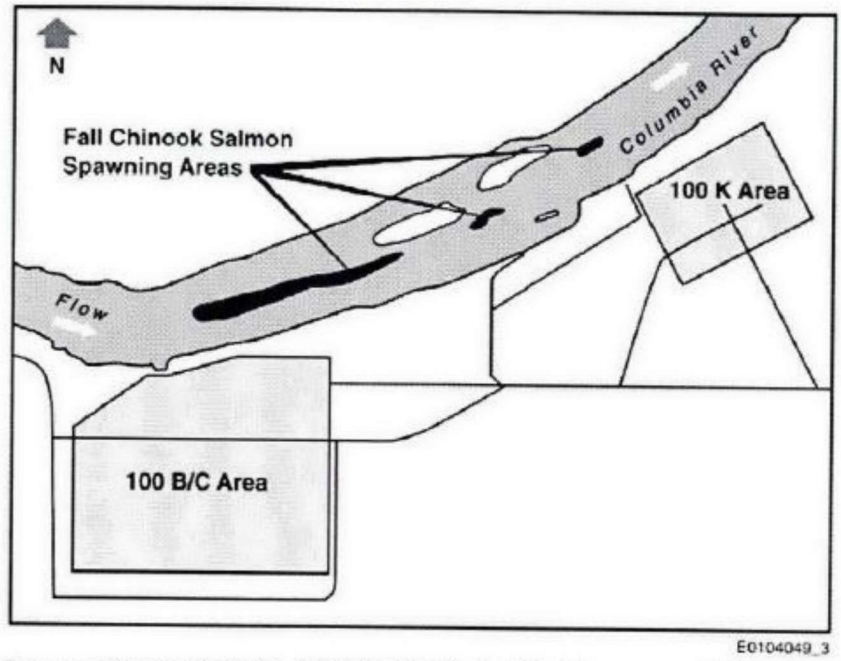

Source: DOE/RL 2005-40, *100-B/C Pilot Project Risk Assessment Report*.

Figure 3-21. Approximate Location of Fall Chinook Spawning Areas

The low concentrations of residual Cr(VI) in the VZ soils and the widespread groundwater distribution of Cr(VI) show that the great majority of Cr(VI) passed entirely through the VZ and into the unconfined aquifer or the Columbia River. Estimates of travel time to the Columbia River from 100 Area facilities were on the order of weeks during operations. Despite the clear indications of highly efficient transport through the VZ, a small residual amount remains, suggesting other chemical or physical mechanisms that

influenced the transport of a small fraction of the total discharged inventory. The summary discussion of the distribution of the residual contamination of Cr(VI) in both the groundwater and the VZ follows.

Groundwater

Cr(VI) concentrations in the groundwater plumes near the 100 Area are summarized each year by the Hanford Area Groundwater Monitoring Report (DOE/RL-2010-11, *Groundwater Monitoring and Performance Report for 2009: Volumes 1 and 2*). Chromate contamination is found at levels above drinking water standards (100 µg/L) in the 100-K Area, 100-D Area, and 100-H Area, and at lower concentrations in the 100-B Area, 100-N Area, and 100-F Area (Hartman et al., 2007). The highest groundwater concentrations are found in the 100-D Area, with concentrations greater than 1,500 µg/L in 2006. Concentrations considerably less than the drinking water standard are also of concern because the Washington State ambient WQS for chronic exposure is 11 µg/L for aquatic biota. Groundwater pump-and-treat systems are active for chromate remediation in the 100-K, 100-D, and 100-H Areas. At the 100-D Area, chromate contamination is also being treated by ISRM (PNNL-16346. *Hanford Site Groundwater Monitoring for Fiscal Year 2006*). Groundwater chromate concentrations found in the 100-D Area at levels greater than that in the cooling water and the contaminant distribution in the 100-D, 100-K, and other areas implicate dichromate leaks or spills and/or liquid waste disposal facilities as likely sources for some of the groundwater contamination (PNNL-16346; Peterson et al., 1996; Rohay et al., 1999). Figure 3-22 illustrates the extent of Cr contamination in the 100 Areas based on the recent groundwater monitoring report.

Vadose Zone

Cr(VI) is the most significant contaminant at each of the 100 Area OU's with the exception of 100-N. Due to the low propensity of Cr(VI) to adsorb to soil in the VZ, the majority of the Cr(VI) has likely passed through the VZ into the groundwater. Results from leachability tests (see next section) indicate that this is the case. The highest soil contaminant concentrations are expected within and near the point of release. Sufficiently high volumes of liquids discharged into a waste site can increase the vertical extent of contamination in the VZ. Where little or no liquid effluents were discharged to a waste site, soil contamination is expected to remain within and only slightly below the point of release. The available data indicate residual concentrations of Cr(VI) remain in the VZ where remedial actions have been completed. However, few data are available to quantify total VZ Cr(VI) quantities and distribution. Soil samples collected and analyzed during interim remedial actions (Borehole B8786 at 116-DR-1&2) indicate that residual contamination is located above the water table and the periodically re-wetted zone. The profiles of the 116-F-4 crib and 116-F-14 retention basin show that contaminant concentrations generally decrease with depth, with the exception of total Cr. Higher concentrations are generally present between 1.5 to 3 m (10 ft) bgs and are associated with the bottom of the engineered structure. Total Cr concentrations increase with depth at the 116-F-4 crib toward the bottom of the borehole.

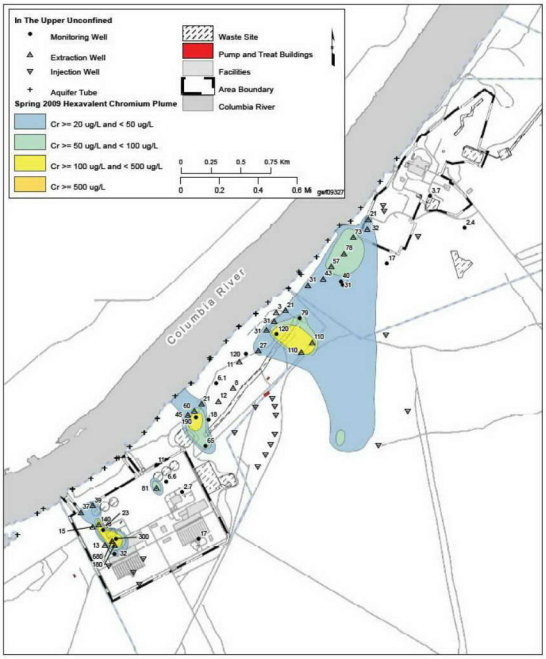

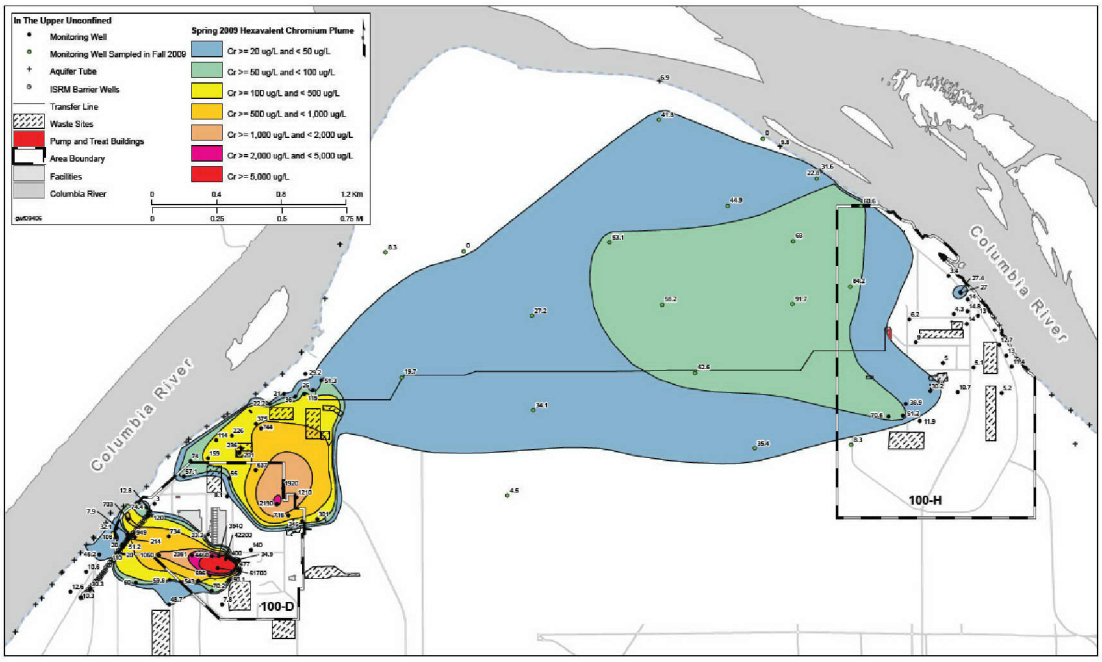

Figure 3-22. Extent of Cr(VI) Contamination in the 100 Areas

3.3.4 Cr(VI) Leachability

Leaching tests have been conducted on Cr-contaminated soils collected under retention basins at 100-D and 100-H geographic areas and under the liquid discharge trench 1301-N in the 100 N Area. In all cases, the leachable fraction of Cr(VI) was less than 1% for a variety of experimental conditions. A detailed description of leaching experiments in soils retrieved below the 116-D-7 retention basin is provided in a remediation description document for that facility (CVP-99-00007, *Cleanup Verification Package for 116-D-7 Retention Basin*). Total Cr concentrations were about 177 mg/kg including a Cr(VI) portion of about 6 mg/kg. It should be noted that the authors put forth the possibility that the measured Cr(VI) could have been Cr(III) that was oxidized to Cr(VI) by the sample preparation process. In standard batch leaching tests with several soil samples, Cr(VI) was detected at very low concentrations (about 2 to 20 µg/L) or could not be measured. In the flow through column tests, steady state concentrations of 1 to 2 µg/L were measured by Inductively Coupled Plasma Mass Spectrometry (ICP-MS) and about 11 µg/L by colorimetry. The authors considered the ICP-MS measurements to be more accurate. After 12 pore volumes, less than 0.1% of the initial Cr(VI) had passed through the column assuming ICP-MS measurements.

A detailed leaching and characterization study has also been completed using near surface soils (less than 3 m [10 ft] bgs) collected near sodium dichromate storage tanks and railroad tracks in the 100-BC geographic area (PNNL-17674, *Geochemical Characterization of Chromate Contamination in the 100 Area Vadose Zone at the Hanford Site*). Unlike the leaching sediments described above, these soils were only leached by natural infiltration. In this study, two types of leaching behavior were observed. First, large fractions of Cr(VI) in the contaminated soil were eluted in the first pore volume (about 65%) and about 4% of the initial mass was released in the next five pore volumes. After five pore volumes, the leachate concentration had decreased about three orders of magnitude. For example, in one soil sediment initially containing Cr(VI) concentrations of about 550 mg/kg, the first pore volume concentration was greater than 8,000 mg/L. After five pore volumes, the concentration was approximately 2 mg/L.

As part of the leachability tests (PNNL-17674), modeling using the CXTFIT code (Parker and van Genuchten, 1984, "*Determining Transport Parameters from Laboratory and Field Tracer Experiments*"; Toride et al., 1999, *The CXTFIT Code for Estimating Transport Parameters from Laboratory or Field Tracer Experiments*) was performed to calculate transport parameters. This code includes a two-site model for adsorption, including a kinetic model and an equilibrium model. Parameter estimation for the CXTFIT model was completed for dispersivity, Peclet Number, K_d (kinetic and equilibrium), and equilibrium site fraction. The two-site model fit Cr(VI) desorption profiles well for columns 3, 4, 5, and 6 (Figure 3-23). The modeling exercise indicated that the majority of the mass of Cr(VI) can be described using the equilibrium model, while a small portion is kinetically controlled with percent equilibrium sites of 97.5, 95, 98.7, and 97 for columns 3, 4, 5, and 6, respectively. Table 3-15 indicates a K_d of 0 or close to 0 is appropriate for equilibrium controlled Cr(VI). The calculated values of dispersivity were close to or within the range of typical values observed in packed laboratory columns (dispersivity less than 2 cm) (Jury et al., 1991, *Soil Physics*). The values of the Peclet number (PN = L/λ, where L is the column length) varied between 2.8 and 12.4 (Table 3-16). Generally, the majority of the Cr(VI) mass present in the sediment was removed during the initial leaching phase. A small fraction of the total mass exhibited time-dependent desorption. This fraction released Cr(VI) with reaction half-lives that varied from 76.1 to 126 hours represented a small portion of the total mass of Cr(VI) in the column.

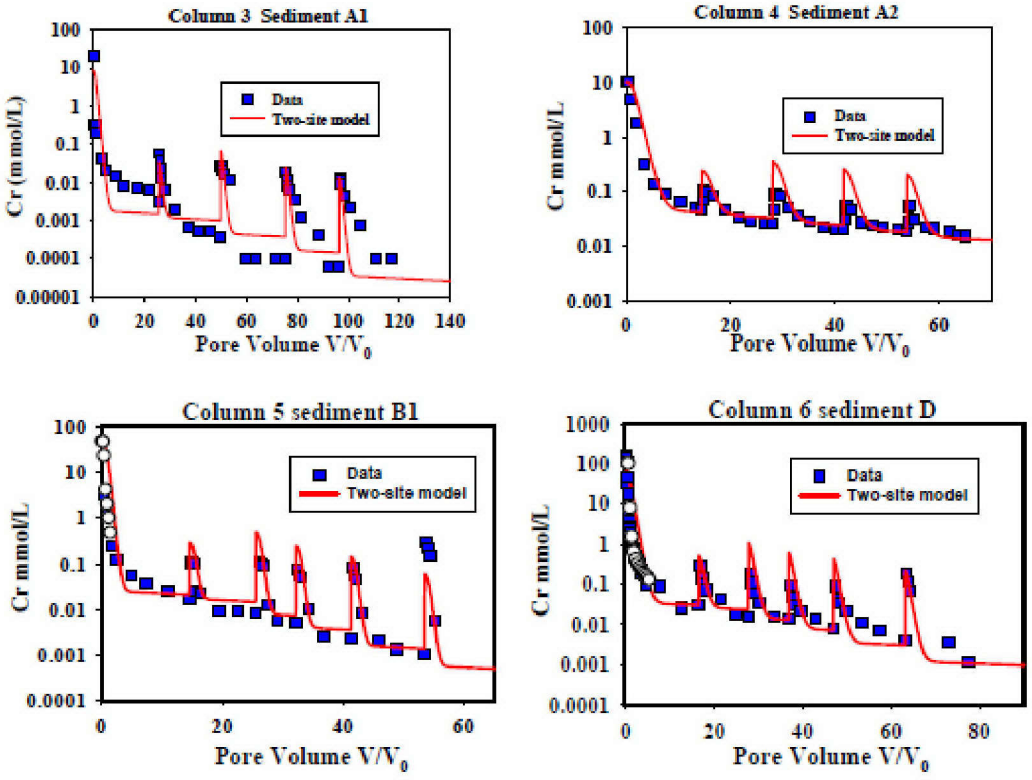

Source: PNNL-17674

Figure 3-23. The Results from Fitting the Two-Site (Two-Region) Model to Experimental Data for Column Experiments 3, 4, 5, and 6

Table 3-15. Results from Modeling the Cr(VI) Desorption Data Using a Two-Site Equilibrium and Kinetic Model (PNNL-17674)

Parameters	Column 3 Sediment A1	Column 4 Sediment A2	Column 5[c] Sediment B1	Column 6[c] Sediment D
K_d – kinetic (ml g^{-1})	0	45	13	4.8
K_d – equilibrium (ml g^{-1})	0	0.33	0	0
Equilibrium site fraction (%)	97.5	95	98.7	97
Rate constant (kinetic site fraction) (h^{-1})	0.0082	0.0055	0.0091	0.0068
Reaction half-life[a] (h)	84.5	126	76.1	101.9
Reaction characteristic time[b] (h)	121.9	181.8	109.8	147.1

[a]Reaction half-life: [ln(2)/rate constant].

[b]Reaction characteristic time: (1/rate constant).

[c]Data from other columns were included in these simulations to better represent Cr(VI) effluent concentrations in the first pore volumes.

Table 3-16. Selected Measured and Calculated Physical Properties in Column Experiments 1, 2, 3, 4, 5, and 6 (PNNL-17674)

Column	1 Sediment D	2 Sediment B2	3 Sediment A1	4 Sediment A2	5 Sediment B1	6 Sediment D
Pore Volume[b] (cm^3)	26.51	19.12	19.79	20.89	19.19	19.70
Water Content[b] (cm^3 cm^{-3})	0.47	0.52	0.37	0.41	0.38	0.37
Residence Time[b] (h)	2.41	2.46	1.13	1.77	1.65	1.32
Bulk Density[b] (g cm^{-3})	1.40	1.25	1.68	1.57	1.65	1.66
Flow Rate[a] (cm^3 min^{-1})	0.183 ± 0.011	0.197 ± 0.014	0.333 ± 0.015	0.196 ± 0.008	0.194 ± 0.012	0.248 ± 0.035
Water Flux (cm min^{-1})	0.034	0.037	0.065	0.039	0.039	0.048
Pore Water Velocity (cm h^{-1})	4.32	4.26	10.56	5.76	6.24	7.92
Dispersion Coefficient (cm^2 h^{-1})			27.3	10.1	5.21	29.3
Dispersivity (cm)			2.58	1.75	0.83	3.69
The Péclet number			4.1	5.9	12.4	2.8

[a]The average flow rate was calculated from experimental measurements (the standard deviation is given in squared brackets, more than 100 experimental measurements were taken in each column to determine the average flow rate).

[b]Pore volume, water content, residence time and bulk density were calculated based on the amount of sediments added in each column and the mass of water used to saturate the columns.

Considered collectively, these experimental results suggest that after Cr(VI) is discharged to the soil column, two primary chemical stages of Cr reactivity occur, which influence its transport characteristics. First, the majority of Cr(VI) remains mobile, transports readily, and contributes groundwater concentrations commensurate with source term strength. Second, some Cr(VI) is sequestered by a variety of mechanisms on some sorption sites that retard further migration. The effectiveness of these sequestration processes increases over time. In the retention basin soil, it appears that the initial highly mobile component of discharged Cr(VI) has already been flushed from the sampled soil. This is expected, given the high leakage volume from the retention basins during operations. Conversely, the reactor area soil has been contacted by much smaller volumes of water since the contaminating event. Therefore, extensive flushing of the soil has not been completed in the natural setting.

The number of pore volumes of groundwater passed through contaminated soil in the 100 Area VZ is not well understood. Additionally, the experimental column soil conditions present a highly idealized environment for groundwater contact and transport with regard to the irregular subsurface features found in the local 100 Area geology. These features could harbor concentrated dichromate solutions or limit contact with groundwater and introduce more complex release mechanisms than those observed in the column tests. Therefore, studies and data collection focused on understanding the long-term hydrology, geological influences, and spatial distribution of Cr(VI) at work in various locations may be needed.

Batch leaching studies have been performed on the soil samples (<2 mm size) taken underneath various waste sites as part of the River Corridor remedial investigation efforts. The results of the batch leach tests are summarized in ECF-Hanford-11-0165 Rev. 0 (*Evaluation of Hexavalent Chromium Leach Test Data Conducted on Vadose Zone Sediment Samples from the 100 Area*). A total of 509 samples from 58

locations were analyzed. Only 39 samples from 15 locations had detectable Cr(VI) in the soil and only 10 samples from 4 locations had detectable Cr(VI) in both the soil and leachate. For each sample, analyses were performed using three ratios of soil to leachant (1:1, 1:2.5, and 1:5) by weight. One of the three ratios was randomly selected to be run as a duplicate analysis totaling four analyses for each soil sample. The Cr(VI) concentration in the soil samples ranged from 4.31 mg/kg to undetectable levels and the pH of the leachant added to the soil sample was held at pH of 5 to simulate the rain water. Quadruplicate analyses were conducted for each soil sample and if the sorbed mass on any of the quadruplicate samples was flagged as a non-detect then they were excluded from analysis and considered unreliable for K_d determination. However, if the leachate concentration was flagged as a non-detect, the K_d was calculated as a greater than value by assuming the practical quantitation limit (PQL) as the solute concentration. An empirical cumulative distribution function (ECDF) is created from the resulting K_d values (after adjusting for the dilution factors). The ECDF indicates a 90^{th}, 50^{th}, and 10^{th} percentile exceedance of approximately 0.8 ml/g, 9 ml/g, and 29 ml/g, respectively. For the purpose of PRG and soil screening level calculations the K_d of 0.8 ml/g was chosen (equivalent to the 90^{th} percentile exceedance).

4. Model Implementation

Numerical predictions of groundwater concentrations from soil contamination are founded on a conceptual model of solute fate and transport for the Hanford Site VZ. Numerous characterization and modeling efforts have yielded ample information with which to construct the conceptual model. Important conceptual model components include the hydrologic driving forces, especially recharge, waste discharges, and aquifer flow; the interaction between the flowing fluids and the sediments of the different hydrostratigraphic units; the interactions between the sediments and the solutes; and the initial distributions of water pressure and solute concentration. The conceptual model also provides an understanding of the uncertainties about model components (e.g., hydraulic properties) and a context for evaluating the relative conservatism of different modeling assumptions.

Peak groundwater concentrations were simulated using 1-D STOMP numerical fate and transport simulations under variably saturated conditions. Simulated transport processes included sorption to sediments and contaminant degradation from radioactive decay. Each model domain comprised a VZ and an underlying aquifer, wherein the peak groundwater concentration was determined. Recharge, gravity, and matric potential gradients were assumed to drive water downward through the VZ's contaminated interval into the aquifer, where a hydraulic gradient was assumed to drive water horizontally towards the simulated monitoring well screen. Two- or three-dimensional STOMP simulations could also be used, but would require greater resources and would yield less-conservative (lower) peak groundwater concentrations. The STOMP code was selected to perform the simulations on the basis of its ability to provide an adequate simulation of the VZ FEPs relevant to calculating PRGs for the Hanford site and to satisfy the other code criteria and attributes (DOE/RL-2011-50 Rev. 0). Model development was completed in accordance with the *Quality Assurance Project Plan for Modeling* (Appendix G of CHPRC-00189 Rev. 9).

4.1 Governing Equations

STOMP was used to solve the Richards equation and the Advection-Dispersion equation that govern water flow and solute transport, respectively, under variably saturated conditions beneath the waste sites.

4.1.1 Flow and Solute Transport Equations

The governing equation for variably saturated flow through porous media was simulated using STOMP's single phase water-only mode. As such, the principle processes that drive water flow are gravity and gradients in pressure or volumetric water content. No momentum is transferred from the liquid phase to the vapor phase. The overall equation governing liquid phase flow for STOMP is written as:

$$\frac{\partial}{\partial t}(n_D\,\rho\,s) = \frac{\rho k_r \boldsymbol{k}}{\mu}\left(\nabla P + \rho\, g\, \mathbf{z}_g\right) + \tau\, n_D\,\rho\, s\, \frac{M^w}{M} D^w\, \nabla X^w + \dot{m}^w \qquad \text{(Eqn. 4-1)}$$

where t is time (T), n_D is diffusive porosity (L^3L^{-3}), ρ is liquid density (ML^{-3}), s is saturation (-), k_r is relative permeability (-), $\boldsymbol{k}$ is the permeability tensor (L^2), μ is dynamic viscosity ($ML^{-1}T^{-1}$), P is pressure ($ML^{-1}T^{-2}$), g is gravitational acceleration (LT^{-2}), $\mathbf{z}_g$ is the unit vector for the z axis (-), τ is tortuosity (-), M^w is molecular weight of water (M/mole), M is molecular weight of the liquid phase (M/mole), D_w is the self-diffusion coefficient of water (L^2T^{-1}), X^w is the mole fraction of water in the liquid phase (-), and $\dot{m}^w$

is the mass source rate (MT^{-1}), i.e., aggregate rate of sources and sinks. As the gradient of the mole fraction of water in water is zero, the second term on the right-hand side is zero, leaving the well known Richards equation:

$$\frac{\partial}{\partial t}(n_D\ \rho\ s) = \frac{\rho k_r\ \boldsymbol{k}}{\mu}\left(\nabla P + \rho\ g\ \boldsymbol{z}_g\right) + \dot{m}^w \qquad \text{(Eqn. 4-2)}$$

Solving Equation 4-2 requires stipulation of appropriate boundary conditions, initial conditions, and parameter values. Net Infiltration was represented by a specified flux boundary condition along the top boundary of the numerical model domain. Lateral groundwater flow was simulated using specified pressure boundaries on the upgradient and downgradient edges of the aquifer portion of the numerical domain. Initial conditions were specified for pressure throughout the model domain. Parameter values were taken from approved Hanford databases and reports.

Solute transport in a variably saturated liquid is governed by water movement, diffusion, dispersion, sorption, decay, and chemical reactions. STOMP employs the Advection-Dispersion equation as the governing equation for transport of solutes in the liquid phase:

$$\frac{\partial C}{\partial t} = -(\nabla C \cdot \boldsymbol{V}) + \dot{m}^c - R^c\ C + \nabla[(\tau\ n_D\ s\ D^c + n_D\ s\ \mathbf{D}_h)\nabla C] \qquad \text{(Eqn. 4-3)}$$

where C is solute concentration (ML^{-3}), $\boldsymbol{V}$ is the seepage velocity vector (LT^{-1}), $\dot{m}^c$ is the solute source rate (MT^{-1}), R^C is the solute decay rate (T^{-1}), D^C is the solute diffusion coefficient for variably saturated media (L^2T^{-1}), $\mathbf{D}_h$ is the hydraulic dispersion coefficient (L^2T^{-1}), and all other variables are defined as above. Sorption, which is the interchange of solute molecules between the dissolved phase and the adsorbed phase onto the geologic material, can be linear or nonlinear, equilibrium or non-equilibrium. STOMP calculates equilibrium distribution of the solute molecules between the dissolved and sorbed phases with a general equation of the following form:

$$C_T = n_D\ s\ C_l + (1 - n_T)C_s \qquad \text{(Eqn. 4-4)}$$

Here C_T is the total concentration of the contaminant in a given pore volume, C_l is the dissolved phase concentration (solute concentration), C_s is the sorbed phase concentration, and n_T is total porosity (L^3L^{-3}). STOMP can handle nonlinear equilibrium sorption isotherms such as the Freundlich and Langmuir isotherms, but the linear equilibrium sorption isotherm is the only sorption behavior considered in this report. It is defined as:

$$K_d = \frac{C_s}{C_l} \qquad \text{(Eqn. 4-5)}$$

where K_d is the distribution coefficient (L^3M^{-1}). Solving the Advection-Dispersion governing equation and the linear sorption equations above requires stipulation of appropriate boundary conditions, initial conditions, and parameter values. The seepage velocity **V** in Equation 4-3 is taken from a solution of the

Richards equation (Equation 4-2), so the flow system at each time step must be solved prior to solving for concentration in the same time step. Boundary conditions for concentration were typically specified as zero flux or zero concentration. For example, the net infiltration water or aquifer water entering the domain were each assumed to have a zero contaminant concentration. Initial conditions were specified for contaminant soil concentration, C_s in Equations 4-4 and 4-5, by the user. Values for the dispersivity, diffusion coefficient, and K_d parameters were taken from approved Hanford databases and reports.

4.1.2 Constitutive Relations

Solving the Richards Equation (Section 4.1.1) requires adequately defined soil-moisture retention and relative permeability functions. The VZ and aquifer sediments were assumed to follow the van Genuchten (1980) moisture retention constitutive relation and the Mualem (1976) relative permeability constitutive relation. The moisture retention constitutive relation defines the relationship between volumetric water content and matric potential, $\theta(\psi)$, and is also known as the pore-pressure–saturation curve or the characteristic curve. According to van Genuchten (1980), the relationship is defined as:

$$\theta(\psi) = \theta_r + (\theta_s - \theta_r)(1 + |\alpha\psi|^n)^{-m} \qquad \text{(Eqn. 4-6)}$$

for which α is proportional to the inverse of the air-entry matric potential (L^{-1}), θ_s is saturated volumetric water content (L^3L^{-3}), θ_r is the residual volumetric water content (L^3L^{-3}), and n and m are dimensionless fitting parameters with $m = (n\text{-}1)/n$. In terms of STOMP's state variables and parameters, volumetric water content is the product of water saturation and diffusive porosity, $\theta = s\, n_D$, and matric potential ψ is the ratio of gas-aqueous capillary pressure to the product of liquid density and the gravitational acceleration constant.

The Mualem–van Genuchten relative permeability in terms of matric potential, $K(\psi)$, is defined as:

$$K(\psi) = K_s + (1 + |\alpha\psi|^n)^{-m\beta}\{1 - [(1 - |\alpha\psi|^n)^{-1}]^m\}^2 \qquad \text{(Eqn. 4-7)}$$

where K_s is the saturated hydraulic conductivity (LT^{-1}) and β is Mualem's dimensionless fitting parameter. Solving the characteristic equation for matric potential and substituting the result into the above equation yields the relative permeability in terms of volumetric water content:

$$K(\theta) = K_s \left(\frac{\theta-\theta_r}{\theta_s-\theta_r}\right)^{\beta} \left\{1 - \left[1 - \left(\frac{\theta-\theta_r}{\theta_s-\theta_r}\right)^{\frac{1}{m}}\right]^m\right\}^2 \qquad \text{(Eqn. 4-8)}$$

The n parameter is an index of the pore size variability, which is commonly taken as the inverse of the pore size standard deviation, for the Mualem-van Genuchten parameterization, whereas β represents the tortuosity and the partial correlation in pore radius between two adjacent pores at a given saturation (Mualem, 1976).

4.2 Software Used

STOMP (PNNL-11216; PNNL-12030; PNNL-15782) was selected to simulate the transport of contaminants in the vadose zone of the 100 Area because it fulfills the following specifications:

- The STOMP simulator operational modes needed for implementation of this model is available for free for government use under a limited government-use agreement.
- The STOMP simulator solves the necessary governing equations (see Section 4.1 above).
- It is capable of directly simulating the principal FEPs that are relevant (see Section 3.2 above).
- The STOMP simulator is well documented (PNNL-11216; PNNL-12030; PNNL-15782).
- The STOMP simulator development is compliant with DOE O 414.1c requirements (PNNL-SA-54022, *STOMP Software Test Plan Rev. 1.0*; PNNL-SA-54023, *STOMP Software Configuration Management Plan Rev. 1.3*; PNNL-SA-54079, *Requirements for STOMP Subsurface Transport Over Multiple Phases*).
- The STOMP simulator is distributed with source code, enhancing transparency.
- The modeling team implementing this model has expertise in use of this simulator.
- There is an extensive history of application of STOMP at Hanford and elsewhere including verification, validation, and benchmarking (see Appendix C, *CHPRC Fact Sheet: STOMP: Validation and Extent of Application*).
- Use of STOMP is in keeping with DOE direction for simulation of VZ flow and transport at the Hanford Site (*Hanford Groundwater Modeling Integration* [Klein, 2006]).

The software used to implement this model and perform calculations was approved under the requirements of, and use was compliant with, PRC-PRO-IRM-309 Rev. 1, *Controlled Software Management*. This software is managed under the following software quality assurance documents consistent with PRC-PRO-IRM-309 Rev. 1:

- CHPRC-00222 Rev. 1, *STOMP Functional Requirements Document*
- CHPRC-00176 Rev. 2, *STOMP Software Management Plan*
- CHPRC-00211 Rev. 1, *STOMP Software Test Plan*
- CHPRC-00515 Rev. 1, *STOMP Acceptance Test Report*
- CHPRC-00269 Rev. 1, *STOMP Requirements Traceability Matrix*

4.2.1 STOMP Controlled Calculation Software

The following describes the STOMP Controlled Calculation software:

- Software Title: STOMP-W (a scientific tool for analyzing single- and multiple-phase subsurface flow and transport using the integrated finite volume discretization technique with Newton-Raphson iteration).
- Software Version: STOMP-W was provided by PNNL on December 16, 2010, and was tested and approved for use by CHPRC as "CHPRC Build 2."

- Hanford Information System Inventory Identification Number: 2471 (Safety Software S3, graded Level C).

4.2.2 Software Installation and Checkout

Safety Software (CHPRC Build 2 of STOMP) is checked out in accordance with procedures specified in CHPRC-00176 Rev. 2. Source or executables are obtained from the CHPRC software owner, who maintains the configuration-managed copies in MKS Integrity™. Installation tests identified in CHPRC-00211 Rev. 1, are performed and successful installation confirmed, and software installation and checkout forms are required and must be approved for installations used to perform model runs. Approved users are registered in the Hanford Information System Inventory for safety software.

4.2.3 Statement of Valid Software Application

Use of the STOMP software for implementing the model described in this report is consistent with its intended use for CHPRC, as identified in CHPRC-00222 Rev. 1. A fact sheet that provides a brief overview of work that has validated the STOMP simulator software and the breadth of applications to which this simulator has been applied is presented in Appendix C.

4.3 Spatial and Temporal Discretization

STOMP, or any numerical modeling code, solves the governing equations (see Section 4.1) at user-specified locations and times. For STOMP, the conceptual model's physical domain is discretized into grid blocks within which the governing equations are solved on the centroids at times determined by the code's time-stepping algorithm and, in part, by the user. The governing equations are solved using integral volume finite-difference method.

As described in Section 3, the conceptual model represents a column of sediments that comprise a VZ and an underlying aquifer. Recharge-driven flow moves downward through the VZ, where it encounters contamination that is eventually transported to the aquifer, across which a pressure gradient drives horizontal flow. The conceptual model is represented numerically as a vertical, one-dimensional column of evenly-spaced grid blocks with boundary conditions defined on the grid block faces (see Section 4.4.1) and initial conditions defined at the centroids (see Section 4.4.2). The number of grid blocks in the vertical column is varied to match the length of each representative stratigraphic column, and the hydraulic and transport properties assigned to each grid block is also changed to match the lithologic composition of each stratigraphic column (see Section 4.5). The simulated time span was divided into two intervals, one that represents the period prior to the year 2010 (pre-2010 period), during which only flow was simulated, and one that represents the period after the year 2010 (post-2010 period), during which both flow and solute transport were simulated (see Section 4.3.2).

Given the differences in the representative stratigraphic columns, each grid block was assigned a constant thickness and length. Grid block thickness was set to 0.25 m to represent the changes in lithology and to avoid large grid-block Courant numbers (see Section 4.3.3). A length of 10 m for 100-D/H, 100-K, 100-BC, 100-F, 100-UI-2/6, and 100-N geographic area was selected to avoid large grid-block Courant numbers in the aquifer grid blocks during transport simulations (see Section 4.3.3) and the results were scaled down to produce results appropriate for a column of a unit length (1 m).

™ MKS Integrity is a trademark of MKS, Incorporated.

4.3.1 Representative Stratigraphic Columns

A total of 28 different representative stratigraphic columns were simulated for the five different geographic areas: 100-D/H, 100-K, 100-BC, 100-F, and 100-IU-2/6 (Figures 4-1 and 4-2). Some of the representative stratigraphic columns for 100-BC, 100-F and 100-IU-2/6 may be revised based on reevaluation of extent and thickness of Ringold E unit. The thickness of the representative columns ranged between 8 and 40 m (Tables 3-2 to 3-7), with a corresponding range of 32 to 160 grid blocks. Model domain dimensions and discretization were held constant for the pre-2010 and post-2010 simulations.

The thickness of the VZ, excluding the 4.5 m of clean fill at the top, ranges between 3.5 and 35.5 m across all geographic areas. Aquifer thickness was set equal to the observed thickness for each representative column unless that thickness was less than 5 m, in which case the minimum thickness was set to a minimum thickness of 5 m. This was necessitated by the model requirement that groundwater concentrations were representative of a water table monitoring well constructed with a 6 m (20 ft) screen in such a way that a 5-m-long span was below the water table. However, it was observed that using 5 m deep SZ instead of deeper SZ didn't change the peak concentration at the water table. On the other hand, run time for the simulation reduced significantly because the number of active nodes in the model is less than the model with the deeper SZ. So, a 5 m thick SZ was used for all the representative columns.

Depending on source-area-specific geology, the VZ comprises either Hanford formation alone or a combination of Hanford and Ringold E units (Tables 3-2 to 3-7 and Figures 4-1 to 4-2). At the start of each post-2010 simulation, the VZ spans a cover of clean fill with constant thickness as well as contaminated and uncontaminated sediments of varying thickness. The SZ can comprise of, only Hanford formation, a combination of Hanford formation and Ringold E unit, or only Ringold E unit (Tables 3-2 to 3-7 and Figures 4-1 to 4-2). If present, the contact between the Ringold E unit and the RUM forms the bottom of the unconfined aquifer.

4.3.2 Simulation Periods

Two sequential STOMP simulations were used to determine peak groundwater concentrations. The first stage model, called the pre-2010 model, simulated flow through the representative columns for a 2,010-year period (an arbitrary long period chosen to allow establishment of pressures in equilibrium with the present day conditions). Results from the pre-2010 simulations provided initial aqueous pressure conditions for the 1,000-year-long second stage simulation, the post-2010 model, which is solved for both flow and solute transport. The post-2010 solute transport simulations track the fate of contaminants with different distribution coefficients (K_d) and decay constants through the VZ and into the aquifer. These results were used to identify the peak groundwater concentrations.

As described below, recharge rates varied with time during the pre-2010 simulations to represent changes in land cover with the start of operations at the Hanford site in the year 1944. Aqueous pressure and saturation values were reviewed at least every ten years after the start of operations to ensure that the values had reached equilibrium prior to the end of the simulation period.

4.3.3 Grid and Time-Step Constraints

The choice of grid block dimensions and time step intervals can affect solution convergence and mass balance errors. Deleterious effects can be minimized by choosing grid-block and time step sizes that yield acceptable Peclet and Courant numbers for the model. Defined as the product of the seepage velocity and

the ratio of the time step and the grid block dimension, dimensionless Courant numbers provide a stability constraint and should ideally be less than 1 to minimize convergence and mass balance problems (for example, see page 231 in Celia and Gray, 1992, *Numerical Methods for Differential Equations*). Courant numbers for the aquifer grid blocks, in which flow is horizontal under fully saturated conditions, were all less than 1.00. Courant numbers for the VZ grid blocks, in which flow is vertical under variably saturated conditions, were all less 1.00 for all recharge scenarios. No grid size constraints were placed based on Peclet numbers because dispersion was assumed to be negligible (see Section 4.5).

4.4 Initial and Boundary Conditions

Solving the governing equations for variably-saturated flow and transport requires stipulation of boundary conditions and initial conditions. A complete set of boundary and initial conditions must be stipulated for each scenario.

Representative Stratigraphic Columns for 100-D

Vadose Zone Thickness:

(1) 25-m

(100% Hanford in VZ)

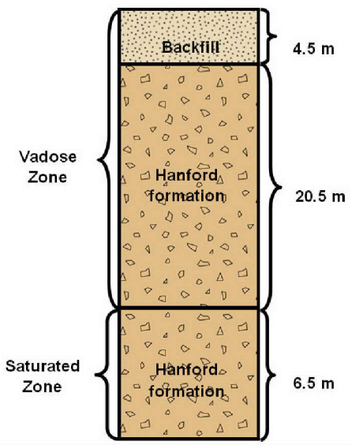

(2) 20-m

(100% Hanford in VZ)

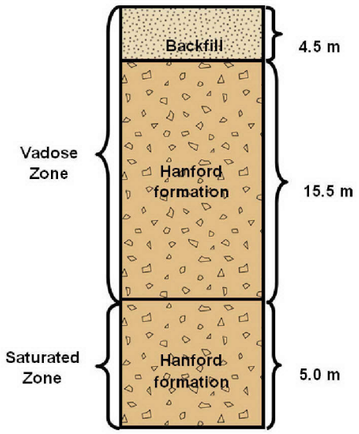

(3) 25-m

(75% Hanford 25% Ringold E in VZ)

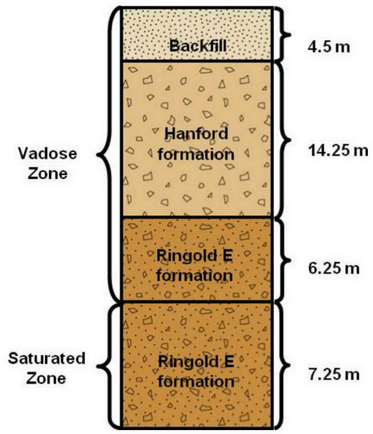

(4) 20-m

(80% Hanford 20% Ringold E in VZ)

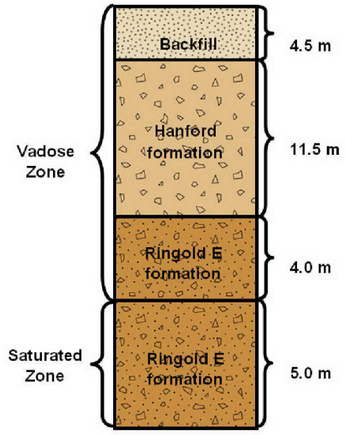

(5) 25-m

(60% Hanford 40% Ringold E in VZ)

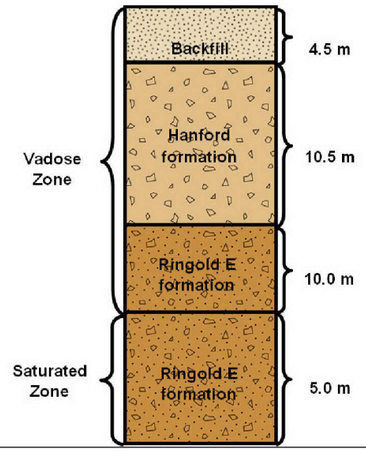

(6) 15-m

(60% Hanford 40% Ringold E in VZ)

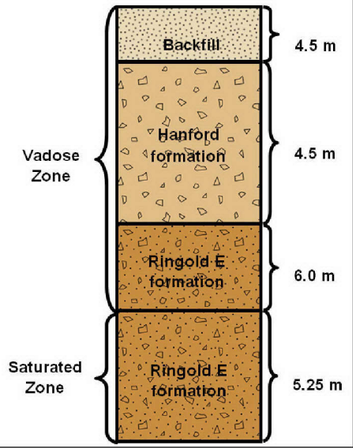

Representative Stratigraphic Columns for 100-H

(1) 12-m

(100% Hanford in VZ)

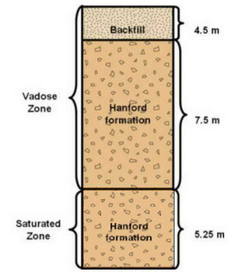

Representative Stratigraphic Columns for 100-K

Vadose Zone Thickness:

(1) 25-m

(40% Hanford 60% Ringold E in VZ)

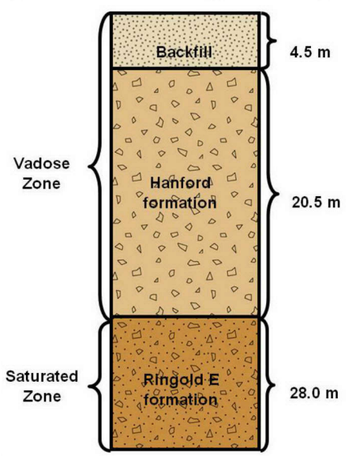

(2) 15-m

(70% Hanford 30% Ringold E in VZ)

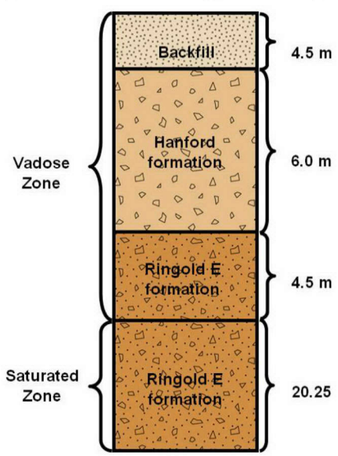

(4) 20-m

(50% Hanford 50% Ringold E in VZ)

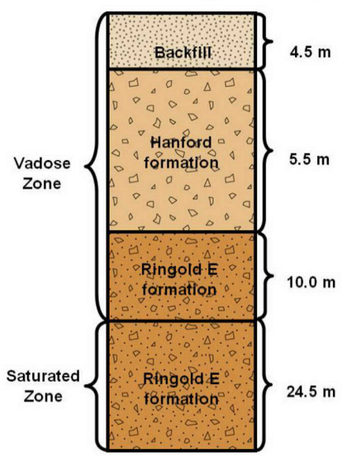

(4) 20-m

(60% Hanford 40% Ringold E in VZ)

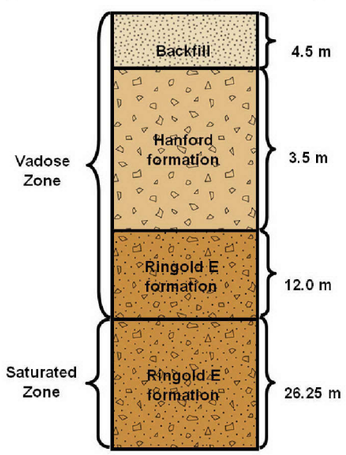

(5) 20-m

(30% Hanford 70% Ringold E in VZ)

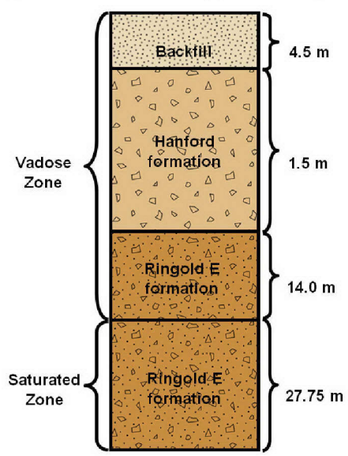

(2) 8-m

(100% Hanford in VZ)

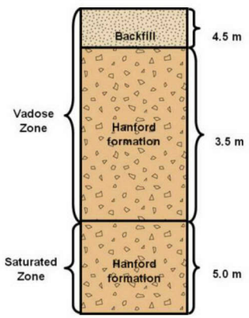

Figure 4-1. Representative Stratigraphic Columns for 100-D, 100-H, and 100-K Geographic Areas

Representative Stratigraphic Columns for 100-BC

Vadose Zone Thickness:

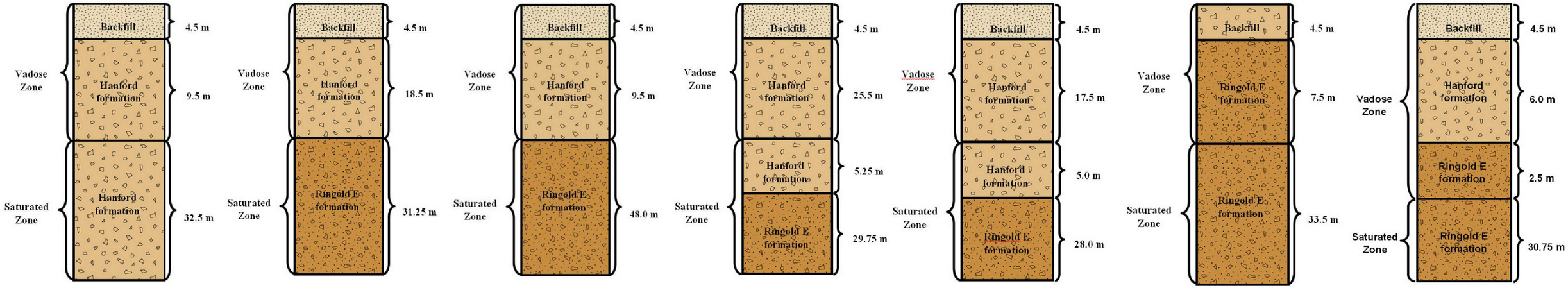

Representative Stratigraphic Columns for 100-F

Vadose Zone Thickness:

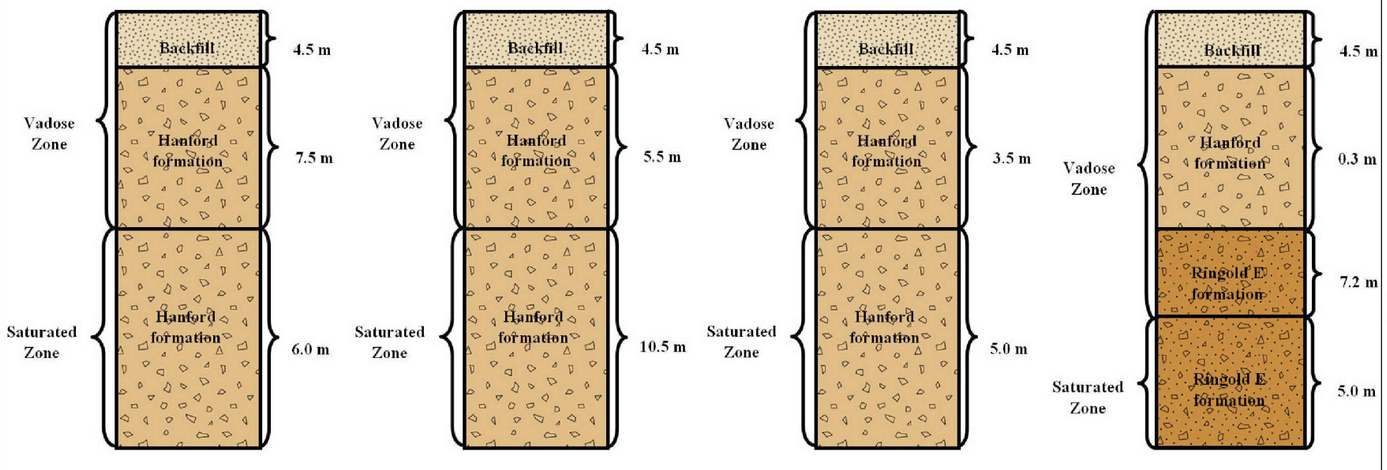

Representative Stratigraphic Columns for 100-IU-2 and 100-IU-6

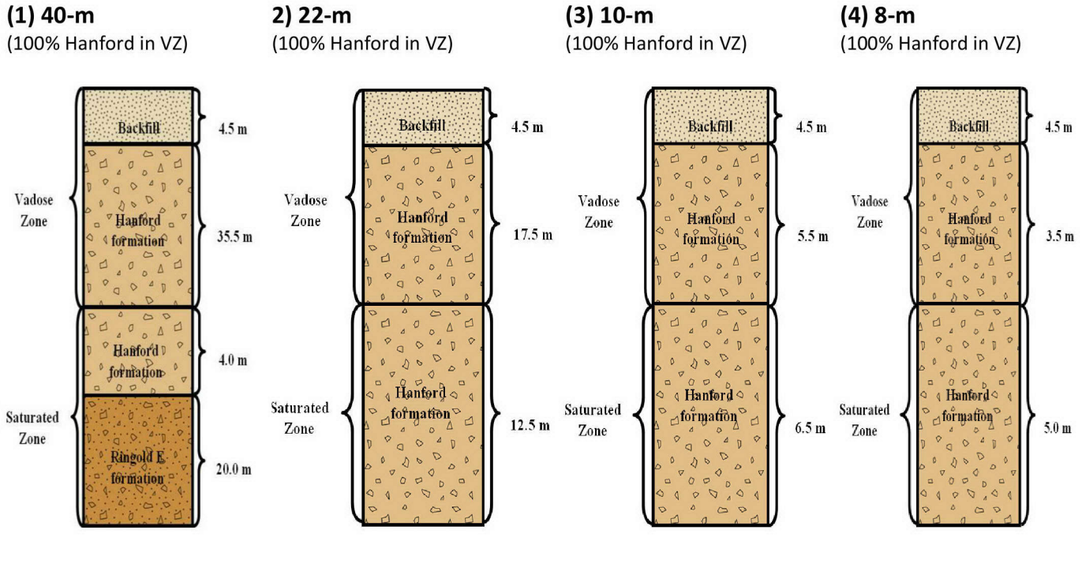

Note: Some representative columns for 100-BC, 100-F, 100-IU-2, and 100-IU-6 are subject to revision based on reevaluation of extent of Ringold E unit.

Figure 4-2. Representative Stratigraphic Columns for 100-BC, 100-IU-2 and 100-IU-6, and 100-F Geographic Areas

4.4.1 Flow and Transport Boundary Conditions

For water flow a specified-flux boundary condition was applied at the surface to simulate recharge. No-flow boundary conditions were assigned to the edges of the VZ (assuming only vertical flow) and the bottom of the aquifer (assuming only horizontal flow). Prescribed pressure boundaries were assigned to the edges of the aquifer (Figure 4-3). The prescribed pressures were selected to create the water table at the desired elevation and with the desired hydraulic gradient.

For solute transport, specified zero flux boundaries were applied at the top of the model domain, along the upgradient edges of the aquifer grid blocks, along both edges of the VZ, and the bottom of the aquifer (Figure 4-3). The downgradient edges of the aquifer grid blocks were assigned STOMP's outflow solute boundary condition (see page 6.21 of PNNL-12030 and page 4.4 of PNNL-15782), which transports solute out of the domain according to the advective flux term in the governing equation and does not allow solute to enter into the domain (Figure 4-3).

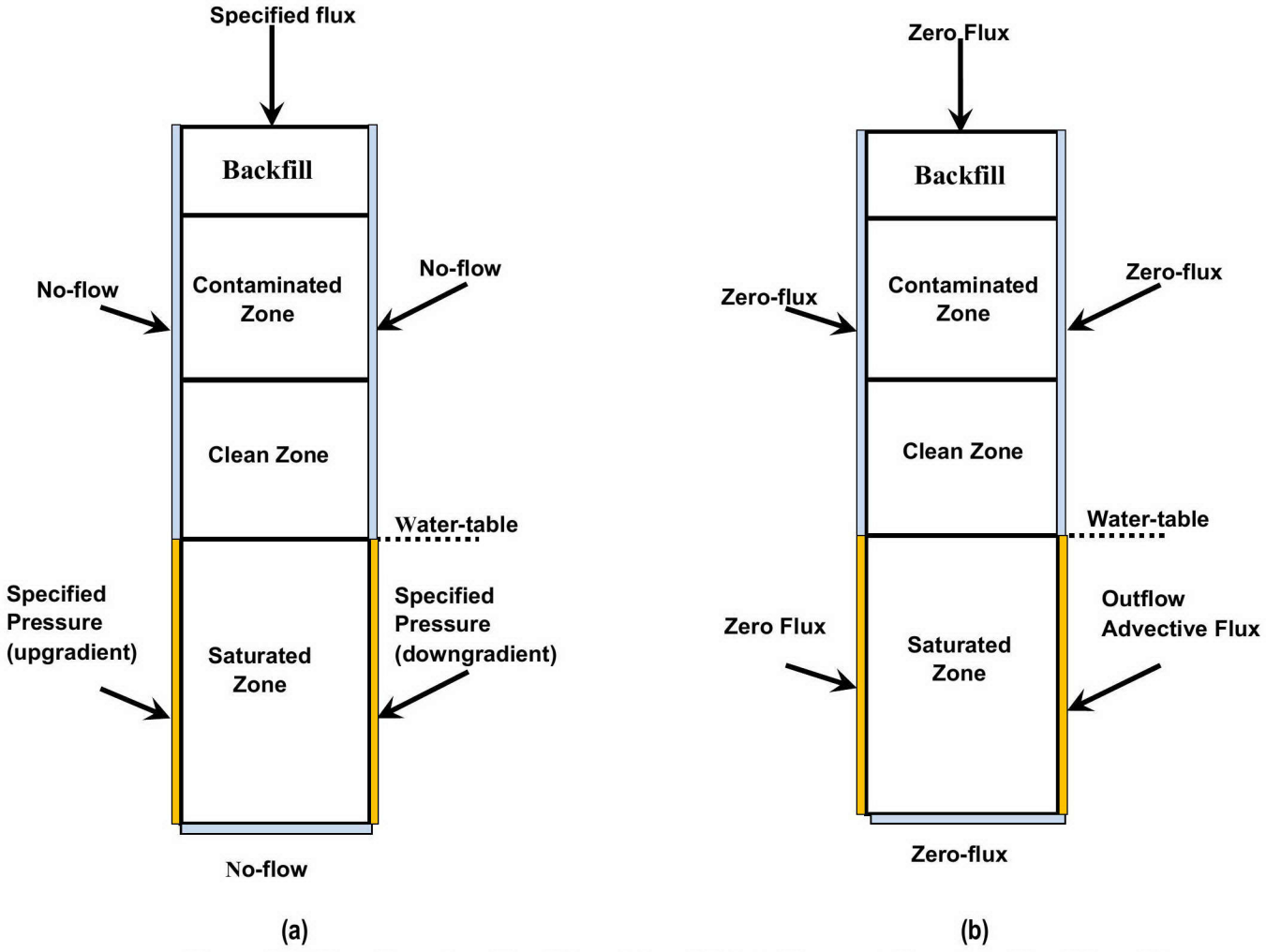

Figure 4-3. Flow Boundary Conditions (a) and Solute Transport Boundary Conditions (b)

Recharge

The net infiltration into the VZ, which is used in the model to represent recharge into the aquifer, is driven by the competition between precipitation, potential evaporation, transpiration, run-off, and run-on. In an arid climate, downward fluxes resulting from this competition are episodic and usually infrequent.

A number of studies have been carried out at the Hanford site to ascertain representative long-term averages of the episodic fluxes, i.e., recharge rates, such as those compiled in PNNL-14702 Rev. 1, for the 100 Area. The 100 Area-specific recharge rates in PNNL-14702 Rev. 1 varied with surface soil type and therefore provide an estimate of the range of possible recharge rates for various land uses. The four surface soil types were the Ephrata Sandy Loam, Ephrata Stony Loam, Burbank Loamy Sand, and Rupert Sand; however, recharge rates for the Ephrata Sandy Loam and the Ephrata Stony Loam were described as being identical (PNNL-14702 Rev. 1) and have been combined. Thus the three resulting surface soil types were assumed to represent recharge rate variability.

Two different scenarios of land use or land cover were evaluated: (1) Base case scenario and (2) Irrigation scenario. The calculations are performed differently for the pre-2010 simulations and the post-2010 simulations as the land use or land cover is expected to vary over time. For the pre-2010 simulations, the land use is the same for both scenarios and is broken into two periods defined by pre-operations period at Hanford (up to Year 1944) and operations period (from Year 1944 to 2010). For the post-2010 simulations the land cover for the base case scenario is varied over time to model the transition from bare soil to mixed grass and shrub cover to mature shrub steppe cover while for the irrigation scenario it is based on the assumption of bare soil cover throughout the simulation.

Recharge rates for each scenario were determined using the rates for each of the three surface soil types. In the STOMP simulations, recharge rates were conservatively simulated as a specified flux boundary condition applied to the uppermost boundary of the model (Figure 4-4) for each recharge scenario and each soil type. Rates were assumed to change over time in step function-fashion for the two scenarios.

For the pre-2010 simulations, land use and recharge rates were assumed to change from shrub-steppe (pre-operations) to bare soil (operations). Recharge rates for each type of land cover for each soil type were applied to the top boundary from the year 0 to 1944 for the pre-operations period and from 1944 to 2010 for the operations period (Table 4-1). Same conditions were applied to both the base case and irrigation scenario.

Three recharge time periods are specified in the post-2010 simulations to represent changes in recharge rates as listed in Table 4-2 and shown in Figure 4-4. Bare soil is assumed to be the land cover above the waste site during the first recharge period, which spans from 2010 to 2015. Same conditions were applied to both the base case and irrigation scenario. The second recharge period, which is 30 years in duration, for the base case scenario represents grasses and shrubs covering bare soil, followed by establishment of a mature shrub steppe for the remainder of the simulation period (third recharge period); thus recharge rates decrease with time (Table 4-2).

Table 4-1. Recharge Rates for Pre-2010 Simulations

Soil Type	Recharge Scenario	Recharge Rate (mm/yr)	
		0-1944	1944-2010
Ephrata Sandy Loam and Stony Loam	Base	1.5	17.0
	Irrigation		
Burbank Sandy Loam	Base	3.0	52.0
	Irrigation		
Rupert Sand	Base	4.0	44.0
	Irrigation		

Table 4-2. Recharge Rates for Post-2010 Simulations

Soil Type	Recharge Scenario	Recharge Rate (mm/yr)		
		2010-2015	2015-2045	2045-5010
Ephrata Sandy Loam and Stony Loam	Base case	17.0	3.0	1.5
	Irrigation	17.0	71.4	69.9
Burbank Sandy Loam	Base case	52.0	6.0	3.0
	Irrigation	52.0	74.4	71.4
Rupert Sand	Base case	44.0	8.0	4.0
	Irrigation	44.0	76.4	72.4

Note: Bare soil was assumed to be the land cover above the waste site for first recharge period from 2010 to 2015. The second recharge period, from 2015 to 2045, represents grasses and shrubs covering bare soil, while the third recharge period represents establishment of a mature shrub steppe for the remainder of the simulation.

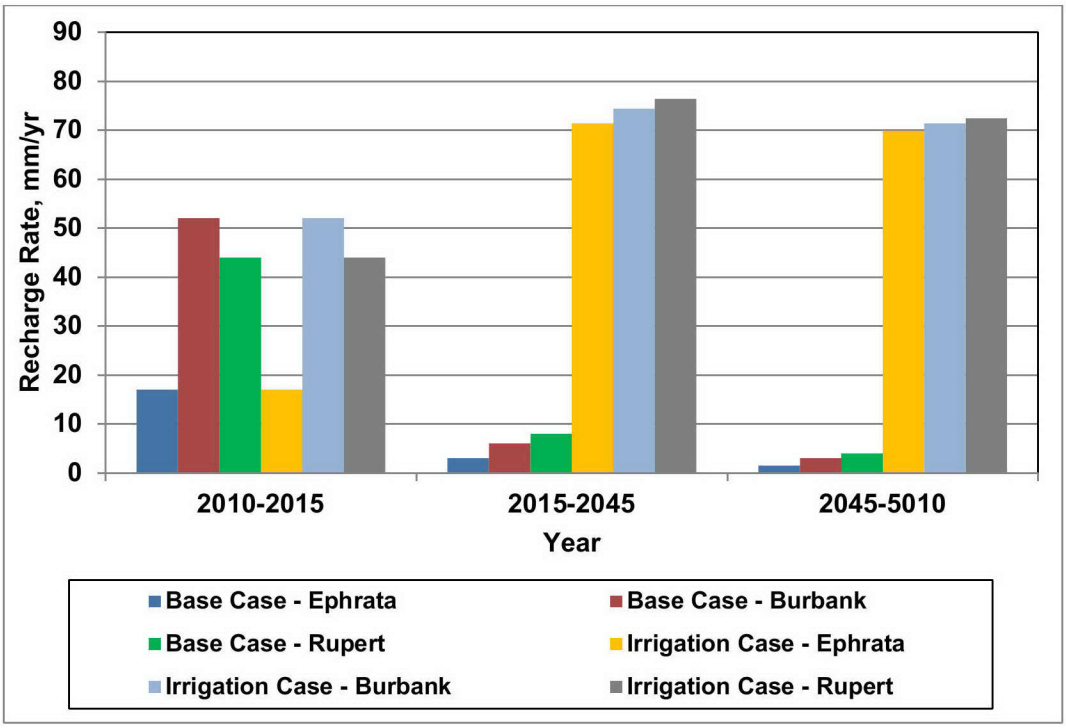

Figure 4-4. Recharge Rates Used for Modeling

For the irrigation scenario, the recharge rates in the second and third recharge periods were estimated using the same approach employed to assess interim remediation at 100 Area waste sites (DOE/RL-96-17 Rev. 6, *Remedial Design Report/Remedial Action Work Plan for the 100 Area*). These site assessments used Remedial Action Goals calculated from RESRAD simulations that assumed total recharge was a combination of irrigation and non-irrigation (base case) recharge rates. As the base case rates used in the RESRAD simulations were different than those adopted from PNNL-14702 Rev. 1, the RESRAD equation for total recharge was solved to determine the rate attributable to irrigation alone. According to the RESRAD manual, total recharge is a function of precipitation, evapotranspiration, run-off, and applied irrigation, and is defined as

$$I = (1 - C_e)[(1 - C_r)P_r + I_{rr}] \qquad \text{(Eqn. 4-9)}$$

in which I = annual recharge rate (LT^{-1}), C_e = evapotranspiration coefficient (dimensionless), C_r = runoff coefficient (dimensionless), P_r = annual precipitation rate (LT^{-1}), and I_{rr} = annual irrigation rate (LT^{-1}). Using Equation 4-9 and the RESRAD values for these parameters, C_e = 0.91, C_r = 0.2, P_r = 0.16 m/yr, and I_{rr} = 0.76 m/yr, yielded a total recharge rate of 80 mm/yr. Solving Equation 4-9 with I_{rr} = 0 yielded the non-irrigation total recharge rate of 11.6 mm/yr and therefore the recharge attributable to irrigation alone was 68.4 mm/yr, which was then added to the base case recharge rates to determine a recharge rate for the irrigation scenario for each soil type. For example, the irrigation scenario for the Ephrata soils set the recharge rate to 17 mm/yr from 2010 to 2015, 71.4 mm/yr from 2015 to 2045, and 69.9 mm/yr from 2045 to 5010 (Table 4-2).

Aquifer Flux

The specified pressure values assigned to the edges of the aquifer grid blocks were selected to create a hydraulic gradient across the model domain representative of each geographic area The hydraulic gradients used for the simulations were based on head data for March 2008 because the greatest number of wells was measured in that month, yielding the greatest number of measurements for all 100 Area source OUs. Triangulated Irregular Networks (TINs) were developed for the wells using ArcGIS, and hydraulic gradients were computed for each TIN (Table 4-3). The gradient magnitudes typically varied across two or more orders of magnitude, so the median, a measure of the central tendency of the computed gradients, was selected as a representative value, yielding hydraulic gradients of 0.0011 m/m at 100-D, 0.0021 m/m at 100-H, 0.0039 at 100-K, 0.0019 m/m at 100-BC, 0.0010 m/m at 100-F, 0.0014 m/m at 100-IU-2, and 0.0025 at 100-IU-6.

Table 4-3. Hydraulic Gradients for March 2008

		Hydraulic Gradient (m/m)				
Geographic Area	Number of TINs	Minimum	Maximum	Median	Arithmetic Average	Geometric Average
100-D	82	0.00018	0.00664	0.00110	0.00153	0.00113
100-H	28	0.00014	0.00592	0.00214	0.00258	0.00195
100-K	35	0.00085	0.00759	0.00389	0.00379	0.00341
100-F	14	0.0002	0.0025	0.0010	0.0011	0.0009
100-IU-2	8	0.0006	0.0024	0.0014	0.0014	0.0013
100-IU-6	14	0.0001	0.0071	0.0025	0.0028	0.0013
100-BC	14	0.000012	0.0469	0.0019	0.0018	0.00064

Note: TINs = Triangular Irregular Networks

4.4.2 Flow and Transport – Initial Conditions

For the pre-2010 flow simulations, initial pressure of 86,656.7 Pa, approximately equivalent to -1.5 m matric potential, was assigned to the nodes in the VZ, whereas the aquifer grid blocks were assigned values that matched the boundary condition pressures for the pre-2010 flow simulations. The purpose of the pre-2010 flow simulations is to develop a pressure field that is in equilibrium with the imposed boundary conditions appropriate to the geographic area. Final pressures from the pre-2010 simulations were used as the initial pressures for the post-2010 flow and transport simulations. Thus, the somewhat arbitrary initial condition selected for the pre-2010 flow simulations does not affect the screening level and PRG calculations.

Based on SGW-51818, *Conceptual Basis for Distribution of Highly Sorbed Contaminants in 100 Areas Vadose Zone*, all contaminants were grouped into two groups, one with lower distribution coefficients in the range $K_d < 2$ mL/g, and other with the higher distribution coefficients in the range ≥2 mL/g. For the lower K_d contaminants ($K_d < 2$ mL/g), a uniform concentration of 1.0 mg/kg was applied in the entire

vadose zone below the clean backfill up to 0.5 m (two grid blocks) above the water table for the low K_d contaminants; this is termed the effective 100:0 initial source distribution. Initial concentration in the 0.5 m zone above the water table was not applied due to the physical presence of capillary fringe and water table movement in the periodically rewetted zone that would result from river stage fluctuations. Placing the initial mass at the water table can also result in unrepresentative large peak releases in the simulation start because of the extreme concentration gradients created by the application of this initial condition. According to SGW-51818, for the higher K_d contaminants ($K_d \geq 2$ mL/g) if the soil column is shown to be not contaminated throughout the vertical profile, the most conservative assumption (i.e., contamination throughout the full thickness of the vadose zone) can be considerably relaxed with respect to soil cleanup decisions at waste sites in the 100 Areas. Based on this conclusion, for the high K_d contaminants the upper 70% of the vadose zone below the clean backfill was assumed to be contaminated while the lower 30% is treated as uncontaminated; this is termed the 70:30 initial source distribution. The 70:30 initial source distribution assumption is still conservative for the high K_d contaminants with respect to peak concentration based on observed limited vertical extent (SGW-51818).

A notable exception to the K_d based assignment of an initial source distribution was made for strontium-90. Because field data reveal that this contaminant is found throughout the vadose zone at several sites, use of the 70:30 initial source distribution for this contaminant would clearly be non-conservative. Accordingly, SSL and PRG values were calculated for strontium-90 using the 100:0 initial source distribution at all sites. Strontium-90 is distributed throughout the vadose zone despite its relatively high K_d value for reasons having to do with historic discharge practices that no longer dominate the subsurface. The unit initial concentration is arbitrary, but was chosen only for convenience in calculating PRG values and has no effect on the PRG values since the initial concentration C_I is accounted for in Equation 2-1.

In the calculation methodology, the saturated zone is assumed to be initially uncontaminated, which may not always be true since plumes can migrate from upgradient locations over time. However, due to several in-built modeling conservatisms, the screening level and PRG calculations are deemed to remain bounding when compared to the results derived from a more sophisticated site-specific predictive model that incorporates all the features and processes relevant at the scale of the model, including any contaminant migration from upgradient locations.

4.5 Model Parameterization

4.5.1 Parameters and ranges

To the extent possible, geographic area-specific hydraulic and transport parameter values were used in the STOMP simulations. Based on previous Hanford studies and on the fact that all available measurements of hydraulic properties made the same assumption, the sediments were assumed to follow the van Genuchten (1980) moisture-retention constitutive relation and the Mualem–van Genuchten relative-permeability constitutive relation (Mualem, 1976), thus requiring values to be specified in STOMP for each lithologic unit for:

- Saturated hydraulic conductivity, (LT^{-1}).
- Total porosity (L^3L^{-3}).
- Saturated volumetric water content, called diffusive porosity in STOMP (L^3L^{-3}).

- Residual saturation (dimensionless), equal to the residual volumetric water content divided by the saturated volumetric water content.
- van Genuchten α (L^{-1}), proportional to the inverse of the air entry matric potential.
- The dimensionless van Genuchten n fitting parameter.

The van Genuchten m parameter was assumed to be fixed and equal to $(n - 1)/n$ and the Mualem β exponent was assumed to be fixed at 0.5 (Mualem, 1976; RPP-20621 Rev. 0, *Far-Field Hydrology Data Package for the Integrated Disposal Facility Performance Assessment*).

Hanford and Ringold E units are well to poorly sorted sandy gravels or sandy silty gravels, whereas the backfill consists of poorly sorted sand and gravel with varying fractions of eolian loess and silt (RPP-20621 Rev. 0; SGW-44022 Rev. 1, *Geologic Data Package in Support of 100-BC-5 Modeling*; SGW-46279 Rev. 0, *Conceptual Framework and Numerical Implementation of 100 Areas Groundwater Flow and Transport Model*; PNNL-18564, *Selection and Traceability of Parameters to Support Hanford-Specific RESRAD Analyses Fiscal Year 2008 Status Report*). Within the 100-BC, 100-D, 100-H, 100-K, 100-F, 100-IU-2, and 100-IU-6 geographic areas, the Hanford formation tends to be coarser grained than the Ringold E. The former tends to contain larger gravel clasts than the latter. The Ringold E unit in the 100-BC VZ consists of semi-indurated clay, silt, fine- to coarse-grained sand, and pebble- to cobble-size gravel (SGW-44022 Rev. 1). Near the 100-D, 100-H, and 100-K geographic areas the Ringold E unit can locally contain significant amounts of gravel (SGW-40781 Rev. 1; SGW-41213 Rev. 0; and SGW-46279 Rev. 0). The 100-F, 100-IU-2, and 100-IU-6 geographic areas contain larger gravel clasts than the latter, but the Ringold E unit can locally contain significant amounts of gravel (SGW-46279 Rev. 0). Where present, the RUM was assumed to act as a lower bound (aquitard) for the aquifer (SGW-46279 Rev. 0) and so was not directly included in the STOMP simulations.

Geographic area specific values for several Mualem-van Genuchten hydraulic parameters were obtained for the Hanford formation from data package SGW-46279 Rev. 0 (entire 100 Area). This data package cites the data table for the unsaturated hydraulic properties of 15 samples of sandy gravels from the 100 Area, which were originally described in RPP-20621 Rev. 0. These 100 Area sediments are dominated by the gravel fraction (> 2 mm size), with gravel clasts accounting for 43% to 75% of the total sample mass (Table 4-4; RPP-20621 Rev. 0). Moisture-retention data were measured on the non-gravel sediment fraction (less than 2 mm size) and then corrected for the gravel fraction, whereas hydraulic conductivities were measured on the bulk samples that included the gravel fraction using the constant-head permeameter method for saturated hydraulic conductivity (K_s) and the unit gradient method for unsaturated hydraulic conductivity (RPP-20621 Rev. 0). Given the absence of any indication in the source document, the samples in Table 4-4 were assumed to represent the Hanford formation due to shallow sampling depth and high gravel content. Note that the Hanford formation is the most gravel-rich of the 100 Area lithologies. The K_s measurements were assumed to represent vertical hydraulic conductivity.

Table 4-4. Mualem-van Genuchten Hydraulic Parameters for Sandy Gravels in the 100 Area VZ

Sample	HSU[a]	Geographic area	Well Number	Depth (m)	% Gravel	θ_s (cm^3/cm^3)	θ_r (cm^3/cm^3)	α (1/cm)	n (-)	Fitted K_s (cm/s)*
2-1307	Ringold	100-HR-3	199-D5-14	18.90	43	0.236	0.0089	0.0130	1.447	1.29E-04
2-1308	Ringold	100-HR-3	199-D5-14	30.64	58	0.120	0.0208	0.0126	1.628	6.97E-05
2-1318	Hanford	100-HR-3	199-D8-54A	15.54	60	0.124	0.0108	0.0081	1.496	1.67E-04
2-2663	Hanford	100-BC-5	199-B2-12	8.20	61	0.135	0.0179	0.0067	1.527	6.73E-05
2-2664	Ringold	100-BC-5	199-B2-12	24.84	73	0.125	0.0136	0.0152	1.516	1.12E-04
2-2666	Hanford	100-BC-5	199-B4-9	21.49	71	0.138	0.00	0.0087	1.284	1.02E-04
2-2667	Hanford	100-BC-5	199-B4-9	23.93	75	0.094	0.00	0.0104	1.296	1.40E-04
3-0570	Hanford	100-KR-1	116-KE-4A	3.50	60	0.141	0.00	0.0869	1.195	2.06E-02
3-0577	Hanford	100-FR-3	199-F5-43B	7.16	66	0.107	0.00	0.0166	1.359	2.49E-04
3-0686	Hanford	100-FR-1	116-F-14	6.49	55	0.184	0.00	0.0123	1.600	5.93E-04
3-1702	Hanford	100-DR-2	199-D5-30	9.78	68	0.103	0.00	0.0491	1.260	1.30E-03
4-1086	Ringold	100-K	199-K-110A	12.77	65	0.137	0.00	0.1513	1.189	5.83E-02
4-1090	Hanford	100-K	199-K-111A	8.20	50	0.152	0.0159	0.0159	1.619	4.05E-04
4-1118	Hanford	100-K	199-K-109A	10.30	66	0.163	0.00	0.2481	1.183	3.89E-02
4-1120	Ringold	100-K	199-K-109A	18.90	63	0.131	0.0070	0.0138	1.501	2.85E-04

Source: RPP-20621 Rev .0

*Assumed to represent vertical hydraulic conductivity

a. HSU=hydrostratigraphic unit

The Mualem-van Genuchten hydraulic properties for the Hanford formation in the vadose zone were estimated for each geographic area by averaging the individual parameter values for all samples collected from that geographic area (Table 4-5). For example, four samples from boreholes 199-D5-14, 199-D5-30, and 199-D8-54A were selected to provide mean properties for 100-D and 100-H areas for the Hanford formation. Vertical saturated hydraulic conductivity of Hanford formation was averaged using the geometric mean of the four measurements whereas the other parameters were averaged using the arithmetic mean. An exception is the saturated volumetric water content, called θ_s in the van Genuchten moisture retention relation and diffusive porosity in STOMP. The θ_s values listed in Table 4-4 were determined by applying a gravel correction factor to the values determined in the laboratory on the < 2 mm fraction. However, the θ_s values appear to be underestimated and are hard to reconcile with the high K_s values estimated. Therefore, the site wide estimate of 0.25 was used for Hanford formation.

Mualem-van Genuchten parameters for the Hanford formation in 100-K were determined from the five samples taken from boreholes 116-KE-4A, 199-K-110A, 199-K-111A, and 199-K-109A. However, three of the samples have vertical K_s values that are roughly two orders of magnitude larger than the values for the other two measurements (Table 4-4). Consequently, two sets of Mualem-van Genuchten parameters were calculated. For vertical K_s, the first set was calculated by averaging the three large values using the geometric mean while the second set was calculated by taking the geometric mean of the two smaller values. The first set resulted in vertical K_s of 0.036 cm/s whereas the second set resulted in vertical K_s of 0.00034 cm/s. Since there were no aquifer test data for the Hanford in 100-K, the horizontal aquifer K_s was estimated as 10 times the vertical K_s.

The document and database review did not yield geographic area specific Mualem-van Genuchten property values for the Ringold E unit or the backfill material. In the absence of more site-specific data, Hanford-wide mean parameter values for the backfill and the Ringold E units were taken from Table A.12 of PNNL-18564. Mean hydraulic parameters for six samples of backfill and 18 samples of Ringold E gravels that were collected within the Hanford site (PNNL-18564) were selected to represent these units within the 100 Area (Tables 4-5, 4-6, and 4-7).

Geographic area-specific values for Hanford and Ringold E saturated hydraulic properties were presented in a separate chapter from the VZ properties in SGW-40781 Rev. 1; SGW-41213 Rev. 0; and SGW-46279 Rev. 0. Horizontal saturated hydraulic conductivity measurements from aquifer (pump) tests and slug tests for the several geographic areas presented therein were reviewed, and geometric means were calculated for each geographic area aquifer test measurements only (Table 4-5). Geometric means were used instead of arithmetic means because the K_s values spanned several orders of magnitude. The mean K_s values ranged between 3 and 98 m/day (Table 4-5). There were no pumping test data for the Hanford formation in the 100-K geographic area, so the horizontal K_s was set to be ten times the geometric mean vertical K_s for samples from the 100-K geographic area on the basis of an assumed horizontal to vertical anisotropy ratio of 10:1. Since there are no measurements for 100-IU-2 and 100-IU-6 geographic areas (Table 4-5), the parameters for Hanford formation in the VZ at 100-F are used to represent those at 100-IU-2 and 100-IU-6. The geometric mean of horizontal K_s for Hanford formation in the 100-H geographic area based on pumping tests is 97.9 m/day while the horizontal K_s for Hanford formation in the VZ is 2.10E-03 cm/s at 100-H (ECF-Hanford-11-0063 Rev. 5). The ratio of horizontal K_s for Hanford formation between the SZ and VZ is about 53.8 at 100-H, which was also used to determine the K_s for Hanford in the SZ at 100-BC since there are no measurements of K_s for Hanford formation in the SZ. The horizontal K_s for Hanford formation in the VZ at 100-BC is 1.02E-03 cm/s, and the corresponding horizontal K_s for Hanford formation in the SZ is about 47.4 m/day at 100-BC based on the

above ratio (Table 4-4). In addition, the horizontal K_s for Ringold E in the SZ is about 6.2 m/day based on the currently calibrated 100 Area groundwater flow and transport model.

The horizontal K_s value for the Hanford unit in the aquifer at 100-F is determined by the current 100 Area groundwater flow and transport model, which is about 48.3 m/day. The vertical K_s value for Hanford unit in the aquifer is assumed to be ten times smaller than horizontal K_s at 100-F, which is 4.83 m/day. At 100-IU-2 and 100-IU-6, the horizontal and vertical K_s values for the Hanford unit in the aquifer are represented by the corresponding values at 100-K (ECF-Hanford-11-0063 Rev. 5). Furthermore, the corresponding values at 100-D (ECF-Hanford-11-0063 Rev. 5) are used to represent the horizontal and vertical K_s values for Ringold E unit in the aquifer at the 100-F, 100-IU-2, and 100-IU-6 OUs. Table 4-5 lists all the hydraulic parameters used in the STOMP simulations at 100-D, 100-H, and 100-K. Table 4-6 lists all the hydraulic parameters used in the STOMP simulations at 100-F, 100-IU-2, and 100-IU-6. Table 4-7 lists all the hydraulic parameters used in the STOMP simulations at 100-BC.

Table 4-5. Hydraulic Parameters Used for Geographic Areas 100-D, 100-H and 100-K

Geographic Area	Zone*	Unit	Total porosity n_T	Diffusive porosity n_D	van Genuchten α (1/cm)	van Genuchten n	Residual saturation s_r	Horizontal Saturated K (cm/s)	Vertical Saturated K (cm/s)
100-D	BF	Hanford	0.276	0.262	0.019	1.4	0.162	5.98E-04	5.98E-04
	VZ	Hanford	0.28	0.25	0.029	1.378	0.02	4.66E-03	4.66E-04
	VZ	Ringold E	0.28	0.28	0.013	1.538	0.054	9.48E-04	9.48E-05
	SZ	Hanford	0.28	0.25	0.021	1.458	0.04	6.42E-02	6.42E-03
	SZ	Ringold E	0.28	0.28	0.008	1.66	0.093	2.59E-02	2.59E-03
100-H	BF	Hanford	0.276	0.262	0.019	1.4	0.162	5.98E-04	5.98E-04
	VZ	Hanford	0.28	0.25	0.029	1.378	0.02	4.66E-03	4.66E-04
	VZ	Ringold E	0.28	0.28	0.013	1.538	0.054	9.48E-04	9.48E-05
	SZ	Hanford	0.28	0.25	0.021	1.458	0.04	1.13E-01	1.13E-02
	SZ	Ringold E	0.28	0.28	0.008	1.66	0.093	4.28E-03	4.28E-04
100-K1	BF	Hanford	0.276	0.262	0.019	1.4	0.162	5.98E-04	5.98E-04
	VZ	Hanford	0.28	0.25	0.168	1.189	0	2.83E-01	2.83E-02
	VZ	Ringold E	0.28	0.28	0.151	1.189	0	5.83E-01	5.83E-02
	SZ	Hanford	0.28	0.25	0.162	1.189	0	3.60E-01	3.60E-02
	SZ	Ringold E	0.28	0.28	0.008	1.66	0.093	4.86E-03	4.86E-04
100-K2	BF	Hanford	0.276	0.262	0.019	1.4	0.162	5.98E-04	5.98E-04
	VZ	Hanford	0.28	0.25	0.016	1.619	0.064	4.05E-03	4.05E-04
	VZ	Ringold E	0.28	0.28	0.014	1.501	0.025	2.85E-03	2.85E-04
	SZ	Hanford	0.28	0.25	0.014	1.56	0.04	1.13E-01	1.13E-02
	SZ	Ringold E	0.28	0.28	0.008	1.66	0.093	4.86E-03	4.86E-04

*BF = Backfill; VZ = Vadose Zone; SZ = Saturated Zone

Table 4-6. Hydraulic Parameters† Used for Geographic Areas 100-F, 100-IU2 and 100-IU6

Geographic Area	Zone*	Unit	Total porosity n_T	Diffusive porosity n_D	van Genuchten α (1/cm)	van Genuchten n	Residual saturation s_r	Horizontal Saturated K (cm/s)	Vertical Saturated K (cm/s)
100-F	BF	Hanford	0.276	0.262	0.019	1.4	0.162	5.98E-04	5.98E-04
	VZ	Hanford	0.28	0.25	0.0145	1.48	0	3.83E-03	3.84E-04
	VZ	Ringold E	0.28	0.28	0.008	1.66	0.093	4.13E-03	4.14E-04
	SZ	Hanford	0.28	0.25	0.0145	1.48	0	5.59E-02	5.59E-03
	SZ	Ringold E	0.28	0.28	0.008	1.66	0.093	2.59E-02	2.59E-03
100-IU-2 & 100-IU-6	BF	Hanford	0.276	0.262	0.019	1.4	0.162	5.98E-04	5.98E-04
	VZ	Hanford	0.28	0.25	0.0145	1.48	0	3.83E-03	3.84E-04
	SZ	Hanford	0.28	0.25	0.0145	1.48	0	1.13E-01	1.13E-02
	SZ	Ringold E	0.28	0.28	0.008	1.66	0.093	2.59E-02	2.59E-03

*BF = Backfill; VZ = Vadose Zone; SZ = Saturated Zone

† The dataset is preliminary and may be subject to revision.

Table 4-7. Hydraulic parameters used for Geographic Area 100-BC

Geographic Area	Zone*	Unit	Total porosity n_T	Diffusive porosity n_D	van Genuchten α (1/cm)	van Genuchten n	Residual saturation s_r	Horizontal Saturated K (cm/s)	Vertical Saturated K (cm/s)
100-BC	BF	Hanford	0.276	0.262	0.019	1.4	0.162	5.98E-04	5.98E-04
	VZ	Hanford	0.28	0.25	0.009	1.369	0.024	9.87E-04	9.87E-05
	VZ	Ringold E	0.28	0.28	0.015	1.516	0.050	1.12E-03	1.12E-04
	SZ	Hanford	0.28	0.25	0.009	1.369	0.024	5.49E-02	5.49E-03
	SZ	Ringold E	0.28	0.28	0.015	1.516	0.050	7.18E-03	7.18E-04

*BF = Backfill; VZ = Vadose Zone; SZ = Saturated Zone

For transport simulations, STOMP requires the particle density (ρ_p) values of the backfill, Hanford formation, and Ringold units. The particle density of each unit can be calculated using the bulk density (ρ_B) and dividing it by 1- Total Porosity term. Bulk density is necessary for retardation scaling factor calculations. Estimates of bulk density for Hanford formation and Ringold E unit were obtained from PNNL-14702 Rev. 1, which gave 1.91 g/cm^3 for the Hanford formation and 1.90 g/cm^3 for the Ringold E unit. The bulk density estimate of 1.94 g/cm^3 for backfill was obtained from PNNL-18564. Dispersion was conservatively assumed to be negligible, so dispersivity values were all set to zero. Barring numerical dispersion introduced by the solution method, setting dispersivity values to zero yields higher peak concentrations than setting non-zero values and therefore yields conservative PRG values.

4.5.2 Sorption Partition Coefficients

Partition coefficient, K_d, values for sorption along with the radionuclide half-lives were taken from ECF-Hanford-10-0442 Rev. 0, *Calculation of Nonradiological Preliminary Remediation Goals using the Fixed Parameter 3-Phase Equilibrium Partitioning Equation for Groundwater Protection in the 100 Areas and 300 Area*. As described in Section 5, simulations were run to produce peak groundwater concentrations for a subset of the range of distribution coefficients required for all contaminants of interest. Typically, the subset comprised 26 distribution coefficients (Table 4-8) between 0 and 16 ml/g. Dividing the K_d range from 0 to 16 ml/g into 26 distribution coefficients and performing calculations provides enough resolution for interpolation in peak concentration when the K_d for a given contaminant falls between the two values for which simulations were performed. For analytes whose K_d values are greater than 16 ml/g the peak concentration was calculated by using the scaling methods described in Section 5.

4.6 Implementation Using STOMP

Calculations using STOMP are performed in two modeling steps. The first step, called the pre-2010 model, is used to simulate flow through the representative column up to Year 2010. A long-term transient-state simulation is performed so that near steady-state hydrologic conditions are reached in the model domain based on the prescribed boundary conditions. The result of this model is used to set up the initial conditions for the second modeling step where both flow and transport are simulated for a period of 1,000 years (starting from year 2010). A detailed description of the STOMP input files [2]for both models is presented in Appendix B for a representative column chosen from 100-D geographic area.

[2] The parameter values are presented for the purpose of illustration of the model set-up only and do not necessarily imply that the final calculations were run with this parameter set.

Table 4-8. Distribution Coefficients (K_d) used in STOMP Simulations

Distribution Coefficient (ml/g)
0
0.00001
0.0001
0.001
0.01
0.02
0.04
0.06
0.08
0.1
0.2
0.3
0.4
0.5
0.6
0.7
0.8
0.9
1.0
2.0
4.0
8.0
10.0
12.0
14.0
16.0

5. Model Results and Application

The peak groundwater concentrations obtained by employing STOMP were used to identify those constituents that pose a significant risk from a fate and transport perspective. The objective was to determine concentration of contaminants in the VZ that will not cause an exceedance of groundwater and surface water regulatory standards for the ranges of conditions observed within the 100 Area. Two sets of residual contaminant concentrations for the VZ were developed: screening levels and PRGs, each with its own specific purpose.

The screening level for each analyte is defined as the larger of a background level, a practical quantification limit, or a calculated screening level that was computed using STOMP and a highly conservative set of assumptions on contaminant distribution and recharge rates. Screening levels are used to separate analytes from COPCs and determine which COPCs warrant further evaluation or investigation (EPA/540/R-96/018; EPA/540/R-95/128; DOE-STD-1153-2002). PRGs are defined as the allowable concentrations or activities of constituents in the VZ that are protective of groundwater and surface water quality. PRGs are calculated for COPCs that failed the screening process. For the lower K_d contaminants ($K_d < 2$ mL/g), a uniform concentration of 1.0 mg/kg was applied in the entire vadose zone below the clean backfill up to 0.5 m (two grid blocks) above the water table for the low K_d contaminants; this is termed the effective 100:0 initial source distribution. Initial concentration in the 0.5 m zone above the water table was not applied due to the physical presence of capillary fringe and water table movement in the periodically rewetted zone that would result from river stage fluctuations. Placing the initial mass at the water table can also result in unrepresentative large peak releases in the simulation start because of the extreme concentration gradients created by the application of this initial condition. According to SGW-51818, for the higher K_d contaminants ($K_d \geq 2$ mL/g) if the soil column is shown to be not contaminated throughout the vertical profile, the most conservative assumption (i.e., contamination throughout the full thickness of the vadose zone) can be considerably relaxed with respect to soil cleanup decisions at waste sites in the 100 Areas. Based on this conclusion, for the high K_d contaminants the upper 70% of the vadose zone below the clean backfill was assumed to be contaminated while the lower 30% is treated as uncontaminated; this is termed the 70:30 initial source distribution. The 70:30 initial source distribution assumption is still conservative for the high K_d contaminants with respect to peak concentration based on observed limited vertical extent (SGW-51818)

5.1 Peak Concentration Calculation and Scaling

Peak concentrations for use in calculating SSLs or PRGs were obtained by running multiple simulations using STOMP for the set of Kd values listed in Table 4-8 for the irrigation recharge scenario in the case of SSLs, and for the native vegetation recharge scenario in the case of PRGs. Peak concentrations are then estimated based on the Kd value of each contaminant from linear interpolation of the results of the STOMP simulations as follows:

1. For contaminants in the range $1.0 < K_d < 2.0$, a fitted linear regression equation created by performing a linear regression of STOMP simulated peak concentrations against K_d values in the range $0.5 < K_d < 2.0$. This range is estimated separately from higher K_d values because a different initial solute condition (100:0 initial distribution) is used for $K_d < 2.0$ than for higher values. An example is shown in Figure 5-1 using 100-D representative stratigraphic column 1 with irrigation recharge for Ephrata sandy loam soil. For the contaminants with higher K_d values, the inverse of peak concentrations ($1/CPK$) varies nonlinearly with K_d values.

2. For the contaminants in the range $2.0 \leq K_d \leq 8.0$, the 'FORECAST' function in Excel® that uses a best fit (least squares) linear regression is used to perform a linear regression of STOMP simulated peak concentrations against K_d values over the same range. This range is estimated separately from lower K_d values because a 70-30 distribution is used (in contrast to the 100:0 initial solute distribution applied for lower Kd values).

3. For contaminants in the range $K_d > 8.0$, a fitted linear regression equation created by performing a linear regression of STOMP simulated peak concentrations against Kd values in this range is used. The peak concentrations beyond the simulated K_d values were estimated using regression equation mentioned. An example is shown in Figure 5-2 using 100-D column 1 with irrigation recharge scenario rates for Ephrata sandy loam or stony loam surface soil.

The numerical threshold for breakthrough within 1000 years was set to 1.0×10^{-4} µg/L for non-radionuclide contaminants and 1.0×10^{-4} pCi/L for radionuclide contaminants. If breakthrough above this threshold was not simulated in more than one of the representative stratigraphic columns, and/or when the SSL value for any analyte exceeded 384,000 µg/kg (a physical upper bound developed in Section **Error! Reference source not found.**1 below), then the results were assigned the code "NR" to designate a non-representative result. For SSLs, this condition was observed for contaminants with K_d values greater than 22 mL/g; therefore the SSLs for all contaminants with K_d greater than 22 mL/g were coded "NR." For PRGs, this condition was observed for contaminants with K_d values greater than 1 mL/g; therefore the PRGs for all contaminants with K_d greater than 1 mL/g were coded "NR."

If simulated peak concentrations are very small, application of Equation 2-1 can lead to physically unrealistic soil concentrations (e.g., 10 kg of aluminum per kg of soil) for the screening levels or PRGs. Although not strictly necessary, the maximum PRG value was capped at an estimate of the total contaminant mass that could occupy the void volume within a kg of soil.

The bulk density (ρ_B) of the soil in the 100 Area is 1930 kg/m^3. For 1 kg of soil, the total volume (V_T) of the soil is:

$$\frac{1\ kg}{1930\ kg/m^3} = 5.18\times10^{-4}\ \mathrm{m}^3$$

The contaminant is assumed to fully occupy all of the pores. Thus, the maximum mass of contaminant in the soil is:

$$n \times V_T \times \rho_p$$

where n is the total porosity and ρ_p is the particle density of the contaminant. In the 100 Area, the total porosity of Hanford formation or Ringold E unit is 0.28, and the particle density of the contaminant is assumed to equal the particle density of the soil, 2650 kg/m^3. The maximum mass of contaminant in 1 kg soil is given by:

$$0.28\times5.18\times10^{-4}\ \mathrm{m}^3\times2650\ \mathrm{kg/m}^3 = 0.384\ \mathrm{kg} = 3.84\times10^5\ \mathrm{mg}$$

Thus the maximum PRG for non-radionuclides is 384,000 mg per kg of soil. Any non-radionuclide PRG with a larger value was replaced by 384,000 mg per kg of soil.

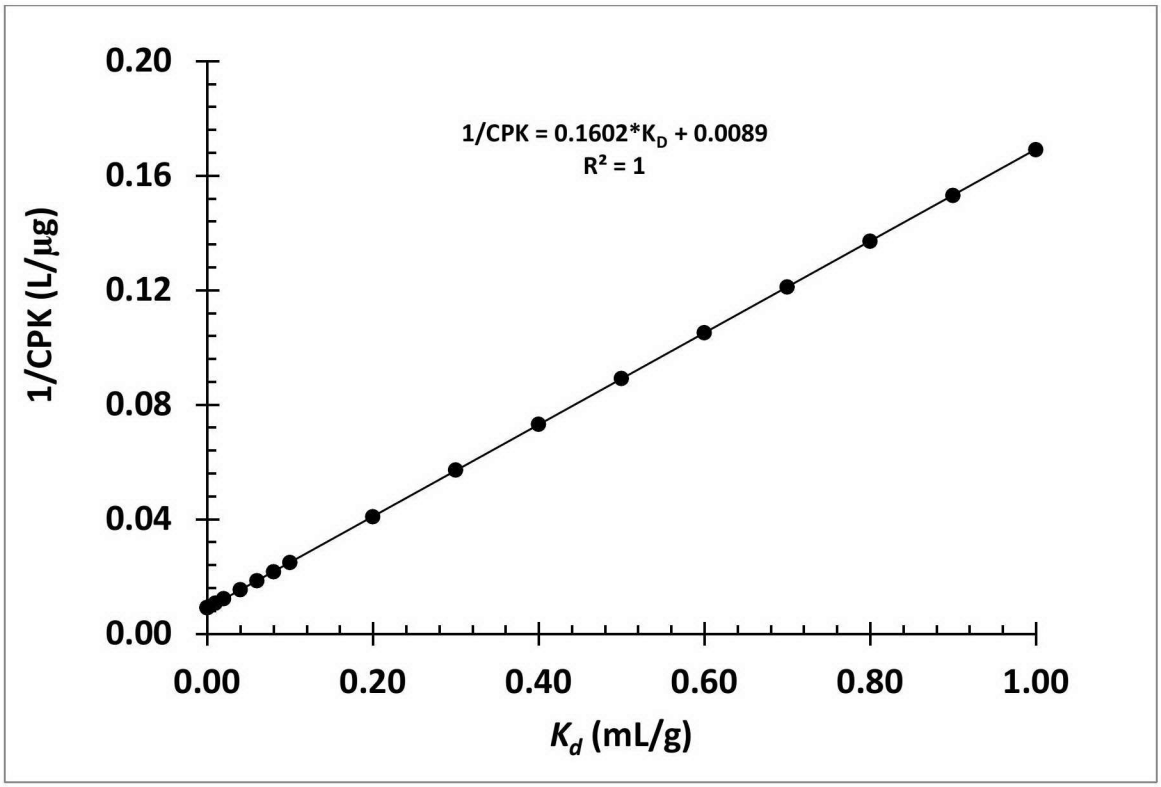

Figure 5-1. Linear Regression Equation for Low K_d Contaminants for 100-D Column 1 and Irrigation Case Recharge with Ephrata Sandy Loam soil

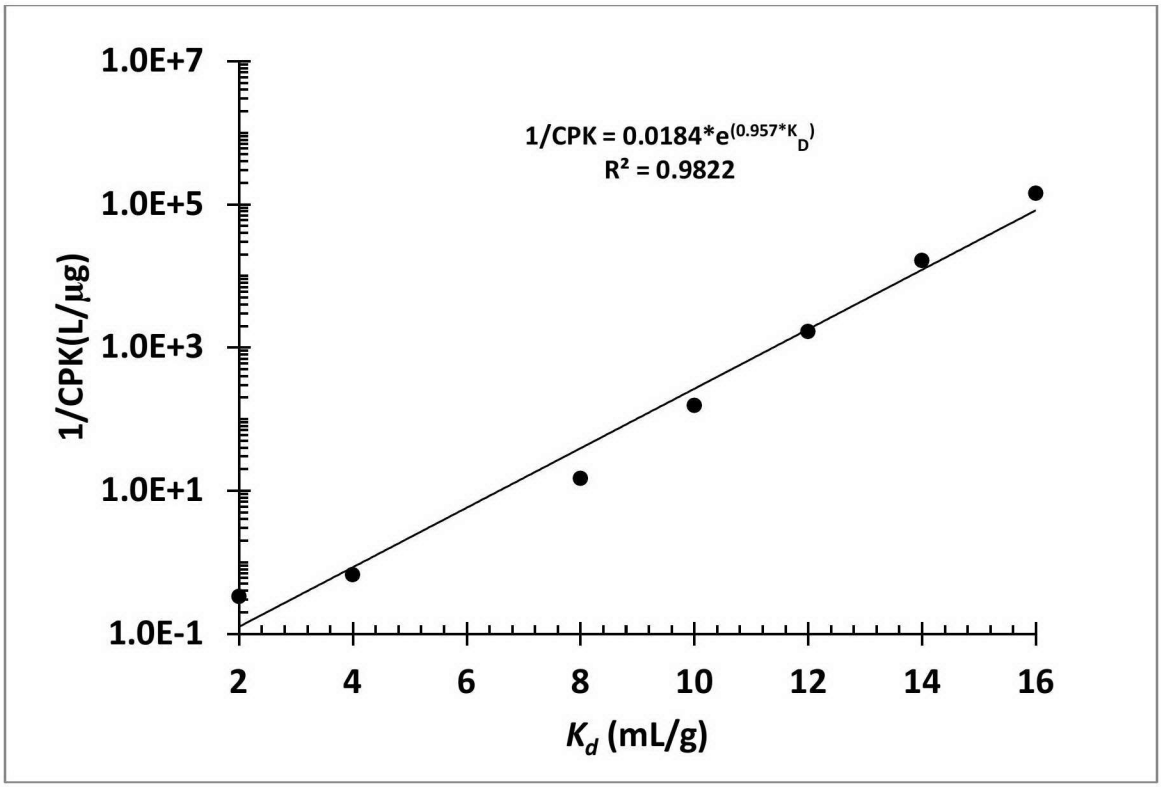

Figure 5-2. Linear Regression Equation for High K_d Contaminants for 100-D Column 1 and Irrigation Case Recharge with Ephrata Sandy Loam soil

For radionuclides in groundwater, the maximum contaminant mass was transformed into a maximum radionuclide activity using the specific activity of each radionuclide. The specific activity is defined as the amount of radioactivity of a particular radionuclide per unit mass of the radionuclide, which is calculated by:

$$SpA\ (pCi/g) = 3.578 \times 10^{17}/(m_{amu} \times t_{1/2}) \qquad \text{(Eqn. 5-1)}$$

where SpA is the specific activity (pCi/g), m_{amu} is the atomic mass unit (amu), and $t_{1/2}$ is the decay rate (yr). The specific activities for nickel-63, tritium, and strontium-90, which were the only radionuclides with very large PRG values, were calculated using Equation 5-1, and the maximum PRG values were obtained by multiplying the specific activity by the maximum contaminant mass (Table 5-1).

Table 5-1. Specific Activity and Maximum PRG Value for Selected Radionuclides

Radionuclide	Atomic mass	Half-life (yr)	Specific Activity (pCi/g)	Maximal PRG (pCi/g)
Nickel-63	58.6934	96	6.35E+13	2.44E+13
Tritium	3.0160492	12.35	9.61E+15	3.69E+15
Strontium-90	89.9	29.12	1.37E+14	5.26E+13

5.2 Screening Level and PRG Results

Soil screening level and PRG development captures the effects of geologic variability by simulating flow and transport through a set of representative stratigraphic columns within a given geographic area. The calculations are performed using same modeling assumptions except that the irrigation recharge rates are applied for the soil screening level calculations while the base case (ambient) recharge rates are applied for the PRG calculations. Peak groundwater concentrations are simulated for each representative column and using Equation 2-1 the screening levels and PRGs are calculated separately for each representative column in the geographic area. The screening levels and PRGs for each representative column are compared for a given contaminant and a minimum value is adopted as the final screening level and final PRG value for each geographic area.

The screening level and PRG values are computed separately for the protection of groundwater and surface water (using Equation 2-1) because of different water quality standards. The federal and/or state drinking water standards are used for groundwater protection and aquatic water quality standards are used for surface water protection. The final screening level and PRG values for groundwater and surface water are developed to guide risk assessment decisions and for evaluation of selected remedies.

The STOMP simulations provide predictions of peak groundwater concentration for given recharge rates, sediment types, thicknesses, and properties appropriate to the geographic areas. The peak concentration within the 1000 year simulation was used to calculate the screening value and PRG value. Note that, particularly for contaminants with greater sorption, peaks may occur beyond 1000 years but these are not calculated or reported because a 1000-year limit was established for purposes of PRG calculation by agreement with regulatory agencies. One set of test case simulations were run for selecting the low K_d and high K_d contaminants. Column 1 from 100-D OU was chosen for the test case. The native vegetation recharge scenario rates for Ephrata sandy loam soil was applied and effective 100:0 distribution was applied for the initial contaminant source distribution. The breakthrough curves for different distribution

coefficients are shown in Figure 5-3. Observation of the breakthrough curves in Figure 5-3 reveals that for the distribution coefficients <2 mL/g the peak concentration occurs within 1000 years and for the distribution coefficients >2 mL/g the peak concentration occurs after 1000 years. As a result, the contaminants were grouped into two groups, one with low distribution coefficients < 2 mL/g and another one with the high distribution coefficients ≥ 2 mL/g for both screening value and PRG calculation.

For the low K_d contaminants effective 100:0 source distribution was used and for the high K_d contaminants 70:30 source distribution was used. The final screening value and PRG value for each recharge scenario is chosen by selecting the minimum value (lowest PRG calculated) from all of the representative columns for that geographic area. If the minimum value calculated is below the estimated quantitation limit (EQL) for soil then EQL was substituted for screening and PRG value (as a lower threshold). The soil EQL values represent the lowest concentration that can be reliably measured within specified limits of precision and accuracy during routine laboratory operating conditions. EQLs are normally arbitrarily set rather than explicitly determined; for this calculation EQLs are those specified in Appendix A of DOE/RL-2009-41 Rev. 0, *Sampling and Analysis Plan for the 100-K Decision Unit Remedial Investigation/Feasibility Study,* and DOE/RL-2009-40 Rev. 0, *Sampling and Analysis Plan for the 100-K Decision Unit Remedial Investigation/Feasibility Study*.

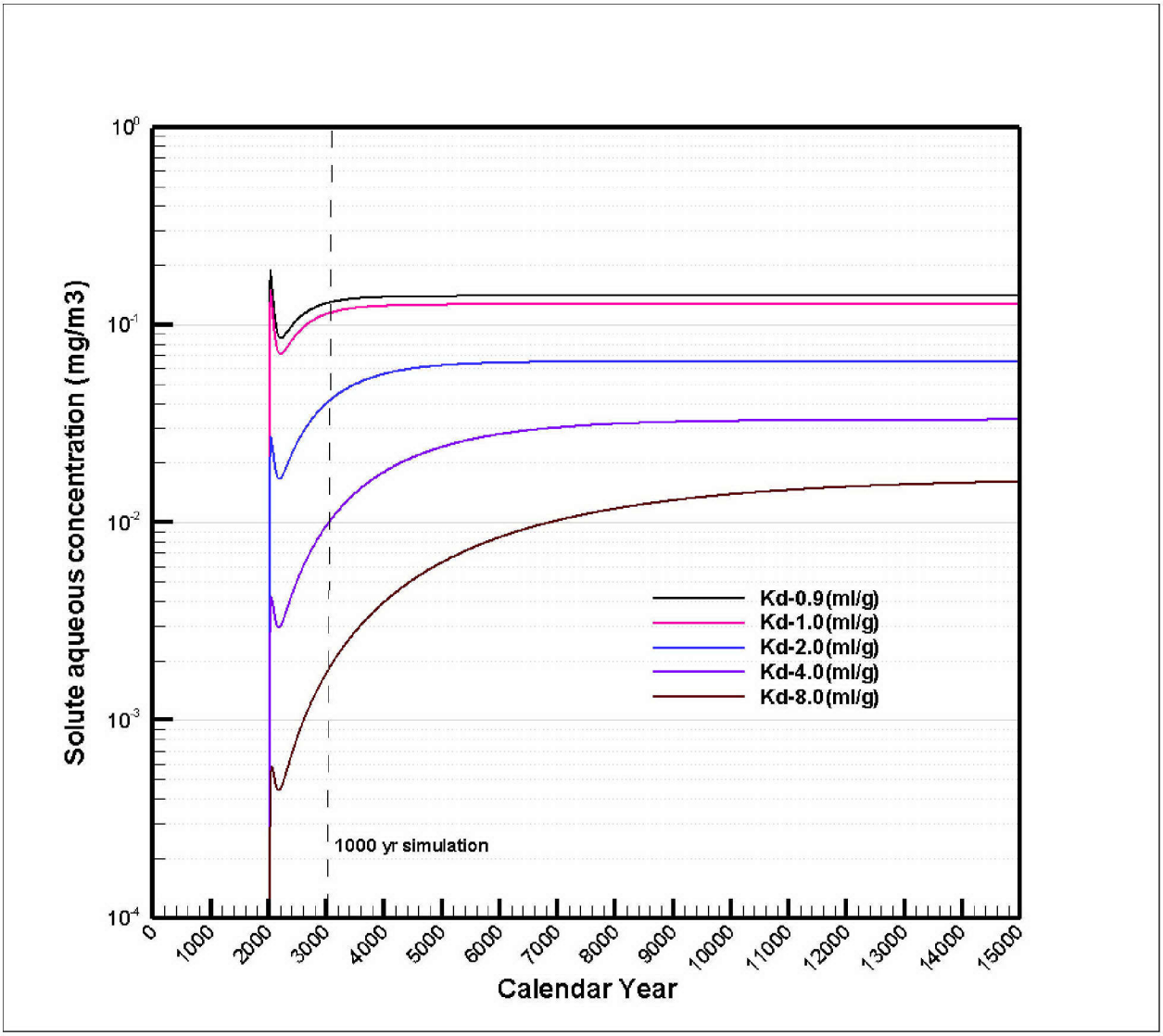

Figure 5-3. Breakthrough Curves for Different Distribution Coefficients with Base Case Recharge (Column1 0f 100-D OU)

In the absence of sufficient data to determine the subsurface extent of any contaminant, the contaminated interval was assumed to be full thickness of the vadose zone below the waste site in calculating soil screening levels and PRGs. This is a conservative assumption for many of the 100 Area waste sites, especially for those waste sites where large volumes of liquid wastes were discharged to the vadose zone.

Table 5-2 summarizes the representative 1-D columns evaluated in the calculations along with their composition in terms of geologic units and soil type for each geographic area. The 1-D column chosen for screening level and PRG calculations are listed. Note that the representative columns for 100-F and 100-IU geographic areas are based on preliminary information and may be revised.

Examples of the soil screening levels and groundwater PRG values for three contaminants for the representative Column 1 in 100-D geographic area are shown in Table 5-3. As expected, soil screening levels for the irrigation recharge scenario are smaller than the PRGs for the base case scenario. As the magnitude of K_d increases, the magnitude of the PRG also increases, all other conditions held constant.

Examination of results reveals that PRG values for the Rupert sand soil type are smaller than those for the Ephrata soils. This behavior is a direct result of the relatively high recharge rates for the Rupert sand and the relatively small recharge rate for the Ephrata soils.

Table 5-2. Representative Soil Column Characteristics and Column Number Used for Screening Level and PRG Calculation

Geographic Area	Representative Column Index	Representative VZ thickness (m)	Representative VZ Composition	Thickness of Hanford fm. in VZ (m)	Thickness of Ringold E in VZ (m)	SZ Composition	Column Index Used For Screening Level	Soil Type Used For Screening Level	Column Index Used For PRG Calculation	Soil Type Used For PRG Calculation
100-D	1	25	100% Hanford fm.	25.0	0.0	100% Hanford	3 and 4	Ephrata Sandy Loam and Rupert Sand	5	Burbank Sandy Loam
	2	20	100% Hanford fm.	20.0	0.0	100% Hanford				
	3	25	75% Hanford 25% Ringold E	20.0	5.0	100% Ringold E				
	4	20	80% Hanford 20% Ringold E	16.0	4.0	100% Ringold E				
	5	25	60% Hanford 40% Ringold E	15.0	10.0	100% Ringold E				
	6	15	60% Hanford 40% Ringold E	9.0	6.0	100% Ringold E				
100-H	1	12	100% Hanford fm.	12.0	0.0	100% Hanford	1	Ephrata Sandy Loam and Rupert Sand	1	Burbank Sandy Loam
	2	8	100% Hanford fm.	8.0	0.0	100% Hanford				
100-K	1	25	40% Hanford 60% Ringold E	10.0	15.0	100% Ringold E	2 and 3	Rupert Sand	1	Burbank Sandy Loam
	2	15	70% Hanford 30% Ringold E	10.5	4.5	100% Ringold E				
	3	20	50% Hanford 50% Ringold E	10.0	10.0	100% Ringold E				
	4	20	40% Hanford 60% Ringold E	8.0	12.0	100% Ringold E				
	5	20	30% Hanford 70% Ringold E	6.0	14.0	100% Ringold E				
100-BC	1	14	100% Hanford fm.	14.0	0.0	100% Hanford	NA	NA	NA	NA
	2	23	100% Hanford fm.	23.0	0.0	100% Ringold E				
	3	12	100% Hanford fm.	12.0	0.0	100% Ringold E				
	4	30	100% Hanford fm.	30.0	0.0	15% Hanford 85% Ringold E				
	5	22	100% Hanford fm.	22.0	0.0	15% Hanford 85% Ringold E				
100-F*	1	12	100% Hanford fm.	12.0	0.0	100% Hanford	NA	NA	NA	NA
	2	10	100% Hanford fm.	10.0	0.0	100% Hanford				
	3	8	100% Hanford fm.	8.0	0.0	100% Hanford				
	4	9	80% Hanford 20% Ringold E	7.2	1.8	100% Ringold E				
	5	12	40% Hanford 60% Ringold E	4.8	7.2	100% Ringold E				
100-IU*	1	40	100% Hanford fm.	40.0	0.0	17% Hanford 83% Ringold E	NA	NA	NA	NA
	2	22	100% Hanford fm.	22.0	0.0	100% Hanford				
	3	10	100% Hanford fm.	10.0	0.0	100% Hanford	NA	NA	NA	NA
	4	8	100% Hanford fm.	8.0	0.0	100% Hanford				

NA = Information not available currently

* Some representative columns and thicknesses are preliminary and subject to revision

Table 5-3. Example Groundwater Protection Concentration Results for the First Representative Column in 100-D Geographic Area

Contaminant	K_d Value (ml/g)	Ground Water Standard (μg/L)	Soil Screening Level (mg/kg)			PRG (mg/kg)		
			Effective 100-0 source distribution: Irrigation Scenario			Effective 100-0 source distribution: Base Case Scenario		
			Ephrata Loam	Burbank Loam	Rupert Sand	Ephrata Loam	Burbank Loam	Rupert Sand
Cr(VI)	0.8	48	66	65	63	1950	311	410
Benzene	0.062	0.8	0.15	0.15	0.15	0.97	0.25	0.30
Trichloro-ethene	0.094	0.49	0.12	0.12	0.11	0.81	0.20	0.24

5.3 Validation of Conservative Basis for 70:30 Source Distribution for High K_d Contaminants

SGW-51818, *Conceptual Basis for Distribution of Highly Sorbed Contaminants in 100 Areas Vadose Zone*, recommends that for higher K_d contaminants ($K_d \geq 2$ mL/g) the most conservative assumption that contamination is uniformly distributed throughout the full thickness of the vadose zone can be considerably relaxed with respect to soil cleanup decisions at waste sites in the 100 Areas. Based on this conclusion, for higher K_d contaminants the upper 70% of the vadose zone below the clean backfill was assumed to be contaminated while the lower 30% was assumed uncontaminated. This is termed the 70:30 initial source distribution assumed for higher K_d contaminants, in contrast with the 100:0 initial source distribution assumed for lower K_d contaminants. However, the possibility that contaminant of higher K_d contaminants could be present in the deeper portions of the vadose zone was recognized, and such case could be addressed if appropriate using site-specific modeling under the graded approach (DOE/RL-2011-50).

RI borehole data collected in the 100-D/H area provided many indications that some higher K_d contaminants ($K_d \geq 2$ mL/g) were present in the lower portion of the vadose zone, leading to the need to evaluate the appropriateness of the 70:30 initial contaminant distribution in these locations. The process for identifying specific waste sites and contaminants that merit further consideration is found in Appendix D, and excluded cases for which:

- boreholes did not sample the lower 30 percent of the vadose zone
- contaminants had no background values
- reported concentrations in the lower 30 percent of the vadose zone were within the range of background
- contaminants had $K_d > 25$ mL/g
- contaminants was strontium-90

The reason for the $K_d > 25$ mL/g exclusion basis was that results from vadose zone modeling to develop SSLs show that contaminants with K_d values higher than 25 mL/g result in non-representative (NR) values based on peak groundwater concentrations simulated within 1000 years for 100:0 initial

distributions; thus there is no need to evaluate these cases further. Strontium-90 was excluded because it was decided to assign the 100:0 initial concentration distribution to this constituent throughout the D/H area based on its prevalence throughout the vadose zone in many locations, presence in groundwater, and recognition that this contaminant is a recognized risk driver in the 100 Area.

Based on the evaluation above, the following waste sites and contaminants were identified as potential cases for which the 70:30 initial distribution representations may be non-conservative:

- 116-D-1A (trench), neptunium-237
- 116-D-7 (retention basin), antimony
- 116-DR-9 (retention basin), acenaphthene
- 116-H-1 (trench), phenanthrene
- 116-H-1 (trench), antimony
- 116-H-4 (pluto crib), antimony
- 116-H-6 (solar evaporation basin), antimony
- 116-H-7 (retention basin), antimony
- 116-H-7 (retention basin), molybdenum
- 118-H-6 (reactor fuel storage basin), neptunium-237

For each case on the above list, the conservatism of the 70:30 initial concentration representations requires testing because the 70:30 initial source distribution was not intended to exclude of the possibility any deep contamination, but rather was to serve as a conservative representation of higher K_d contaminants. Therefore, the conservatism of the cases identified in Appendix D was tested to determine if any were non-conservative and therefore would need to be considered for a site-specific evaluation. To test, simulations are performed in pairs: once with the actual vertical contamination profile reported for the RI borehole, and again using the 70:30 representation with the uniform concentration equal to the peak observed concentration in the RI borehole (matching the essential function of the 70:30 representation relative to SSL and PRG values). The peak groundwater discharge predicted by the model were obtained from in each case in these pairs of simulations and compared. The conservatism of the 70:30 initial concentration distribution was considered validated if:

- The simulated peak groundwater concentration obtained from observed contaminant distribution was less than the peak groundwater concentration obtained from the 70:30 distribution, and
- The simulated peak groundwater concentration was less than the MCL for the constituent simulated.

The observed contaminant distribution in the vadose zone for different waste sites is presented in Figure 5-4. For these waste sites site specific modeling was performed. Two conceptual site models (CSMs) were evaluated: (1) the actual contaminant distribution (labeled CSM1) using data from the RI borehole, and (2) the 70:30 distribution with maximum concentration observed (labeled CSM2).

Figure 5-5 represents the two conceptual models. For each of the waste sites a single representative soil column was selected that represents the site specific conditions. The specific surface soil identified for

each waste site location is used to select the most site-specific appropriate recharge rates, which depend on surface soil type (Table 4-2). The irrigation recharge rates corresponding to the surface soil type was applied in the model. The representative column and surface soil type used in these site specific modeling is presented in Table 5-4.

For CSM1 (with actual contaminant distribution) the vertical distribution of contaminant observed in the borehole was input to the STOMP model. Concentration in the STOMP model nodes were interpolated using Excel "FORECAST" function from the vertical distribution of the observed data. The concentration was distributed along the entire 10m width of the waste site. Concentration was not applied in the 0.5-m zone above the water table for reasons discussed in Section 4.4.2. For CSM2 (70:30 distribution) the maximum concentration used in CSM2 was applied uniformly in the 70% of the vadose zone below backfill. The lower 30% of the vadose zone was assigned zero concentration.

Results for the conservatism test modeling are presented in Table 5-5. For the 70:30 distribution (CSM2) peak concentrations are higher than the actual distribution (CSM1) in all cases evaluated, indicating that the 70:30 distribution model (CSM2) is more conservative than the actual distribution model (CSM1) for every case evaluated. The peak concentrations within the first 1000 years are well below the applicable protection standard for all cases. Figure 5-6 presents an example pair of breakthrough curves, in this case for neptunium-237 at waste site 116-D1-A, for both the actual and 70:30 initial conditions, illustrating the impact of the two initial conditions as well as the higher peak groundwater concentration for the 70:30 representation.

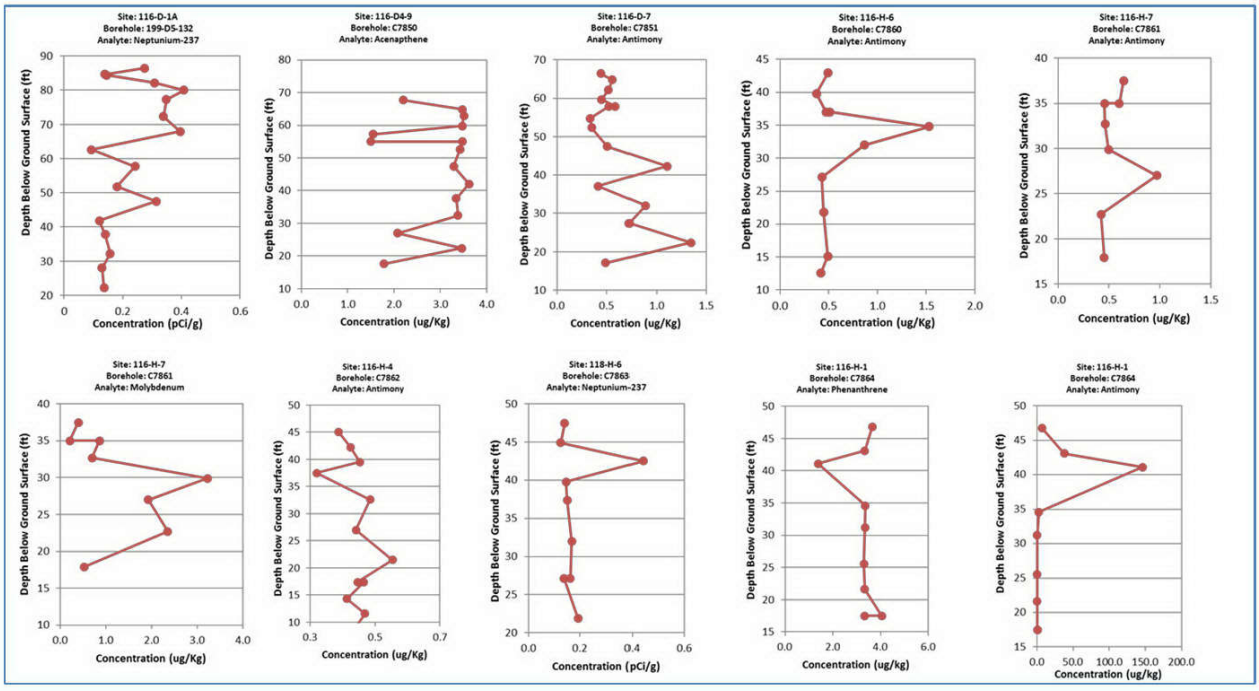

Figure 5-4. Observed Contaminant Distribution in the Vadose Zone

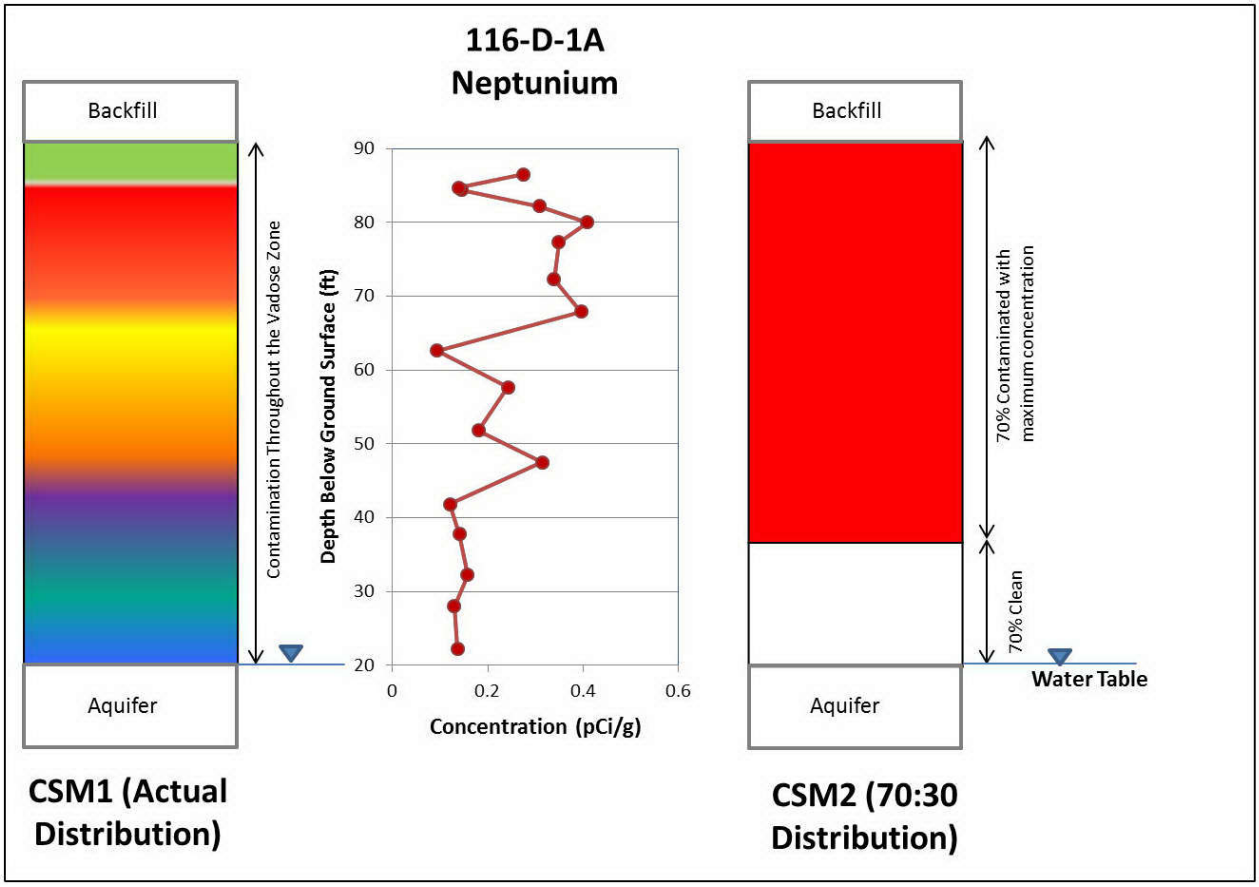

Figure 5-5. Illustrative Comparison Initial Contaminant Source Distributions for the CSM1 (Actual) and CSM2 (70:30) Cases Evaluated for Testing Conservatism of the 70:30 Distribution

Table 5-4. Representative Column and Surface Soil Type Used in the Evaluation of Conservatism of the 70:30 Initial Distribution for Potentially Unrepresentative Cases

Waste Site	Borehole	Analyte	Representative Stratigraphic Column	Surface Soil Type
116-D-1A	199-D5-132	Neptunium-237	5	ESL
116-D-7	C7851	Antimony	6	ESL
116-D4-9	C7850	Acenaphthene	1	RS
116-H-1	C7864	Phenanthrene	1	BSL
116-H-1	C7864	Antimony	1	BSL
116-H-4	C7862	Antimony	1	BSL
116-H-6	C7860	Antimony	1	BSL
116-H-7	C7861	Antimony	1	BSL
116-H-7	C7861	Molybdenum	1	BSL
118-H-6	C7863	Neptunium-237	1	BSL

Table 5-5. Results for the 70:30 Initial Concentration Distribution Conservatism Testing Simulations

Waste Site	Borehole	Analyte	K_d (mL/g)	Ground-water Standard (µg/L)[a]	Peak Concentration (µg/L)[a]		Peak Concentration in 1000 yr (µg/L)[a]		Surface Soil Type
					Actual Distribution (CSM1)	70:30 Distribution (CSM2)	Actual Distribution (CSM1)	70:30 Distribution (CSM2)	
116-D-1A	199-D5-132	Neptunium-237	15	15	3.59E-01	4.17E-01	3.59E-01	< 1E-04	ESL
116-D-7	C7851	Antimony	3.76	6	3.64E-03	5.40E-03	3.64E-03	5.40E-03	ESL
116-D4-9	C7850	Acenaphthene	6.12	960	9.01E-03	9.32E-03	1.11E-03	9.45E-04	RS
116-H-1	C7864	Phenanthrene	16.7	No Value	3.71E-04	4.46E-04	3.71E-04	2.32E-04	BSL
116-H-1	C7864	Antimony	3.76	6	1.44E-02	3.01E-02	1.44E-02	3.01E-02	BSL
116-H-4	C7862	Antimony	3.76	6	2.52E-04	2.67E-04	2.52E-04	2.67E-04	BSL
116-H-6	C7860	Antimony	3.76	6	5.20E-04	7.38E-04	5.20E-04	7.38E-04	BSL
116-H-7	C7861	Antimony	3.76	6	3.24E-04	4.67E-04	3.24E-04	4.67E-04	BSL
116-H-7	C7861	Molybdenum	20	80	2.07E-04	2.97E-04	2.07E-04	2.97E-04	BSL
118-H-6	C7863	Neptunium-237	15	15	2.00E-02	2.30E-02	2.00E-02	1.50E-02	BSL

a. Neptunium-237 values are activity concentrations, expressed in units pCi/L

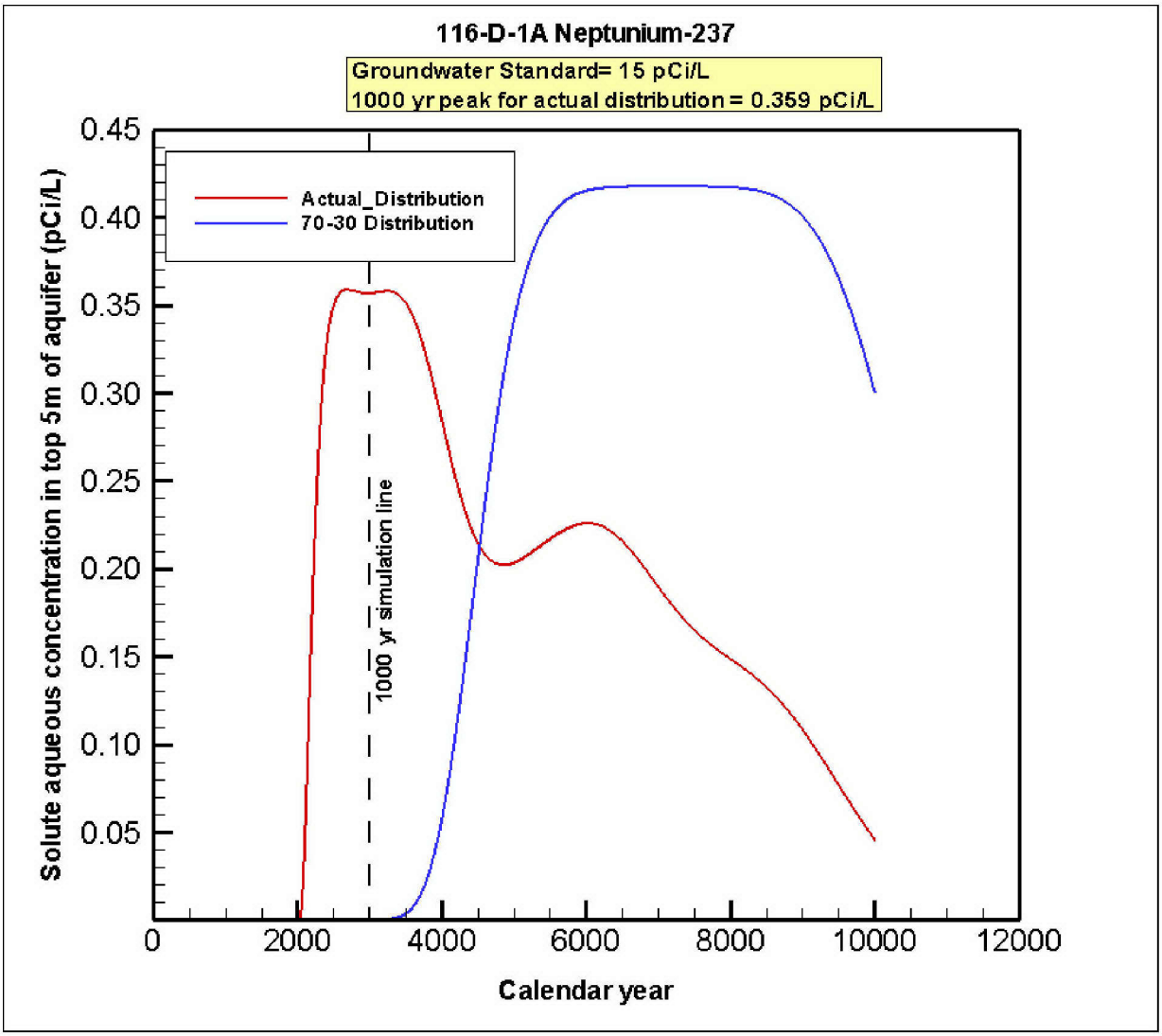

Figure 5-6. Breakthrough Curves for Neptunium-237 Simulated in Conservatism Testing for 70:30 Representation

5.4 Calculating Dilution Factors

As the contaminant mass enters the aquifer from the vadose zone the aqueous concentration reduces due to dilution. Since the screening level and PRG calculations are a function of the peak concentration it is important to understand the dilution factor within the saturated zone. As defined in the Washington Administrative Code (WAC 173-340-747), the dilution factor is the ratio of the combined aquifer and vadose zone water fluxes to the vadose zone water flux:

$$Df = \frac{Q_{VZ}+Q_A}{Q_{VZ}} \qquad \text{(Eqn. 5-2)}$$

for which Df = the dimensionless dilution factor, Q_{VZ} equals the volumetric flux from the vadose zone into the aquifer (L^3T^{-1})and Q_A represents the volumetric flux through the topmost five meters of the aquifer (L^3T^{-1}) representing the screened interval in the borehole. The dilution factors for different

recharge scenarios are shown in Figure 5-7. For each scenario the results are presented for the three soil types indicating minor effects on the dilution factors. Because of the high hydraulic conductivity in the aquifer and low recharge rates the dilution factors vary from 1e+02 to 1e+06, indicating significant dilution of the concentration in the saturated zone. The dilution factors for representative columns with aquifers of Ringold E are smaller than the dilution factors for Hanford aquifers for all recharge scenarios (Figure 5-7).

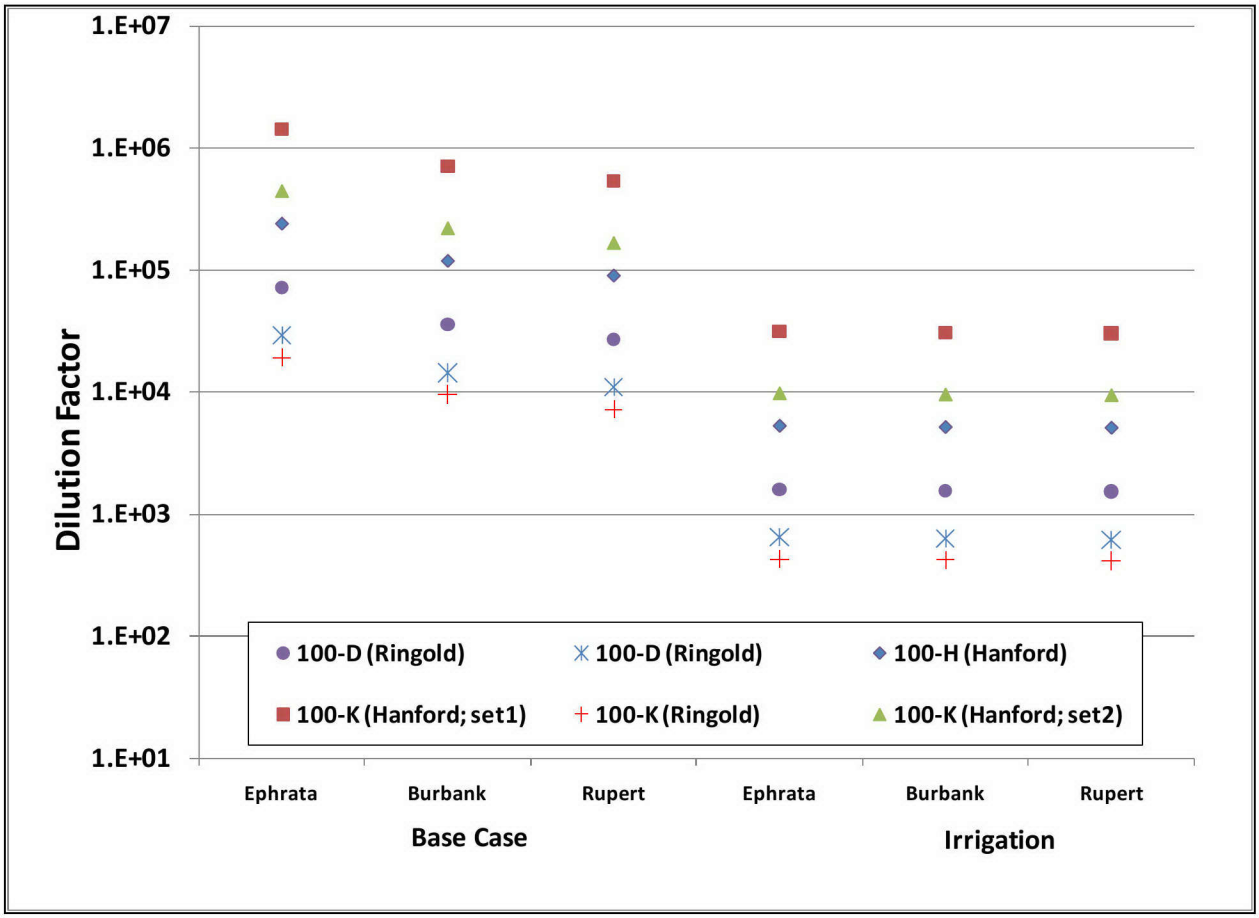

Figure 5-7. Dilution Factors for Representative Columns. The Lithology in the Saturated Zone is Listed in Parenthesis.

5.5 Application

Detailed tables of soil screening level and PRG values calculated using the methods described in this report for representative stratigraphic columns in 100-D, H, and K geographic areas can be found in the various attachments of ECF-Hanford-11-0063 Rev. 5. The values reported in these tables are used to identify those constituents that pose a significant risk to surface water and groundwater. Table 5-6 provides a list of the contaminants for the 100-D, H, and K geographic areas along with their calculated soil screening level and PRG values. The values are selected by choosing the lowest value (most conservative) from calculations performed on each representative stratigraphic column (Table 5-2) under various recharge rates for three soil types for the protection of groundwater and surface water. Final calculations have not been performed on 100-BC, 100-F, and 100-IU-2/6 geographic areas.

The PRG values resulting from simulations and back-calculations are only intended to be applied to sites that share the same set of conditions and assumptions underpinning these calculations. The results, in general, should not be applied to other geographic areas. Questions about whether the PRG values are appropriate for a given site should be directed to the CH2M Hill Plateau Remediation Company (CHPRC) lead for modeling and risk assessment. Some waste sites may require a more rigorous investigation of site specific conditions than those underlying the PRG values. Other simulations and back calculations may be necessary if the assumptions and conditions for a particular site do not match those used in these calculations.

Table 5-6. PRG and Soil Screening Level (SSL) values for 100-D, H, and K geographic areas

Contaminants of Interest	PRG (mg/kg or pCi/g)	SSL (mg/kg or pCi/g)	Contaminants of Interest	PRG (mg/kg or pCi/g)	SSL (mg/kg or pCi/g)
100-K			100-D		
Carbon-14	9.2E+01	4.27E+01	Chromium	NR	NR
Chromium	NR	NR	Hexavalent Chromium	6 *	6 *
Hexavalent Chromium	6 *	6 *	Nitrate	3.48E+03	1.65E+03
Nitrate	2.07E+03	9.6E+02	100-H		
Strontium-90	NR	2.23E+04	Hexavalent Chromium	6 *	6 *
Tritium	1.01E+03	4.27E+02	Strontium-90	NR	9.93E+04

Note: Minimum of surface water and groundwater protection related screening levels and PRGs are shown here. The "NR" sign designates a non-representative result for analytes were breakthrough was not simulated to occur in more than one representative stratigraphic column within 1000 years, where breakthrough is defined as concentration exceeding 1.0E-04 µg/L (limit of numerical significance). The Cr(VI) soil screening level is limited to a maximum value of 6.0 mg/kg because the Kd value used in the model was derived from experiments with soil concentrations less than that value.

6. Model Sensitivity and Uncertainty

This section presents the modeling conservatism and the results of the sensitivity and uncertainty analyses conducted to gain understanding of the important parameters that can impact the screening level and PRG calculations.

6.1 Modeling Conservatisms

Application of the PRG and screening level values calculated herein requires an understanding of which assumptions and modeling choices were conservative and which were not. Conservative assumptions and modeling choices include:

- The assumption of effective 100-0 source distribution (fully contaminated vadose zone) is likely to be a significant overestimate of the actual source distribution beneath many 100 Area waste sites, even for waste sites where high volume, low concentration discharges occurred during operations.

- PRG and screening values are selected by taking the minimum soil concentration value calculated for all of the representative columns simulated for the particular area.

- Recharge was represented in the numerical model by uniform flux rates specified over particular time periods so that vadose zone flow is always downward. In contrast, recharge in an arid vadose zone occurs only as often as the combination of precipitation and antecedent moisture conditions allow, i.e., sporadically or infrequently, so that there can be long periods when shallow vadose-zone porewater movement is controlled more by evaporation and transpiration near the surface than gravity, resulting in some upward movement or reduced downward seepage velocity.

- The smallest base case recharge rates are larger than the minimum of the range of rates determined for the Hanford shrub steppe.

- The one-dimensional simulations force all contamination through the vadose zone down to the aquifer, whereas infiltrating water and solutes tend to migrate laterally and vertically as the wetting front redistributes following an infiltration event.

- Dilution upon mixing of groundwater with Columbia River water is assumed to be negligible.

- Dispersion is assumed to be negligible, which leads to larger peak concentrations than if dispersion had been included.

- Volatile organic compounds are assumed to have negligible volatilization so that the resulting peak concentrations are larger than if volatilization had been included.

- Geometric means of measured aquifer horizontal hydraulic conductivity values are lower, and thus more conservative than arithmetic means because the values typically span several orders of magnitude.

- Initial contaminant mass within the domain is conservatively calculated by assuming that all the sediments, gravels and finer-grained materials (<2 mm size fraction) are active in transporting water and solutes. Majority of the residual contamination is found to be associated with the fine-

grained (<2 mm size) portion of the sediments in the vadose zone. However, considerable uncertainty exists due to the spatial variation in fraction of fine grained material within the vadose zone. For the purpose of modeling, the residual contaminant concentration determined in the laboratory on the fine-grained sediments is applied to the bulk volume thereby increasing the initial mass estimate. Under the recharge scenarios considered for the simulations, pore-waters do not have significant interaction with the gravel clasts because pore-waters are mostly restricted to the finer-grained materials due to capillary forces under relatively dry conditions. Thus the resulting PRG and screening level values are highly conservative because the initial dissolved contaminant concentrations are over predicted.

- Contaminant source mass within the domain is calculated using the bulk density value for gravels and finer-grained materials, whereas laboratory measurements of soil concentrations typically exclude the gravel fraction and measure the concentration of the finer-grained materials only. The bulk density for Hanford formation and Ringold E sediments with gravels is 1.93 gm/cm^3, whereas the bulk density of the < 2 mm fraction is lower. Because initial mass loading (applied on a bulk volume basis) is calculated by multiplying the sorbed concentration with the bulk density using a larger bulk density is conservative as it will lead to larger peak concentration.

- The simulations do not explicitly represent the alternation of thin intervals of finer-grained material with thicker intervals of coarser-grained materials commonly observed in the 100 Area, even though such alternations create local capillary impedances to downward transport through the juxtaposition of intervals with large pores below intervals with small pores. The alternations can lead to spreading of the plume thereby reducing the peak concentration.

Assumptions that may or may not be conservative include:

- The median hydraulic gradient value for each source area may be too small for waste sites near the Columbia River (at certain times of the day) and may be several times too large for waste sites that are far inland from the river. Since volumetric flux through the SZ is a function of hydraulic gradient and affects the dilution factor the peak concentrations will be impacted based on value chosen.

- The assumption of a five-meter-thick aquifer may or may not be conservative for those 100 Area locations with aquifer thicknesses less than five meters.

The calculations are performed with numerous conservative assumptions. Due to conservative choice of modeling inputs and boundary conditions, the screening levels and PRG concentrations are deemed to be bounding estimates (i.e., lead to the lowest threshold concentrations).

In the calculation methodology, the saturated zone is assumed to be initially uncontaminated, which may not always be true since plumes can migrate from upgradient locations over time. However, due to several in-built modeling conservatisms mentioned above, the screening level and PRG calculations are deemed to remain bounding when compared to the results derived from a more sophisticated site-specific predictive model that incorporates all the features and processes relevant at the scale of the model, including any contaminant migration from upgradient locations. Stated differently, groundwater is not expected to remain contaminated above cleanup levels (or discharge to the Columbia River above ambient water quality standards) any longer because former waste sites are closed with the screening values or PRGs calculated using this methodology.

6.2 Sensitivity Analyses

Sensitivity analyses provide information on how PRGs and screening levels might be affected by changes in input parameters. The stratigraphic columns used for performing the sensitivity analyses, when not specified, are restricted to 100-BC and 300 geographic areas in order to reduce the number of calculations. The calculations are further restricted to certain selected stratigraphic columns. Column 2 was selected for 100-BC area and Column 5 was selected for 300 area. Results are presented for the base case scenario for Burbank sandy loam soil recharge rate when not specified in the sensitivity analysis.

6.2.1 Evaluation of K_d Influence on Contaminant Breakthrough

In order to evaluate the influence of K_d on contaminant breakthrough behavior, the 100-D column 1 was run with irrigation recharge case for Ephrata sand with effective 100:0 source distribution. Figure 6-1 shows the breakthrough curves for different K_d values ranging from 0.8 to 9.0 mL/g. Observation of the break through curves from Figure 6-1 reveals that all the peak concentrations occur within 1000 year simulation time. As the irrigation recharge is really high it flushes the contaminants very fast through the vadose zone even with higher K_d values. The irrigation recharge scenario does not represent actual site conditions; it is used as a limiting conservative (bounding) condition for the purpose of calculating screening values only.

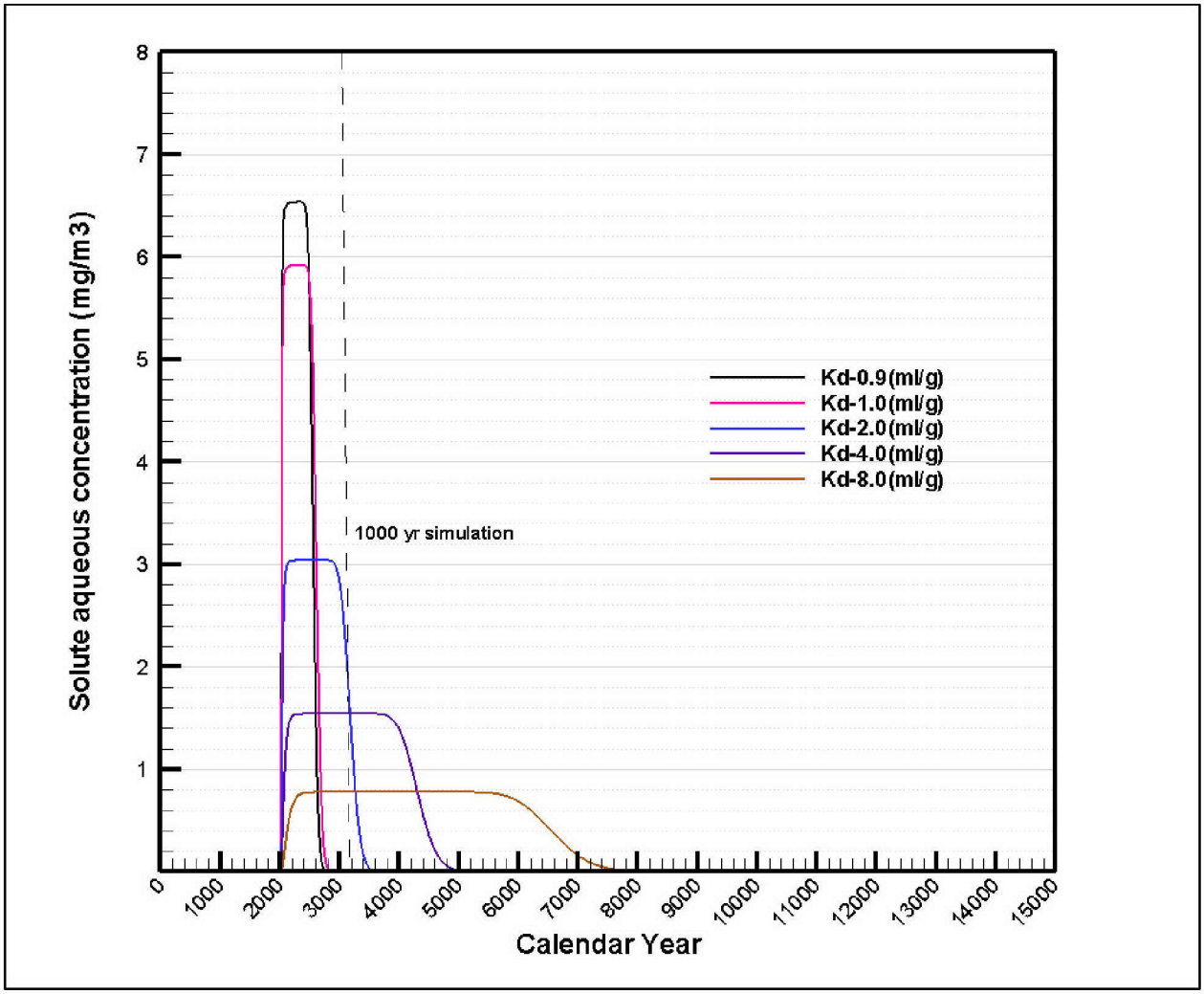

Figure 6-1. Breakthrough Curves for Different Distribution Coefficients with Irrigation Recharge Rate

6.2.2 Sensitivity to Long Term Recharges

Sensitivity to long-term recharge is presented by ignoring the step change in recharge due to establishment of mature shrub steppe vegetation. Because of the frequent occurrence (a once-a-decade cycle) of natural fires on the Hanford reservation, it is possible that mature shrub steppe may not get established. To evaluate the impact of this on the base case, a sensitivity analysis is conducted where the two-step change in recharge imposed in the base case is changed to a one-step change, essentially assuming that immature shrub steppe is the dominant land cover condition. Figure 6-2 shows the change in recharge for Burbank sandy loam. The change in PRG for Cr(VI) is presented in Table 6-1 and graphically presented in Figure 6-3. As the peak concentration occurs before the Year 2045 there is no or negligible change in PRG values in the two recharge scenarios.

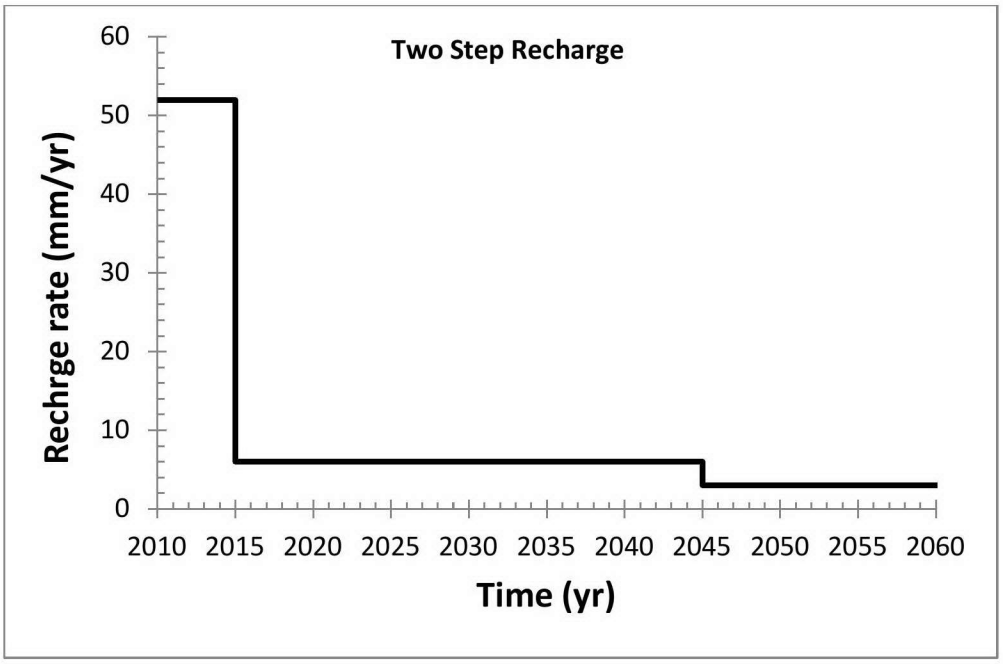

(a)

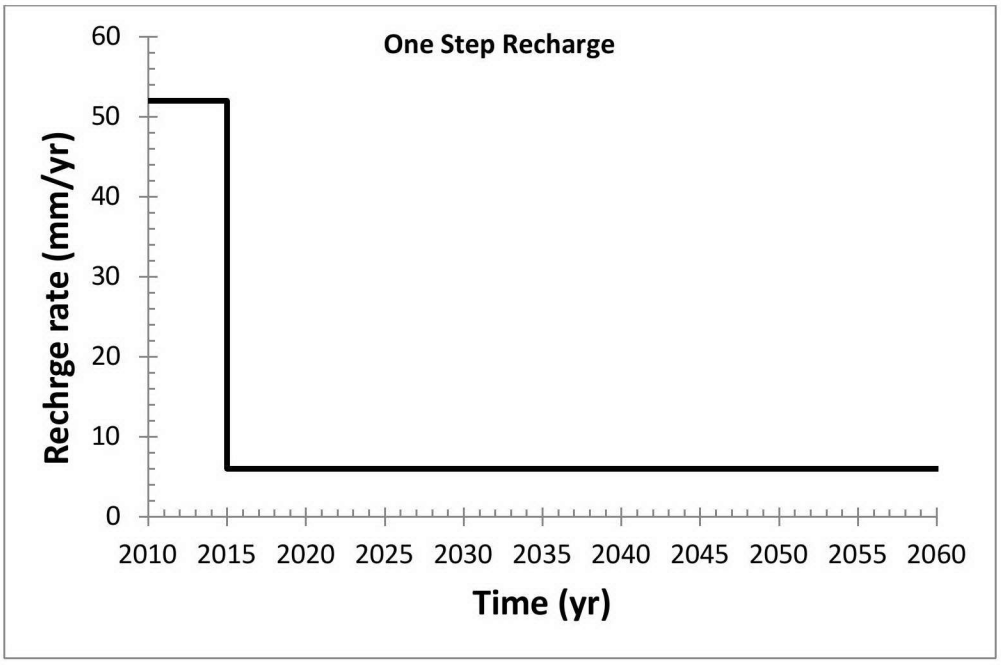

(b)

Figure 6-2. Long-Term Recharge Rate for Burbank Sandy Loam: (a) Two-Step Recharge; (b) One- Step Recharge

Table 6-1. Surface Water PRG for Cr(VI) for Two Step vs. One Step Change in Recharge.

Operable Unit	Column No	Soil Type	Recharge	Surface Water PRG (mg/Kg)
100-BC	2	Burbank Sandy Loam	Two Step	17.7
			One Step	17.7
300	5	Burbank Sandy Loam	Two Step	971.0
			One Step	971.0

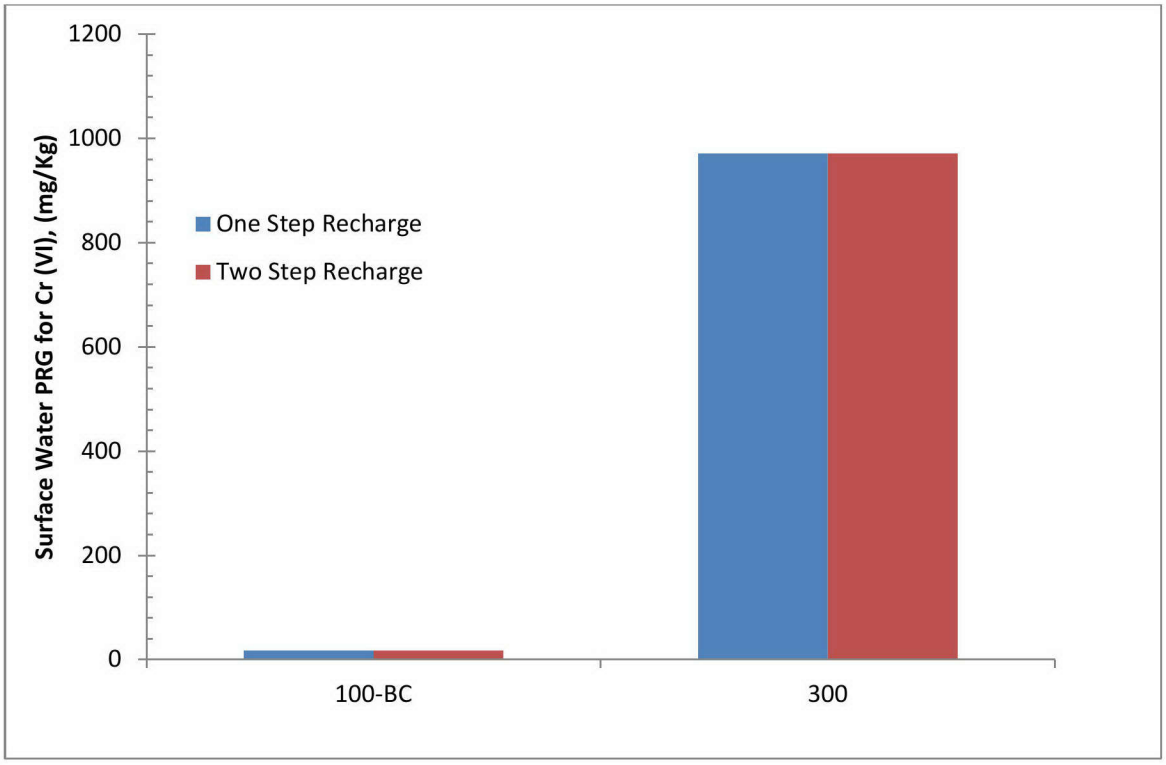

Figure 6-3. Surface Water PRG for Cr(VI) for Different Long-Term Recharge

6.2.3 Effects of Different Source Distribution

This sensitivity analysis focuses on discerning the effects of different source distributions on PRGs. Using the base case recharge, five new source distributions (50-50, 60-40, 70-30, 80-20, and 90-10) were simulated and compared to the PRG values for the effective 100-0 source distribution already computed. A 60-40 source distribution indicates that the top 60% of the VZ thickness beneath the clean cover (backfill) was contaminated with a uniform concentration of 1 mg/kg soil, whereas the remaining 40% contained no contamination.

Figure 6-4 shows the final PRG values of Cr(VI) in surface water from the six source distributions in the 100-BC and 300 geographic areas. This sensitivity analysis was performed for Column 2 and 5 for 100-BC and 300 areas, respectively. As expected, step-wise decreases in the source distribution from 100% to 50% of the VZ thickness beneath the clean cover yields decreasing peak groundwater concentrations and

increasing PRG values. Although the source distribution decreased linearly from effective 100-0 to 50-50, the PRG values do not appear to follow a linearly increasing trend.

The VZ thickness for the 300 area column (16.5 m) chosen for the sensitivity analysis is smaller than 100-BC column (23 m) and SZ is made of Hanford fm. as compared to the Ringold E unit leading to higher hydraulic conductivity. Because of these differences the initial mass in the 300 area column is smaller and dilution factor is higher in the SZ compared to the 100-BC column used in the sensitivity analysis. This results in lower peak concentration for the 300 area column and therefore higher PRG values and relatively larger sensitivity to the source distribution particularly when the source extent is reduced.

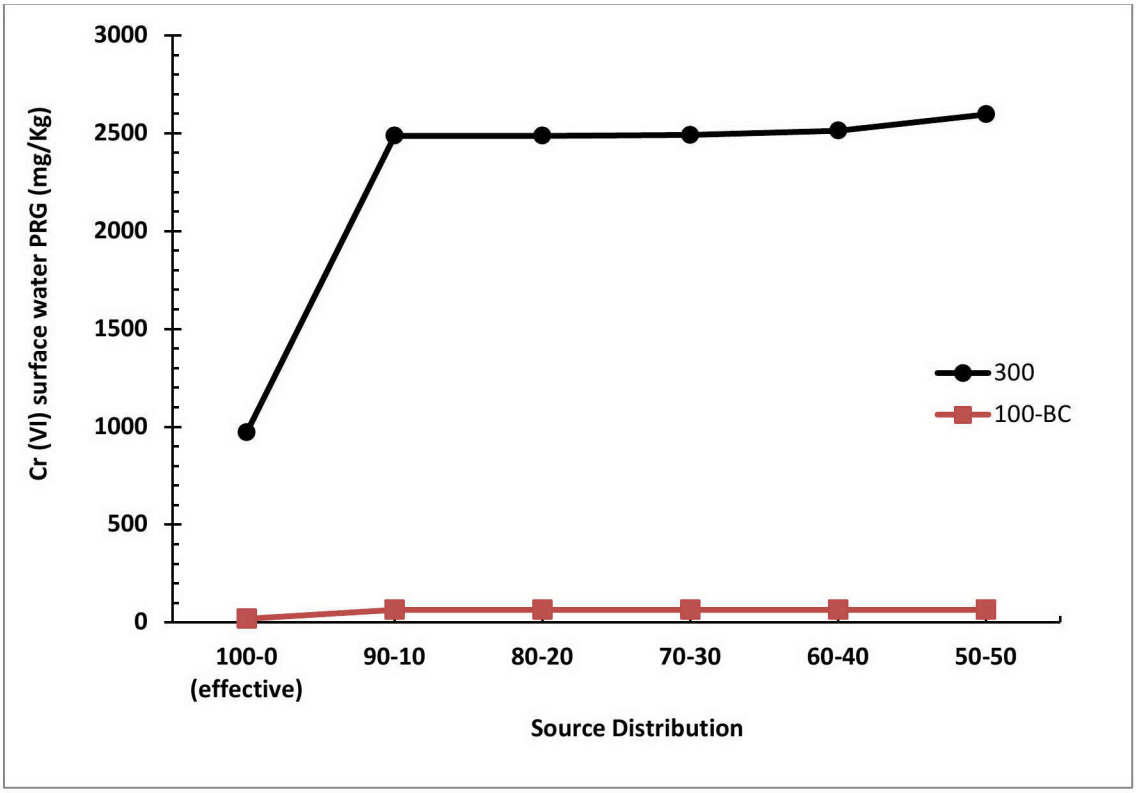

Figure 6-4. Surface water PRG for Cr(VI) for Different Source Distributions in Soil

6.2.4 Effects of Extending Bare Soil Recharge Period

For the base case scenario, bare soil is assumed to be the land cover between Year 2010 and 2015 (Table 4-2), after which time grasses and shrubs are expected to colonize the bare soil. Accordingly, the recharge rate associated with bare soil is higher than those associated with immature and mature shrub-steppe cover. The effect of extending the bare soil recharge period on surface water PRG for Cr(VI) is evaluated for the base case. Two sensitivity analyses were conducted with the bare soil recharge rate extended to Year 2020 and Year 2030, thereby resulting in application of the bare soil recharge rate for 10 and 20 years, respectively. Simulation time remained at 1,000 years and the duration of the second recharge period, which simulated an immature shrub-steppe cover, remained at 30 years. Significant difference in PRG values has been found for both 100-BC and 300 areas, as the peak concentration occurs after the

bare soil recharge case time period. Extended bare soil recharge scenario caused more mass going down to the SZ and eventually, increased the peak concentration. Extending the bare soil recharge scenario from 2010-2015 to 2010-2030 caused 3 to 5 times decrease in PRG values for both 100-BC and 300 areas (Figure 6-5).

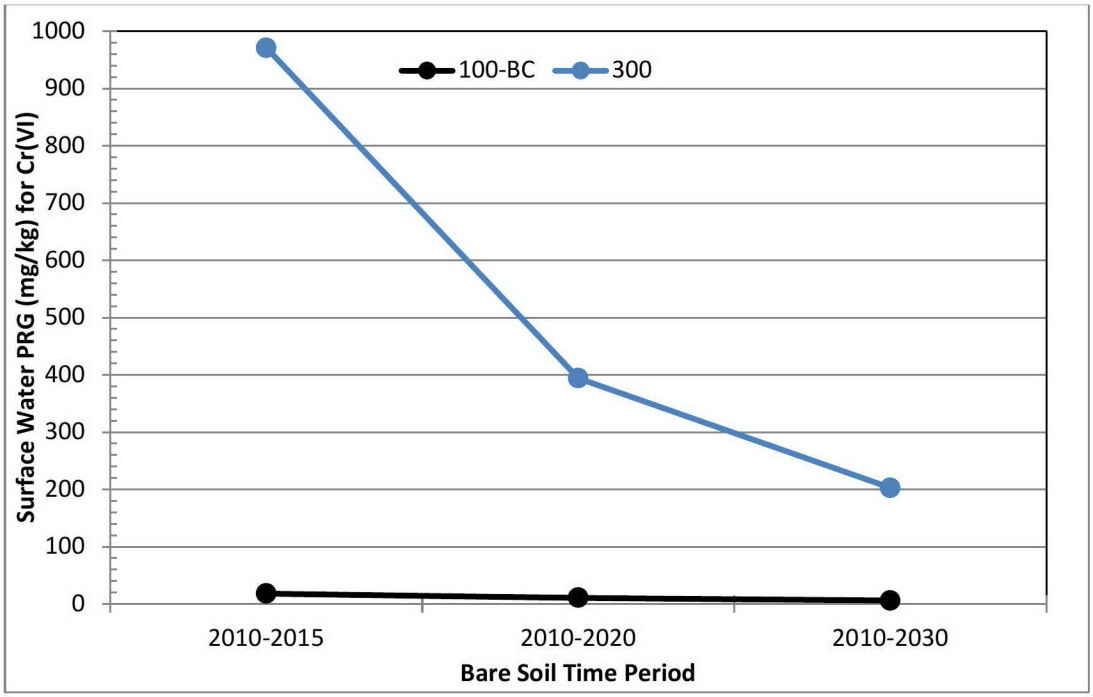

Figure 6-5. Surface water PRG for Cr(VI) for different bare soil time periods under the base case scenario

6.2.5 Sensitivity to Solute Transport Solution Methodology

In STOMP, the governing mass transport equations can be solved with either the power-law scheme of Patankar (1980) or with a third-order scheme using Total Variation Diminishing (TVD) criteria. The Patankar solution scheme was employed in the calculations and is based on the fully implicit finite-difference methodology. In an advection-dominated system (characterized by large Peclet number) the Patankar solution scheme can suffer from numerical dispersion that can result in smearing of otherwise sharp concentration fronts and could also lead to artificial oscillations at the concentration front. The smearing is a result of the first-order approximation of the advective term in the transport equation. The third-order TVD solution methodology does not suffer from numerical errors and can avoid the artificial oscillations with appropriate flux limiting function even for advection-dominated system. A sensitivity analysis was performed to compare the results of the two solution methodologies in terms of peak concentration and the timing of the peak concentration. The calculations were performed for Column 2 in 100-BC geographic area using the effective 100-0 distribution of contaminants for Burbank sandy loam and base case recharge. The K_d for the contaminant simulated was set to zero. Figure 6-6 shows the solute concentration for a node that is located at the water table. The magnitude of peak concentration and the time to peak concentration is nearly identical for both solution methods.

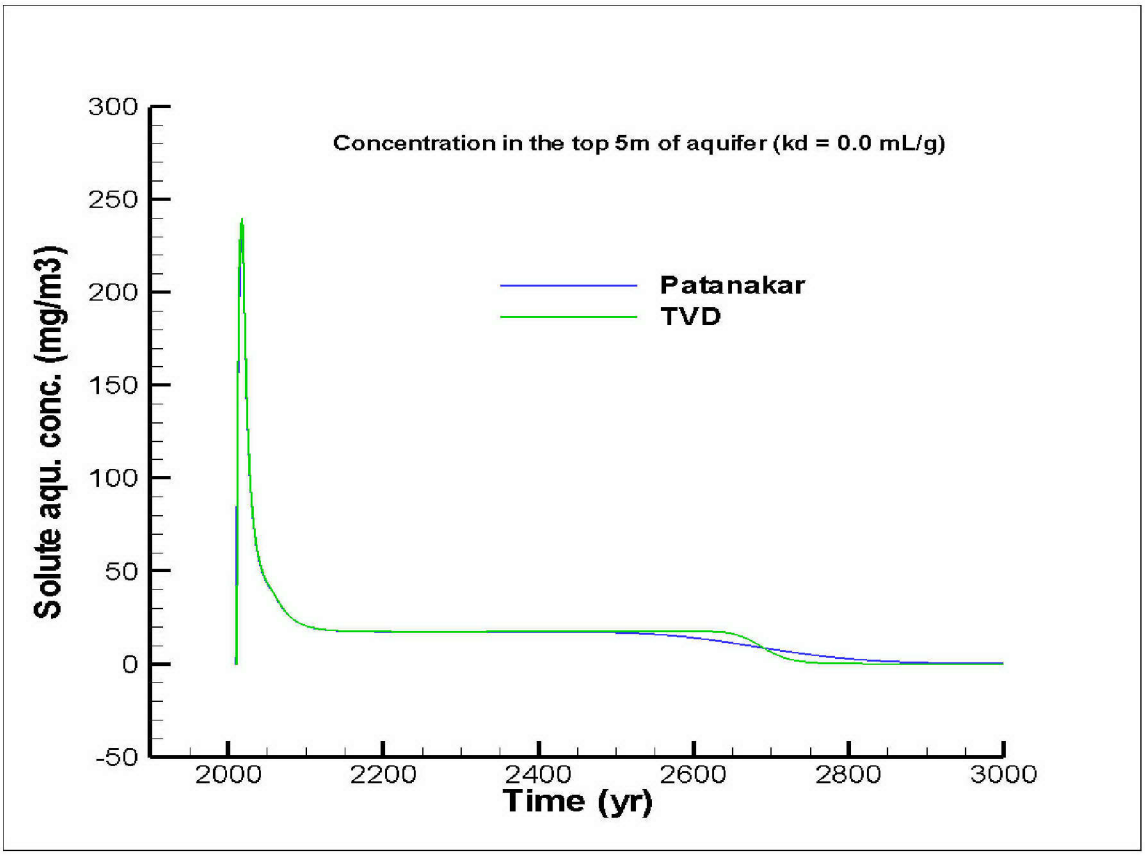

Figure 6-6. Comparison of Non-Sorbing Solute Concentration using Patankar and TVD Solution Methodologies for Column 2 of 100-BC Geographic Area with Burbank Sandy Loam recharge and effective 100-0 Contaminant Distribution.

6.3 Uncertainty Analyses

The vadose zone models described in this modeling report were developed in order to calculate clean-up levels necessary for the protection of groundwater and surface water. To do this the models predict concentration levels in groundwater and surface water resulting from soil contamination in the vadose zone. As all models are approximations of the real world, it is a given that uncertainty exists within these predictions. Methods have been developed for estimating the contribution to total uncertainty in a prediction from each model parameter. One qualified support software that includes algorithms for estimating the relative contribution to uncertainty is PEST (Doherty, 2010). PEST is graded as support software and was used under the guidance of the software management plan CHPRC-00258 Rev. 2, *MODFLOW and Related Software Codes Software Management Plan*. Based on the model inputs and outputs generated and read by PEST, parameters values that best fit observed data can be estimated in an automated fashion. Beyond parameter estimation, the most recent versions also include algorithms for working with predictive uncertainty with model predictions. These algorithms can combine uncertainty introduced by the variability in observed data and uncertainty introduce by the numerical model itself. This section of the report summarizes an application of linear predictive uncertainty analysis (Moore and Doherty, 2005), implemented using PEST, to two of the alternative conceptual models (ACM) described in this document, specifically, the 100-BC column 2 and 100-F column 3. These columns were picked

randomly from Table 5-2. First, a discussion of the definition of contribution to prediction uncertainty and how it is calculated is presented. Then, the set up of the model files and parameter values and statistics used in uncertainty analysis are discussed. Finally, relative contribution to prediction uncertainty is presented in the results section.

6.3.1 Contribution to Prediction Uncertainty

All numerical models are approximations of the real world. Predictions made using these models are not exact. Predictive uncertainty of numerical simulation results can be developed by investigating the affect of changing model input parameters on the model predictions. One method for quantifying the uncertainty of predictions comes from frequentist statistical techniques for calculation of the mean and variance of distribution. Figure 6-7(a) shows a normal distribution curve fitted to a set of field parameters. The normal distribution is used to approximate the field observed data over the range of values expected to exist for the given phenomena using a continuous function. The same method can be used to describe a prediction from a numeric model shown in Figure 6-7(b). The most likely simulated result and the variance describe the mean and range of values that may be simulated given the variation in the input parameters. In frequentist statistics the mean and variance are estimated from a discrete number of field observed measurements. The distribution of the prediction uncertainty is estimated from the results of a discrete number of numerical simulations based on the perturbation of model inputs and fitting a mean and variance distribution to the range of simulated results. Moore and Doherty (2005) illustrated that this type of conceptual framework can be used to combine statistical measures for field data with the uncertainty introduced through the numerical modeling to develop an estimate of predictive uncertainty including both types of data. In this manner the uncertainty from the field data and uncertainty introduced by the model calculations can be combined into a final prediction and variance that describe the certainty of a prediction.

PEST includes algorithms to estimate relative contribution of model input parameters to the uncertainty in a prediction produced from a numerical model. This is accomplished by perturbing model inputs in a systematic fashion and recording sensitivity of the value of the prediction to changes in model inputs. In this case, PEST will be run using the linear predictive error estimator documented in the PEST manual (Doherty, 2010). Other methods for estimating uncertainty in the prediction exist. However, given the domain of the models (1-D), the linear predictive error estimator was deemed adequate for this analysis. For the linear predictive error analysis PEST required two STOMP simulations for every model input parameter investigated as part of the analysis. In each of these simulations one parameter is perturbed from its original (initial) value, once above and once below the initial value, hence the need for two simulations per parameter. Based on the sensitivity of the prediction to the change in the parameter value a covariance matrix of model parameters and the prediction can be created. At this point the uncertainty in the model prediction based on parameter inputs can be estimated by PEST.

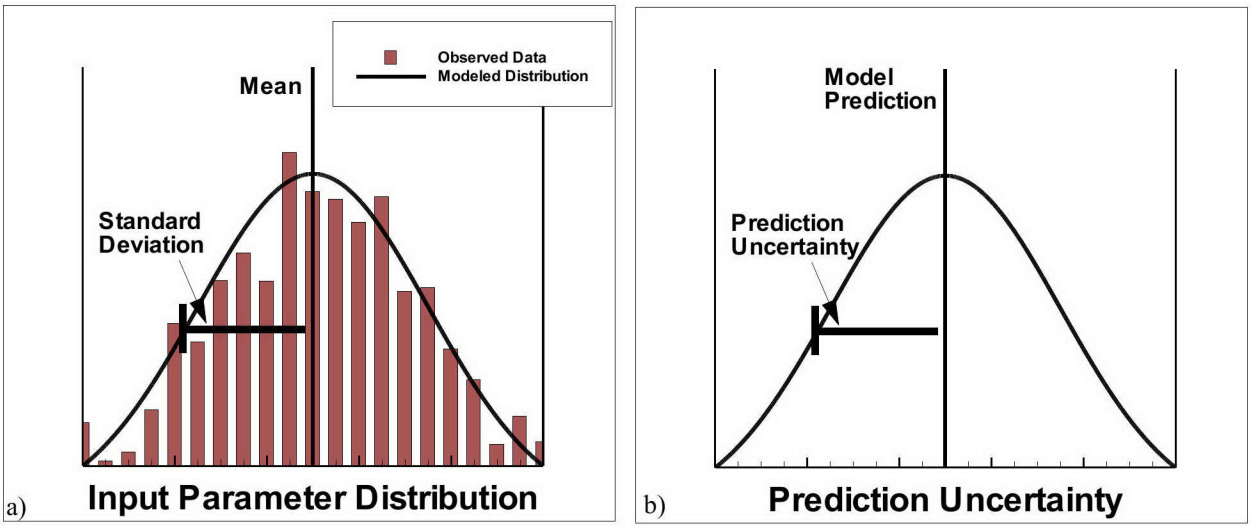

Figure 6-7. Illustration of how Statistical Distributions for Model Input Parameters and Simulated Predictions can be approached with Similar Methods

The PEST documentation notes that the algorithms for this type of analysis depend on model linearity. However, they may be applied to non-linear models (i.e., vadose zone models) for ranking parameters and their ability "to reduce the potential wrongness of a key model prediction" (Doherty, 2010). In line with this observation the results presented in this analysis are relative contribution of each parameter on the total uncertainty in the prediction rather than presenting the absolute value of uncertainty.

6.3.2 Model Files and Parameters

Two separate analyses are conducted using stylized conceptual model so that the epistemic uncertainty (uncertainty due to lack of knowledge) in model input parameters can be evaluated. For this purpose two different soil columns with different vertical extent of contaminated zones (100-0 and 50-50) and recharge conditions are selected to evaluate the relative effect of different model input parameters on the resulting soil concentrations used in calculating screening levels and PRGs. The first analysis is based on selecting Column 2 from 100-BC geographic area [Figure 6-8(a)] using Ephrata Loam soil cover under irrigation recharge scenario and assuming 100-0 extent of contamination. The second analysis is based on choosing Column 3 from 100-F geographic area [Figure 6-8(b)] using Burbank Sandy Loam soil cover under base recharge scenario and assuming 50-50 extent of contamination in the vadose zone.

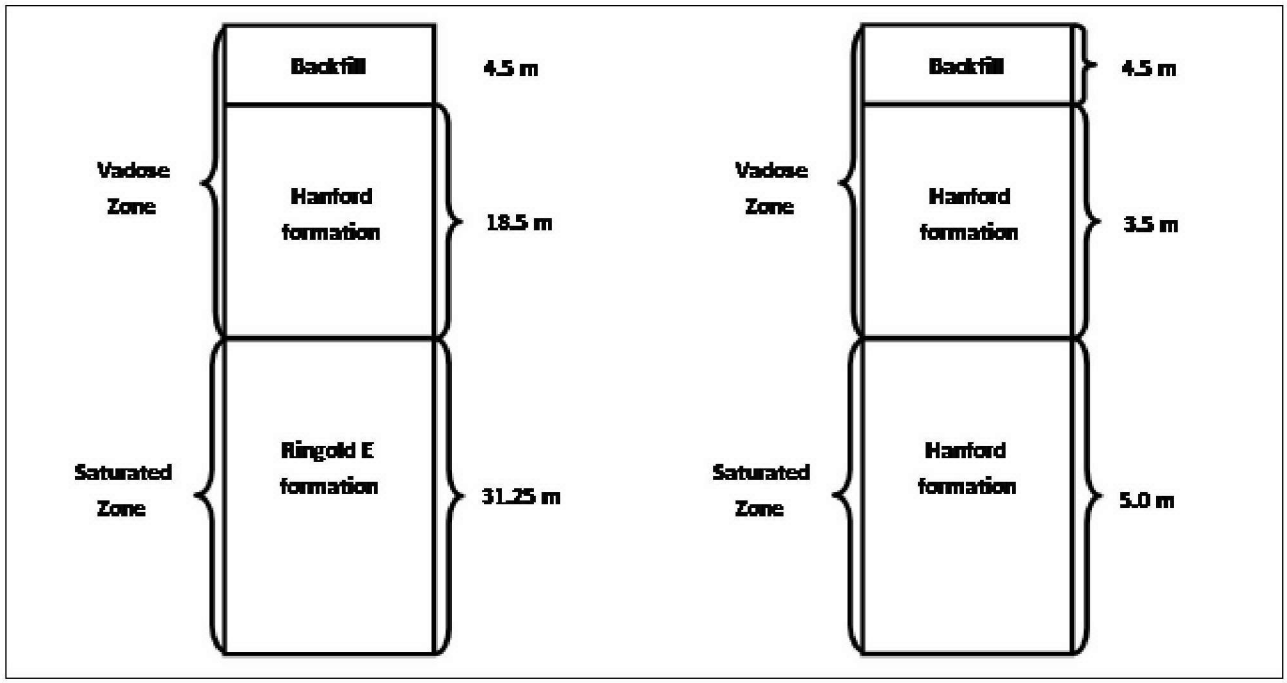

(a) **(b)**

Figure 6-8. (a) Column 2 of 100-BC geographic area and (b) Column 3 of 100-F geographic area

Once the above soil columns along with the soil type are selected in the model the basic structure of the stylized conceptual model is ready for evaluation of epistemic uncertainty. Some of model parameters and their ranges for 100 Area soils were derived from the available experimental data and are presented in Table 6-2. Other parameter values were derived from other sources (e.g., PNNL-14702 Rev. 1). Table 6-2 shows the list of parameters included in the uncertainty analysis. The table includes the parameter values used in developing the model, the range of values, and the standard deviations for each parameter. Sources for these data are also included in the tables. PEST execution required STOMP simulations be carried out two times the number of parameters in the uncertainty file. Therefore, a total of 28 numerical simulations were required for developing the predictive uncertainty distributions for each ACM.

The vadose zone fate and transport calculations were performed using the STOMP Version 3.2 code, Hanford Information System Inventory (HISI) identification number 2471. STOMP and PEST were executed on the RANSAC Linux®[3] Cluster (ransac-0.pnl.gov) that is managed by Pacific Northwest National Laboratory (PNNL). The computer property tag identifier for the frontend node is WD56054 (PNNL Property System). The frontend hardware (controller node) is a Dell® PowerEdge® 2550 with dual 3.00-GHz (Intel® Xeon®[4]) processors and 2 GB of RAM loaded with the Red Hat®[5] Enterprise Linux® Client release 5.5 (Tikanga) operating system.

The results of CHPRC acceptance testing (CHPRC-00515 Rev. 1) demonstrate that the STOMP software is acceptable for its intended use by the CHPRC. Installations of the software are operating correctly, as

[3] Linux is a registered trademark of Linux Tovalds in the United States and other countries.

[4] Intel and Xeon are registered trademarks of Intel in the United States and other countries.

[5] Red Hat is a registered trademark of Red Hat, Inc.

demonstrated by the RANSAC Linux Cluster system producing the same results as those presented for selected problems from the STOMP Application Guide (PNNL-11216). PEST is graded as support software and was used under the software management plan CHPRC-00258 Rev. 2.

6.3.3 Results Summary

Figures 6-9 and 6-10 show charts of the relative uncertainty with respect to predicted groundwater contaminant concentration for each of the parameters listed in Table 6-2. The relative minimized error variance is calculated by dividing the minimized error variance for a given parameter by the sum of all values for minimized error variance for all parameters. The error variance in output for a parameter perturbation is calculated with respect to the results obtained from initial parameter value (base case).

Figure 6-9 illustrates results for Column 2 from 100-BC geographic area and Figure 6-10 shows results from Column 3 from 100-F geographic area. Uncertainty contributions vary significantly from one another. Hydraulic gradient is the largest contributor to uncertainty in 100-BC simulation while van Genuchten parameters play the largest role in the 100-F simulation. The van Genuchten parameters also contribute significantly to predictive uncertainty in the 100-BC simulation. The difference can be explained in the differences in model setup. The 100-F simulation contaminant concentration only covers top half of the vadose zone and the recharge is from a base case recharge scenario. In contrast, the 100-BC contaminant distribution covers the entire vadose zone and has a much larger recharge due to irrigation. The uncertainty estimate illustrates the decreased travel time in the vadose zone to produce the peak groundwater concentration. Because the contaminant in 100-F simulation must travel through the vadose zone for a larger distance above the water table and in much drier conditions, the parameters affecting fate and transport through this portion of the model contribute most to the difference in calculated peak concentrations. In the 100-BC simulation, where contamination exists right above the water table, the uncertainty analysis indicates that travel through the vadose zone is not as important to final predicted concentrations as the amount of clean ground water entering the groundwater system through saturated groundwater flow.

Table 6-2. Model Input Parameters included as Part of the Sensitivity Analysis and their Input Value Ranges and Standard Deviations

Parameter	Units	Formation	Initial	Max	Min	Standard Deviation	Reference
Total Porosity	-	Hanford	0.28	0.40	0.14	7.889E-02	PNNL-14702 Rev.1 via SGW-44022 Rev. 0 Table 8-2
Diffusive Porosity†	-	Hanford	0.25	0.37	0.11	2.813E-02	SGW-40781 Rev. 1, Table 6.1
Total Porosity	-	Ringold	0.28	0.39	0.19	5.597E-02	PNNL-14702 Rev.1 via SGW-44022 Rev. 0 Table 8-2
Diffusive Porosity†	-	Ringold	0.28	0.39	0.19	2.813E-02	SGW-40781 Rev. 1, Table 6.1
Hydraulic Conductivity	cm/s	Hanford	1.02E-03	3.89E-02	6.73E-05	2.777E+00	SGW-40781 Rev. 1, Table 6.1
Hydraulic Conductivity	cm/s	Ringold-S	7.18E-03	6.48E-01	4.63E-05	1.916E-03	SGW-40781 Rev. 1, Table 7.1
van Genuchten α	1/cm	Hanford	0.0100	0.2481	0.0067	1.190E+00	SGW-40781 Rev. 1, Table 6.1
van Genuchten n	-	Hanford	1.41	1.62	1.18	1.649E-01	SGW-40781 Rev. 1, Table 6.1
van Genuchten α	1/cm	Ringold	0.080	0.1513	0.0126	1.079E+00	SGW-40781 Rev. 1, Table 6.1
van Genuchten n	-	Ringold	1.66	1.63	1.19	1.632E-01	SGW-40781 Rev. 1, Table 6.1
Recharge	mm/yr	Natural	1.5	2.25	0.75	7.500E-01	PNNL-14702 Rev.1
Recharge	mm/yr	Production	17	25.5	8.5	8.500E+00	PNNL-14702 Rev.1
Recharge	mm/yr	Early Irrigation	71.4	107.1	35.7	3.570E+01	PNNL-14702 Rev.1
Recharge	mm/yr	Late Irrigation	69.9	104.85	34.95	3.495E+01	PNNL-14702 Rev.1
Head Boundary*	Pa		406148.3	406148.3	406148.3	1.000E+00	Gradient Calculations, ECF-Hanford-11-0063
Head Boundary	Pa		405962.2	406119.3	405589	1.574E+02	Gradient Calculations, ECF-Hanford-11-0063
Dispersivity	m		0.000	1.000	0.000	1.000E+00	PNNL-14702 Rev.1
Distribution Coefficient*	g/cm^3		0.00	500.00	0.00	1.000E+00	PNNL-14702 Rev.1

†Parameter was "tied" to the parameter listed above it. Parameters values changed relative to the other.

*Parameter was set to either "fixed" at the initial value. These parameters were not used as part of the uncertainty analysis

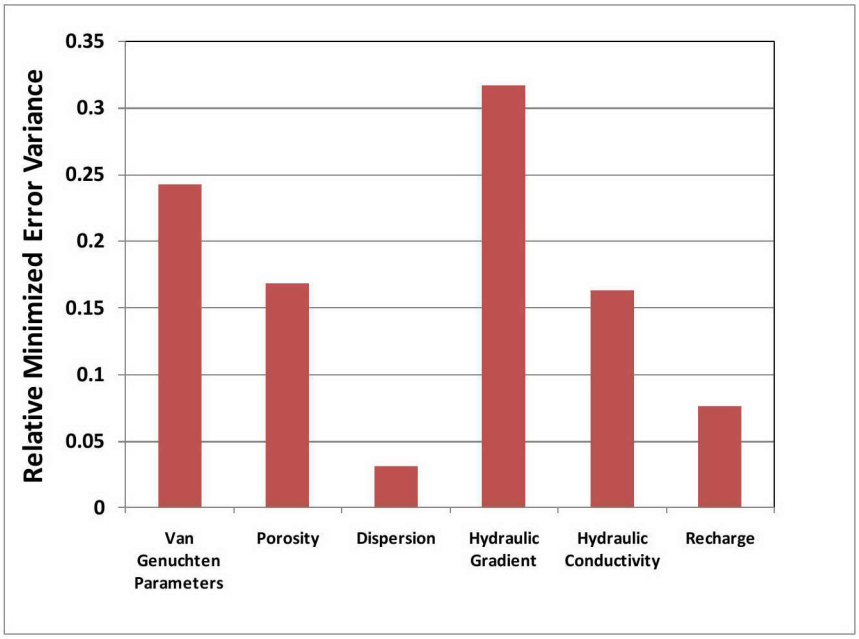

Figure 6-9. Relative Contribution of Parameter Groups to Uncertainty of the Peak Concentration Calculation for Column 2 in the 100-BC Geographic Area

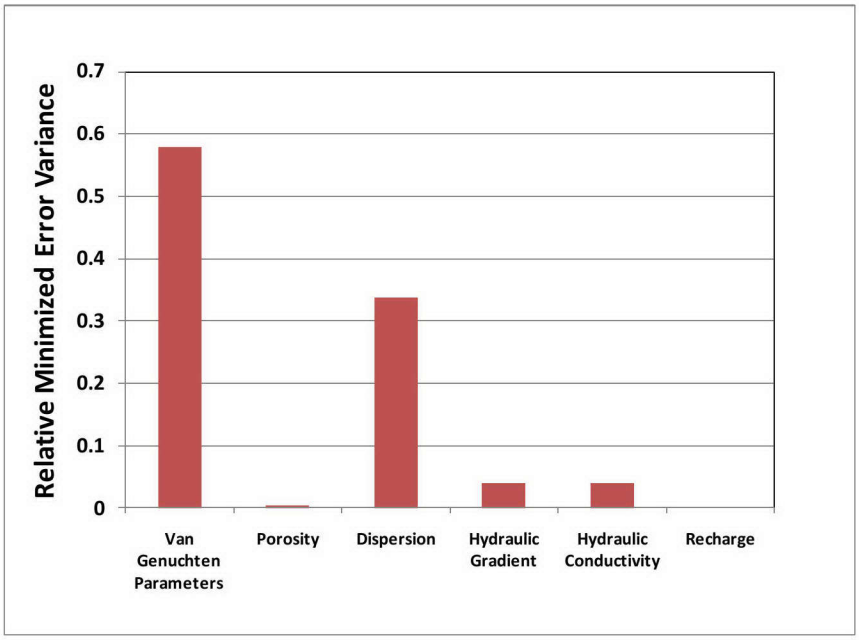

Figure 6-10. Relative Contribution of Parameter Groups to Uncertainty of the Peak Concentration Calculation for Column 3 in the 100-F Geographic Area Ringold Units

6.3.4 Effect of Gravel Correction

Geochemical analysis of soil samples at the Hanford site are typically conducted on soil with the gravel (particles less than 2 mm in diameter) removed. Analysis of these soil samples are corrected based on the percentage of gravel that is in the sample. One model input parameter that can be affected by this correction is the bulk density. The bulk density directly changes the solute concentration used as the initial condition in the model. As described in the methodology section of this report, 1 mg/kg of soil contamination is used as the input to the model. However, STOMP does not support soil concentration as an input in the version (STOMP-W) of STOMP used in the analysis. The input parameter used is titled "Solute Volumetric Concentration" (which is the total mass in a grid-block per unit bulk volume of the grid-block). In order to ensure that 1 mg/kg of contamination is entered into the model, the following equation was used to adjust the value of 1 mg/kg of soil contamination to the Solute Volumetric Concentration.

$$C_v = C_s * \gamma_b \qquad \text{Eq. 6-1}$$

Where, C_v is the solute volume concentration (mg/m^3), C_s is the soil concentration (1 mg/kg), and γ_b is the bulk density in (kg/m^3). Gravel correction directly changes the concentration used in the STOMP input based on the changes in bulk density.

The bulk density and soil concentration were altered in a series of simulations to illustrate the level of conservatism used in the modeling. The bulk density values were taken based on the gravel percentages listed in Table 4-4. The change in bulk density resulted in a proportional change in the Solute Volumetric Concentration. This in turn resulted in a proportional change to the resulting simulated peak concentration. For example, the gravel correction of 43 percent produces a peak concentration 43 percent smaller than the original result. Not utilizing the gravel correction factor in establishing the initial condition provides more conservative result for clean-up level with respect to simulated peak concentration.

7. Model Configuration Management

Consistent with the requirements of CHPRC-00189 Rev. 9 (Appendix G), all inputs and outputs for the development of the soil screening level and PRG models are committed to the Environmental Model Management Archive (EMMA) to maintain and preserve configuration managed models. Basis information (that information collected to form the basis for model input parameterization) is also stored in the EMMA for traceability purposes.

The STOMP software is used to implement the models collectively described in this report. These models are configuration managed as discussed in Section 4.2. Safety Software (CHPRC Build 2 of STOMP) is checked out in accordance with procedures specified in CHPRC-00176 Rev. 2. Source or executable files are obtained from the CHPRC software owner, who maintains the configuration-managed copies in MKS Integrity™. Installation tests identified in CHPRC-00211 Rev. 1 are performed and successful installation confirmed, and software installation and checkout forms are required and must be approved for installations used to perform model runs. Approved users are registered in the Hanford Information System Inventory for Safety Software.

Use of the STOMP software for implementing the model described in this report is consistent with its intended use for CHPRC, as identified in CHPRC-00222 Rev. 1.

7.1 Model Version History

This is the first edition of the RCVZ models. Future revisions to this report will include a history to date of versions issued for the models collectively described by this model package report.

™ MKS Integrity is a trademark of MKS, Incorporated.

8. References

BHI-00917, 1996, *Conceptual Site Models for Groundwater Contamination at 100-BC-5, 100-KR-4, 100-HR-3, and 100-FR-3 Operable Units*, Bechtel Hanford, Inc., Richland, Washington. Available at: http://www5.hanford.gov/arpir/?content=findpage&AKey=D197142704.

Celia, M.A. and W.G. Gray, 1992, *Numerical Methods for Differential Equations*, Prentice Hall, Englewood Cliffs, New Jersey.

Chandler, D.P., F.J. Brockman, T.J. Bailey and J.K. Fredrickson, 1997, "Phylogenetic Diversity of Archaea and Bacteria in a Deep Subsurface Paleosol," *Microbial Ecology*, Vol. 36, No. 1, pp. 37 50.

CHPRC-00176, 2011, *STOMP Software Management Plan*, Rev. 2, CH2M HILL Plateau Remediation Company, Richland, Washington.

CHPRC-00189, *CH2M HILL Plateau Remediation Company Environmental Quality Assurance Program Plan*, Rev. 9, CH2M HILL Plateau Remediation Company, Richland, Washington.

CHPRC-00211, 2011, *STOMP Software Test Plan*, Rev. 1, CH2M HILL Plateau Remediation Company, Richland, Washington.

CHPRC-00222, 2011, *STOMP Functional Requirements Document*, Rev. 1, CH2M HILL Plateau Remediation Company, Richland, Washington.

CHPRC-00258, 2010, *MODFLOW and Related Codes Software Management Plan*, Rev. 2, CH2M HILL Plateau Remediation Company, Richland, Washington.

CHPRC-00269, 2011, *STOMP Requirements Traceability Matrix*, Rev. 1, CH2M HILL Plateau Remediation Company, Richland, Washington.

CHPRC-00515, 2011, *STOMP Acceptance Test Report*, Rev. 1, CH2M HILL Plateau Remediation Company, Richland, Washington.

CRC Press, 2005, *Chromium(VI) Handbook*, Independent Environmental Technical Evaluation Group, Guertin, J., J.A. Jacobs, and C.P. Avakian eds., CRC Press, New York, New York.

CVP-99-00007, 2000, *Cleanup Verification Package for 116-D-7 Retention Basin*, Rev. 0, Bechtel Hanford, Inc., Richland, Washington. Available at: http://www5.hanford.gov/arpir/?content=findpage&AKey=D5615147.

DOE/RL-92-24, 2001, *Hanford Site Background*, Rev. 4, U.S. Department of Energy, Richland Operations Office, Richland, Washington. Available at: http://www5.hanford.gov/arpir/?content=findpage&AKey=0096062, http://www5.hanford.gov/arpir/?content=findpage&AKey=0096061.

DOE/RL-93-37, *Limited Field Investigation Report for the 100-BC-5 Operable Unit*, Rev. 0, U.S. Department of Energy, Richland Operations Office, Richland, Washington. Available at: http://www5.hanford.gov/arpir/?content=findpage&AKey=D196075584.

DOE/RL-93-43, *Limited Field Investigation Report for the 100-HR-3 Operable Unit*, Rev. 0, U.S. Department of Energy, Richland Operations Office, Richland, Washington. Available at: http://www5.hanford.gov/arpir/?content=findpage&AKey=D196060716.

DOE/RL-93-83, *Limited Field Investigation Report for the 100-FR-3 Operable Unit*, Rev. 0, U.S. Department of Energy, Richland Operations Office, Richland, Washington. Available at: http://www5.hanford.gov/arpir/?content=findpage&AKey=D196084471.

DOE/RL-96-17, *Remedial Design Report/Remedial Action Work Plan for the 100 Area*, Rev. 6, U.S. Department of Energy, Richland Operations Office, Richland, Washington. Available at: http://www5.hanford.gov/arpir/?content=findpage&AKey=0810240391.

DOE/RL-2002-39, *Standardized Stratigraphic Nomenclature for Post-Ringold-Formation Sediments within the Central Pasco Basin*, U.S. Department of Energy, Richland Operations Office, Richland, Washington.

DOE/RL-2005-40, *100-BC Pilot Project Risk Assessment Report*, Draft B, U.S. Department of Energy, Richland Operations Office, Richland, Washington. Available at: http://www5.hanford.gov/arpir/?content=findpage&AKey=DA01944866, http://www5.hanford.gov/arpir/?content=findpage&AKey=DA01945154, http://www5.hanford.gov/arpir/?content=findpage&AKey=DA01945466, http://www5.hanford.gov/arpir/?content=findpage&AKey=DA01945824, http://www5.hanford.gov/arpir/?content=findpage&AKey=DA01946039.

DOE/RL-2008-46-ADD1, *Integrated 100 Area Remedial Investigation/Feasibility Study Work Plan Addendum 1: 100-DR-1, 100-DR-2, 100-HR-1, 100-HR-2, and 100-HR-3 Operable Units*, Rev. 0, U.S. Department of Energy, Richland Operations Office, Richland, Washington. Available at: http://www5.hanford.gov/arpir/?content=findpage&AKey=0084374.

DOE/RL-2008-46-ADD2, *Integrated 100 Area Remedial Investigation/Feasibility Study Work Plan Addendum 2: 100-KR-1, 100-KR-2, and 100-KR-4 Operable Units*, Rev 0, U.S. Department of Energy, Richland Operations Office, Richland, Washington. Available at: http://www5.hanford.gov/arpir/?content=findpage&AKey=0906110864.

DOE/RL-2008-46-ADD3, *Integrated 100 Area Remedial Investigation Feasibility Study Work Plan Addendum 3 100-BC-1 100-BC-2 And 100-BC-5 Operable Units 100BC Area Base Map and BC Reactor Map*, Rev. 0, U.S. Department of Energy, Richland Operations Office, Richland, Washington. Available at: http://www5.hanford.gov/arpir/?content=findpage&AKey=0084266.

DOE/RL-2008-46-ADD4, *Integrated 100 Area Remedial Investigation/Feasibility Study Work Plan Addendum 4: 100-FR-1, 100-FR-2, 100-FR-3, 100-IU-2, and 100-IU-6 Operable Units*, Rev. 0 REISSUE, U.S. Department of Energy, Richland Operations Office, Richland, Washington. Available at: http://www5.hanford.gov/arpir/?content=findpage&AKey=1006220804.

DOE/RL-2008-46-ADD5, *Integrated 100 Area Remedial Investigation Feasibility Study Work Plan Addendum 5 100-NR-1 and 100-NR-2 Operable Units*, Rev. 0, U.S. Department of Energy, Richland Operations Office, Richland, Washington. Available at: http://www5.hanford.gov/arpir/?content=findpage&AKey=1105031084, http://www5.hanford.gov/arpir/?content=findpage&AKey=1105031085, http://www5.hanford.gov/arpir/?content=findpage&AKey=1105031086, http://www5.hanford.gov/arpir/?content=findpage&AKey=1105031087,

http://www5.hanford.gov/arpir/?content=findpage&AKey=1105031088,
http://www5.hanford.gov/arpir/?content=findpage&AKey=1105031089,
http://www5.hanford.gov/arpir/?content=findpage&AKey=1105031090,
http://www5.hanford.gov/arpir/?content=findpage&AKey=1105031091,
http://www5.hanford.gov/arpir/?content=findpage&AKey=1105031092,
http://www5.hanford.gov/arpir/?content=findpage&AKey=1105031093,
http://www5.hanford.gov/arpir/?content=findpage&AKey=1105031094,
http://www5.hanford.gov/arpir/?content=findpage&AKey=1105031095,
http://www5.hanford.gov/arpir/?content=findpage&AKey=1105031096,
http://www5.hanford.gov/arpir/?content=findpage&AKey=1105031097,
http://www5.hanford.gov/arpir/?content=findpage&AKey=1105031098,
http://www5.hanford.gov/arpir/?content=findpage&AKey=1105031099,
http://www5.hanford.gov/arpir/?content=findpage&AKey=1105031100,
http://www5.hanford.gov/arpir/?content=findpage&AKey=1105031101,
http://www5.hanford.gov/arpir/?content=findpage&AKey=1105031102,
http://www5.hanford.gov/arpir/?content=findpage&AKey=1105031103,
http://www5.hanford.gov/arpir/?content=findpage&AKey=1105031104,
http://www5.hanford.gov/arpir/?content=findpage&AKey=1105031105,
http://www5.hanford.gov/arpir/?content=findpage&AKey=1105031106,
http://www5.hanford.gov/arpir/?content=findpage&AKey=1105031107,
http://www5.hanford.gov/arpir/?content=findpage&AKey=1105031108.

DOE/RL-2009-42, *Sampling and Analysis Plan for the 100-NR-1 and 100-NR-2 Operable Units Remedial Investigation/Feasibility Study*, Rev. 0, U.S. Department of Energy, Richland Operations Office, Richland, Washington. Available at: http://www5.hanford.gov/arpir/?content=findpage&AKey=0084103.

DOE/RL-2010-11, *Hanford Site Groundwater Monitoring and Performance Report for 2009: Volumes 1 and 2*, U.S. Department of Energy, Richland Operations Office, Richland, Washington. Available at: http://www5.hanford.gov/arpir/?content=findpage&AKey=0084237.

DOE/RL-2011-50, 2011, *Regulatory Basis and Implementation of a Graded Approach to Evaluation of Groundwater Protection*, Rev. 0, U.S. Department of Energy, Richland Operations Office, Richland, Washington.

DOE-STD-1153-2002, 2002, *A Graded Approach for Evaluating Radiation Does to Aquatic and Terrestrial Biota*, U.S. Department of Energy, Washington, DC. Available at: http://www.hss.doe.gov/nuclearsafety/techstds/docs/standard/1153_Frontmatter.pdf.

Doherty, John E. and Randall J. Hunt, 2010, *Approaches to Highly Parameterized Inversion: A Guide to Using PEST for Groundwater-Model Calibration*, U.S. Geological Survey Scientific Investigations Report 2010-5169, Washington, DC.

ECF-Hanford-10-0442, 2010, *Calculation of Nonradiological Preliminary Remediation Goals using the Fixed Parameter 3-Phase Equilibrium Partitioning Equation for Groundwater Protection in the 100 Areas and 300 Area*, Rev. 0, CH2M HILL Plateau Remediation Company, Richland, Washington, Richland, Washington.

ECF-Hanford-11-0038, 2011, *Soil Background Data for Interim Use at the Hanford Site*, Rev.0, CH2M HILL Plateau Remediation Company, Richland, Washington, Richland, Washington.

ECF-Hanford-11-0063, 2011, *STOMP 1-D Vadose Zone Modeling for Determination of Preliminary Remediation Goals for 100 Area D, H, and K Source Operable Units*, Rev. 5, CH2M HILL Plateau Remediation Company, Richland, Washington.

ECF-Hanford-11-0165, 2011, *Evaluation of Hexavalent Chromium Leach Test Data Conducted on Vadose Zone Sediment Samples from the 100 Area*, Rev. 0, CH2M HILL Plateau Remediation Company, Richland, Washington.

EPA/540/R-95/128, *Soil Screening Guidance: Technical Background Document*, U.S. Environmental Protection Agency, Washington, DC.

EPA/540/R-96/018, *Soil Screening Guidance: Users Guide*, U.S. Environmental Protection Agency, Washington, DC.

EPA/ROD/R10-99/039, *EPA Superfund Record of Decision: Hanford 200-Area (USDOE) and Hanford 100-Area (USDOE)*, U.S. Environmental Protection Agency, Washington, DC.

Gee, G.W., J.M. Keller and A.L. Ward, 2005, *Measurement and Prediction of Deep Drainage from Bare Sediments at a Semiarid Site,* Vadose Zone Journal, Vol. 4, No. 1, p. 9.

Gee, G.W., M. Oostrom, M.D. Freshley, M.L. Rockhold, and J.M. Zachara, 2007, *Hanford Site Vadose Zone Studies: An Overview*, Vadose Zone Journal, Vol. 6, No. 4, pp. 899-905.

Han, R., J.T. Geller, L. Yang, E.L. Brodie, R. Chakraborty, J.T. Larsen, and H.R. Beller, 2010, *Physiological and Transcriptional Studies of Cr(VI) Reduction Under Aerobic and Denitrifying Conditions by an Aquifer-Derived Pseudomonad*, Environmental Science Technology, 44, 7491-7497.

HW-34499, 1955, *Adsorption and Retention of Strontium by Soils of the Hanford Project*, General Electric, Hanford Atomic Products Operation, Richland, Washington.

HW-56582, 1958, *Influence of Limestone Neutralization on the Soil Uptake of Sr-90 from a Radioactive Waste*, General Electric Company, Hanford Atomic Products Operation, Richland, Washington.

Jury, W.A., W.R. Gardner, and W.H. Gardner, 1991, *Soil Physics*, 328 pp., John Wiley, Hoboken, New Jersey.

Klein, K.A., 2006, Letter: Contract No. DE-AC06-96RL13200 - Hanford Groundwater Modeling Integration, to R. G. Gallagher, Richland, Washington, U.S. Department of Energy, Richland Operations Office.

Moore, C. and J. Doherty, 2005. *The role of the calibration process in reducing model predictive error.* Water Resources Research. Vol 41, No 5: W05020.

Mualem, Y., 1976, *A New Model for Predicting the Hydraulic Conductivity of Unsaturated Porous Media*, Water Resources Research, Vol. 12, pp. 513-522.

Nichols, W.E., N.J. Aimo, M. Oostrom, and M.D. White, 1997. Subsurface Transport Over Multiple Phases Applicaton Guide, PNNL-11216, Pacific Northwest National Laboratory, Richland, Washington.

Patankar, S.V., 1980, *Numerical heat transfer and fluid flow*. Hemisphere Publishing Corporation, Washington, D.C.

Parker, J.C. and M.Th. van Genuchten, 1984. *Determining Transport Parameters from Laboratory and Field Tracer Experiments*, Virginia Agricultural Experiment Station Bulletin 84-3.

Peterson, R.E., R.F. Raidl, and C.W. Denslow, 1996. *Conceptual Site Models for Groundwater Contamination at 100-BC-5, 100-KR-4, 100-HR-3, and 100-FR-3 Operable Units,* BHI-00917 Rev. 0, Bechtel Hanford, Inc., Richland, Washington.

PNL-6403, 1987, *Recharge at the Hanford Site: Status Report*, Pacific Northwest Laboratory, Richland, Washington. Available at: http://www.osti.gov/bridge/servlets/purl/5539519-iBxaB8/5539519.pdf.

PNL-6456, 1998, *Hazard Ranking System Evaluation of CERCLA Inactive Waste Sites at Hanford*, Pacific Northwest National Laboratory, Richland, Washington. Available at: http://www5.hanford.gov/pdw/fsd/AR/FSD0001/FSD0041/D196006954/D196006954_2395.pdf.

PNL-6810, 1989, *The Field Lysimeter Test Facility (FLTF) at the Hanford Site: Installation and Initial Tests*, Pacific Northwest National Laboratory, Richland, Washington. Available at: http://www.osti.gov/bridge/servlets/purl/6518216-fj8Lhm/6518216.pdf.

PNL-7209, 1990, *Field Lysimeter Test Facility: Second Year (FY 1989) Test Results*, Pacific Northwest National Laboratory, Richland, Washington. Available at: http://www.osti.gov/bridge/servlets/purl/6973885-0GBmG8/6973885.pdf.

PNL-10285, 1995, *Estimated Recharge Rates at the Hanford Site*, Pacific Northwest Laboratory, Richland, Washington. Available at: http://www.osti.gov/energycitations/servlets/purl/10122247-XORHkt/webviewable/10122247.pdf.

PNNL-11216, 1997, *STOMP Subsurface Transport Over Multiple Phases: Application Guide*, Pacific Northwest National Laboratory, Richland, Washington. Available at: http://stomp.pnnl.gov/documentation/guides/application.pdf.

PNNL-12030, 2000, *STOMP Subsurface Transport Over Multiple Phases Version 2.0 Theory Guide*, Pacific Northwest National Laboratory, Richland, Washington. Available at: http://stomp.pnnl.gov/documentation/guides/theory.pdf.

PNNL-13033, 1999, *Recharge Data Package for the Immobilized Low-Activity Waste 2001 Performance Assessment*, Pacific Northwest National Laboratory, Richland, Washington. Available at: http://www.pnl.gov/main/publications/external/technical_reports/13033.pdf.

PNNL-13674, 2001, *Zone of Interaction Between Hanford Site Groundwater and Adjacent Columbia River*, Pacific Northwest National Laboratory, Richland, Washington. Available at: http://www.pnl.gov/main/publications/external/technical_reports/pnnl-13674.pdf.

PNNL-13688, 2001, *Vascular Plants of the Hanford Site*, Pacific Northwest National Laboratory, Richland, Washington. Available at: http://www.pnl.gov/main/publications/external/technical_reports/pnnl-13688.pdf.

PNNL-14202, 2003, *Mineralogical and Bulk-Rock Geochemical Signatures of Ringold and Hanford Formation Sediments*, Pacific Northwest National Laboratory, Richland, Washington. Available at: http://www.pnl.gov/main/publications/external/technical_reports/pnnl-13688.pdf.

PNNL-14702, 2006, *Vadose Zone Hydrogeology Data Package for Hanford Assessments*, Rev. 1, Pacific Northwest National Laboratory, Richland, Washington. Available at: http://www.pnl.gov/main/publications/external/technical_reports/PNNL-14702rev1.pdf.

PNNL-14744, 2004, *Recharge Data Package for the 2005 Integrated Disposal Facility Performance Assessment*, Pacific Northwest National Laboratory, Richland, Washington. Available at: http://www.pnl.gov/main/publications/external/technical_reports/PNNL-14744.pdf.

PNNL-15160, 2005, *Hanford Site Climatological Summary 2004 with Historical Data*, Pacific Northwest National Laboratory, Richland, Washington. Available at: http://www.pnl.gov/main/publications/external/technical_reports/PNNL-15160.pdf.

PNNL-15782, 2006, *STOMP Subsurface Transport Over Multiple Phases Version 4.0 User's Guide*, Pacific Northwest National Laboratory, Richland, Washington. Available at: http://www.pnl.gov/main/publications/external/technical_reports/PNNL-15782.pdf.

PNNL-16346, 2007, *Hanford Site Groundwater Monitoring for Fiscal Year 2006*, Pacific Northwest National Laboratory, Richland, Washington. Available at: http://www.pnl.gov/main/publications/external/technical_reports/PNNL-16346.pdf.

PNNL-16688, 2007, *Recharge Data Package for Hanford Single-Shell Tank Waste Management Areas*, Pacific Northwest National Laboratory, Richland, Washington. Available at: http://www.pnl.gov/main/publications/external/technical_reports/PNNL-16688.pdf.

PNNL-17674, 2008, *Geochemical Characterization of Chromate Contamination in the 100 Area Vadose Zone at the Hanford Site*, Pacific Northwest National Laboratory, Richland, Washington. Available at: http://www.pnl.gov/main/publications/external/technical_reports/PNNL-17674.pdf.

PNNL-17841. 2008, *Compendium of Data for the Hanford Site (Fiscal Years 2004 to 2008) Applicable to Estimation of Recharge Rates*, Pacific Northwest National Laboratory, Richland, Washington. Available at: http://www.pnl.gov/main/publications/external/technical_reports/PNNL-17841.pdf.

PNNL-18564, 2009, *Selection and Traceability of Parameters to Support Hanford-Specific RESRAD Analyses Fiscal Year 2008 Status Report*, Pacific Northwest National Laboratory, Richland, Washington. Available at: http://www.pnl.gov/main/publications/external/technical_reports/PNNL-18564.pdf.

PNNL-18577, 2009, *A Review of Metal Concentrations Measured in Surface Soil Samples Collected on and Around the Hanford Site*, Pacific Northwest National Laboratory, Richland, Washington. Available at: http://www.pnl.gov/main/publications/external/technical_reports/PNNL-18577.pdf.

PNNL-18784, 2009, *Hanford 100-D Area Biostimulation Treatability Test Results*, Pacific Northwest National Laboratory, Richland, Washington. Available at: http://www.pnl.gov/main/publications/external/technical_reports/PNNL-18784.pdf.

PNNL-6415, *Hanford Site National Environmental Policy Act (NEPA) Characterization*, Rev. 18, Pacific Northwest National Laboratory, Richland, Washington. Available at: http://www.pnl.gov/main/publications/external/technical_reports/PNNL-6415Rev18.pdf.

PNNL-SA-54022, 2007, *STOMP Software Test Plan Rev. 1.0*, Pacific Northwest National Laboratory, Richland, Washington. Available at: http://stomp.pnnl.gov/documentation/qa/qa_software_testplan.pdf.

PNNL-SA-54023, 2007, *STOMP Software Configuration Management Plan Rev. 1.3*, Pacific Northwest National Laboratory, Richland, Washington. Available at: http://stomp.pnnl.gov/documentation/qa/qa_configuration_mgmt_plan.pdf.

PNNL-SA-54079, 2007, *Requirements for STOMP Subsurface Transport Over Multiple Phases*, Pacific Northwest National Laboratory, Richland, Washington. Available at: http://stomp.pnnl.gov/documentation/qa/qa_requirements.pdf.

PRC-PRO-IRM-309, *Controlled Software Management*, Rev. 1, CH2M-HILL Plateau Remediation Company, Richland, Washington.

Rohay, V.J., D.C. Weeks, W.J. McMahon, and J.V. Borghese, 1999. *The Chromium Groundwater Plume West of the 100-D/DR Reactors: Summary and Fiscal Year 1999 Update*. BHI-01309 Rev. 0, Bechtel Hanford, Inc, Richland, Washington.

RPP-20621, 2004, *Far-Field Hydrology Data Package for the Integrated Disposal Facility Performance Assessment*, Rev. 0, CH2M HILL Hanford Group, Inc., Richland, Washington.

Selker, J., C. Kent, and J. McCord, 1999, *Vadose Zone Processes*, Lewis Publishers, New York, New York.

SGW-39305 Rev. 0, 2008, *Technical Evaluation of the Interaction of Groundwater with the Columbia River at the Department of Energy Hanford Site, 100-D Area*, Fluor, Richland, Washington. Available at: http://www.osti.gov/bridge/servlets/purl/943297-EPtwMW/943297.pdf.

SGW-40781, 2009, *100-HR-3 Remedial Process Optimization Modeling Data Package*, Rev. 1, CH2M HILL Plateau Remediation Company, Richland, Washington.

SGW-41213, 2009, *100-KR-4 Remedial Process Optimization Modeling Data Package*, Rev. 0, CH2M HILL Plateau Remediation Company, Richland, Washington. Available at: http://www5.hanford.gov/arpir/?content=findpage&AKey=0908311235.

SGW-44022, *Geologic Data Package in Support of 100-BC-5 Modeling*, Rev. 0, CH2M HILL Plateau Remediation Company, Richland, Washington. Available at: http://www5.hanford.gov/arpir/?content=findpage&AKey=1003100446.

SGW-44022, *Geologic Data Package in Support of 100-BC-5 Modeling*, Rev. 1, CH2M HILL Plateau Remediation Company, Richland, Washington.

SGW-46279, 2010, *Conceptual Framework and Numerical Implementation of 100 Areas Groundwater Flow and Transport Model*, Rev. 0, CH2M HILL Plateau Remediation Company, Richland, Washington.

Świetlik, R., 2002, *Kinetic Study of Redox Processes of Chromium in Natural River Water*, Polish Journal of Environmental Studies, Vol. 11, No. 4, 441-447.

Toride, N., F. J. Leij, and M.Th. van Genuchten, 1999, *The CXTFIT Code for Estimating Transport Parameters from Laboratory or Field Tracer Experiments*, Research Report No. 137, US Salinity Laboratory, Agricultural Research Service, U.S. Department of Agriculture, Riverside California.

van Genuchten, M. T., 1980, *A Closed-Form Solution for Predicting the Conductivity of Unsaturated Soils*, Soil Science Society of America Journal, Vol. 44, pp. 892-898.

WCH-380, 2010, *Field Summary Report for Remedial Investigation of Hanford Site Releases to the Columbia River, Hanford Site, Washington*, Rev. 0, Washington Closure Hanford, Richland, Washington. Available at: http://www.washingtonclosure.com/documents/mission_complete/WCH-380%20Rev.%200/WCH-380%20Rev%200.pdf.

WHC-SD-EN-DP-090, *Borehole Data Package for the 100-K Area Ground Water Wells, CY 1994*, Rev. 0, Westinghouse Hanford Company, Richland, Washington.

Appendix A

Method for Determining Representative Stratigraphic Columns For Various Geographic Areas

The following are the steps taken to produce the representative geology for each OU.

1) Began with data from GRAM, Inc.
    a. 100 Area RUM and RE elevation master_10-19-10.xls
        i. Contained borehole location/depth information and elevations of Hanford/RE and RUM contacts.
2) Brought data into ArcGIS and used GIS techniques to select "representative" boreholes of the waste sites in each of the 100 D,H,K, BC, F, IU, and N vadose zone OUs.
    a. Selection Criteria:
        i. Within 35 m of waste sites (if none then further)
        ii. Representation to RUM (didn't use wells that ended mid upper formations)
        iii. If no borehole representation where needed then used interpolated surfaces to determine formation elevations.
3) Calculations
    a. GIS
        i. Water Level Jun 2008 elev (m)
            1. surfer grid head elevation file from SSPA's 100 area groundwater model
        ii. LiDAR
            1. 2010 terrain/surface elevation ArcGIS grid
        iii. Vadose Thickness (m)
            1. *VZTHICK=Ground surface (GS) – Water Table (WT)*
        iv. Aquifer Thickness (m)
            1. *AQTHICK=WT-RUM*
        v. Waste Site Closest to Well
            1. Spatial Join (ArcGIS tool)
        vi. Distance Well is from Wastesite (m)
            1. Spatial Join (ArcGIS tool)
    b. Excel—for each representative borehole/location
        i. Total Thickness (m)
            1. *TOTTHICK=GS-RUMCONTACT*
        ii. Hanford (%) in Vadose
            1. *VZHF=IF(WT>HFRECONTACT, 1,(GS-HFRECONTACT)/VZTHICK)*
        iii. RE (%) in Vadose
            1. *VZRE=1-VZHF*
        iv. Hanford saturated (%)
            1. *SATHF=IF(VZHF<1,0,(IF(HFRECONTACT>RUMCONTACT,(WT-HFRECONTACT)/AQTHICK,1)))*
        v. RE saturated (%)
            1. *SATRE=1-SATHF*
        vi. Total Hanford (%)
            1. *HFTOT=IF(HFRECONTACT>RUMCONTACT,(GS-HFRECONTACT)/TOTTHICK,(GS-RUMCONTACT)/TOTTHICK)*
        vii. Total RE (%)
            1. *=1-HFTOT*

Appendix B

Description of STOMP Input File

STOMP INPUT FILE

A STOMP input file is composed of cards, some of which are required and others which are optional or unused depending on the operational mode. In the STOMP-W mode following card are necessary for simulating flow and transport.

1. Simulation Control Card
2. Solution Control Card
3. Grid Card
4. Rock/Soil Zonation Card
5. Mechanical Properties Card
6. Hydraulic Properties Card
7. Saturation Function Card
8. Aqueous Relative Permeability Card
9. Initial Conditions Card
10. Boundary Conditions Card
11. Solute/Fluid Interactions Card
12. Solute/Porous Media Interactions Card
13. Surface Flux Card
14. Output Control Card

Descriptions of these cards can be found in STOMP user guide (PNNL-15782) and input file formats can be found in Appendix A of the user guide. For an example of input files[6] one column (column 3) from 100-D area is chosen. Figure B-1 shows the column with different zone thickness. Two sequential STOMP simulations were used. The first stage, called the pre-2010 model, simulated flow through the representative columns for a 2,010-year period. Results from the pre-2010 simulations provided initial aqueous pressure conditions for the 3,000-year-long second stage simulation in a file called restart. This restart file was used for the post-2010 model, which is solved for both flow and solute transport. Both of the input files are explained below.

[6] The parameter values in the input file are presented for the purpose of illustration of the model set-up only and do not necessarily imply that the final calculations were run with this parameter set.

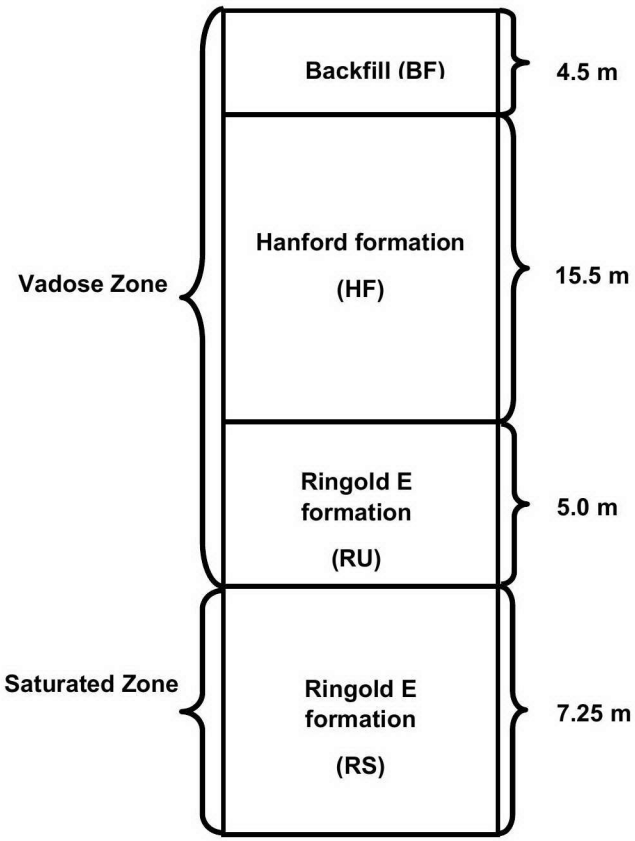

Figure B-1: Stratigraphic columns for 100-D (Column 3).

Pre-2010 Model

Note: Text in black color indicates STOMP inputs while text in blue color is explanation of the inputs.

~Simulation Title Card

#card name start with ~ symbol

1,

#STOMP version number,

100 DR 1D,

#Simulation Title,

C Cheng,

#User name,

Intera Inc.,

#Company name,

Feb 2nd 2011,

#Input creation date,

12:00 PM MST,

#Input creation time,

1,

#Number of simulation note lines,

This input file is a 1D scoping model for 100 Area site D.

#Simulation notes

~Solution Control Card

#card name start with ~ symbol

Normal,

#Execution mode option,

Water,,

#Operation mode option,

1,

#Number of execution time periods,

0.,yr,2010.,yr,1.0e-09,yr,0.01,yr,1.25,8,1.e-6,

#intial time,unit,final time, unit, initial time step, unit, maximum time step, unit, time step acceleration factor, maximum number of Newton-Raphson iterations, convergence criteria,

500000,

#maximum number of time step,

0,

#number of interfacial averaging variables,

~Grid Card

#card name start with ~ symbol

cartesian,

#coordinate system option,

1, 1,129,

#number of X-direction nodes, number of Y-direction nodes, number of Z-direction nodes,

0.0, m, 10, m,

X dir surface position, unit, surface position, unit,

0, m, 1.0, m,

Y dir surface position, unit, surface position, unit,

110.75,m,129@0.25,m,

Z dir surface position, unit, numberof nodes@node width,

~Rock/Soil Zonation Card

#card name start with ~ symbol

4,

#number of rock/soil zone,

RS, 1,1,1,1,1,29,

#zone name (Ringold saturated), X-dir starting node, X-dir ending node, Y-dir starting node, Y-dir ending node, Z-dir starting node, Z-dir ending node,

RU, 1, 1,1,1,30,49,

#zone name (Ringold unsaturated), X-dir starting node, X-dir ending node, Y-dir starting node, Y-dir ending node, Z-dir starting node, Z-dir ending node,

HF, 1, 1, 1,1,50,111,

#zone name (Hanford), X-dir starting node, X-dir ending node, Y-dir starting node, Y-dir ending node, Z-dir starting node, Z-dir ending node,

BF, 1,1,1,1,112,129,

#zone name (Backfill) , X-dir starting node, X-dir ending node, Y-dir starting node, Y-dir ending node, Z-dir starting node, Z-dir ending node,

~Mechanical Properties Card

#card name start with ~ symbol

BF,2.68,g/cm^3,0.276,0.262,,,Millington and Quirk,

#zone name, particle density, unit, total porosity, diffusive porosity, specific storativity - default = 1E-07*diff porosity, units - default = 1/m, tortuosity function,

HF,2.68,g/cm^3,0.280,0.25,,,Millington and Quirk,

#zone name, particle density, unit, total porosity, diffusive porosity, specific storativity - default = 1E-07*diff porosity, units - default = 1/m, tortuosity function,

RU,2.68,g/cm^3,0.280,0.28,,,Millington and Quirk,

#zone name, particle density, unit, total porosity, diffusive porosity, specific storativity - default = 1E-07*diff porosity, units - default = 1/m, tortuosity function,

RS,2.68,g/cm^3,0.280,0.28,,,Millington and Quirk,

#zone name, particle density, unit, total porosity, diffusive porosity, specific storativity - default = 1E-07*diff porosity, units - default = 1/m, tortuosity function,

~Hydraulic Properties Card

#card name start with ~ symbol

BF,5.98E-04,hc:cm/s,,,5.98E-04,hc:cm/s,

#zone name, X-direction hydraulic conductivity, units, Y-direction hydraulic conductivity (zero), units, Z-direction hydraulic conductivity, units,

HF,2.10E-03,hc:cm/s,,,2.10E-04,hc:cm/s,

#zone name, X-direction hydraulic conductivity, units, Y-direction hydraulic conductivity (zero), units, Z-direction hydraulic conductivity, units,

RU,4.13E-03,hc:cm/s,,,4.13E-04,hc:cm/s,

#zone name, X-direction hydraulic conductivity, units, Y-direction hydraulic conductivity (zero), units, Z-direction hydraulic conductivity, units,

RS,2.59E-02,hc:cm/s,,,2.59E-03,hc:cm/s,

#zone name, X-direction hydraulic conductivity, units, Y-direction hydraulic conductivity (zero), units, Z-direction hydraulic conductivity, units,

~Saturation Function Card

#card name start with ~ symbol

BF, Nonhysteretic van Genuchten, 0.019, 1/cm,1.4,0.162,,

#zone name, moisture retention function, vG alpha, units, vG n, residual saturation, vG m - default = 1 - 1/n,

HF, Nonhysteretic van Genuchten, 0.021, 1/cm,1.458,0.04,,

#zone name, moisture retention function, vG alpha, units, vG n, residual saturation, vG m - default = 1 - 1/n,

RU, Nonhysteretic van Genuchten, 0.008, 1/cm,1.66,0.093,,

#zone name, moisture retention function, vG alpha, units, vG n, residual saturation, vG m - default = 1 - 1/n,

RS, Nonhysteretic van Genuchten, 0.008, 1/cm,1.66,0.093,,

#zone name, moisture retention function, vG alpha, units, vG n, residual saturation, vG m - default = 1 - 1/n,

~Aqueous Relative Permeability Card

#card name start with ~ symbol

BF, Mualem,,

#zone name, permeability function name, vG m parameter (default =1-1/n),

HF,Mualem,,

#zone name, permeability function name, vG m parameter (default =1-1/n),

RU,Mualem,,

#zone name, permeability function name, vG m parameter (default =1-1/n),

RS,Mualem,,

#zone name, permeability function name, vG m parameter (default =1-1/n),

~Initial Conditions Card

#Initial conditions area applied at node center

#card name start with ~ symbol

Aqueous Pressure, Gas Pressure,

#initial saturation optionA, initial saturation optionB,

2,

#number of initial conditions,

Aqueous Pressure,1.7110383E+05,Pa,,,,,-9793.52,1/m,1,1,1,1,1,29,

#variable name, magnitude,unit,X-dir pressure gradient,unit, Y-dir pressure gradient,unit,Z-dir pressure gradient,unit, X-dir starting node ,X-dir ending node,Y-dir starting node, Y-dir ending node,Z-dir starting node, Z-dir ending node,

*# Notes: Calculation of base pressure: saturated thickness = 7.25 m, Atmospheric pressure = 1.01E+05 Pa, water unit weight = 9793.52 N/m^3, node spacing = 0.25m, so base pressure (at the center of bottom node) = 101325 + 9793.52 * (7.25-0.125) = 1.711E+05 Pa.*

Aqueous Pressure,86656.7554,Pa,,,,,-100.,1/m,1,1,1,1,30,129,

#variable name,magnitude,unit,X-dir pressure gradient,unit, Y-dir pressure gradient,unit,Z-dir pressure gradient,unit, X-dir starting node ,X-dir ending node,Y-dir starting node, Y-dir ending node,Z-dir starting node, Z-dir ending node,

~Boundary Conditions Card #Boundary conditions area applied at node face

#card name start with ~ symbol

3,

number of boundary conditions,

top, neumann,

1(Recharge) boundary surface direction, aqueous phase boundary type,

1, 1,1,1,129,129,4,

X-dir starting, node,X-dir ending node,Y-dir starting node, Y-dir ending node,Z-dir starting node, Z-dir ending node,number of bondary times,

0.,yr,-1.5000000E+00,mm/yr,

#boundary time, unit, aqueous volumetric flux (recharge rate), unit,

1944, yr,-1.5000000E+00,mm/yr,

#boundary time, unit, aqueous volumetric flux (recharge rate), unit,

1944, yr,-1.7000000E+01,mm/yr,

#boundary time, unit, aqueous volumetric flux (recharge rate), unit,

2010, yr,-1.7000000E+01, mm/yr,

#boundary time, unit, aqueous volumetric flux (recharge rate), unit,

west, hydraulic gradient,

#2 boundary surface direction, aqueous phase boundary type,

1, 1,1,1,1,29,1,

X-dir starting, node,X-dir ending node,Y-dir starting node, Y-dir ending node,Z-dir starting node, Z-dir ending node,number of bondary times,

0., yr, 1.7110383E+05,Pa,

#boundary time, unit, base aqueous pressure, unit,

east, hydraulic gradient,

#3 boundary surface direction, aqueous phase boundary type,

1, 1,1,1,1,29,1,

X-dir starting, node,X-dir ending node,Y-dir starting node, Y-dir ending node,Z-dir starting node, Z-dir ending node,number of bondary times,

0., yr, 1.7099610E+05, Pa,

#boundary time, unit, base aqueous pressure, unit,

#Notes: hydraulic gradient 0.0011m was applied from west to east, distance between west and east surface = 10m, so pressure at the east surface
*= west pressure – 0.0011*10*9793.52 = 1.711E+05-107.73 = 1.7099E+05 Pa*

~Output Control Card

#card name start with ~ symbol

1,

#number of reference node at which output will be taken

1,1,29,

#reference node X index, reference node Y index, reference node Z index,

50, 50, yr, m, 6, 6, 9,

#reference node screen output frequency (every 50 time step),reference node output file frequency (every 50 time step), time unit, length unit, screen significant digits, output file significant digits, plot file significant digits,

8,

#number of output files variables

aqueous saturation,,

#variable name, unit,

aqueous matric potential, m,

#variable name,unit,

aqueous moisture content,,

#variable name, unit,

xnc aqueous vol, m/yr,

#variable name, unit,

znc aqueous vol, m/yr,

#variable name,unit,

aqueous courant number,,

#variable name, unit,

total water mass,,

#variable name, unit,

water mass source int,,

#variable name, unit,

1,

#number of plot files time

2010. yr,

#plot/restart file time, unit,

8,

#number of plot files variables

aqueous saturation,,

#variable name, unit,

aqueous matric potential, m,

#variable name, unit,

aqueous moisture content,,

#variable name, unit,

xnc aqueous vol, m/yr,

#variable name, unit,

znc aqueous vol, m/yr,

#variable name, unit,

aqueous courant number,,

#variable name, unit,

total water mass,,

#variable name, unit,

water mass source int,,

#variable name,unit,

Post-2010 Model

~Simulation Title Card

#card name start with ~ symbol

1,

#STOMP version number,

100 DR 1D,

#Simulation Title,

C Cheng,

#User name,

Intera Inc.,

#Company name,

Feb 2nd 2011,

#Input creation date,

12:00 PM MST,

#Input creation time,

1,

#Number of simulation note lines,

This input file is a 1D scoping model for 100 Area site D.

#Simulation notes

~Solution Control Card

#card name start with ~ symbol

restart,

#Execution mode option, (restart file was created from the previous flow simulation)

Water w/ transport courant,,

#Operation mode option, (transport simulation will be carried with Patankar solute transport) maximum courant number= 1(default),

1,

#Number of execution time periods,

2010.,yr,6010,yr,1.0e-09,yr,0.01,yr,1.25,8,1.e-6,

#intial time,unit,final time, unit, initial time step, unit, maximum time step, unit, time step acceleration factor, maximum number of Newton-Raphson iterations, convergence criteria,

900000,

#maximum number of time step,

0,

#number of interfacial averaging variables,

~Grid Card

#card name start with ~ symbol

cartesian,

#coordinate system option,

1, 1,129,

#number of X-direction nodes, number of Y-direction nodes, number of Z-direction nodes,

0.0, m, 10, m,

X dir surface position, unit, surface position, unit,

0., m, 1.0, m,

Y dir surface position, unit, surface position, unit,

110.75000,m,129@0.25,m,

Z dir surface position, unit, number of nodes@node width,

~Rock/Soil Zonation Card

#card name start with ~ symbol

4,

#number of rock/soil zone,

RS, 1,1,1,1,1,29,

#zone name, X-dir starting node, X-dir ending node,Y-dir starting node, Y-dir ending node,Z-dir starting node, Z-dir ending node,

RU, 1, 1,1,1,30,49,

#zone name, X-dir starting node, X-dir ending node, Y-dir starting node, Y-dir ending node, Z-dir starting node, Z-dir ending node,

HF, 1, 1, 1,1,50,111,

#zone name, X-dir starting node, X-dir ending node, Y-dir starting node, Y-dir ending node,Z-dir starting node, Z-dir ending node,

BF, 1,1,1,1,112,129,

#zone name, X-dir starting node, X-dir ending node, Y-dir starting node, Y-dir ending node, Z-dir starting node, Z-dir ending node,

~Mechanical Properties Card

#card name start with ~ symbol

BF,2.68,g/cm^3,0.276,0.262,,,Millington and Quirk,

#zone name, particle density, unit, total porosity, diffusive porosity, specific storativity - default = 1E-07*diff porosity, units - default = 1/m, tortuosity function,

HF,2.68,g/cm^3,0.280,0.25,,,Millington and Quirk,

#zone name, particle density, unit, total porosity, diffusive porosity, specific storativity - default = 1E-07*diff porosity, units - default = 1/m, tortuosity function,

RU,2.68,g/cm^3,0.280,0.28,,,Millington and Quirk,

#zone name, particle density, unit, total porosity, diffusive porosity, specific storativity - default = 1E-07*diff porosity, units - default = 1/m, tortuosity function,

RS,2.68,g/cm^3,0.280,0.28,,,Millington and Quirk,

#zone name, particle density, unit, total porosity, diffusive porosity, specific storativity - default = 1E-07*diff porosity, units - default = 1/m, tortuosity function,

~Hydraulic Properties Card

#card name start with ~ symbol

BF,5.98E-04,hc:cm/s,,,5.98E-04,hc:cm/s,

#zone name, X-direction hydraulic conductivity, units, Y-direction hydraulic conductivity (zero), units, Z-direction hydraulic conductivity, unit,

HF,2.10E-03,hc:cm/s,,,2.10E-04,hc:cm/s,

#zone name, X-direction hydraulic conductivity, units, Y-direction hydraulic conductivity (zero), units, Z-direction hydraulic conductivity, unit,

RU,4.13E-03,hc:cm/s,,,4.13E-04,hc:cm/s,

#zone name, X-direction hydraulic conductivity, units, Y-direction hydraulic conductivity (zero), units, Z-direction hydraulic conductivity, unit,

RS,2.59E-02,hc:cm/s,,,2.59E-03,hc:cm/s,

#zone name, X-direction hydraulic conductivity, units, Y-direction hydraulic conductivity (zero), units, Z-direction hydraulic conductivity, unit,

~Saturation Function Card

#card name start with ~ symbol

BF, Nonhysteretic van Genuchten, 0.019, 1/cm,1.4,0.162,,

#zone name, moisture retention function, vG alpha, units, vG n, residual saturation, vG m - default = 1 - 1/n,

HF, Nonhysteretic van Genuchten, 0.021, 1/cm,1.458,0.04,,

#zone name, moisture retention function, vG alpha, units, vG n, residual saturation, vG m - default = 1 - 1/n,

RU, Nonhysteretic van Genuchten, 0.008, 1/cm,1.66,0.093,,

#zone name, moisture retention function, vG alpha, units, vG n, residual saturation, vG m - default = 1 - 1/n,

RS, Nonhysteretic van Genuchten, 0.008, 1/cm,1.66,0.093,,

#zone name, moisture retention function, vG alpha, units, vG n, residual saturation, vG m - default = 1 - 1/n,

~Aqueous Relative Permeability Card

#card name start with ~ symbol

BF, Mualem,,

#zone name, permeability function name, vG m parameter (default =1-1/n),

HF, Mualem,,

#zone name, permeability function name, vG m parameter (default =1-1/n),

RU, Mualem,,

#zone name, permeability function name, vG m parameter (default =1-1/n),

RS, Mualem,,

#zone name, permeability function name, vG m parameter (default =1-1/n),

~Initial Conditions Card #Initial conditions area applied at node center

#card name start with ~ symbol

Aqueous Pressure, Gas Pressure,

#initial saturation optionA, initial saturation optionB,

3,

#number of initial conditions,

Aqueous Pressure,1.7110383E+05,Pa,,,,,-9793.52,1/m,1,1,1,1,1,1,29,

#variable name,magnitude,unit,X-dir pressure gradient,unit, Y-dir pressure gradient,unit,Z-dir pressure gradient,unit,X-dir starting node,X-dir ending node,Y-dir starting node, Y-dir ending node,Z-dir starting node, Z-dir ending node,

Aqueous Pressure,86656.7554,Pa,,,,,-100.,1/m,1,1,1,1,1,30,129,

#variable name,magnitude,unit,X-dir pressure gradient,unit, Y-dir pressure gradient,unit,Z-dir pressure gradient,unit,X-dir starting node,X-dir ending node,Y-dir starting node, Y-dir ending node,Z-dir starting node, Z-dir ending node,

Solute Volumetric Overwrite,Con100,1930,1/m^3,,,,,,,1,1,1,1,1,71,111,

#variable name,solute name,solute initial concentration,unit,X-dir gradient,unit, Y-dir gradient,unit,Z-dir gradient,unit,X-dir starting node,X-dir ending node,Y-dir starting node, Y-dir ending node,Z-dir starting node, Z-dir ending node,

#Notes: calculation of solute concentration: Particle density = 2.68
*Bulk density = (1-porosity)*particle density = (1-0.28)*2.68 = 1.93 gm/cc = 1930 Kg/m^3*
solute initial concentration = 1mg/Kg = 1930 mg/m^3

*#depth of contamination = (111-71+1)*0.25 = 10.25m = 50% of total vadose zone below the clean back fill which is 20.5 m (Figure B-1).*

~Boundary Conditions Card #Boundary conditions area applied at node face

#card name start with ~ symbol

3,

number of boundary conditions,

top,neumann,zero flux,

1(Recharge) boundary surface direction, aqueous phase boundary type, solute boundary type for number of solutes (here only one Con100),

1, 1,1,1,129,129,6,

#X-dir starting node,X-dir ending node,Y-dir starting node, Y-dir ending node,Z-dir starting node, Z-dir ending node,number of bondary times,

2010., yr, -1.7000000E+01, mm/yr,,,

#boundary time, unit, aqueous volumetric flux (recharge rate), unit, solute flux (zero), unit,

2015.0000000, yr, -1.7000000E+01,mm/yr,,,

#boundary time, unit, aqueous volumetric flux (recharge rate), unit, solute flux (zero), unit,

2015.0000000, yr, -3.0000000E+00, mm/yr,,,

#boundary time, unit, aqueous volumetric flux (recharge rate), unit, solute flux (zero), unit,

2045.0000000, yr, -3.0000000E+00, mm/yr,,,

#boundary time, unit, aqueous volumetric flux (recharge rate), unit, solute flux (zero), unit,

2045.0000000, yr, -1.5000000E+00, mm/yr,,,

#boundary time, unit, aqueous volumetric flux (recharge rate), unit, solute flux (zero), unit,

5010, yr, -1.5000000E+00, mm/yr,,,

#boundary time, unit, aqueous volumetric flux (recharge rate), unit, solute flux (zero), unit,

west,hydraulic gradient,zero flux,

#2 boundary surface direction, aqueous phase boundary type, solute boundary type,

1, 1,1,1,1,29,1,

#X-dir starting node,X-dir ending node,Y-dir starting node, Y-dir ending node,Z-dir starting node, Z-dir ending node,number of boundary times,

2010, yr, 1.7110383E+05, Pa,,,

#boundary time, unit, base aqueous pressure, unit, solute flux, unit,

east,hydraulic gradient,outflow,

#2 boundary surface direction, aqueous phase boundary type, solute boundary type,

1, 1,1,1,1,29,1,

#X-dir starting node, X-dir ending node, Y-dir starting node, Y-dir ending node, Z-dir starting node, Z-dir ending node, number of boundary times,

2010,yr,1.7099610E+05,Pa,,,

#boundary time, unit, base aqueous pressure, unit, solute flux, unit,

~Solute/Fluid Interactions Card

#card name start with ~ symbol

1,

#number of solutes,

Con100,conventional,0.0,m^2/s,continuous,1.0E+20,yr,

#solute name, Effective diffusion calculation method, aqueous molecular diffusion coefficient@20 degree Celsius, unit, solute partitioning option, half life, unit,

0,

#number of chain decay lines (for radioactive solute),

~Solute/Porous Media Interaction Card

#card name start with ~ symbol

BF, 0.0, m, 0.0, m,

#zone name, longitudinal dispersivity, unit, transverse dispersivity, unit,

Con100, 0.140, cm^3/g,

#solute name, solute aqueous partitioning coefficient, unit,

HF, 0.0, m, 0.0, m,

#zone name, longitudinal dispersivity, unit, transverse dispersivity, unit,

Con100, 0.140, cm^3/g,

#solute name, solute aqueous partitioning coefficient, unit,

RU, 0.0, m, 0.0, m,

#zone name, longitudinal dispersivity, unit, transverse dispersivity, unit,

Con100, 0 .140, cm^3/g,

#solute name, solute aqueous partitioning coefficient, unit,

RS, 0.00, m, 0.00, m,

#zone name, longitudinal dispersivity, unit, transverse dispersivity, unit,

Con100, 0.140, cm^3/g,

#solute name, solute aqueous partitioning coefficient, unit,

~Surface Flux Card

#card name start with ~ symbol

2,

#Total number of surface flux inputs,

2, gw_conc.srf,

#number of surface flux inputs in file, file name,

Aqueous Volumetric Flux, m^3/yr, m^3, east, 1, 1,1,1,10,29,

#surface flux type,unit,unit(integral),surface orientation,X-dir starting node,X-dir ending node,Y-dir starting node, Y-dir ending node,Z-dir starting node, Z-dir ending node,

Solute Flux,Con100,1/yr,,east,1,1,1,1,10,29,

#surface flux type,unit,unit(integral),surface orientation,X-dir starting node,X-dir ending node,Y-dir starting node, Y-dir ending node,Z-dir starting node, Z-dir ending node,

~Output Control Card

#card name start with ~ symbol

1,

#number of reference node at which output will be taken

1,1,28,

#reference node X index, reference node Y index, reference node Z index,

50, 50, yr, m, 6, 6, 9,

#reference node screen output frequency (every 50 time step),reference node output file frequency (every 50 time step), time unit, length unit, screen significant digits, output file significant digits, plot file significant digits,

11,

#number of output file variables

aqueous saturation,,

#variable name, unit,

aqueous pressure,Pa,

#variable name,unit,

aqueous hydraulic head, m,

#variable name,unit,

aqueous matric potential,cm,

#variable name, unit,

aqueous moisture content,,

#variable name,unit,

xnc aqueous vol, m/yr,

#variable name,unit,

znc aqueous vol, m/yr,

#variable name, unit,

aqueous courant number,,

#variable name, unit,

total water mass,,

#variable name, unit,

solute aqueous concentration, Con100, 1/m^3,

#variable name, unit,

Solute volumetric concentration, Con100, 1/m^3,

#variable name, unit,

1,

#number of plot files time

5010, yr,

#plot/restart file time, unit,

11,

#number of plot file variables

aqueous saturation,,

#variable name, unit,

aqueous pressure, Pa,

#variable name, unit,

aqueous hydraulic head, m,

#variable name, unit,

aqueous matric potential, cm,

#variable name, unit,

aqueous moisture content,,

#variable name, unit,

xnc aqueous vol, m/yr,

#variable name, unit,

znc aqueous vol, m/yr,

#variable name, unit,

aqueous courant number,,

#variable name, unit,

total water mass,,

#variable name, unit,

solute aqueous concentration, Con100, 1/m^3,

#variable name, unit,

solute volumetric concentration, Con100, 1/m^3,

#variable name, unit,

Appendix C

CHPRC Fact Sheet

STOMP: Validation and Extent of Application

The STOMP (Subsurface Transport Over Multiple Phases) simulator software was developed at Pacific Northwest National Laboratory in the early 1990s and has been subject to extensive use and improvement since that time. The fundamental purpose of the STOMP simulator software is to produce numerical predictions of thermal and hydrogeologic flow and transport phenomena in variably saturated subsurface environments, which are contaminated with volatile or non-volatile organic compounds. Auxiliary applications include numerical predictions of solute transport processes including reactive transport. This fact sheet provides a brief overview of work that has validated the STOMP simulator software and the breadth of applications to which this simulator has been applied.

EXAMPLES OF VALIDATION, BENCHMARKING, AND VERIFICATION FOR STOMP

Document	Validation/Benchmark/Verification Performed
STOMP Subsurface Transport Over Multiple Phases: Application Guide PNNL-11216, Nichols et al. 1997, Pacific Northwest National Laboratory, Richland, Washington	• Saturated Flow – validation against analytical solution of Theis (1935) • Saturated Flow – validation against analytical solution of the leaky aquifer problem • Saturated Flow – benchmark against numerical solution of Morris and Reddell (1991) for flow to two wells in a non-homogenous domain • Saturated Transport – validation against analytical solution of van Genuchten and Alves (1982) for one-dimensional transport in a uniform steady flow field • Saturated Transport – validation against analytical solution of Cleary and Ungs (1978) for the "patch source" problem for transport in a steady uniform two-dimensional flow field • Sea-Water Intrusion: validation against the analytical solution of Henry's Problem for steady-state diffused seat water wedging within a confined aquifer balanced against a fresh-water field as revisited by Ségol (1994) • Density-Driven Flow: verification against Elder's Problem for transient thermal convection in porous media (Voss and Souza 1987). • Flow and Transport in Unsaturated Porous Media: verification against results for infiltration of water into a uniform laboratory scale soil column filled with very dry soils as reported by Haverkamp et al. (1977) • Flow and Transport in Unsaturated Porous Media: verification and benchmark against experimental and numerical simulation results reported by Touma and Vauclin (1986) for two-phase (air and water), one-dimensional infiltration into a soil column • Energy and Phase Mass Conservation: validation against hand calculations to demonstrate conservation of energy and phase mass in multiple phases for single-node system undergoing the following phase changes: evaporation, condensation, and thawing; and for flow from hot, two-phase conditions • Heat Pipe Flow and Transport: validation against the heat pipe problem posed and solved analytically by Udell and Fitch (1985) • Heat Pipe Flow and Transport: verification against the experimental results reported by Jame and Norum (1980) for a freezing/thawing heat pipe problem • Non-Aqueous Phase Liquid Flow and Transport: benchmark against the simulations conducted with the MOFAT code reported by Kaluarachchi and Parker (1989) for infiltration and redistribution of oil in a hypothetical, two-dimensional aquifer • Non-Aqueous Phase Liquid Flow and Transport: verification against experimentally determined fluid saturations during the infiltration and redistribution of a LNAPL and a DNAPL in a partly saturated one-dimensional column reported in Oostrom et al (1995). • Non-Aqueous Phase Liquid Flow and Transport: verification against experimentally determined Trichloroethlene (TCE) gaseous concentrations reported in Lenhard et al. (1985)

Simulation of Unsaturated Flow and Nonreactive Solute Transport in a Heterogeneous Soil at the Field Scale NUREG/CR-5998 & PNL-8496, 1993, Pacific Northwest Laboratory, Richland, Washington	Verification of unsaturated flow and nonreactive solute transport in a heterogeneous soil at the field scale using the Las Cruces trench site in New Mexico.
Application of similar media scaling and conditional simulation for modeling water flow and tritium transport at the Las Cruces Trench Site Rockhold et al. (1996), Water Resources Research 32(3):595-609	
Numerical modeling of hysteretic multiphase flow: 1. Model description and verification and 2. A validation exercise White et. al (1993) in *EOS Transactions,* 74(16), AGU	Verification conducted to test the hysteretic permeability-saturation-pressure (k-S-P) relations that were embodied in the numerical simulator STOMP. The data used in the validation exercise were measured during a multiphase one-dimensional flow experiment where the elevation of the water table was fluctuated to produce wetting and drying fluid saturation paths. Water and NAPL contents were measured nondestructively at specified flow-cell locations via radiation attenuation. These measurements were compared to simulations of the experiment using STOMP. Close agreement was obtained between the experimental data and the numerical results, except for the highest and lowest measurement elevations. For the highest position, a slight modification to the relative permeability function provided better agreement with the experimental NAPL data. For the lowest position, the discrepancy between experimental data and numerical simulations is attributed to an absence of a nonwetting-fluid entry-pressure concept in the k-S-P model.
Numerical analysis of a three-phase system with a fluctuating water table White and Lenhard (1993) in *Proceedings of Thirteenth Annual AGU Hydrology Days*	Verification against multiphase flow experiment measurements involving subjecting an initially water-drained, three-phase (air-oil-water) to a fluctuating water table to quantify the entrapment of air an NAPL by phases of greater wettability under dynamic conditions.
Measurement and predictions of density-driven vapor flow of trichloroethylene in sandy porous media Oostrom et al. (1994) in *EOS,* 75(16), American Geophysical Union	Verification against experimental measurements of spatial and temporal evolution of gaseous-phase trichloroethylene (TCE) in a variably saturated 1-m-hight by 2-m-long flow cell.

An experimental and numerical study of LNAPL and DNAPL movement in the subsurface Oostrom et al. (1994), *EOS*	Verification against experimental measurements of the multiphase transport of LNAPL and DNAPL in a one-m-long glass column.
Models to determine first order rate coefficients from single-well push-pull tests. Schroth and Istok (2006), Ground Water 44(2): 275–283	Validation against analytical solution for a push-pull test (injection and extraction from a single well) used for in situ determination of a variety of aquifer properties. The results of a STOMP based numerical model were in good agreement with the results of the analytical solution.
Intercomparison of Numerical Simulation Codes for Geologic Disposal of CO2 Pruess et al. (2002), LBNL-51813, Lawrence Berkeley National Laboratory, Berkeley, California	Benchmark with other numerical simulation codes, including the TOUGH2 family of codes, MUFTE_UG, SIMUSCOPP, GEM, FLOTRAN, ECLIPSE 300, and NUFT.

EXAMPLES OF THE BREADTH OF STOMP APPLICATIONS (ASIDE FROM THE HANFORD SITE)

Document(s)	**Location** / Application
	Yucca Mountain, Nevada
Preliminary Total-System Analysis of a Potential High-Level Nuclear Waste Repository at Yucca Mountain PNNL-8444, Eslinger et al. (1993), Pacific Northwest National Laboratory, Richland, Washington	Simulation of long-term gas phase transport of carbon-14 in potential high-level waste repository in unsaturated volcanic tuff
Simulation of Two-phase Carbon-14 Transport at Yucca Mountain, Nevada White et al. (1992) in *Proceedings of Solving Ground Water Problems with Models*	
	Edwards Air Force Base near Mohave, California
Numerical Analysis of the In-Well Vapor-Stripping System Demonstration at Edwards Air Force Base PNNL-11348, White and Gilmore (1996), Pacific Northwest National Laboratory, Richland, Washington	In support of interim cleanup activities, simulation of in-well vapor stripping remediation technology designed to remove dissolved volatile organic compounds from groundwater. The in-well vapor-stripping system comprises an engineered and a hydrologic component that operate in unison to form an in situ recirculation pattern. The engineered system is driven with compressed air, utilizing an air-lift pumping scheme that volatilizes dissolved organic compounds. The volatile vapors are removed from the gas stream above the ground surface and pumped water is infiltrated into the hydrologic system below the ground surface.
Performance Assessment of the In-Well Vapor-Stripping System PNNL-11414, Gilmore et al. (1996), Pacific Northwest National Laboratory, Richland, Washington	

NAPL Migration in Response to Hydraulic Controls at the Brooklawn Site near Baton Rouge, Louisiana White and Oostrom (1997) in *Proceedings of Twenty First Annual American Geophysical Union Hydrology Days*	**Brooklawn Site, Baton Rouge, Louisiana** Evaluation of the effectiveness of the hydraulic containment strategy being implemented at the Brooklawn Site to control DNAPL migration toward a fresh water aquifer. The investigation comprised experimental and numerical components. Laboratory experiments on soil samples and pumped DNAPL from the Brooklawn site were conducted to determine hydrologic properties of the soils and physical and chemical composition of the liquid. Numerical simulations were conducted using a multifluid simulator for multiple realizations of a two dimensional cross-section through the Brooklawn site transecting the region of known DNAPL contamination. Multifluid flow behavior considered included three-phase retention and relative permeability characteristics, nonwetting fluid entrapment, and multiphase pumping. The principal objective of the simulations was to generate quantitative comparisons between various hydraulic control options, thus providing a stronger scientific rationale for future environmental management decisions at the site. Results indicate that under current conditions the pumping wells peripheral to the DNAPL plume do not significantly contribute to hydraulic control of DNAPL migration or source recovery.
Transport of Carbon-14 in a Large Unsaturated Soil Column Plummer et al. (2004), Vadose Zone Journal 3 (1): 109-121	**Idaho National Engineering and Environmental Laboratory, Idaho Falls, ID** Estimation of solid-aqueous distribution coefficient for sediments through inverse modeling of carbon-14 transport data using both a simple gas-diffusion model and STOMP to support work on the Radioactive Waste Management Complex (RWMC) of the Idaho National Engineering and Environmental Laboratory (INEEL) that includes activated metals that release radioactive C-14 as they corrode.
The Ohio River Valley CO_2 Storage Project Final Technical Report Gupta (2008)	**Mountaineer Power Plant, New Haven, West Virginia** A series of numerical simulations of CO_2 injection were conducted as part of a program to assess the potential for geologic sequestration in deep geologic reservoirs, the Rose Run formation and the Copper Ridge formation, at the AEP Mountaineer Power Plant outside of New Haven, West Virginia. The simulations were executed using the H2O-CO2-NaCl operational mode of the Subsurface Transport Over Multiple Phases (STOMP) simulator.

Validation of CO2 Injection simulations with Monitoring Well Data Bacon et al. (2009), Energy Procedia	**Midwest Regional Carbon Sequestration Partnership geologic field test site, Otsego County, Michigan** STOMP used to assess potential carbon dioxide (CO_2) injection rates into saline formations at several sites for the MRCSP. An injection test of approximately 10,000 metric tons into the Bass Islands Dolomite with CO_2 injection rates from 250–500 tons per day, was performed in the test well at the MRCSP geologic field test site. Reservoir simulations were performed to estimate injection parameters, such as bottom hole pressures and pressure response over time in the storage formation, and compared to measurements taken during the test.
Geological sequestration of carbon dioxide in the Cambrian Mount Simon Sandstone: Regional storage capacity, site characterization, and large-scale injection feasibility, Michigan Basin Barnes et al. (2009), Environmental Geosciences: 16(3), 163-183	
Quantification of Microbial Methane Oxidation in an Alpine Peat Bog Urmann et al. (2007), Vadose Zone Journal 6:705-712	**Drained but partially regenerated raised peat bog in Eigenthal above the city of Lucerne, Switzerland** STOMP used to simulate a gas push-pull test to quantify methanotrophic activity in situ in the vadose zone above a petroleum-contaminated aquifer.
Hydrology and subsurface transport of oil-field brine at the U.S. Geological Survey OSPER site "A", Osage County, Oklahoma Herkelrath et al. (2007), Applied Geochemistry 22(10):2155-2163	**U.S. Geological Survey OSPER site "A", Osage County, Oklahoma** STOMP used to simulate a subsurface salt plume.
Modeling of Bromide in a Single-well Injection-Withdraw Experiment Hellerich et al. (1999) in Hazardous and Industrial Wastes, Proceedings of the 31st Mid-Atlantic Industrial and Hazardous Waste Conference.	**National Chromium, Inc. chromium metal plating facility located in northeastern Connecticut** Mechanisms controlling the transport of bromide in a single-well injection-withdrawal experiment determined through modeling using the STOMP simulator.
Thermal Analysis of GCLs at a Municipal Solid Waste Landfill Hanson et al. (2005), Civil and Environmental Engineering	**An undisclosed solid waste landfill, Michigan** STOMP used to simulate in one dimension heat transfer near the center of the landfill.

Phytocapping: An alternative technique to reduce leachate and methane generation from municipal landfills Venkatraman and Ashwath (2007), The Environmentalist 27(1):1573-2991	**Queensland, Australia** Trial use of STOMP to calculate daily water balance to identify suitable plant species and optimize thickness of soil cover for use in phytocapping.
Numerical Analysis to Investigate the Effects of the Design and Installation of Equilibrium Tension Plate Lysimeters on Leachate Volume Mertensa et al. (2005) 4:488-499	**Lake Taupo catchment, New Zealand** Applied STOMP to a two-dimensional model for a range of subsurface conditions to examine the effect of the lower boundary condition on solute transport in lysimeters.
Degassing of $^3H/^3He$, CFCs and SF_6 by denitrification: Measurements and two-phase transport simulations Visser et al. (2008), Journal of Contaminant Hydrology 103(3-4):206-218	**The Netherlands** Used STOMP as a two-phase flow and transport model to study reliability of $^3H/^3He$, CFCs and SF_6 as groundwater age tracers under agricultural land where denitrification causes degassing.

Appendix D

Identification of Waste Sites and Contaminants of Potential Concern Requiring Evaluation of the Conservatism of the 70:30 Initial Contaminant Distribution for Soil Screening Level and Preliminary Remedial Goal Development

Table D-1 contains the full list of waste sites and contaminants with apparent deep contamination that may indicate non-conservative representation by the 70:30 initial concentration distribution assumption used in modeling of the vadose zone for purposes of calculating SSL and PRG values.

Table D-2 contains the filtered list after the following exclusions are applied:

- boreholes that did not sample the lower 30 percent of the vadose zone
- contaminants that had no background values
- contaminants with reported concentrations in the lower 30 percent of the vadose zone that were within the range of background
- contaminants had $K_d > 25$ (will not yield numerical SSL or PRG values under 100:0)
- Strontium-90 (already using 100:0 model per other considerations)

Table D-1. Preliminary Identification of Waste Sites and Contaminants that Appear Non-Conservative with Respect to the 70:30 Initial Concentration Distribution based on Review of RI Borehole Data

Vadose Zone re-evaluation for groundwater protection at 100-DH.

Identifying vadose zone conditions for constituents with higher Kd, but exhibiting full-thickness contamination (i.e., non-70:30 conditions).

Inspection of data performed by:	CW Miller/PRC
Inspection Date:	10-Oct-12

Approach to Data Inspection:

Reviewed vertical distribution profiles from Chap 4 of RI/FS Report. Identified by inspection contaminants that were not constrained to 70:30 distribution.

Data conditions that preclude using 70:30 distribution model:

1. The constituent typically exhibits a reference K_d of 2 ml/g or greater.

2. An anthropogenic (non-background) contaminant is present throughout the vadose, including within the lower 30% of the vadose thickness.

3. An anthropogenic contaminant with an established background level exceeds the 90th percentile background at some depth interval(s) and reported MDCs for the remaining

measurements are greater than the 90th percentile background.

4. An anthropogenic contaminant is present in the deepest sample of a vadose profile, if sampling did not examine the entire vadose.

5. An anthropogenic contaminant was not detected, however, all non-detects exhibit MDCs greater than the 90th percentile background concentration.

6. An anthropogenic contaminant exhibits increasing concentration with depth in the lower 30% of the vadose.

Uncertainties to

a. Not all naturally-occurring metals have established background concentration statistics (e.g., Sr, Sn)

Consider:

This precludes assessing whether or not the observed concentrations exceed background.

b. Some investigative wells and borings did not fully penetrate the vadose zone. This results in obvious uncertainty in the distribution of contaminants within the deeper vadose, particularly where the contaminant(s) are consistently detected in the upper vadose portion and are detected in the deepest vadose samples analyzed. This does not provide a basis for concluding the absence of the contaminant in deeper vadose.-

c. Unacceptably-high minimum detectable concentrations (e.g., MDCs greater than the 90th percentile background concentration, or MDCs greater than quantified detections) do not provide a basis for concluding the absence of a contaminant in vadose zone samples.

d. Some constituents may exhibit site-specific, or historical waste stream-specific Kd that results in historic migration differing substantially from predicted future migration.

e. Established soil background statistics may not be representative of actual naturally-occurring concentrations at various depths within the vadose zone.

Note: Contaminants highlighted in BLUE are selected for alternative SSL/PRG calculation. Contaminants highlighted in ORANGE are not selected because background statistics have not been developed.

Note: Applicable uncertainties are dominated by partial vadose characterization at locations with apparent residual vadose contamination and high analyte MDCs that do not support exclusion from vadose transport analysis.

Note: Sr-90 (highlighted in GREEN) has already been simulated under 100:0 distribution scenario; it is included in this table for completeness.

Waste Site	Sample Location	Contaminants	Rationale for non-70:30 Distribution	Applicable Uncertainty

Waste Site	Sample Location	Contaminants	Rationale for non-70:30 Distribution	Applicable Uncertainty
116-D-1A	199-D5-21	Am-241	Detected in every vadose sample	Boring did not penetrate entire vadose zone; partial characterization.
116-D-1A	199-D5-21	Co-60	Detected throughout vadose	Boring did not penetrate entire vadose zone; partial characterization.
116-D-1A	199-D5-21	Cr	Detected throughout vadose exceeding 90% background	Boring did not penetrate entire vadose zone; partial characterization.
116-D-1A	199-D5-21	Cs-137	Detected in every vadose sample	Boring did not penetrate entire vadose zone; partial characterization.
116-D-1A	199-D5-21	Eu-152	Detected throughout vadose	Boring did not penetrate entire vadose zone; partial characterization.
116-D-1A	199-D5-21	Eu-154	Detected throughout vadose	Boring did not penetrate entire vadose zone; partial characterization.
116-D-1A	199-D5-21	Hg	Detected throughout vadose exceeding 90% background	Boring did not penetrate entire vadose zone; partial characterization.
116-D-1A	199-D5-21	Pb	Detected throughout vadose exceeding 90% background	Boring did not penetrate entire vadose zone; partial characterization.
116-D-1A	199-D5-21	Pu-239	Detected in every vadose sample	Boring did not penetrate entire vadose zone; partial characterization.
116-D-1A	199-D5-21	Sr-90	Detected in every vadose sample	Boring did not penetrate entire vadose zone; partial characterization.

Waste Site	Sample Location	Contaminants	Rationale for non-70:30 Distribution	Applicable Uncertainty
116-D-4	199-D5-24	Ag	Detected in deepest vadose sample, high MDC	Boring did not penetrate entire vadose zone; partial characterization.
116-D-1B	199-D5-29	Ag	MDCs exceed 90% background	Boring did not penetrate entire vadose zone; partial characterization.
116-D-1B	199-D5-29	Am-241	Detected in every vadose sample	Boring did not penetrate entire vadose zone; partial characterization.
116-D-1B	199-D5-29	Cd	MDCs exceed 90% background	Boring did not penetrate entire vadose zone; partial characterization.
116-D-1B	199-D5-29	Co-60	Detections near deepest zone sampled.	Boring did not penetrate entire vadose zone; partial characterization.
116-D-1B	199-D5-29	Cs-137	Detected in every vadose sample	Boring did not penetrate entire vadose zone; partial characterization.
116-D-1B	199-D5-29	Eu-152	Detections near deepest zone sampled.	Boring did not penetrate entire vadose zone; partial characterization.
116-D-1B	199-D5-29	Eu-154	Detections near deepest zone sampled.	Boring did not penetrate entire vadose zone; partial characterization.
116-D-1B	199-D5-29	Hg	MDCs exceed 90% background	Boring did not penetrate entire vadose zone; partial characterization.
116-D-1B	199-D5-29	Pu-239	Detected in every vadose sample	Boring did not penetrate entire vadose zone; partial characterization.

Waste Site	Sample Location	Contaminants	Rationale for non-70:30 Distribution	Applicable Uncertainty
116-D-1B	199-D5-29	Sr-90	Detected in every vadose sample	Boring did not penetrate entire vadose zone; partial characterization.
116-D-7	199-D8-60	Ag	Detected in vadose at, or above, 90% background, high MDCs	Boring did not penetrate entire vadose zone; partial characterization.
116-D-7	199-D8-60	Cr	Detected in vadose at, or above, 90% background, high MDCs	Boring did not penetrate entire vadose zone; partial characterization.
116-D-7	199-D8-60	Cs-137	Detected in deepest vadose sample	Boring did not penetrate entire vadose zone; partial characterization.
116-D-7	199-D8-60	Sr-90	Detected in deepest vadose sample	Boring did not penetrate entire vadose zone; partial characterization.
116-DR-1&2	199-D8-61	Ag	Detected in vadose, high MDC	Boring did not penetrate entire vadose zone; partial characterization.
116-DR-1&2	199-D8-61	Am-241	Detected in deepest vadose sample	Boring did not penetrate entire vadose zone; partial characterization.
116-DR-1&2	199-D8-61	Cs-137	Detected in deepest vadose sample	Boring did not penetrate entire vadose zone; partial characterization.
116-DR-1&2	199-D8-61	Eu-152	Detected in deepest vadose sample	Boring did not penetrate entire vadose zone; partial characterization.
116-DR-1&2	199-D8-61	Eu-154	Detected in deepest vadose sample	Boring did not penetrate entire vadose zone; partial characterization.

Waste Site	Sample Location	Contaminants	Rationale for non-70:30 Distribution	Applicable Uncertainty
116-DR-1&2	199-D8-61	Hg	Detected in vadose, high MDC	Boring did not penetrate entire vadose zone; partial characterization.
116-DR-1&2	199-D8-61	Pu-239	Detected in deepest vadose sample	Boring did not penetrate entire vadose zone; partial characterization.
116-DR-1&2	199-D8-61	Sr-90	Detected in deepest vadose sample	Boring did not penetrate entire vadose zone; partial characterization.
116-DR-1&2	199-D8-62	Ag	Present in all vadose samples above 90% background	Boring did not penetrate entire vadose zone; partial characterization.
116-DR-1&2	199-D8-62	Co-60	Detected in deepest vadose sample	Boring did not penetrate entire vadose zone; partial characterization.
116-DR-1&2	199-D8-62	Cs-137	Detected in deepest vadose sample	Boring did not penetrate entire vadose zone; partial characterization.
116-DR-1&2	199-D8-62	Eu-152	Detected in deepest vadose sample	Boring did not penetrate entire vadose zone; partial characterization.
116-DR-1&2	199-D8-62	Hg	Present in vadose, high MDCs	Boring did not penetrate entire vadose zone; partial characterization.
116-DR-1&2	199-D8-62	Pu-239	Detected in deepest vadose sample	Boring did not penetrate entire vadose zone; partial characterization.
116-DR-1&2	199-D8-62	Sr-90	Detected in deepest vadose sample	Boring did not penetrate entire vadose zone; partial characterization.

Waste Site	Sample Location	Contaminants	Rationale for non-70:30 Distribution	Applicable Uncertainty
116-DR-9	199-D8-64	Aroclor-1260	Detected in deep vadose, high MDC	Boring did not penetrate entire vadose zone; partial characterization.
116-DR-9	199-D8-64	Cd	Hi MDCs	Boring did not penetrate entire vadose zone; partial characterization.
116-DR-9	199-D8-64	Hg	Detected in deep vadose, high MDCs	Boring did not penetrate entire vadose zone; partial characterization.
116-DR-9	199-D8-64	Sr-90	Present in vadose, no background	Boring did not penetrate entire vadose zone; partial characterization.
116-DR-9	199-D8-65	Ag	Detected throughout vadose in excess of 90% background	Boring did not penetrate entire vadose zone; partial characterization.
116-DR-9	199-D8-65	Cd	Detected in deep vadose sample, high MDC	Boring did not penetrate entire vadose zone; partial characterization.
116-DR-9	199-D8-65	Cs-137	Detected in deep vadose	Boring did not penetrate entire vadose zone; partial characterization.
116-DR-9	199-D8-65	Eu-152	Detected in deepest sample	Boring did not penetrate entire vadose zone; partial characterization.
116-DR-9	199-D8-65	Hg	Detected in deep sample, high MDC	Boring did not penetrate entire vadose zone; partial characterization.
116-DR-9	199-D8-65	Pu-239	Detected in deepest sample, increasing with depth	Boring did not penetrate entire vadose zone; partial characterization.

Waste Site	Sample Location	Contaminants	Rationale for non-70:30 Distribution	Applicable Uncertainty
116-DR-9	199-D8-65	Sr-90	Detected throughout vadose	Boring did not penetrate entire vadose zone; partial characterization.
116-DR-9	199-D8-66	Ag	Present in vadose, high MDCs	Boring did not penetrate entire vadose zone; partial characterization.
116-DR-9	199-D8-66	Cd	Detected in deepest sample, increasing with depth	Boring did not penetrate entire vadose zone; partial characterization.
116-DR-9	199-D8-66	Co-60	Detected in deepest vadose sample	Boring did not penetrate entire vadose zone; partial characterization.
116-DR-9	199-D8-66	Cs-137	Detected in deepest vadose sample	Boring did not penetrate entire vadose zone; partial characterization.
116-DR-9	199-D8-66	Eu-152	Detected in deepest vadose sample	Boring did not penetrate entire vadose zone; partial characterization.
116-DR-9	199-D8-66	Eu-154	Detected in deepest vadose sample	Boring did not penetrate entire vadose zone; partial characterization.
116-DR-9	199-D8-66	Sr-90	Detected throughout vadose	Boring did not penetrate entire vadose zone; partial characterization.
Non-specific	199-D3-5	Mo	Detected in deep vadose at, or above 90% background	May reflect variability in background concentrations with depth.
Non-specific	199-D3-5	Sn		Detected throughout vadose, no background established

Waste Site	Sample Location	Contaminants	Rationale for non-70:30 Distribution	Applicable Uncertainty
116-H-6	199-H4-50	Ag	Detected in vadose, high MDC	Boring did not penetrate entire vadose zone; partial characterization.
116-H-6	199-H4-50	Cs-137	Detected in vadose samples	Boring did not penetrate entire vadose zone; partial characterization.
116-H-6	199-H4-50	Hg	Detected in vadose, high MDC	Boring did not penetrate entire vadose zone; partial characterization.
116-H-6	199-H4-50	Sb	Detected in vadose samples, high MDC	Boring did not penetrate entire vadose zone; partial characterization.
116-H-6	199-H4-50	U-234	Detected in all vadose samples above 90% b ackground	Boring did not penetrate entire vadose zone; partial characterization.
116-H-6	199-H4-50	U-235	Detected in all vadose samples above 90% b ackground	Boring did not penetrate entire vadose zone; partial characterization.
116-H-6	199-H4-50	U-238	Detected in all vadose samples above 90% b ackground	Boring did not penetrate entire vadose zone; partial characterization.
116-H-6	199-H4-51	Cd	Detected at, or above, 90% background, increasing with depth	Boring did not penetrate entire vadose zone; partial characterization.
116-H-6	199-H4-52	Ag	Detected in deepest vadose sample, high MDC	Boring did not penetrate entire vadose zone; partial characterization.
116-H-6	199-H4-52	Cd	Detected exceeding 90% background in deepest sample, high MDC	Boring did not penetrate entire vadose zone; partial characterization.

Waste Site	Sample Location	Contaminants	Rationale for non-70:30 Distribution	Applicable Uncertainty
116-H-6	199-H4-52	Hg	Detected in deepest vadose sample, high MDC	Boring did not penetrate entire vadose zone; partial characterization.
116-H-6	199-H4-52	Sb	Detected in deepest vadose sample, high MDC	Boring did not penetrate entire vadose zone; partial characterization.
116-H-6	199-H4-53	Hg	Detected in vadose zone, MDC exceeds 90% bckground by 10x	Boring did not penetrate entire vadose zone; partial characterization.
116-H-6	199-H4-53	Sb	Detected over vadose zone exceeding 90% background, high MDC	Boring did not penetrate entire vadose zone; partial characterization.
116-H-6	199-H4-55	Cd	Detected at, or above, 90% background, high MDC	Boring did not penetrate entire vadose zone; partial characterization.
116-H-6	199-H4-55	Hg	Detected at, or above, 90% background, high MDC	Boring did not penetrate entire vadose zone; partial characterization.
116-H-6	199-H4-55	Sb	Detected throughout vadose above 90% background	Boring did not penetrate entire vadose zone; partial characterization.
116-H-6	199-H4-55	Se	Detected above 90% background, high MDC	Boring did not penetrate entire vadose zone; partial characterization.
116-H-6	199-H4-56	Pb	Detected throughout vadose at, or above 90% background	Boring did not penetrate entire vadose zone; partial characterization.
116-H-6	199-H4-56	Sb	Detected throughout vadose above 90% background	Boring did not penetrate entire vadose zone; partial characterization.

Waste Site	Sample Location	Contaminants	Rationale for non-70:30 Distribution	Applicable Uncertainty
116-H-6	199-H4-57	Sb	Detected throughout vadose above 90% background, High MDC	Boring did not penetrate entire vadose zone; partial characterization.
116-H-1	199-H4-58	Eu-152	Present in deepest sample	Boring did not penetrate entire vadose zone; partial characterization.
116-H-1	199-H4-58	Eu-154	Present in deepest sample	Boring did not penetrate entire vadose zone; partial characterization.
116-H-1	199-H4-58	Pu-239/240	Present in deepest sample	Boring did not penetrate entire vadose zone; partial characterization.
116-H-1	199-H4-58	Se	Present in vadose, high MDCs	Boring did not penetrate entire vadose zone; partial characterization.
116-H-2	199-H4-59	Cr	Present in all vadose samples, increasing with depth	Boring did not penetrate entire vadose zone; partial characterization.
116-H-2	199-H4-59	Ni	Present in all vadose samples, increasing with depth	Boring did not penetrate entire vadose zone; partial characterization.
116-H-7	199-H4-61	Co-60	Detected in deep vadose	Boring did not penetrate entire vadose zone; partial characterization.
116-H-7	199-H4-61	Cr	Detected in deep vadose above 90% background	Boring did not penetrate entire vadose zone; partial characterization.
116-H-7	199-H4-61	Cs-137	Detected in deep vadose	Boring did not penetrate entire vadose zone; partial characterization.

Waste Site	Sample Location	Contaminants	Rationale for non-70:30 Distribution	Applicable Uncertainty
116-H-7	199-H4-61	Eu-152	Detected in all vadose samples	Boring did not penetrate entire vadose zone; partial characterization.
116-H-7	199-H4-61	Eu-154	Detected in all vadose samples	Boring did not penetrate entire vadose zone; partial characterization.
116-H-7	199-H4-61	Hg	Detected throughout vadose, high MDC	Boring did not penetrate entire vadose zone; partial characterization.
116-H-7	199-H4-61	Pu-239/240	Detected in deep vadose	Boring did not penetrate entire vadose zone; partial characterization.
116-H-7	199-H4-61	Se	MDC exceeds 90% background	Boring did not penetrate entire vadose zone; partial characterization.
116-H-7	199-H4-61	Sr-90	Detected in deep vadose	Boring did not penetrate entire vadose zone; partial characterization.
1607-H4	Test Pit	Acenaphthene	Detected in deepest vadose sample	Boring did not penetrate entire vadose zone; partial characterization.
1607-H4	Test Pit	Acenaphthylene	Detected in deepest vadose sample	Boring did not penetrate entire vadose zone; partial characterization.
1607-H4	Test Pit	Antrhacene	Detected in deepest vadose sample	Boring did not penetrate entire vadose zone; partial characterization.
1607-H4	Test Pit	Benzo(a)pyrene	Detected in deepest vadose sample	Boring did not penetrate entire vadose zone; partial characterization.

Waste Site	Sample Location	Contaminants	Rationale for non-70:30 Distribution	Applicable Uncertainty
1607-H4	Test Pit	Benzo(b)fluoranthene	Detected in deepest vadose sample	Boring did not penetrate entire vadose zone; partial characterization.
1607-H4	Test Pit	Benzo(k)Anthracene	Detected in deepest vadose sample	Boring did not penetrate entire vadose zone; partial characterization.
1607-H4	Test Pit	Bezo(a)anthracene	Detected in deepest vadose sample	Boring did not penetrate entire vadose zone; partial characterization.
1607-H4	Test Pit	Chrysene	Detected in deepest vadose sample	Boring did not penetrate entire vadose zone; partial characterization.
1607-H4	Test Pit	Fluoranthene	Detected in deepest vadose sample	Boring did not penetrate entire vadose zone; partial characterization.
1607-H4	Test Pit	Fluorene	Detected in deepest vadose sample	Boring did not penetrate entire vadose zone; partial characterization.
1607-H4	Test Pit	Pb	Detected in deepest vadose sample above 90% background	Boring did not penetrate entire vadose zone; partial characterization.
1607-H4	Test Pit	Phenanthrene	Detected in deepest vadose sample	Boring did not penetrate entire vadose zone; partial characterization.
1607-H4	Test Pit	Pyrene	Detected in deepest vadose sample	Boring did not penetrate entire vadose zone; partial characterization.
100-D-56	199-D5-143	Sr-90	Detected in deep vadose zone	Duplicate sample was non-detect.
Non-specific	199-D3-5	Sr		Detected throughout vadose, no background established

Waste Site	Sample Location	Contaminants	Rationale for non-70:30 Distribution	Applicable Uncertainty
Non-specific	199-D5-133	Mo	Detected in deep vadose at, or above 90% background	
100-D-12	199-D5-144	Tl	MDCs exceed 90% background	High MDCs do not support exclusion from GW protection analysis.
100-D-56	199-D5-143	Cr	Detected throughout vadose, increasing with depth	
116-D-1A	199-D5-132	Hg	MDCs exceed 90% background	High MDCs do not support exclusion from GW protection analysis.
116-D-1A	199-D5-132	Sb	MDCs exceed 90% background	High MDCs do not support exclusion from GW protection analysis.
116-D-1A	199-D5-132	Np-237	Present over vadose thickness	
116-D-7	C7851	Cs-137	Detected in deep vadose	
116-D-7	C7851	Mo	Detected in deep vadose at, or above 90% background	
116-D-7	C7851	Cr	Detected in vadose at, or above, 90% background	
116-D-7	199-D8-60	Hg	Detected in vadose at, or above, 90% background, high MDCs	High MDCs do not support exclusion from GW protection analysis.
116-D-7	C7851	Hg	Detected in vadose at, or above, 90% background, high MDCs	High MDCs do not support exclusion from GW protection analysis.
Non-specific	199-D5-133	Pb	Detected in deep vadose at, or above 90% background	

Waste Site	Sample Location	Contaminants	Rationale for non-70:30 Distribution	Applicable Uncertainty
Non-specific	199-D5-133	Sn		Detected throughout vadose, no background established
116-D-7	C7851	Sb	Detected in vadose at, or above, 90% background, high MDCs	
116-DR-1&2	C7852	Hg	Detected in deep profile, high MDC	High MDCs do not support exclusion from GW protection analysis.
116-DR-1&2	199-D8-62	Tl	Detected in vadose soil, high MDCs	High MDCs do not support exclusion from GW protection analysis.
116-DR-1&2	B8786	Hg	Present in vadose, high MDCs	High MDCs do not support exclusion from GW protection analysis.
116-DR-9	C7850	Acenaphthene	Detected in deep vadose, high MDCs	High MDCs do not support exclusion from GW protection analysis.
116-DR-9	C7850	Aroclor-1260	Detected in deep vadose, high MDCs	High MDCs do not support exclusion from GW protection analysis.
116-H-1	C7864	Chrysene	Detected in deep vadose	High MDCs do not support exclusion from GW protection analysis.
Non-specific	199-D5-133	Sr		Detected throughout vadose, no background established
116-H-1	C7864	Fluoranthene	Detected in deep vadose	
Non-specific	199-D5-134	Sb	Detected in all vadose samples above 90% b ackground	May reflect variability in background concentrations with depth.

Waste Site	Sample Location	Contaminants	Rationale for non-70:30 Distribution	Applicable Uncertainty
116-H-1	C7864	Phenanthrene	Detected in deep vadose	High MDCs do not support exclusion from GW protection analysis.
116-H-1	C7864	Pyrene	Detected in deep vadose	
116-H-1	C7864	Cs-137	Present in deep vadose	
116-H-1	C3048	Eu-152	Present in deep vadose	
116-H-1	C7864	Eu-152	Present in deep vadose	
100-D-12	199-D5-144	Sr-90	Detected throughout vadose, increasing with depth	Kd may differ from reference value.
Non-specific	199-D5-134	Sn		Detected throughout vadose, no background established
116-D-1A	199-D5-132	Cr	Detected throughout vadose	May reflect variability in background concentrations with depth.
116-D-1A	199-D5-132	Mo	Exceeds background over vadose	May reflect variability in background concentrations with depth.
116-D-1A	199-D5-132	Ni	Detected throughout vadose	May reflect variability in background concentrations with depth.
Non-specific	199-D5-134	Sr		Detected throughout vadose, no background established

Waste Site	Sample Location	Contaminants	Rationale for non-70:30 Distribution	Applicable Uncertainty
Non-specific	199-D5-140	Hg	MDCs exceed 90% background	High MDCs do not support exclusion from GW protection analysis.
Non-specific	199-D5-140	Cr	Detected throughout vadose at, or above, 90% background	May reflect variability in background concentrations with depth.
Non-specific	199-D5-140	Mo	Presented throughout vadose exceeding 90% background	May reflect variability in background concentrations with depth.
Non-specific	199-D5-140	Ni	Detected throughout vadose, increasing with depth	May reflect variability in background concentrations with depth.
100-D-56	199-D5-143	Li	Detected throughout vadose, increasing with depth	May reflect variability in background concentrations with depth.
100-D-56	199-D5-143	Mo	Detected throughout vadose exceeding 90% background	May reflect variability in background concentrations with depth.
116-D-1A	199-D5-21	Cd	Detected throughout vadose exceeding 90% background	May reflect variability in background concentrations with depth.
Non-specific	199-D5-140	Sn		Detected throughout vadose, no background established
Non-specific	199-D5-140	Sr		Detected throughout vadose, no background established
Non-specific	199-D5-141	Mo	Detected throughout vaadose at, or above, 90% background	May reflect variability in background concentrations with depth.

Waste Site	Sample Location	Contaminants	Rationale for non-70:30 Distribution	Applicable Uncertainty
Non-specific	199-D5-141	Sb	Detected throughout vadose above 90% background, High MDC	High MDCs do not support exclusion from GW protection analysis.
Non-specific	199-D5-141	Sn		Detected throughout vadose, no background established
Non-specific	199-D5-141	Sr		Detected throughout vadose, no background established
Non-specific	199-D6-3	Cr	Detected in deep vadose at, or above 90% background	
Non-specific	199-D6-3	Cs-137	Detected in deep vadose	
116-H-1	C3048	Hg	Present in deep vadose	May reflect variability in background concentrations with depth.
116-DR-9	C7850	Mo	Present throughout vadose at, or above, 90% background	May reflect variability in background concentrations with depth.
116-D-7	C7851	Ni	Detected in deep vadose at, or above 90% background	May reflect variability in background concentrations with depth.
116-DR-1&2	C7852	Mo	Present throughout vadose at, or above, 90% background	May reflect variability in background concentrations with depth.
116-D-1B	C7855	Hg	Detections exceed background throughout vadose	May reflect variability in background concentrations with depth.

Waste Site	Sample Location	Contaminants	Rationale for non-70:30 Distribution	Applicable Uncertainty
116-D-1B	C7855	Mo	Detections exceed background throughout vadose	May reflect variability in background concentrations with depth.
116-D-1B	C7855	Sb	Detections exceed background throughout vadose	May reflect variability in background concentrations with depth.
116-H-1	C7864	Cu	Present over vadose at, or greater than, 90% background	May reflect variability in background concentrations with depth.
116-H-1	C7864	Hg	Present at, or greater than, 90% background, elevated MDCs	May reflect variability in background concentrations with depth.
116-H-1	C7864	Mo	Present over vadose at, or greater than, 90% background	May reflect variability in background concentrations with depth.
116-H-1	C7864	Pb	Present over vadose at, or greater than, 90% background	May reflect variability in background concentrations with depth.
116-H-1	C7864	Sb	Present in deep vadose	May reflect variability in background concentrations with depth.
100-D-12	199-D5-144	Mo	Detected throughout vadose exceeding 90% background	Range of background conditions may differ in deep vadose.
116-H-1	C7864	Cr	Present over vadose at, or greater than, 90% background	
116-D-1A	199-D5-132	Sr-90	Present over vadose thickness	
116-H-4	C7862	Sb	Present in deep vadose, high MDC	High MDCs do not support exclusion from GW protection analysis.

Waste Site	Sample Location	Contaminants	Rationale for non-70:30 Distribution	Applicable Uncertainty
Non-specific	199-D6-3	Sn		Detected throughout vadose, no background established
Non-specific	199-D6-3	Sr		Detected throughout vadose, no background established
116-D-4	199-D5-24	Sr-90	Detected in deepest vadose sample	
Non-specific	199-H1-7	Cr	Detected in deep vadose, increasing concentration	Boring did not penetrate entire vadose zone; partial characterization.
Non-specific	199-H1-7	Mo	Detected throughout vadose at, or above, 90% background	Boring did not penetrate entire vadose zone; partial characterization.
116-H-4	C7862	Cr	Present in vadose samples at, or above, 90% background	
Non-specific	199-H3-6	Sr-90	Detectedin deep vadose	
Non-specific	199-H3-9	Sr-90	Detected in deep vadose	
116-H-4	C7862	Mo	Present in vadose samples at, or above, 90% background, increasing with depth	
116-DR-1&2	B8786	Sr-90	Present throughout vadose	
116-H-6	199-H4-54	Cd	Detected at, or above 90% background over vadose; MDC exceeds background level	High MDCs do not support exclusion from GW protection analysis.

Waste Site	Sample Location	Contaminants	Rationale for non-70:30 Distribution	Applicable Uncertainty
116-H-1	C3048	Sr-90	Present throughout vadose	
116-DR-9	C7850	Sr-90	Present in deep vadose	
116-H-6	C7863	Np-237	Detected in deep vadose	
116-H-6	199-H4-54	Sb	Detected in the vadose and MDC exceeds 90% background	High MDCs do not support exclusion from GW protection analysis.
116-H-6	C7860	Sb	Detected over vadose above 90% background, high MDC	High MDCs do not support exclusion from GW protection analysis.
116-H-6	C7863	Mo	Detected throughout vadose at, or above, 90% background	
116-D-1B	C7855	Sr-90	Detected throughout entire vadose zone	
116-H-6	C7860	Hg	Detected throughout vadose zone at, or above 90% background	
Non-specific	199-H1-7	Tl	Detected throughout vadose at, or above, 90% background, High MDC	High MDCs do not support exclusion from GW protection analysis.
118-D-6	C7857	Sr-90	Present throught vadose	
116-H-6	C7860	Mo	Detected throughout vadose zone at, or above 90% background	
116-H-6	C7863	Hg	MDC exceeds 90% background	High MDCs do not support exclusion from GW protection analysis.
116-H-6	C7860	Sr-90	Detected in deep vadose	

Waste Site	Sample Location	Contaminants	Rationale for non-70:30 Distribution	Applicable Uncertainty
116-H-7	C7861	Sb	Detected in deep vadose, high MDC	High MDCs do not support exclusion from GW protection analysis.
Non-specific	199-H1-7	Sn		Detected throughout vadose, no background established
116-H-7	C7861	Mo	Detected throughout vadose above 90% background	
116-H-7	C7861	Hg	Detected throughout vadose at, or above 90% background	
116-H-7	C7861	Sr-90	Detected throughout vadose zone, increasing with depth	
116-H-7	C7861	Cr	Detected throughout vadose at, or above, 90% background	
116-H-7	C7861	Cs-137	Detected throughout vadose zone	
118-D-6	C7857	Hg	Detected in vadose, high MDC	High MDCs do not support exclusion from GW protection analysis.
Non-specific	199-H1-7	Sr		Detected throughout vadose, no background established
116-H-6	C7863	Sr-90	Detected in deep vadose	
Non-specific	199-H2-1	Mo	Detected throughout vadose at, or above, 90% background	May reflect variability in background concentrations with depth.
118-D-6	C7857	Cr	present in vadose at greater than 90% background	
118-D-6	C7857	Mo	Present over vadose thickness at greater than90% background	

Waste Site	Sample Location	Contaminants	Rationale for non-70:30 Distribution	Applicable Uncertainty
Non-specific	199-H2-1	Sn		Detected throughout vadose, no background established
Non-specific	199-H2-1	Sr		Detected throughout vadose, no background established
116-H-1	C7864	Sr-90	Present throughout vadose	
Non-specific	199-H3-10	Mo	Detected throughout vadose at, or above, 90% background	
Non-specific	199-H3-10	Sn		Detected throughout vadose, no background established
116-D-1A	199-D5-132	Sn		Detected throughout vadose, no background established
116-D-1A	199-D5-132	Sr		Detected throughout vadose, no background established
Non-specific	199-H3-10	Sr		Detected throughout vadose, no background established
Non-specific	199-H3-6	Sn		Detected throughout vadose, no background established
Non-specific	199-H3-6	Sr		Detected throughout vadose, no background established
Non-specific	199-H3-7	2-Hexanone	Detected in lower vadose zone, High MDC	High MDCs do not support exclusion from GW protection analysis.

Waste Site	Sample Location	Contaminants	Rationale for non-70:30 Distribution	Applicable Uncertainty
Non-specific	199-H3-7	Mo	Detected throughout vadose at, or above, 90% background	High MDCs do not support exclusion from GW protection analysis.
Non-specific	199-H3-7	Styrene	Detected in deep vadose, high MDC	High MDCs do not support exclusion from GW protection analysis.
Non-specific	199-H3-7	Tl	Detected throughout vadose exceeding 90% background	High MDCs do not support exclusion from GW protection analysis.
Non-specific	199-H3-7	Sn		Detected throughout vadose, no background established
100-D-56	199-D5-143	Sn		Detected throughout vadose, no background established
100-D-56	199-D5-143	Sr		Detected throughout vadose, no background established
100-D-12	199-D5-144	Sn		Detected throughout vadose, no background established
100-D-12	199-D5-144	Sr		Detected throughout vadose, no background established
Non-specific	199-H3-7	Sr		Detected throughout vadose, no background established
Non-specific	199-H3-9	Cr	Detected throughout vadose, at, or above 90% background	May reflect variability in background concentrations with depth.

Waste Site	Sample Location	Contaminants	Rationale for non-70:30 Distribution	Applicable Uncertainty
Non-specific	199-H3-9	Cu	Detected in deep vadose at, or above 90% background	May reflect variability in background concentrations with depth.
Non-specific	199-H3-9	Mo	Detected throughout vadose at, or above, 90% background	May reflect variability in background concentrations with depth.
Non-specific	199-H3-9	Ni	Detected in deep vadose above 90% background	May reflect variability in background concentrations with depth.
Non-specific	199-H3-9	Sb	Detected throughout vadose, at, or above 90% background	May reflect variability in background concentrations with depth.
Non-specific	199-H3-9	Sn		Detected throughout vadose, no background established
Non-specific	199-H3-9	Sr		Detected throughout vadose, no background established
Non-specific	199-H6-3	Hg	MDCs exceed 90% background	High MDCs do not support exclusion from GW protection analysis.
Non-specific	199-H6-3	Mo	Detected throughout vadose at, or above, 90% background	May reflect variability in background concentrations with depth.
Non-specific	199-H6-3	Ni	Detected throughout vadose at, or above, 90% background	May reflect variability in background concentrations with depth.
Non-specific	199-H6-3	Sn		Detected throughout vadose, no background established

Waste Site	Sample Location	Contaminants	Rationale for non-70:30 Distribution	Applicable Uncertainty
Non-specific	199-H6-3	Sr		Detected throughout vadose, no background established
Non-specific	199-H6-4	2-Hexanone	Detected in deep vadose, high MDC	High MDCs do not support exclusion from GW protection analysis.
Non-specific	199-H6-4	Mo	Detected throughout vadose at, or above, 90% background	
Non-specific	199-H6-4	Styrene	Detected in deep vadose, high MDC	High MDCs do not support exclusion from GW protection analysis.
Non-specific	199-H6-4	Sn		Detected throughout vadose, no background established
Non-specific	199-H6-4	Sr		Detected throughout vadose, no background established
116-DR-9	C7850	Sn		Detected throughout vadose, no background established
116-DR-9	C7850	Sr		Detected throughout vadose, no background established
116-D-7	C7851	Sn		Detected throughout vadose, no background established
116-D-7	C7851	Sr		Detected throughout vadose, no background established

Waste Site	Sample Location	Contaminants	Rationale for non-70:30 Distribution	Applicable Uncertainty
116-DR-1&2	C7852	Sn		Detected throughout vadose, no background established
116-DR-1&2	C7852	Sr		Detected throughout vadose, no background established
118-D-6	C7857	Sn		Detected throughout vadose, no background established
118-D-6	C7857	Sr		Detected throughout vadose, no background established
116-H-6	C7860	Sn		Detected throughout vadose, no background established
116-H-6	C7860	Sr		Detected throughout vadose, no background established
116-H-7	C7861	Sn		Detected throughout vadose, no background established
116-H-7	C7861	Sr		Detected throughout vadose, no background established
116-H-4	C7862	Sn		Detected throughout vadose, no background established
116-H-4	C7862	Sr		Detected throughout vadose, no background established

Waste Site	Sample Location	Contaminants	Rationale for non-70:30 Distribution	Applicable Uncertainty
116-H-6	C7863	Sn		Detected throughout vadose, no background established
116-H-6	C7863	Sr		Detected throughout vadose, no background established
116-H-1	C7864	Sn		Detected throughout vadose, no background established
116-H-1	C7864	Sr		Detected throughout vadose, no background established
100-D-4	Test Pit	Sn		Detected throughout vadose, no background established
100-D-4	Test Pit	Sr		Detected throughout vadose, no background established
116-D-4	Test Pit	Sn		Detected throughout vadose, no background established
116-D-4	Test Pit	Sr		Detected throughout vadose, no background established
116-H-2	Test Pit	Sn		Detected throughout vadose, no background established
116-H-2	Test Pit	Sr		Detected throughout vadose, no background established

Waste Site	Sample Location	Contaminants	Rationale for non-70:30 Distribution	Applicable Uncertainty
1607-H4	Test Pit	Sn		Detected throughout vadose, no background established
1607-H4	Test Pit	Sr		Detected throughout vadose, no background established

Table D-2. Waste Sites and Contaminants to Test for Conservatism of 70:30 Initial Concentration Distribution (After Exclusion Criteria[a] Applied to List in Table D-1)

Waste Site	Sample Location	Contaminants	Rationale for non-70:30 Distribution	Applicable Uncertainty
116-D-1A	199-D5-132	Np-237	Present over vadose thickness	
116-D-7	C7851	Sb	Detected in vadose at, or above, 90% background, high MDCs	
116-DR-9	C7850	Acenaphthene	Detected in deep vadose, high MDCs	High MDCs do not support exclusion from GW protection analysis.
116-H-1	C7864	Phenanthrene	Detected in deep vadose	High MDCs do not support exclusion from GW protection analysis.
116-H-1	C7864	Sb	Present in deep vadose	May reflect variability in background concentrations with depth; added back
116-H-4	C7862	Sb	Present in deep vadose, high MDC	High MDCs do not support exclusion from GW protection analysis.
116-H-6	C7860	Sb	Detected over vadose above 90% background, high MDC	High MDCs do not support exclusion from GW protection analysis.
116-H-7	C7861	Sb	Detected in deep vadose, high MDC	High MDCs do not support exclusion from GW protection analysis.
116-H-7	C7861	Mo	Detected throughout vadose above 90% background	

Waste Site	Sample Location	Contaminants	Rationale for non-70:30 Distribution	Applicable Uncertainty
118-H-6	C7863	Np-237	Detected in deep vadose	

a. Excluded:

- Boreholes not associated with a waste site (SSLs and PRGs calculated only for waste site evaluation)
- Boreholes that did not sample the lower 30 percent of the vadose zone
- Contaminants that had no background values
- Contaminants with reported concentrations in the lower 30 percent of the vadose zone that were within the range of background
- Contaminants had Kd > 25 (will not yield numerical SSL or PRG values under 100:0)
- Strontium-90 (already using 100:0 model per other considerations)